
ibmcp
Instituto de Biología Molecular y Celular de Plantas
UNIVERSITAT POLITÈCNICA DE VALÈNCIA
iata
EXCELENCIA SEVERO OCHOA
Instituto de Agroquímica y Tecnología de Alimentos
HO
O
O
SYNTHETIC BIOLOGY TOOLS FOR PRODUCTION OF INSECT PHEROMONES IN PLANTS & FILAMENTOUS FUNGI
Doctoral thesis
Elena Moreno Giménez
Advisors:
Diego Orzáez Calatayud
Jose F. Marcos López
Lynne Yenush
Valencia, October 2023

UNIVERSITAT POLITÈCNICA DE VALÈNCIA

Synthetic biology tools for production of insect pheromones in plants and filamentous fungi

Doctoral thesis

Elena Moreno Giménez

Advisors:

Diego Orzáez Calatayud

Jose F. Marcos López

Lynne Yenush

Valencia, October 2023

TABLE OF CONTENTS

ACKNOWLEDGEMENTS

ACKNOWLEDGEMENTS

"¿Y cómo haces para no volverte loca?" Es una pregunta que me han hecho a menudo al mencionar que estaba haciendo la tesis en dos laboratorios a la vez, aunque seguramente sea una cuestión extendida entre doctorandos aún sin este añadido de tener que andar de un lado para otro. Por supuesto la organización es clave, pero sirve de muy poco sin unos directores capaces de entenderse contigo y entre ellos para no acabar sobrecargándote en exceso.

Así pues, como no podía ser de otro modo, agradezco en primer lugar a mis directores Diego, Jose y Lynne porque sin vuestra paciencia y apoyo al único título al que aspiraría hoy es al de demente. Diego, contigo he peleado más que con ninguno, eres exigente pero a la vez muy atento y sobre todo eres un gran profesional, crítico y detallista. Contigo he aprendido muchísimo no sólo de ciencia, pues cada conversación venía acompañada de algún que otro inciso interesante de mil temas distintos. Gracias por aguantarme en mis momentos más bajos y confiar en mi para sacar esto adelante. Jose, gracias por sacar siempre esos 5 minutos entre ser director de centro y de laboratorio cada vez que te necesitaba y por tus palabras de ánimo y de reconocimiento a todo lo que conseguía, por poco que fuera. La biotecnología de hongos es desde luego complicada, pero "if something doesn't works, it doesn't" y no hay que darle más vueltas ni desesperar, pues aún con tantas cosas que no he conseguido que funcionen, también me llevo muchas victorias para continuar por este camino con la cabeza alta. Lynne, tú has sido y siempre serás mi modelo a seguir desde que te conocí allá en la carrera. Aún recuerdo con inmenso cariño mi primer contacto real con el laboratorio a tu lado durante mi TFG. Me viste dar los primeros pasos y a ti te debo el estar hoy aquí al pensar en mí cuando surgió esta maravillosa oportunidad de tesis. Aunque eres a la que menos he disfrutado durante estos años, siempre has estado ahí en mis momentos de crisis para hablar un rato y ayudarme en todo lo que necesitaba. Eres increíble y nunca dejaré de admirarte por la dedicación y trabajo duro que sacas día a día para llevar mil historias a la vez y aun así estar al tanto de todo.

Aunque los directories tienen un papel primordial en la salud mental del doctorando, una estaría totalmente perdida en el laboratorio sin nadie a quien preguntar cuando no encuentras algo o cuando no tienes ni idea de por donde coger las cosas. Los siguientes a los que quiero agradecer este trabajo es a esos "padres de labo", en mi caso "madres", que no dudaron en acoger a esta recién llegada con tanto cariño y paciencia, aún cuando no les daba la vida para terminar su propia faena. Marta, tú eres sin duda la primera y a la que más tengo que agradecer, porque además de tu enorme apoyo en el labo de ti me llevo una gran amiga, atenta y encantadora. Mónica, mi mami del IATA, no dejo de alucinar con la cantidad de cosas que llevas encima, desde luego el laboratorio estaría perdido sin ti (aún se pierde a veces, aunque ya no estés por allí). Asun, Paloma, gracias también a vosotras por ayudarme siempre que lo necesitaba, incluso cuando ni siquiera teníais claro

cómo hacerlo. Silvia, gracias por mantener el laboratorio a flote día tras día, el hecho de estar en dos laboratorios me ha hecho apreciar muchísimo la tarea titánica que esto supone. Sara, tú has sido mi hermanita mayor, gracias por hacer siempre un alto en tu estresada carrera diaria para echarme un cable cuando lo necesitaba. Sandra, gracias por toda tu ayuda con los experimentos y la escritura del artículo, a ti te he disfrutado poco tiempo pero ha sido suficiente para llevarme un gran recuerdo de ti.

A Silvia y Rubén, equipo SUSPHIRE, compañeros de fatigas en los análisis de gases masas, gracias por ayudarme tanto y ahorrarme tantos viajes. A Jose Luis, gracias por tus clases maestras manejando este bendito aparato, este proyecto no habría despegado sin tu ayuda. Gracias también en este respecto a Ana y Teresa, entre todos habéis conseguido que lo que podría haber sido la mayor pesadilla de mi tesis se convirtiera en una tarea amena y entretenida.

Gracias también al resto de compañeros por contribuir al buen ambiente de trabajo y a mi vida social, tan escasa estos años. Victor, Bea, Paloma, Borja, Javi, Camilo, Martita, Carol, Antonella, Moisés, Zara, María, Elena, Sofi, Nuccio… He coincidido con tanta gente durante estos años y sin embargo de todos vosotros me llevo sólo buenos recuerdos y el orgullo de haber conocido a personas increíbles que seguro triunfarán en cualquier ámbito que se propongan.

A mi gente de Albacete, gracias por todas esas quedadas de fin de semana que tanto me ayudaban a resetear y coger fuerzas. A mis chicas Ana y María, gracias por estar siempre ahí, aún en la distancia, dispuestas a escucharme y darme apoyo. A Roci y Aza, mi refugio friki lleno de amor y patitos, gracias por todo vuestro cariño y atención. A mi familia y sobre todo a ti mi amor, gracias por vuestro apoyo incondicional, aunque aún no tengáis muy claro de qué va mi trabajo, si estoy hoy aquí es gracias a vosotros.

Como decía Newton, “If I have seen further, it is by standing on the shoulders of giants”. Desde luego si he podido ver el camino y dar siempre el siguiente paso ha sido gracias a todas estas grandes personas que con tanto cariño y paciencia me han ayudado a ver más allá. A todos y cada uno de vosotros, de corazón, muchas gracias.

Este trabajo ha sido financiado mediante la Ayuda para la Formación de Profesorado Universitario FPU18/02019 (Ministerio de Educación, Cultura y Deporte), así como por el proyecto europeo SUSPHIRE (PCI2018-092893, Era-CoBiotech), y los proyectos de Plan Nacional I+D PID2019-108203RB-100 y PID2021-125858OB-100 (Ministerio de Ciencia e Innovación).

ABSTRACT
RESUMEN
RESUM

ABSTRACT

The use of living organisms as biofactories have gained significant attention in the industry due to the increasing demand for sustainable production systems and the shortage of resources. Among their many applications, biofactories can be engineered to produce insect pheromones, which serve as eco-friendly alternatives to pesticides for pest management in agriculture. As a proof of concept, in this thesis we characterized *Nicotiana benthamiana* plants engineered with a multigene pathway to produce the moth pheromones *(Z)*-11-hexadecenol (Z11-16OH) and *(Z)*-11-hexadecenyl acetate (Z11-16OAc). The resulting transgenic plants produced modest amounts of both pheromones (111.4 μg g^{-1} FW and 11.8 μg g^{-1} FW for Z11-16OH and Z11-16OAc, respectively), and daily emission rates of ~10 ng g^{-1} FW for each pheromone.

Pheromone production in these plants, however, significantly affected their fitness, likely due to the substantial metabolic burden and possible toxicity of lipid-derived products. One strategy to address these developmental abnormalities consists of engineering conditional transgene expression systems, thus allowing plants to grow normally before inducing the production of the metabolically demanding pheromones. To achieve this goal, in this thesis we developed a set of customizable synthetic promoters called GB_SynP, which can be activated by dCasEV2.1, a strong programable transcriptional activator recently developed for plant gene regulation. These GB_SynP promoters enabled tight regulation of single and multiple transgenes, with robust and tunable transcription levels in the ON state (presence of dCasEV2.1 loaded with the corresponding gRNA), and minimal or undetectable expression in the OFF state.

To implement a conditional expression system for pheromone production in plants, a newly engineered multigene pathway for the biosynthesis of moth pheromones was constructed under the control of GB_SynP promoters. In parallel, the dCasEV2.1 activator was transcriptionally regulated with the CUP2:GAL4 sensor for copper sulphate, an agronomically-compatible chemical trigger. The functionality of this system was tested transiently in *N. benthamiana,* resulting in estimated yields of 32.7 μg g^{-1} FW and 25 μg g^{-1} FW for Z11-16OH and Z11-16OAc respectively in the ON state, and negligible levels in the absence of copper. However, stable transformation of the same copper-regulated

pheromone pathway in *N. benthamiana* plants resulted in significantly lower transgene expression levels, which translated into a great reduction of pheromone yields. This makes the system in its current form a non-viable pheromone biofactory in practical terms. Further optimization should focus on the improvement of the activation cascade, the use of alternative plant hosts with more biomass, and/or the enhancement of emission rates *in planta.*

As an alternative to pheromone production in plants, the interchangeability of DNA parts between plants and filamentous fungi could also be exploited to create fungal biofactories for pheromone production. In this regard, our research group previously adapted the GoldenBraid system for filamentous fungi, which we named FungalBraid. In this thesis, we expanded the FungalBraid collection by incorporating 27 new DNA parts, including different selection markers and several constitutive and inducible promoters, all of which were functionally characterized in *Penicillium digitatum* and *P. chrysogenum*. Furthermore, we successfully expressed the GB_SynP promoters developed for plants in *P. digitatum,* in combination with the non-integrative pAMA18-derived vector for the expression of a dCas9-based activator. Although further optimization of GB_SynP in filamentous fungi is required, as expression levels were lower than those previously observed in plants, this and the other tools available in the FungalBraid collection can be effectively employed in the future for the development of fungal biofactories that produce insect pheromones and other high value biomolecules.

RESUMEN

El empleo de organismos vivos como biofactorías ha ganado una atención significativa en la industria debido a la creciente demanda de sistemas de producción sostenible y la escasez de recursos. Entre sus muchas aplicaciones, las biofactorías pueden ser diseñadas para producir feromonas de insectos, las cuales sirven como alternativa ecológica a los pesticidas para el control de plagas en la agricultura. Como prueba de este concepto, en esta tesis doctoral se caracterizaron plantas de *Nicotiana benthamiana* modificadas genéticamente con una ruta multigénica para producir las feromonas de polillas (Z)-11-hexadecenol (Z11-16OH) y (Z)-11-hexadecenil acetato (Z11-16OAc). Las plantas transgénicas resultantes produjeron cantidades moderadas de ambas feromonas (111.4 μg g^{-1} FW y 11.8 μg g^{-1} FW para Z11-16OH y Z11-16OAc, respectivamente), y tasas de emisión diarias de ~10 ng g^{-1} FW para cada feromona.

La producción de feromonas en estas plantas, sin embargo, afectó significativamente a su desarrollo, probablemente debido a la sustancial carga metabólica y la posible toxicidad de estos productos derivados de lípidos. Una estrategia para superar estas anormalidades en el desarrollo es diseñar un sistema de expresión condicional de los transgenes, permitiendo a las plantas crecer con normalidad antes de inducir la producción de feromonas. Para lograr este objetivo, en esta tesis desarrollamos un conjunto de promotores sintéticos personalizables, llamados GB_SynP, que pueden ser activados con dCasEV2.1, un activador transcripcional potente y programable desarrollado recientemente para la inducción de genes en plantas. Estos promotores GB_SynP permitieron una regulación precisa de transgenes individuales y múltiples, con unos niveles de transcripción robustos y modulables en el estado “encendido” (presencia de dCasEV2.1 portando la correspondiente guía de ARN), y una expresión mínima o indetectable en el estado “apagado”.

Con el fin de implementar un sistema de expresión condicional para producir feromonas en plantas, se generó una nueva ruta multigénica para la biosíntesis de feromonas de polilla bajo el control de los promotores GB_SynP. Paralelamente, el activador dCasEV2.1 se reguló transcripcionalmente mediante el módulo CUP2:GAL4 sensible a sulfato de cobre, un inductor químico ampliamente utilizado en la agricultura. La funcionalidad de este sistema se probó mediante expresión transitoria en *N. benthamiana*, lo que resultó en unos rendimientos estimados de 32.7 μg g^{-1} FW and 25 μg g^{-1} FW para Z11-16OH y Z11-16OAc,

respectivamente, en el estado “encendido”, y unos niveles insignificantes en ausencia de cobre. Sin embargo, la expresión en estable de esta ruta de producción de feromonas regulada por cobre en *N. benthamiana* resultó en unos niveles de expresión de los transgenes significativamente reducidos, lo cual se tradujo en una marcada disminución en la producción de feromonas. Esto supone que el sistema en su forma actual resulte inviable como biofactoría de feromonas en términos prácticos. La consiguiente optimización de este sistema debe centrarse en mejorar la cascada de activación, en el uso de especies de plantas alternativas con mayor biomasa, y/o en incrementar las tasas de emisión en planta.

Como alternativa a la producción de feromonas en plantas, la intercambiabilidad de piezas génicas entre plantas y hongos filamentosos podría también aprovecharse para crear biofactorías fúngicas de feromonas. En este sentido, nuestro grupo de investigación adaptó previamente el sistema GoldenBraid a hongos filamentosos, al que llamamos FungalBraid. En esta tesis ampliamos la colección de FungalBraid incorporando 27 piezas nuevas que incluyen diferentes marcadores de selección y varios promotores constitutivos e inducibles, todos los cuales se caracterizaron funcionalmente en *Penicillium digitatum* y *P. chrysogenum*. Además, logramos expresar con éxito los promotores GB_SynP desarrollados para plantas en *P. digitatum*, en combinación con un vector no integrativo derivado de pAMA18 que expresa un sistema de dCas9 activadora. Aunque se requiere una mayor optimización de GB_SynP en hongos filamentosos, pues los niveles de expresión fueron menores que los observados previamente en plantas, ésta y otras herramientas disponibles en la colección FungalBraid pueden utilizarse en el futuro de manera efectiva para el desarrollo de biofactorías fúngicas que produzcan feromonas de insectos y otras biomoléculas de alto valor.

RESUM

L'ús d'organismes vius com biofàbriques ha guanyat una atenció significativa a la indústria a causa de la creixent demanda de sistemes de producció sostenible i l'escassetat de recursos. Entre les seues moltes aplicacions, les biofàbriques poden ser dissenyades per a produir feromones d'insectes, les quals serveixen com a alternativa ecològica als pesticides per al control de plagues a l'agricultura. Com a prova d'aquest concepte, en aquesta tesi doctoral es van caracteritzar plantes de *Nicotiana benthamiana* modificades genèticament plantes de amb una ruta multigènica per a produir les feromones d'arnes (Z)-11-hexadecenol (Z11-16OH) i (Z)-11-hexadecenil acetat (Z11-16OAc). Les plantes transgèniques resultants van produir quantitats moderades de totes dues feromones (111.4 µg g^{-1} FW i 11.8 µg g^{-1} FW per a Z11-16OH i Z11-16OAc, respectivament), i taxes d'emissió diàries d'aproximadament 10 ng g^{-1} FW per a cada feromona.

No obstant això, la producció de feromones en aquestes plantes va afectar significativament el seu desenvolupament, probablement a causa de la substancial càrrega metabòlica i la possible toxicitat d'aquests productes derivats de lípids. Una estratègia per superar aquestes anormalitats en el desenvolupament és dissenyar un sistema d'expressió condicional dels transgens, permetent a les plantes créixer amb normalitat abans d'induir la producció de feromones. Per assolir aquest objectiu, en aquesta tesi hem desenvolupat un conjunt de promotors sintètics personalitzables, anomenats GB_SynP, que poden ser activats amb dCasEV2.1, un activador transcripcional potent i programable desenvolupat recentment per a la inducció de gens en plantes. Aquests promotors GB_SynP van permetre una regulació precisa de transgens individuals i múltiples, amb uns nivells de transcripció robustos i modulables a l'estat “encès” (presència de dCasEV2.1 portant la corresponent guia d'ARN), i una expressió mínima o indetectable a l'estat "apagat".

A fi d'implementar un sistema d'expressió condicional per produir feromones en plantes, es va generar una nova ruta multigènica per a la biosíntesi de feromones d'arna sota el control dels promotors GB_SynP. Paral·lelament, l'activador dCasEV2.1 es va regular transcripcionalment al mòdul CUP2:GAL4 sensible al sulfat de coure, un inductor químic àmpliament utilitzat en l'agricultura. La funcionalitat d'aquest sistema es va provar mitjançant expressió transitòria en *N. benthamiana*, la qual cosa va resultar en uns rendiments estimats de 32.7 g^{-1} FW i 25 µg g^{-1} FW per a Z11-16OH i Z11-16OAc, respectivament, a l'estat "encès", i uns

nivells insignificants en absència de coure. No obstant això, l'expressió estable d'aquesta ruta de producció de feromones regulada pel coure a *N. benthamiana* va resultar en uns nivells d'expressió dels transgens significativament reduïts, la qual cosa es va traduir en una marcada disminució en la producció de feromones. Això suposa que el sistema en la seua forma actual resulte inviable com a biofàbrica de feromones en termes pràctics. La consegüent optimització d'aquest sistema ha de centrar-se en millorar la cascada d'activació, en l'ús d'espècies de plantes alternatives amb major biomassa, i/o en incrementar les taxes d'emissió a la planta.

Com a alternativa a la producció de feromones en plantes, la intercanviabilitat de peces gèniques entre plantes i fongs filamentosos també podria aprofitar-se per crear biofàbriques fúngiques de feromones. En aquest sentit, el nostre grup de recerca va adaptar prèviament el sistema GoldenBraid a fongs filamentosos, al qual vam anomenar FungalBraid. En aquesta tesi, vam ampliar la col·lecció de FungalBraid incorporant 27 peces noves que inclouen diferents marcadors de selecció i diversos promotors constitutius i induïbles, tots els quals es van caracteritzar funcionalment a *Penicillium digitatum* i *P. chrysogenum*. A més, vam aconseguir expressar amb èxit els promotors GB_SynP desenvolupats per a plantes en *P. digitatum*, en combinació amb un vector no integratiu derivat de pAMA18 que expressa un sistema d'activació basat en dCas9. Encara que es requereix una major optimització de GB_SynP en fongs filamentosos, ja que els nivells d'expressió van ser menors que els observats prèviament en plantes, aquesta i altres eines disponibles a la col·lecció FungalBraid poden utilitzar-se en el futur de manera efectiva per al desenvolupament de biofàbriques fúngiques que produeixin feromones d'insectes i altres biomolècules de gran valor.

ABBREVIATIONS

ABBREVIATIONS

2S3*: Arabidopsis thaliana* 2S albumin gene 3
afpB: *Penicillium digitatum* class B antifungal protein gene
ANS*: Solanum lycopersicum* anthocyanidin synthase gene
amdS: *Aspergillus nidulans* acetamidase gene
amyB: *Aspergillus oryzae* α-amylase gene
ATMT: *Agrobacterium tumefaciens*-mediated transformation
AtrΔ11*: Amyelois transitella* Δ11 desaturase
ble: transposon Tn5 bleomycin resistance gene
bp: DNA base pair
CaMV35S: Cauliflower mosaic virus 35S gene
CBS: CUP2 binding site
CHS*: Solanum lycopersicum* chalcone synthase gene
CPH: *Neonothopanus nambi* caffeylpyruvate hydrolase gene
CRISPR: clustered regularly interspaced short palindromic repeats
CRISPRa: CRISPR activation
CUP2: *Saccharomyces cerevisiae* copper-binding transcription factor
dCas9: nuclease-deactivated Cas9 protein
dCasEV2.1: dCas9:EDLL + MS2:VPR + gRNA2.1
DNA: deoxyribonucleic acid
dpi: days post-inoculation
EaDAct: *Euonymus alatus* diacylglycerol acetyltransferase
EAG: electroantennography
ef1A: *Penicillium digitatum* elongation factor 1A gene
eGFP: enhanced green fluorescent protein
ERF2: *Arabidopsis thaliana* Ethylene responsive factor 2
ergA: *Penicillium chrysogenum* squalene epoxidase gene
FAD: fatty acid desaturases
FAR: fatty acyl reductases
FB: FungalBraid
FLuc: firefly luciferase
FOA: fluoroorotic acid
FW: fresh weight

GB: GoldenBraid
GC/MS: gas chromatography/mass spectrometry
glaA: *Aspergillus niger* glucoamylase gene
gpdA: *Aspergillus nidulans* glyceraldehyde-3-phosphate dehydrogenase A gene
GRAS: Generally Recognized as Safe
gRNA: guide RNA
H3H: *Neonothopanus nambi* hispidin-3 hydroxylase gene
HarFAR: *Helicoverpa armigera* fatty acyl reductase gene
HispS: *Neonothopanus nambi* hispidin synthase gene
LB: Luria Bertani medium
Luz: *Neonothopanus nambi* luciferase gene
MES: 2-(N-morpholino)ethanesulfonic acid
MS: Murashige and Skoog medium
NbDFR: *Nicotiana benthamiana* NADPH-dependent dihydroflavonol-4-reductase gene
NLuc: nanoluciferase
NMR: nuclear magnetic resonance
NOS*: A. tumefaciens* nopaline synthase gene
OD: optical density
paf: *Penicillium chrysogenum* antifungal protein gene
pcbC: *Penicillium rubens* Isopenicillin N synthase gene
PCPS2*: Nicotiana tabacum* trichome-specific Class-II terpene synthase gene
PDA: Potato Dextrose Agar
PDB: Potato Dextrose Broth
Phleo^{R}: phleomycin resistance
pkiA: *Aspergillus niger* pyruvate kinase gene
PcMM: *Penicillium chrysogenum* minimal medium
PdMM: *Penicillium digitatum* minimal medium
RLuc: Renilla luciferase
RNA: ribonucleic acid
RPU: relative promoter unit
ScFv: single-chain variable fragment
SlDFR: *Solanum lycopersicum* NADPH-dependent dihydroflavonol-4-reductase gene

ScATF1: *Saccharomyces cerevisiae* alcohol acetyl transferase 1 gene
***SpATF1*-2**: *Saccharomyces pastorianus* alcohol acetyl transferase 1-2 gene
SxP: SexyPlant
SynBio*:* synthetic biology
TA29: *Nicotiana tabacum*
TALE: Transcription activator-like effector
Terb^{R}: Terbinafine resistance
TF: transcription factor
TSS: transcriptional start site
TU: transcriptional unit
VOC: volatile organic compound
VPR: VP64- p65-Rta transcription factor
WT: wild type
xlnA: *Aspergillus nidulans* Endo-1,4-beta-xylanase A gene
YFP: yellow fluorescent protein
Z11-16OH: *(Z)*-11-hexadecenol
Z11-16OAc: *(Z)*-11-hexadecenyl acetate
Z11-16Ald: *(Z)*-11-hexadecenal

GENERAL INTRODUCTION

GENERAL INTRODUCTION

1. Biofactories: a leading force for industrial development

The origins of biomanufacturing date back to fermentation practices more than 9000 years ago (McGovern et al., 2004), but it was not until the early 1900s when microbial fermentation was industrialized powered by the identification of the microorganisms involved and the use of monocultures in large-scale fermentations (Fulmer, 1930). Industrial production was still limited to naturally occurring fermentations, such as the production of alcohols (ethanol, butanol), or organic acids (citrate, lactate). A big revolution came during the Second World War with the advent of fermentation to produce penicillin and the subsequent attention gained for secondary metabolites to produce not only antibiotics but also flavors and scents (Zhang et al., 2017). The development of advanced cell culture systems and recombinant DNA technology in the 1970s was the next breakthrough. These advancements allowed for the large-scale biomanufacturing of custom-made proteins, such as insulin to be used as biopharmaceuticals, or amylases and proteases for industrial enzyme-based catalysis (Demain and Adrio, 2008; Zhang et al., 2017).

Nowadays, the emergence of genome and metabolic engineering approaches has put biomanufacturing again in the spotlight, as industries face multiple challenges stemming from the increasing shortage of resources. Current efforts are focused on the development of sustainable low-carbon bioproduction systems or biofactories that operate using renewable feedstocks or even carbon dioxide to produce a wide array of complex and valuable compounds by more efficient means (Aguilar and Twardowski, 2022; Antonovsky et al., 2016; Clarke and Kitney, 2020; Perathoner and Centi, 2014; Zhang et al., 2017). Moreover, political decisions favoring sustainability penalize single-use technologies with large ecological impacts, thus increasing the cost of waste disposal (Smith et al., 2021) and highlighting the need for waste utilization strategies and biodegradable materials. Compared to chemical manufacturing, biofactories operate at lower temperatures and pressures without compromising production efficiencies, reducing technological complexity (Clomburg et al., 2017). Moreover, the use of

biofactories is more easily distributed, as developed strains and organisms can be shared for their direct use or further optimization (Cravens et al., 2019).

Among the different organisms employed as biofactories, bacteria are by far the most extensively engineered platform due to their simplicity and long history of tool development for molecular processing and engineering. The use of *Escherichia coli* to produce insulin was the beginning of a long list of protein therapeutics that are currently manufactured using bacterial hosts. In fact, one fourth of the recombinant proteins that are commercially available nowadays are produced in *E. coli* and other prokaryotic hosts (Grand View Research, 2021). The industrial use of bacterial cells has also allowed for the scalable and cost-effective production of a wide range of fine chemicals. For instance, Actinomycetes are widely used in industry to manufacture more than 705 antibiotics (Sarmidi and Enshasy, 2012). Recent developments of bacterial biofactories have expanded their application to the fields of biofuels, biosensors, waste valorization, biomaterials and bioremediation (Antonovsky et al., 2016; Vitorino and Bessa, 2017).

In addition to bacteria, the role of yeast in industry is also widespread, as this eukaryotic host overcomes the biosynthetic and metabolic limitations of prokaryotic cells, while avoiding phage contamination and maintaining the advantages of cell cultures and bioreactors. In addition to their major role in industrial fermentations, *Saccharomyces cerevisiae, Pichia pastoris* and other yeast species have proven particularly adept at producing complex proteins like silk (Xia et al., 2010) or therapeutics like artemisinic acid (Paddon and Keasling, 2014). Co-cultures of yeast and bacteria are also being employed as a way of combining the overall high yields of bacteria with the capability of yeast to express complex pathways (Cravens et al., 2019; Süntar et al., 2021). Limitations are still encountered regarding source materials, since all these biofactories rely on carbon feedstocks, and their suitability for more delicate applications, like the production of some therapeutic proteins. Regarding feedstock, plant and algae cultures are increasingly employed due to their photosynthetic capabilities that enable carbon fixation, mainly for the production of biofuels (Rodionova et al., 2017). Regarding therapeutics, mammalian cell lines such as the well-known Chinese hamster ovary (CHO) are commonly employed to produce antibodies,

vaccines and anticancer drugs, as they better fit the required cellular environment. However, yields are usually low and the production process can be costly and prone to contaminations (Warner, 1999).

1.1 Fungal biofactories

Filamentous fungi are, like bacteria, well-established biofactories with a long history of use in industry to produce a vast array of enzymes, proteins and other bio-based products. Fungal biofactories are characterized by their biochemical versatility, their highly developed secretory capacity, and their efficient utilization of many renewable feedstocks (Troiano et al., 2020). Their high capacity for protein expression and secretion reduces the burden of downstream purification, making them a well-suited platform for large-scale, high-yield production (Jo et al., 2023). In fact, fungal biofactories such as yeast and microscopic filamentous fungi often exceed bacterial biofactories in terms of versatility and secretory capacity. For instance, production of citric acid in *Aspergillus niger*, one of the organic acid most extensively used in industry, greatly exceeds production when compared to bacterial fermentation (Behera, 2020; Berovic and Legisa, 2007).

Half of the commercially available enzymes are produced in fungal biofactories, and this increases to 80% when considering only the food industry (Arnau et al., 2020; de Vries et al., 2020; Dhevagi et al., 2021). The enzymes manufactured in fungal biofactories are used in a wide range of industrial sectors, such as the production of paper (xylanases), food and feed (amylases, proteases, pectinases, xylanases, phytases) or detergents (lipases, endo-glucanases). Many fungal species have been established as industrial workhorses, including *Aspergillus niger*, *A. oryzae*, *Trichoderma reesei*, or *Penicillium chrysogenum*, which are employed not only for the production of enzymes, but also for biomanufacturing different organic acids (citric acid, gluconic acid) or pharmaceuticals (penicillin and other β-lactams) (Jo et al., 2023).

Emerging applications are expanding the use of fungal biomass for producing leather and meat substitutes (González et al., 2020; Jones et al., 2020; Strong et al., 2022), as well as for pigments and colorants (Dufossé et al., 2014; Kalra et al., 2020). Fungal organisms can also be engineered for efficient production of biofuels, as well as for degradation of plastics or recalcitrant pollutants,

contributing to environmental bioremediation efforts (Ferreira et al., 2020; Ning et al., 2021; Spina et al., 2021). The rich diversity of filamentous fungi is still highly under-explored, as it has been estimated that around 25,000 secondary metabolite gene clusters are present in *Aspergillus* and *Penicillium* genera alone, and thus several million for the entire fungal kingdom can still be discovered and exploited (Keller, 2019; Robey et al., 2021).

Despite the long track record of fungal biofactories in industry, knowledge regarding development and optimization of fungal biofactories is very limited. Their secretory physiology, one of their major strong points, is still poorly understood, and the metabolic modelling and engineering of these organisms is greatly hindered by the low efficiency of genetic transformation and the shortage of molecular and genetic tools, as compared to prokaryotic biofactories (Jo et al., 2023; Meyer et al., 2016). Moreover, growth of fungal species is often slow and accompanied with non-optimal and highly variable macroscopic morphologies and the secretion of undesired enzymes (El-Enshasy, 2022; Jo et al., 2023). Key aspects for improving fungal biofactories are therefore expanding the knowledge and toolkits available for improving protein production and understanding culture morphogenesis and its impact on growth, metabolism and secretion.

1.2 Plant biofactories

The use of plants as biofactories offers advantages in terms of cost and scalability, as large-scale production can be achieved through conventional agricultural practices, benefiting from existing infrastructure and expertise in this field. The extensive repertoire of biosynthetic pathways and enzymes available in plants facilitate metabolic engineering processes compared to microbial fermentation, where strategies like supplementation of precursors or pathway division are often required (Patron, 2020; Stephenson et al., 2020; Süntar et al., 2021). Moreover, maintenance of the production lines is cheaper for seed storage than for the freezers required to maintain cell line stocks. Plants also offer the possibility to target expression to specific organs like seeds which can be used to facilitate the storage, extraction, and purification steps. Transient expression is another powerful technology available in plants that involves the introduction of expression vectors directly into plant tissues in the form of plasmids or viral vectors, or indirectly via *Agrobacterium tumefaciens*-mediated transformation

(ATMT). These expression systems ensure high yields in short times, as many copies of the expression vector per cell become transcriptionally active in just a few days. Another advantage of transient expression is the reduced biosafety burden, since transfection procedures are carried out in contained facilities (Mett et al., 2008). Transient expression thus ensures the fast implementation of new production systems and provides flexibility for sectors with oscillating demands like vaccine production (Chen et al., 2013; Hager et al., 2022; Schillberg and Finnern, 2021). Finally, plants can be considered as fully biodegradable, single-use bioreactors, implying that cross-contamination between plant batches is greatly reduced, and that the cleaning and validation processes are highly simplified when compared to fermentation in bioreactors (Buyel, 2019).

An important application of plant biofactories is the so-called molecular pharming field, which emerged in the 1980s when numerous groups focused on the manufacture of high-value biopharmaceuticals in plants (Burnett and Burnett, 2020; Löfstedt and Xia, 2021; Stephenson et al., 2020). In fact, it has been estimated that the production of antibodies using commonly-employed fermentation practices requires almost twice the investment needed for greenhouse production on a similar scale, which could be further reduced to less than one tenth of the cost when considering container-based vertical farms (Buyel, 2019). Despite this, pharmaceuticals are still produced preferably in bacterial and mammalian cell factories, as fermentation processes are better established and characterized. The complexity and toxicity of new pharmaceuticals might however push these production systems beyond their capabilities and a shift towards plant biofactories might occur in the near future (Buyel, 2019; Narayanan and Glick, 2023).

In addition to the biosynthesis of recombinant proteins and pharmaceuticals, plants are also commonly exploited for biofuel production (Rodionova et al., 2017). Moreover, new applications are increasingly being explored, such as phytoremediation of soils and water (Kafle et al., 2022) or the production of fish oils to reduce the burden imposed on marine sources (Beaudoin et al., 2014; Napier and Betancor, 2023). The use of plant cell cultures, a technology which dates back to the 1950s, has also re-emerged with the development of genetic and metabolic approaches that make them highly achievable nowadays. Plant cell

cultures retain the advantages of plant production systems while avoiding expression issues, extraction processes and regulations derived from the use of entire plants (Bapat et al., 2023; Wu et al., 2021). In fact, cell cultures of different plant species have already been implemented in the industry to produce recombinant proteins or secondary metabolites, such as glucocerebrosidase, shikonin, cocovanol or anthocyanins (Appelhagen et al., 2018; Kizhner et al., 2015; Wu et al., 2021).

Current challenges for the application of plant biofactories are mainly the competition with food crops and the extensive downstream processing of plant material (Buyel, 2019). The former can be alleviated by mixed strategies such as the development of edible vaccines (Kurup and Thomas, 2020; Phan et al., 2020; Virdi and Depicker, 2013). For the latter, secretory pathways could be exploited by means of rhizosecretion, as in fungal biofactories, which could also be easily combined with hydroponic cultures (Madeira et al., 2016). Yield rates, slow growth and transgenic regulations are also common key concerns for the development and improvement of plant biofactories, although they can be easily overcome with transient expression systems.

2. Synthetic biology for the development and optimization of biofactories

Synthetic biology (SynBio) is an interdisciplinary field that combines engineering and biology to rationally improve the design, construction, and characterization of biological systems (Endy, 2005). Following the principles of abstraction, decoupling and standardization, biological processes can be divided into different design levels (DNA parts, devices, systems) and independent and simplified tasks can be defined to manage complexity. Interoperability between different tasks and levels is ensured by standardization, which further allows for the easy exchange and reuse of materials between groups using common syntaxes and procedures. Moreover, as DNA synthesis has become increasingly affordable, genetic parts and systems can now be designed and synthesized without the need for physical exchange of materials. Computer sciences are also main contributors to SynBio growth, as advances in the generation and analysis of -omics data open

new opportunities for in silico genetic and metabolic programming to overcome challenges of increasingly complex biological systems (Beal et al., 2020).

SynBio tools and technologies are essential to expand our fundamental understanding of biological processes and to tackle complex bioengineering challenges for the efficient development of biofactories. SynBio has been extensively developed in microbial platforms and is rapidly expanding in plants and filamentous fungi (Meyer et al., 2016; Wang and Demirer, 2023). SynBio tools in plants have been implemented mainly in model species like *Arabidopsis thaliana* or *Nicotiana benthamiana*, thus current efforts are focused on translating them to other plant species with more agronomical relevance. Regarding fungal biofactories, the development of highly productive strains has so far relied mostly on mutagenesis, which led to accumulation of mutations and subsequent impaired fitness. One of the main objectives of Fungal SynBio is therefore to generate precise and targeted edition tools for the development of high-producing strains without growth constraints or production of unwanted secondary metabolites.

2.1 Modular cloning. GoldenBraid and FungalBraid for easy modular assembly of multigene pathways in plants and filamentous fungi

Based on the application of engineering concepts, the improvement of SynBio tools and systems is achieved by means of iterative design-build-test cycles (Clarke, 2017). In this regard, modular DNA cloning provides a versatile and efficient approach for the construction of complex genetic architectures through the precise assembly of functional DNA elements like promoters, terminators or coding regions. Moreover, as genetic architecture can influence the behavior of the genes included in multigene constructs (Johnstone and Galloway, 2022; Patel et al., 2021), testing different construct conformations is often required, and so the application of reusable genetic elements is highly desired.

The standardization of genetic elements further allows for the exchangeability and distribution of DNA parts, promoting collaboration between groups and accelerating research progress. The development of standardized collections of genetic parts and the availability of online design tools have enhanced the accessibility and facilitated the implementation of modular cloning strategies in

many biological platforms, including plants and filamentous fungi (Andreou and Nakayama, 2018; Engler et al., 2014; Hernanz-Koers et al., 2018; Pollak et al., 2019; Sarrion-Perdigones et al., 2011; Weber et al., 2011). Many of these collections are based on the Golden Gate cloning strategy (Engler et al., 2014), which relies on Type IIS enzymes for the efficient assembly of multiple DNA parts in a single reaction. Type IIS enzymes are characterized for cleaving outside their recognition site, allowing for the design of code sequences to create directional assemblies and ensure the correct position of each DNA part in the final construct. As the recognition site is not lost during digestion, assemblies can be further designed to favor the accumulation of the desired final products, while incorrect assemblies are redigested back to the initial form. Moreover, Golden Gate reactions accept both linear and circular DNA substrates, thus avoiding the need of intermediate DNA purification steps. A major advantage of this cloning design is therefore the reproducibility and fidelity of the outcome, which can be used directly for transformation.

Our laboratories have pioneered one adaptation of Golden Gate to plants, which resulted in the creation of GoldenBraid (GB) (Sarrion-Perdigones et al., 2011) and its latter adaptation to filamentous fungi as FungalBraid (FB) (Hernanz-Koers et al., 2018). These systems rely on *Agrobacterium tumefaciens*, which can transform genetically both plants and filamentous fungi (de Groot et al., 1998) and use the same pCAMBIA open-source transformation vectors. The systems make use of multipartite assemblies for the generation of Transcriptional Units (TUs), using DNA parts previously adapted to the system. Adaptation or domestication of DNA parts to GB and FB systems implies the removal of internal recognition sites for the BsaI and BsmBI enzymes employed in the assembly reactions, the addition of 4 specific base pair flanking codes to ensure the directional assembly of each part into the right position, and the final insertion of the DNA part into the pUPD2 entry vector for its replication and storage. Assembled TUs are inserted into level 1 α vectors, which can then be combined in a binary way to form multigenic constructs into the level 2 Ω vectors. The assembly loop is closed as two complementary Ω plasmids can be further combined back into α plasmids, allowing the virtually endless addition of TUs to the growing multigene construct (Figure 1). Compatibility of GB and FB with other Golden Gate-based collections is possible as they make use of a common syntax (Patron 2015) initially proposed in

plants and later expanded to other platforms like bacteria, yeast, filamentous fungi, diatoms, algae, cyanobacteria or amoeba (Bird et al., 2022).

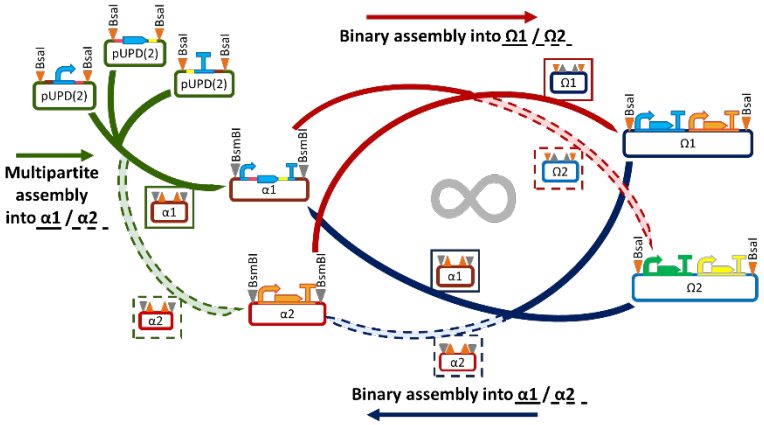

Figure 1. Schematic workflow of GoldenBraid and FungalBraid cloning system. Domesticated parts included in pUPD or pUPD2 entry vectors are assembled into pCAMBIA-based α vectors using BsaI to form Transcriptional Units (TUs), which are then combined in a binary way into pCAMBIA-based Ω vectors using BsmBI. Multigene constructs contained in two compatible Ω vectors can be assembled back into an α vector, which can be combined with a complementary α vector into Ω vector, allowing the endless addition of TU to the growing construct. Figure includes images created with Biorender (biorender.com).

2.2 CRISPR-based technologies are promising tools for the development of fine-tuned biofactories

Originally discovered as part of the adaptive immune system in bacteria, CRISPR/Cas ribonucleoproteins have been repurposed as genome editing tools by harnessing their remarkably accurate ability to target specific DNA sequences. The fast development of CRISPR-based technologies has provided powerful and versatile tools for efficient genome editing in many organisms, including plants and filamentous fungi (Liu et al., 2022; Shen et al., 2023; Zhang et al., 2019). Contrary to other genome-editing nucleases commonly applied like Transcription activator-like effectors (TALEs) or Zinc Fingers that require the re-design of their coding sequence to target different DNA sequences (Morbitzer et al., 2010; Urnov et al., 2010), the activity of Cas nucleases is directed by means of the guide RNA (gRNA) employed, which enhances their customizability and modularity. Moreover, CRISPR-based tools allow for the use of multiple gRNAs to modulate expression of one or various genes simultaneously.

The application of CRISPR-technologies has been further expanded to include gene regulation through the development of a nuclease-deficient Cas9 version (dCas9) that maintains the ability to bind to specific DNA sequences without cleaving them. This enables the regulation of gene expression in a very specific and efficient manner by fusing different transcriptional regulators to this dCas9 protein (Dominguez et al., 2016; Dong et al., 2018), offering novel insights into gene regulatory networks and interactions. CRISPR-based gene regulation, and more precisely CRISPR-based activation (CRISPRa) has been widely implemented in plants (Chavez et al., 2015; Z. Li et al., 2017; Lowder et al., 2018; Pan et al., 2021; Selma et al., 2019) and filamentous fungi (Mózsik et al., 2022; Roux et al., 2020; Schüller et al., 2020). Among the CRISPRa tools available in plants, dCasEV2.1 has excelled due to the strong activation and genome-wide specificity achieved with this tool (Selma et al., 2019). This system makes use of a dCas9 fusion and a modified RNA 2.1 scaffold with two extra aptamer loops that are recognized by the MS2 viral coat protein, thus adding a second anchor point for a transcription factor (Figure 2A). Regarding filamentous fungi, Mózsik et al (2020) reported a non-integrative expression system based on a pAMA1 vector for the expression of a dCas9:VPR fusion and the corresponding gRNA (pAMA18.X). Such non-integrative systems allow for the recycling of the parental strain as the plasmid can be cured in the absence of selection (Figure 2B).

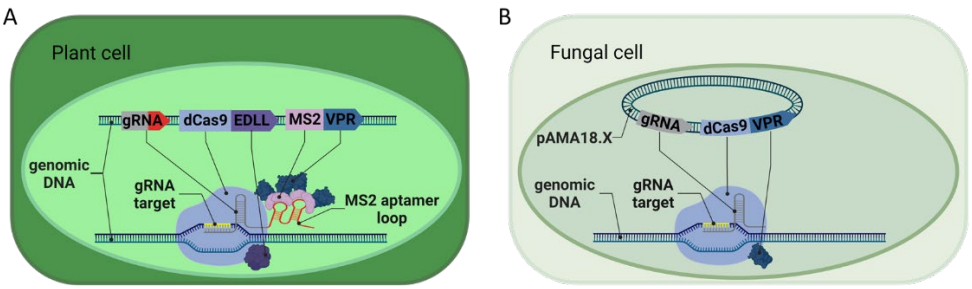

Figure 2. Overview of the CRISPRa tools dCasEV2.1 for plants (A) and pAMA18.X for filamentous fungi (B). The dCasEV2.1 system comprises the dCas9 protein fused to EDLL plant activation domain and the MS2 viral protein fused to the hybrid tri-partite transcriptional activator VP64-p65-Rta (VPR). The gRNA used in dCasEV2.1 includes MS2 aptamer loops to allow the interaction of both dCas9 and MS2 proteins. The pAMA18.X expresses the dCas9:VPR fusion protein and the gRNA in a non-integrative way to allow for the curation of the plasmid and the recycling of the transformed strains. Figure includes images created with Biorender (biorender.com).

3. Combining biofactories and synthetic biology for the sustainable production of insect pheromones

Pheromones are chemical signals that govern communication and coordination processes between individuals of the same species. Among the behaviors influenced by pheromones are mating, aggregation, territory marking and alarm responses. In the agricultural industry, pheromones are mainly applied for mating disruption strategies, followed by mass trapping, and detection and monitoring (Agricultural Pheromone Market report FBI100071, 2021). Mating disruption employs sex pheromones to prevent the identification of members of the opposite gender and subsequent mating, which leads to efficient reduction of pest populations, while preserving natural predators and pollinators (Figure 3A) (Benelli et al., 2019; Cardé and Minks, 1995; Stelinski et al., 2013). For this reason, the employment of pheromones is considered fundamental for the future of sustainable pest control in agriculture. Mating disruption strategies, however, require large amounts of pheromones to be emitted into the environment. Alternative strategies like mass trapping require lower amounts of pheromones (Figure 3B) (El-Sayed et al., 2009; Hossain et al., 2006; Villarreal et al., 2023) but are generally preferred for isolated pest populations and those with low density. Mass trapping is also employed for detection and monitoring, which is essential for the early tracking and removal of pests, and for analyzing population dynamics (Villarreal et al., 2023). Moreover, pheromones can also be employed to attract beneficial insects, such as pollinators or natural predators of pests to promote ecological balance in agricultural landscapes.

Pheromones are applied in the field by means of traps, sprays and dispensers, the latter being the most preferred for their efficient and cheap deployment in the field. Pheromone dispensers release pheromones directly into the environment to influence pest behavior and have been successfully implemented to manage various pests. In orchards, pheromone dispensers are used for controlling codling moths, oriental fruit moths, and apple clearwing moths, while in row crops, they are used to combat destructive pests like European corn borers and bollworms (Agricultural Pheromone Market report FBI100071, 2021). The concept of biodispenser arose from the possibility of using plants as pheromone-emitters for easier deployment and maintenance in comparison to traditional pheromone

dispensers (Bruce et al., 2015; Mateos-Fernández et al., 2021). Pheromone biodispensers are expected to work as passive dispensers for mating disruption, which would remove the need for any downstream processing as they will be intercropped with the plants to be protected (Figure 3C). Plants have already been applied for the emission of other volatiles either to attract predators of herbivore pests (Nishida, 2014; Wei et al., 2007) or to deter the pest itself (Bruce et al., 2015). These examples reinforce the viability of this application and future approaches will include the possibility of producing different pheromones simultaneously to both avoid pest settlement and to attract predators.

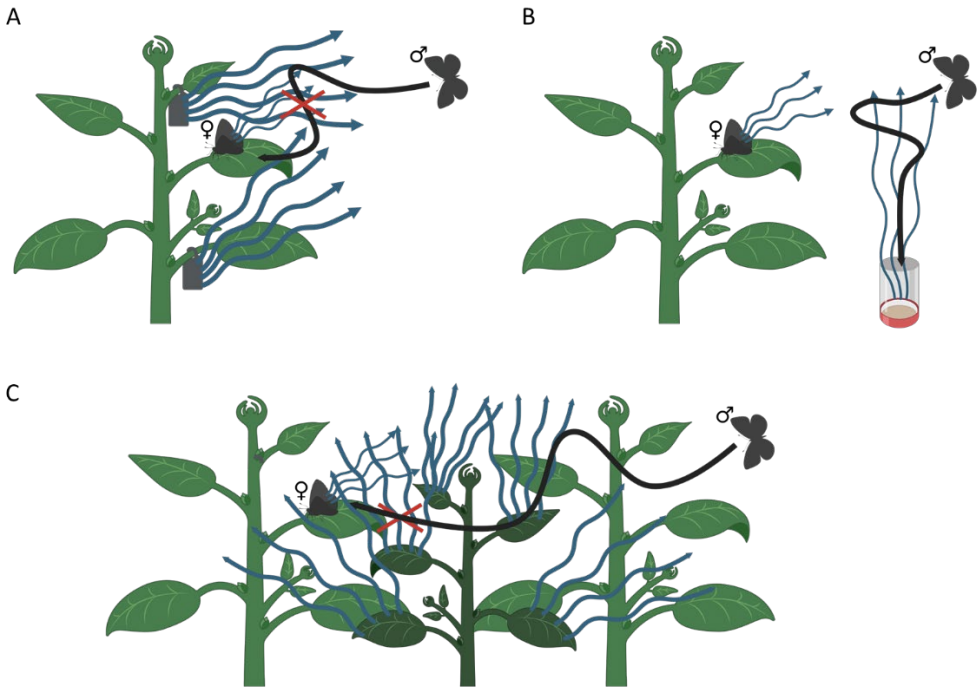

Figure 3. Pheromone-based strategies for pest control. (A) Mating disruption uses sex pheromones to impregnate the field and obstruct the male's orientation towards females, inhibiting mating. (B) Mass trapping employs traps and dispensers to direct and contain males, removing them from the population. (C) Plant Biodispensers envision the use of plants for mating disruption strategies by engineering them to produce and emit pheromones (dark green plant) so that crops (light green plants) can be easily protected by means of intercropping. Figure includes images created with Biorender (biorender.com).

The pheromone market, which is mainly dedicated to sex pheromone production (90%), is currently estimated in 3.7 billion USD and will likely reach 10 billion USD by 2029 (Agricultural Pheromone Market report FBI100071, 2021). However, the costly and laborious processes involved in the chemical synthesis for these molecules, which often involve the generation of toxic byproducts, greatly hamper market growth (Mori, 2010, 2007). Moreover, most pheromones have uncommon chemical structures, which makes their chemical synthesis unfeasible at an industrial scale (Villarreal et al., 2023). In this regard, biofactories offer several advantages, such as reduced environmental impact, stereospecificity, and the potential for tailored production of pheromone blends (Löfstedt and Xia, 2021; Petkevicius et al., 2020). The main biofactories that are currently studied for the production of pheromones include yeast (Hagström et al., 2013; Holkenbrink et al., 2020) and plants (Beale et al., 2006; Ding et al., 2014; Kappers et al., 2005; Nešněrová et al., 2004; Ortiz et al., 2020; Schnee et al., 2006; Xia et al., 2022, 2020). So far, focus has been placed mainly on the production of lepidopteran type I sex pheromones, which comprises C10-C18 mono/di-unsaturated acetates, alcohols or aldehydes. The biosynthesis of these pheromones generally starts from palmitic and stearic acid, produced by common fatty-acid biosynthesis. Although characterization of the key enzymes required for insect pheromones is limited, the biosynthesis of a vast amount of Type I pheromones can be explained using the "Delta 11 hypothesis" which involves a Δ11 desaturation in combination with chain-shortening/elongation step (Bjostad and Roelofs, 1984, 1983). Lepidopteran type I pheromones are widely applied in agriculture, and the first commercial biofactories are starting to emerge, such as the yeast-based production of field-tested moth pheromones by the BioPhero company (https://biophero.com). The oilseed plant *Camelina sativa* has also been postulated as an ideal platform in this regard (Iskandarov et al., 2014; Löfstedt and Xia, 2021; Ortiz et al., 2020; Wang et al., 2022) due to its relatively short lifecycle and the large number of tools available since it is closely related to *A. thaliana* and compatible with ATMT (Lu and Kang, 2008).

This thesis builds upon the idea of the bioproduction of insect pheromones in plant and fungal biofactories, focusing on the production of lepidopteran type I sex pheromones. For this, we have identified major drawbacks linked to constitutive pheromone production in plants, and developed synthetic biology

tools accordingly to maximize yields and better control the timing of the production. Future versions will include the use of an external agent to trigger the production and reduce any expected deleterious effects. Finally, these tools were also implemented and characterized in filamentous fungi, alongside with other promoters and selection markers, to further expand the toolkit available in this alternative production platform.

OBJECTIVES

OBJECTIVES

The main objective of this thesis is the engineering of metabolic pathways for the biosynthesis of Lepidoptera pheromones in plants and filamentous fungi by using synthetic biology.

To achieve this, the following specific objectives are proposed:

1. Analyze the performance of previously developed *N. benthamiana* transgenic plants that constitutively express a multigene pathway to produce the two lepidopteran pheromones *(Z)*-11-hexadecenol (Z11-16OH) and *(Z)*-11-hexadecenyl acetate (Z11-16OAc).

2. Design and validate synthetic regulatory elements based on the GoldenBraid and CRISPR-based activation technologies to enable the tunable and coordinated expression of multigene pathways in plants.

3. Apply the synthetic regulatory elements developed in objective 2 to establish a system for conditional production of pheromones and multigene pathways in plants.

4. Following the guidelines of the GoldenBraid and FungalBraid systems, design and characterize fungal promoters and adapt to filamentous fungi the synthetic inducible genetic constructs developed in plants for gene expression.

CHAPTER I

CHAPTER I

Production of volatile moth sex pheromones in transgenic Nicotiana benthamiana plants

Rubén Mateos-Fernández, **Elena Moreno-Giménez***, Silvia Gianoglio, Alfredo Quijano-Rubio, Jose Gavaldá-García, Lucía Estellés, Alba Rubert, José Luis Rambla, Marta Vazquez-Vilar, Estefanía Huet, Asunción Fernández-del-Carmen, Ana Espinosa-Ruiz, Mojca Juteršek, Sandra Vacas, Ismael Navarro, Vicente Navarro-Llopis, Jaime Primo, and Diego Orzáez.*

BioDesign Research, 2021. DOI: 10.34133/2021/9891082

*These authors contributed equally to this work.

My contribution to this work was essential for its publication. I contributed to most of the analyses performed for SxPv1.0 and the generation of SxPv1.1 and SxPv1.2. I also contributed significantly to manuscript writing. The entire manuscript is presented for clarity.

ABSTRACT

Plant-based bio-production of insect sex pheromones has been proposed as an innovative strategy to increase the sustainability of pest control in agriculture. Here, we describe the engineering of transgenic plants producing *(Z)*-11-hexadecenol (Z11-16OH) and *(Z)*-11-hexadecenyl acetate (Z11-16OAc), two main volatile components in many Lepidoptera sex pheromone blends. We assembled multigene DNA constructs encoding the pheromone biosynthetic pathway and stably transformed them into *Nicotiana benthamiana* plants. The constructs contained the *Amyelois transitella AtrΔ11* desaturase gene, the *Helicoverpa armigera* fatty acyl reductase *HarFAR* gene, and the *Euonymus alatus* diacylglycerol acetyltransferase *EaDAct* gene in different configurations. All the pheromone-producing plants showed dwarf phenotypes, the severity of which correlated with pheromone levels. All but one of the recovered lines produced high levels of Z11-16OH, but very low levels of Z11-16OAc, probably as a result of recurrent truncations at the level of the *EaDAct* gene. Only one plant line (SxPv1.2) was recovered that harbored an intact pheromone pathway and which produced moderate levels of Z11-16OAc (11.8 µg g^{-1} FW) and high levels of Z11-16OH (111.4 µg g^{-1}). Z11-16OAc production was accompanied in SxPv1.2 by a partial recovery of the dwarf phenotype. SxPv1.2 was used to estimate the rates of volatile pheromone release, which resulted in 8.48 ng g^{-1} FW per day for Z11-16OH and 9.44 ng g^{-1} FW per day for Z11-16OAc. Our results suggest that pheromone release acts as a limiting factor in pheromone bio-dispenser strategies and establish a roadmap for biotechnological improvements.

INTRODUCTION

Insect pheromones are a sustainable alternative to broad-spectrum pesticides in pest control. Different pheromone-based pest management approaches can be employed to contain herbivore populations, thus limiting damage to food, feed, industrial crops, and stored goods. These approaches include multiple strategies, such as: (i) attract-and-kill strategies, in which pheromones are used to lure insects into mass traps; (ii) push-pull strategies, in which different stimuli are used to divert herbivores from crops to alternative hosts; and (iii) mating disruption techniques in which mating is prevented or delayed by providing males with misleading pheromone cues (Alfaro et al., 2009; Cardé and Minks, 1995; Cook et al., 2007; Gregg et al., 2018). Broad-spectrum pesticides cause severe toxicity not only towards the targeted insect population, but also towards predatory insects resulting in substantial ecological imbalances (Witzgall et al., 2010). On the contrary, insect sex pheromones usually produced by females to attract males over long distances are highly species-specific and minimize environmental toxicity. Furthermore, pheromone-based pest control approaches are effective against pesticide-resistant insect populations and prevent the emergence of genetic pesticide resistance.

The global insect pheromone market was worth 1.9 billion USD in 2017, with projections reaching over 6 billion USD by 2025 (Agricultural Pheromone Market report FBI100071, 2021). Despite their biological potential and their value to farmers and the environment, their use suffers from some limitations: the chemical synthesis of insect sex pheromones can often be costly and complex and generate polluting by-products, which hamper their sustainability (Mori, 2010, 2007). The cost of chemically synthesized pheromones ranges from 500 to thousands USD kg^{-1}, making this solution profitable only for very high-value end products (Petkevicius et al., 2020). To make pheromone production more sustainable, engineered biological systems can be designed to function as pheromone biofactories from which the molecule(s) of interest can be purified to formulate conventional traps (Löfstedt and Xia, 2021). Ideally, live biodispensers can be envisioned, which directly release pheromones into the environment in an autonomous, self-sustained manner (Bruce et al., 2015).

Around 160,000 lepidopteran species and 700 lepidopteran pheromones are known (Ando, 2021; El-Sayed, 2021; Nieukerken et al., 2011). Many of these moths are relevant for agriculture and rely heavily on pheromones for mating. Lepidopteran sex pheromones have been the focus of many attempts at biotechnological production, because of their relatively simple chemical composition and their economic relevance. Sex pheromones emitted by female moths are composed of a discrete blend of volatile compounds, mostly C10-C18 straight chain primary alcohols, aldehydes, or acetates derived from palmitic and stearic acids (Löfstedt et al., 2016). Although hundreds of species share the same pheromone compounds, the components of the pheromone blend and their relative abundance constitute highly precise, species-specific cues for mating. The biosynthesis of many moth pheromones shares three fundamental steps, which follow fatty acid biosynthesis. Fatty acid desaturases (FADs) introduce double bonds at specific positions in the carbon chain (the most common in Lepidoptera are Δ9 and Δ11). Fatty acyl reductases (FARs) produce fatty alcohols, with different substrate specificities (some accept only a limited range of substrates, while others are more promiscuous). Finally, aldehydes and acetates can be obtained, respectively by oxidation and esterification of these fatty alcohols. In addition, other important modifications can occur before specification of terminal functional groups, especially chain elongation or shortening which, coupled with the desaturation steps, determine the structure of the carbon backbone (Löfstedt et al., 2016). The biosynthesis of the acetate esters is thought to be performed by acetyltransferases, although no insect acetyltransferases have been identified which work on fatty alcohols (Petkevicius et al., 2020). Acetyltransferases from other sources, like plants and yeasts, have nonetheless been discovered, which work efficiently on insect pheromone alcohols (Ding et al., 2016b).

Plants represent an alluring platform to produce moth sex pheromones: the scalability and relatively low costs and infrastructure requirements of plant biofactories make this system versatile and sustainable. In plants, photosynthesis provides the precursors to start fatty acid biosynthesis in the chloroplast. In a pioneering study, Nešněrová et al. (2004), took advantage for the first time of the plant fatty acid pool to produce lepidopteran pheromone precursors in plants. Later, in the most extensive screening of candidate genes so far, Ding et al. (2014) identified the most effective among 50 different gene combinations to produce

moth pheromones by transient expression in *N. benthamiana*. Subsequently, Xia et al. (2020) established stably transformed *N. benthamiana* and *N. tabacum* lines expressing precursors for the synthesis of a wide range of moth pheromones. However, to date, no stable transgenic plants have been reported producing the actual volatile pheromone components.

In this work, we aimed to test the ability of *N. benthamiana* plants to act as constitutive moth pheromone biofactories. *Nicotiana* species (*N. tabacum* and *N. benthamiana*) are ideal chassis for metabolic engineering, due to their large leaf biomass (especially for plastid-derived products) and amenability to genetic manipulation, both through stable transformation and agroinfiltration. For stable pheromone production, we selected three of the genes identified by Ding et al. (2014), namely the *Amyelois transitella AtrΔ11* desaturase, the *Helicoverpa armigera* reductase *HarFAR* and the plant diacylglycerol acetyltransferase *EaDAct* from the bush *Euonymus alatus*. The products of this pathway, *(Z)*-11-hexadecenol (Z11-16OH) and its ester *(Z)*-11-hexadecenyl acetate (Z11-16OAc), are components of the specific pheromone blends of almost 300 lepidopteran species. The generation of transgenic pheromone-producing plants (originally named as "Sexy Plants", SxP) turned out to be severely hampered by a strong growth penalty putatively imposed by the pheromone biosynthetic pathway. In the first round of attempts, only *N. benthamiana* plants accumulating the fatty alcohol were recovered, with all primary transformants showing dwarf phenotypes to different degrees. These transgenic lines were later shown to carry a truncated version of the *EaDAct* gene. This discovery led to the generation of new transformants, with new strategies aimed at ensuring the integrity of the construct that finally yielded a single transgenic line accumulating both the alcohol and the acetate components at relatively high levels, while maintaining acceptable levels of fertility and biomass production. This single line allowed us to gain insights into the challenges associated with fatty-acid derived pheromone production in plants, such as yield-associated growth penalties, changes in volatile profile, and compound volatility.

RESULTS

Assembly of the metabolic pathway

To assess plant-based production of the target moth sex pheromone compounds (Z11-16OH and Z11-16OAc), a T-DNA construct encoding the three biosynthetic genes, each under the control of the constitutive CaMV35S promoter, was agroinfiltrated in plant leaves after being mixed in a 1:1 ratio with an *Agrobacterium* culture carrying the P19 silencing suppressor (Zheng et al., 2009) (Figure 1A). The total volatile organic compound (VOC) composition was analyzed at 5 days post infiltration by gas chromatography/mass spectrometry (GC/MS). GC peaks corresponding to the pheromone compounds Z11-16OH and Z11-16OAc were detected in samples transformed with all three enzymes, but not with P19 alone (Figure 1B). Moreover, both substances were among the most predominant compounds in the leaf volatile profile, indicating that the transgenes were expressed at high levels. Interestingly, a small peak identified as *(Z)*-11-hexadecenal (Z11-16Ald) was also detected in the agroinfiltrated samples, likely due to the endogenous activity of alcohol oxidases, as previously suggested by Hagström et al. (2013). This aldehyde is itself a component of the pheromone blends of around 200 lepidopteran species. Based on these results, a multigene construct (GB1491) for stable transformation of *N. benthamiana* plants was assembled. This construct comprised the three constitutively expressed enzymes, the kanamycin resistance gene *NptII* and the visual selection marker *DsRed* (Figure 1C). Plants resulting from this transformation were denoted as the first version of the pheromone-producing plant (SxPv1.0).

SxPv1.0 stable transformants

The transformation of *N. benthamiana* with the GB1491 construct resulted in the selection of 11 kanamycin-resistant shoots, which also showed red fluorescence resulting from the expression of *DsRed* (T_0 generation SxPv1.0 plants). These shoots were further grown and rooted, and leaf samples were collected at the early flowering stage to assess pheromone production. As observed in Figure 1D, several T_0 plants presented detectable levels of all three pheromone compounds in variable amounts. The relative abundance of all three pheromone compounds was consistent in each plant, despite Z11-16OAc levels being much lower than

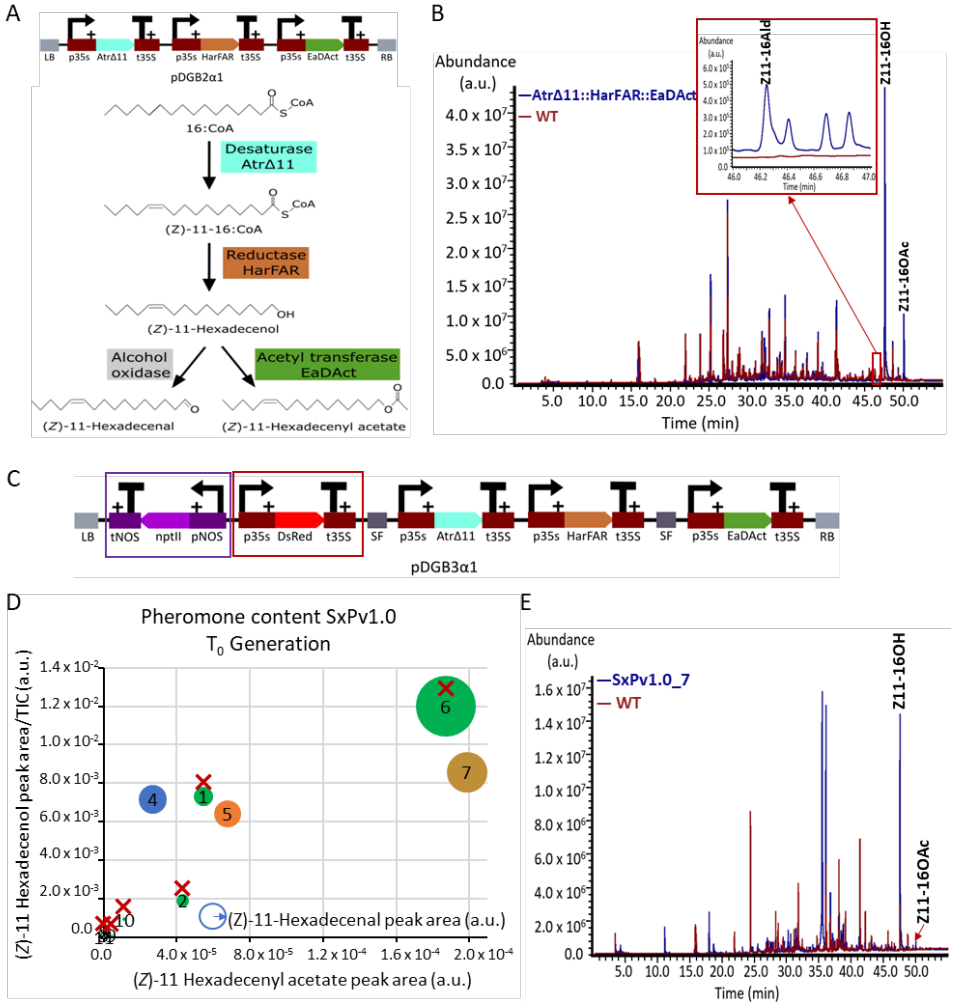

Figure 1. Stable and Transient expression in *Nicotiana benthamiana* of the synthetic moth pheromone pathway. (A) Schematic view of the T-DNA construct used for transient expression, carrying the three transgenes *AtrΔ11*, *HarFAR* and *EaDAct*, each under the control of the constitutive CaMV35S promoter and terminator, and the biosynthetic route of the moth pheromones. (B) GC/MS analysis of the volatile profile of *N. benthamiana* transiently expressing the transgenes (blue line) and a mock infiltrated plant with only P19 (red line). Peaks corresponding to the target insect pheromones are indicated with a label. Highlighted in red is the region of the (*Z*)-11-hexadecenal peak. (C) Schematic view of the T-DNA construct for the SxPv1.0 encoding the three transgenes and two selection markers. The two selection markers DsRed and NptII are highlighted in red and purple, respectively. (D) Pheromone content in SxPv1.0 T_0 plants (numbered from 1 to 11). The diameter of each dot corresponds to the (*Z*)-11-hexadecenal level of each sample. Plants marked with a red cross died before seeds could be collected. (E) Overlapped chromatograms showing the volatile profile of a representative SxPv1.0 T_0 plant (blue line) and a WT plant (red line).

expected in all cases compared to transient pheromone expression. Furthermore, although phenotypic evaluation of *N. benthamiana* T_0 lines is generally cumbersome due to the influence of *in vitro* culture, severe growth penalties were observed in these plants, and only 5 out of 11 plants (SxPv1.0_4, 5, 7, 8, and 9) survived long enough to produce seeds.

To further understand the phenotypic effects of pheromone production, the progeny of plants SxPv1.0_4, SxPv1.0_5 and SxPv1.0_7 was analyzed up to the T_3 generation and the plant size and pheromone production levels were recorded for each individual. In the T_1 generation, growth penalties were also observed in most descendants for all three lines, generally associated with high pheromone production (Figure 2A and 2B, left plot). Several plants could not be phenotyped, as they died soon after germination. Those producing enough seeds were brought to T_2, where a similar trend was also observed (Figure 2B, central panel). A few T_2 plants clearly separated from the rest in terms of high Z11-16OH production, which was again associated with small size and reduced fertility. Neither T_1 or T_2 plants showed signs of recovery in Z11-16OAc levels, although the corresponding GC/MS peak remained detectable in Z11-16OAc levels, although the corresponding GC/MS peak remained detectable and above the wild type (WT) baseline (not shown). At this stage, we decided to re-evaluate the integrity of the T-DNA in T_2 plants, finding that DNA rearrangements had occurred in all three lines in the *EaDAct* coding sequence, resulting in a truncated gene. Rearrangements and truncations of the T-DNA are not uncommon events in stable plant transformation (Bartlett et al., 2014; Forsbach et al., 2003). Interestingly, at least two independent truncation events could be inferred from PCR analysis of gDNA and cDNA samples. In SxPv1.0_7_4 plants, the presence of a ~700bp insertion of a DNA fragment of plasmid origin could be identified at the 3´ end of the *EaDAct* coding sequence. In contrast, the same 700bp genomic PCR fragment could not be recovered from the offspring of SxPv1.0_4_2, SxPv1.0_5_1 and SxPv1.0_5_2 plants, which nevertheless also had a truncated ORF, as evidenced by PCR analysis of cDNA samples (Figure S2). Despite the detection of a T-DNA truncation, the analysis of the SxPv1.0 offspring was continued up to T_3 (Figure 2B, right plot), where a sharp separation between low and high producers was consolidated. Interestingly, the offspring from the SxPv1.0_5_1_7 homozygous line (100% kanamycin resistant) comprised only high producer plants, whereas heterozygous

lines as SxPv1.0_4_2_2 or SxPv1.0_7_4_3 segregated in high and low producers, these correlating with small and large sized individuals, respectively. This observation strongly indicates a drastic effect of transgene copy number on both growth and pheromone production.

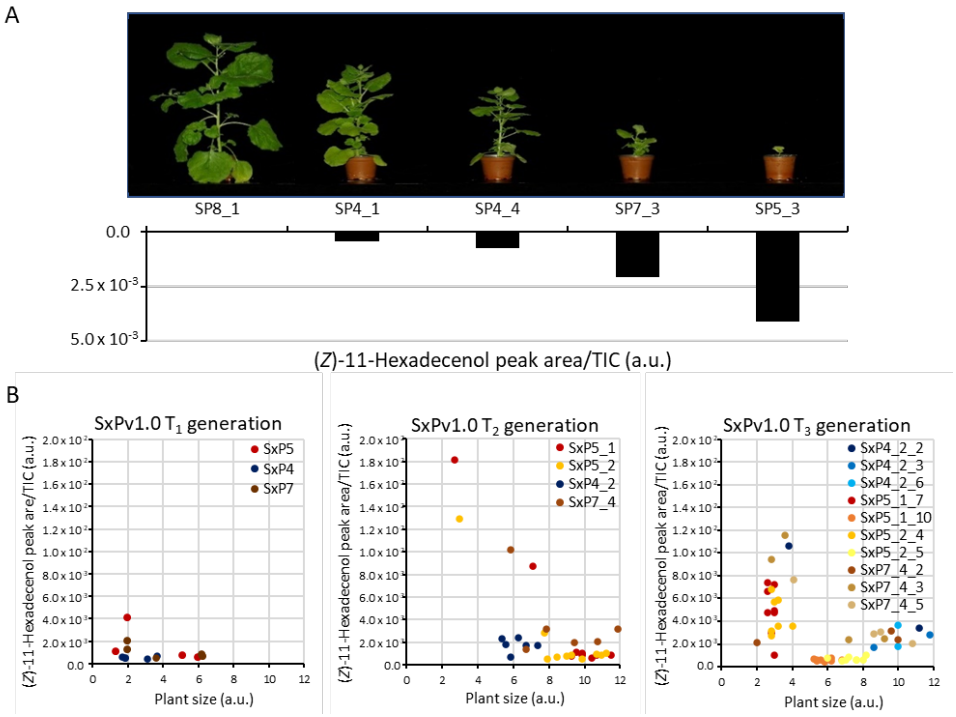

Figure 2. Growth penalty linked to pheromone production in SxPv1.0 plants. (A) Representative SxPv1.0 T_1 plants with their corresponding (*Z*)-11-hexadecenol levels. (B) Correlation between (*Z*)-11-hexadecenol content (arbitrary units, a.u.) and plant size (a.u.) in all three generations of SxPv1.0.

New stable transgenic versions SxPv1.1 and SxPv1.2

The presence of at least two independent truncation events affecting *EaDAct* prompted us to design new transformation strategies by placing a selection marker adjacent to the *EaDAct* gene, ensuring its integrity. Two new DNA constructs were assembled (SxPv1.1 and SxPv1.2) carrying *DsRed* and *NptII* at different relative positions of the T-DNA, as depicted in Figure 3A, B. Five SxPv1.1 and eight SxPv1.2 kanamycin resistant T_0 plants were recovered from each transformation, many of them showing detectable red fluorescence, but

unfortunately all but one failed to produce detectable levels of pheromones. The only exception corresponded to plant SxPv1.2_4, which showed Z11-16OH and Z11-16Ald amounts comparable to the SxPv1.0 plants, but also Z11-16OAc levels close to those measured in transient experiments (Figure 3C, D). SxPv1.2_4 presented premature flowering, a feature that is not unusual in T_0 *N. benthamiana* plants, and produced viable seeds, giving us the opportunity to further investigate the phenotype of stable Z11-16OAc producers.

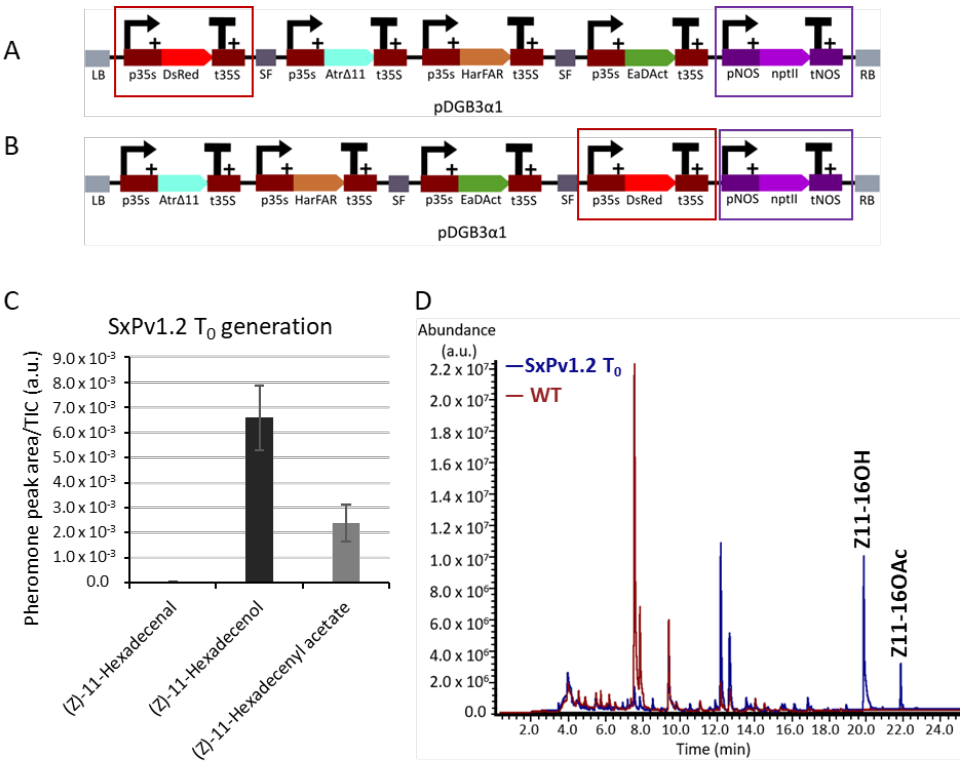

Figure 3. SxP version 1.1 and 1.2 stable plants. (A) Schematic representation of the T-DNA construct employed for stable transgenic SxPv1.1. The two selection markers *DsRed* and *NptII* are highlighted in red and purple, respectively. (B) Schematic representation of the T-DNA construct employed for stable transgenic v1.2. The two selection markers *DsRed* and *NptII* are highlighted in red and purple, respectively. (C) Pheromone content in the surviving SxPv1.2 T_0 plant. Error bars represent the average ± SE of 3 independent replicates. (D) Overlapped chromatograms showing the volatile profile of a SxPv1.2 T_0 plant (blue line) and a WT *Nicotiana benthamiana* (red line).

For a deeper understanding of the effect of fatty-acid-derived pheromone production in plant homeostasis, a comparative study between the progeny of the T_2 SxPv1.0_5_1_7 homozygous line and the T_0 SxPv1.2_4 line was performed. All analyzed SxPv1.2 T_1 plants (>50) were kanamycin resistant, indicating multiple copy insertions. The relative levels of all three pheromone compounds in leaves at two different developmental stages (young and adult) were recorded for twelve T_1 plants per genotype. Similarly, pheromone content in roots was also measured at the adult stage. Plant size was recorded for all analyzed individuals. As expected, all transgenic plants produced detectable levels of both pheromones, but only in the case of SxPv1.2, Z11-16OAc and Z11-16OH accumulated at similar levels. In all the SxPv1.2 samples, the higher Z11-16OAc accumulation seems to result in lower precursor alcohol levels, compared with equivalent SxPv1.0 samples. Both insect pheromones are produced at higher levels in adult plant leaves (Figure 4B) when compared with young plant leaves (Figure 4A) and roots (Figure 4C). All pheromone-producing plants showed considerably reduced plant size, however the growth penalty was significantly more pronounced in plants accumulating mainly Z11-16OH, whereas the conversion into the acetate form in SxPv1.2 seems to partially relieve the dwarf phenotype. Interestingly, both SxPv1.0 and SxPv1.2 plants showed similar morphology, with short petioles curved upwards and resulting in a compact “cabbage-like” characteristic shape (Figure 4D). Both SxP lines showed early senescence symptoms, with premature and progressive yellowing, which led, in the case of SxPv1.0, to the premature death of the plants soon after the fruits set.

The plant volatilome is affected by pheromone production.

A non-targeted analysis of the plant volatile profiles was undertaken to understand the influence of the engineered pheromone pathway on the volatilome. The analysis included leaf samples of 12 young and 12 adult plants from the progeny of SxPv1.0 5_1_7, SxPv1.2_4 and the wild type. The Principal Component Analysis score plot based on the volatile profile showed clustering of the samples based on the different sample classes (Figure 5A). The first component accounted mainly for differences in leaf age, whereas the second principal component separated samples according to their genotype. Remarkably, SxPv1.2 samples have, according to both components, intermediate characteristics between the WT and SxPv1.0. The greater separation of SxPv1.0

and the WT probably reflects the more deleterious phenotypic effects experienced by lines accumulating higher Z11-16OH levels.

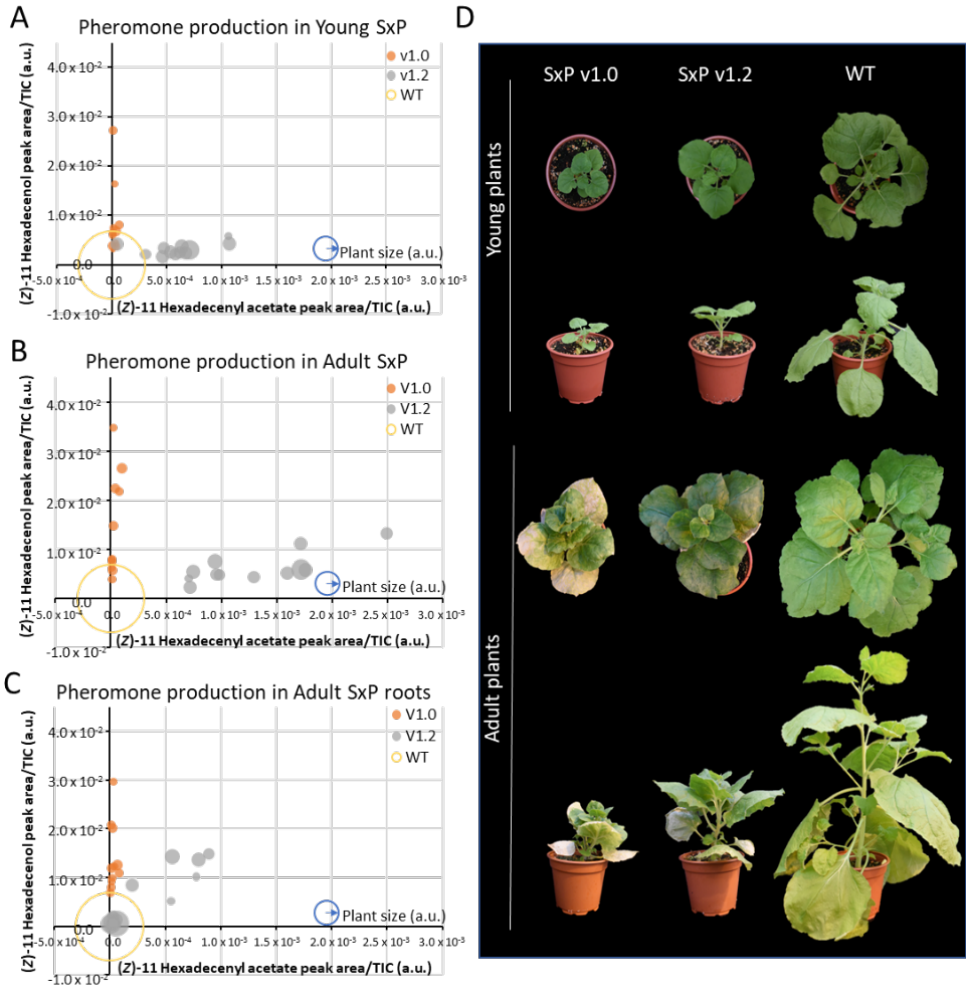

Figure 4. Comparative study between SxPv1.0 T_3 and SxPv1.2 T_1 plants. (A) Pheromone content in leaf samples from young plants of WT, SxPv1.0 and SxPv1.2 lines. (B) pheromone content in leaf samples from adult plants of WT, SxPv1.0 and SxPv1.2 lines. (C) pheromone content in root samples from adult plants of WT, SxPv1.0 and SxPv1.2 lines. The diameter of each dot corresponds to the plant size of each sample. Empty circles correspond to WT plants. (D) Comparative physiological development between SxPv1.0 5_1_7_X (T_3), SxPv1.2 4_X (T_1) and WT *Nicotiana benthamiana* plants at the young and adult stage. Pictures were taken from representative individuals at young (4 weeks after transplant) and adult (7 weeks after transplant) stages.

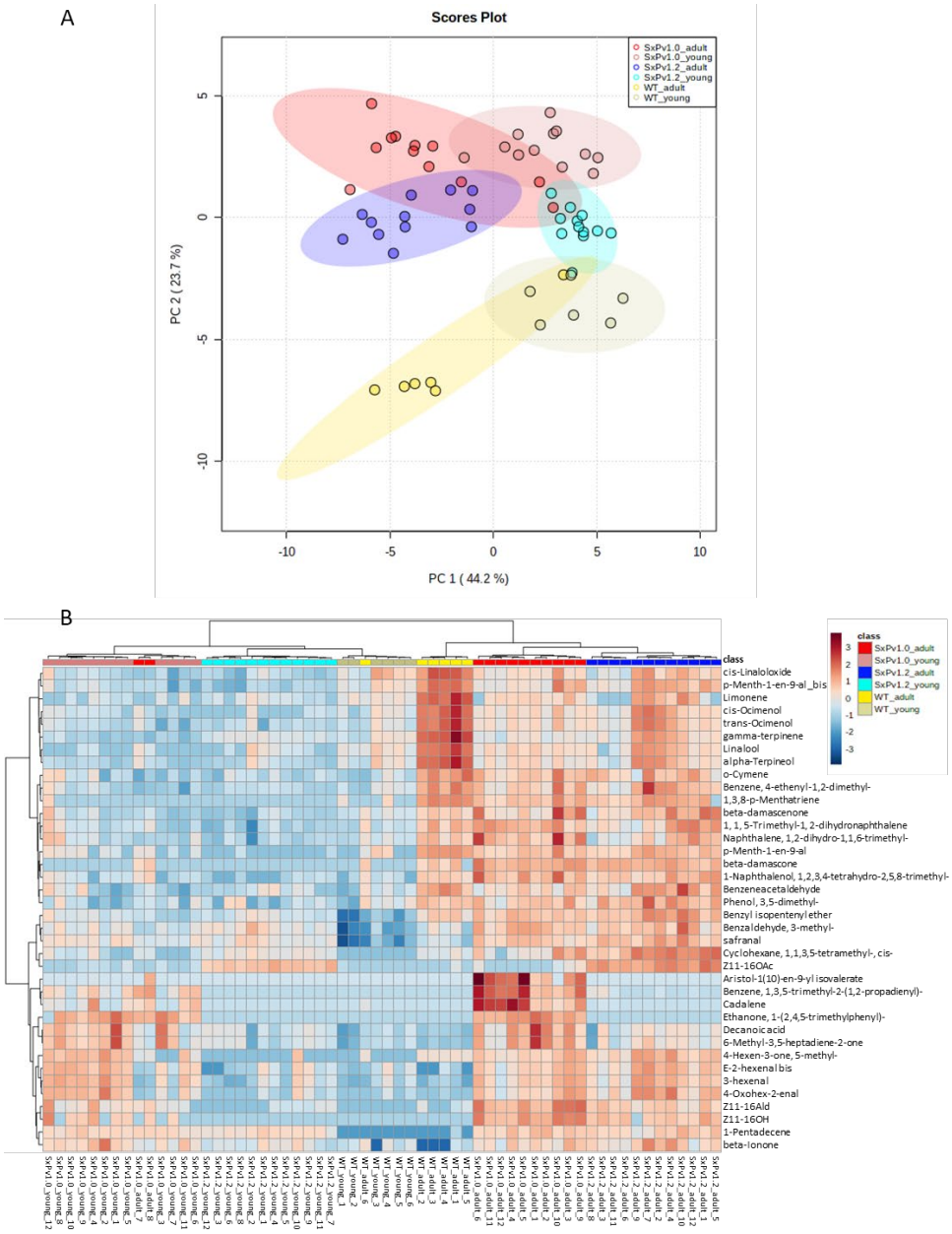

Figure 5. Untargeted analysis of the volatilome of SxPv1.0 and SxPv1.2, and of WT *N. benthamiana*. (A) Principal Component Analysis and (B) Hierarchical clustering and heatmap representation (obtained using Ward's minimum variance method and Euclidean distance) of the composition of the volatilome of SxPv1.0, SxPv1.2 and wild type *N. benthamiana* leaves. Twelve individuals for each SxP genotype and six WT plants were analyzed at two developmental stages, young (4 weeks old) and adult (7 weeks old).

A clustered heatmap provides interesting visual information on the volatile leaf profiles of SxP plants (Figure 5B). The clustering reproduces with few exceptions the different classes, indicating that each genotype and each developmental stage produces a differential and characteristic blend of VOCs. In addition to the pheromone compounds themselves, which are clearly clustered in their respective groups, all SxP plants differentially accumulate other fatty-acid-derived volatile compounds (e.g. (*E*)-2-hexenal, 1-pentadecene), indicating a general activation of this metabolic pathway. Some compounds are characteristic of the adult stage, independently of the genotype. This is the case for some apocarotenoids, such as β-damascenone and β-damascone, and some phenylalanine-derived compounds, such as o-cymene and phenylacetaldehyde. Other VOCs, such as monoterpenoids (α-terpineol, linalool, limonene and ocimenol), are markedly more abundant in WT than in SxP leaf tissues, with a gradient in which SxPv1.2 shows intermediate features between the wild type and the SxPv1.0 genotype. On the other hand, SxPv1.0 plants display a specific subset of volatile compounds (including the sesquiterpene cadalene) that accumulate at increasing levels at the adult stage. Z11-16Ald is detectable in both SxPv1.0 and SxPv1.2, although its levels are higher especially in leaves from adult SxPv1.0 plants, correlating with higher Z11-16OH production. In SxPv1.2 plants, in which Z11-16OH is partially converted to Z11-16OAc, Z11-16Ald is present at lower levels. Z11-16OAc is, instead, clearly restricted to SxPv1.2. The levels of all three pheromones increase with plant age.

Pheromone identification and determination of its biological activity.

Samples of Z11-16OH, Z11-16OAc and Z11-16Ald were synthesized and characterized by GC/MS and nuclear magnetic resonance (NMR) to have analytical standards of the biosynthetic targets. Additionally, to provide unequivocal identification of the plant-made compound, hexane extracts of 120 g of SxPv1.2 leaves were purified by gravity column chromatography after solvent evaporation, and a 2-mg sample of the purest fractions of the biosynthesized alcohol (Z11-16OH) was also analyzed using NMR. The purity assigned by GC/MS was ca. 78 % (Figure S3), and the data extracted from the main signals of both ^{1}H and ^{13}C NMR spectra were fully consistent with those obtained for the synthetic sample of Z11-16OH, confirming the structure and the cis-configuration of the double bond (Figures S4-S5). Further confirmation of the biological activity was provided by

electrophysiological analysis. Hexane extracts of SxPv1.2 leaves were fractionated by column chromatography and the fractions were analyzed by GC/MS. Those fractions that mainly contained Z11-16OH were gathered and employed in electroantennography (EAG) assays with *Sesamia nonagrioides* male moths. The plant-made pheromone was active, since the EAG probe registered significant antennal depolarizations when Z11-16OH reached the antennal preparations (Figure 6; retention time 15.89 min). An unidentified compound with a retention time of 15.54 min also elicited an intense response of the antennae, but did not correspond neither to Z11-16Ald nor to Z11-16OAc.

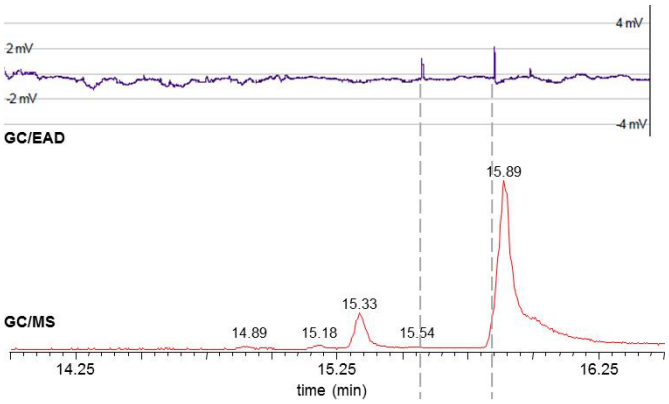

Figure 6. Electrophysiological activity. GC/MS chromatogram and EAD recording showing *Sesamia nonagrioides* male antenna response to the biosynthetic Z11-16OH (retention time = 15.89 min). Other compounds contained in the tested fraction were able to interact with the antennal receptors and triggered antennal responses (e.g. retention time 15.54). The GC/MS-EAD run was performed in a GC column ZB-5MS fused silica capillary column (30 m × 0.25 mm i.d. × 0.25 µm; Phenomenex Inc., Torrance, CA).

Quantification of total pheromone content and release.

The total pheromone content and the rate of volatile emission were both quantified in SxPv1.2 plants. Solvent extraction was carried out in fresh leaves, as well as in leaves stored at -20°C and -80°C to evaluate the total content and the possible loss of pheromone under different storage conditions (Table 1). The Z11-16OH content in leaves was found to be in the range of 0.1 mg g^{-1}, (average 111.4 ± 13.7 µg g^{-1}), whereas Z11-16OAc accumulated at lower levels (average 11.8 ± 1.3 µg g^{-1}). Both pheromones were preserved in frozen leaves, although a part of Z11-16OH could be lost upon storage, although more data will be needed to ensure the actual effect of plant handling and storage temperature. Interestingly, the

unbalanced ratio between the two main compounds was compensated when the rate at which pheromones are released to the environment was estimated. As shown in Table 2, an adult SxPv1.2 plant releases on average 79.3 ± 6.3 ng of Z11-16OH and 88.3 ± 11.5 ng of Z11-16OAc per day, as estimated in volatile collection experiments carried out in dynamic conditions. Not unexpectedly, this indicates a much higher volatility of the acetylated moiety. In terms of pheromone release per biomass unit, both compounds are emitted at levels close to 0.01 µg day^{-1} g^{-1} (FW).

Table 1. Quantity (µg) of (*Z*)-11-hexadecenol (OH) and (*Z*)-11-hexadecenyl acetate (OAc) extracted from SxPv1.2 individuals by solvent extraction and GC/MS/MS quantification.

plant	material	µg OH/g plant	µg OAc/g plant
SxPv1.2 T_1-3	fresh leaves	164,9	9,6
SxPv1.2 T_1-4	fresh leaves	129,9	8,6
SxPv1.2 T_1-5	frozen -20C	78,1	10,5
SxPv1.2 T_1-6	frozen -20C	115,1	17,3
SxPv1.2 T_1-7	frozen -80C	75,8	11,8
SxPv1.2 T_1-8	frozen -80C	104,8	12,9
	mean ± se	**111.4 ± 13.7**	**11.8 ± 1.3**

Table 2. Quantity (ng) of (*Z*)-11-hexadecenol (OH) and (*Z*)-11-hexadecenyl acetate (OAc) released by SxPv1.2 individuals obtained by volatile collection and GC/MS/MS quantification.

plant	ng collected OH	ng OH/day	ng collected OAc	ng OAc/day
SxPv1.2 T_1-1	209,3	69,8	193,3	64,4
SxPv1.2 T_1-2	225,6	75,2	359,4	119,8
SxPv1.2 T_1-3	222,6	74,2	250,7	83,6
SxPv1.2 T_1-4	293,9	98,0	256,8	85,6
mean ± se	**237.8 ± 19.0**	**79.3 ± 6.3**	**265.0 ± 34.6**	**88.3 ± 11.5**

DISCUSSION

This research was initiated as a synthetic biology project in the frame of the iGEM competition, where undergraduate students proposed the use of genetically engineered plants as dispensers of insect sex pheromones. The manufacturing of pheromones and their precursors employing biological factories, such as microbial bioreactors or plant biofactories (Ding et al., 2014; Ortiz et al., 2020; Xia et al., 2020) has become an intensively pursued objective, fueled by the expected gains in sustainability. Beyond the general biofactory concept, our envisioned long-term approach consists of the design of plants that function as autonomous bio-dispensers of semiochemicals. A remarkable precedent of this concept was the engineering of wheat plants releasing the alarm pheromone *(E)*-β-farnesene as a protective strategy against aphid infestation (Bruce et al., 2015). Differently to the alarm pheromone concept, which was produced in the crop itself, the proposed bio-dispenser (originally named as "Sexy Plant", SxP) is based on the intercropping strategy, where a companion crop, rather than the main crop, is engineered to emit the sex pheromone into the environment. From here, two different strategies can be followed. In a mating disruption strategy (Benelli et al., 2019; Cardé and Minks, 1995; Stelinski et al., 2013), the dispensers release pheromones at relatively large quantities, impairing the male's ability to detect females and therefore disrupting the mating. Oppositely, in mass trapping or attract-and-kill strategies (Hossain et al., 2006), dispensers release pheromones to attract males to traps. This later approach often requires lower pheromone levels to be released into the environment, but in turn requires higher semiochemical specificity (in terms of isomeric purity and exact ratios of the pheromone components), and also some associated equipment to trap and eventually kill the attracted insects.

The genetic engineering of *N. benthamiana* shown here was inspired by the seminal work of Ding et al. (2014), where transient expression of various components of moth sex pheromone blends was achieved. Contrary to other insect pests, whose sex pheromones are made of a single, highly specific molecule, as with some mealybugs (Zou and Millar, 2015), lepidopteran sex pheromones are often made of more complex blends of fatty-acid derived compounds, many of them shared by several species. Species-specificity in these cases is provided by the precise ratio in the blend. For instance, Krokos et al. (2002) tested the response of *Sesamia nonagrioides* (Lefèbvre) males to different blends of

pheromone compounds, identifying a 90:10:5 blend of Z11-16OAc:Z11-16OH:Z11-16Ald as the most effective. This feature makes the genetic design of plant emitters for attract-and-kill strategies in moths extremely challenging, because ensuring the right proportions of the three compounds requires a tight control of several factors, from gene expression to enzymatic activity and differential release ratios. Conversely, mating disruption seems a more attainable objective in terms of heterologous pheromone production since, in many cases, the release of non-attractive incomplete mixtures can disrupt mating as effectively as the complete blend (Evenden, 2016). In this case however, the main requirement imposed on a biological dispenser is to produce and release sufficient quantities of one or more compounds in the blend. Therefore, the main objective of this work was to understand the biological constraints accompanying the production and release of two of the most representative compounds of lepidopteran pheromone blends in *N. benthamiana* plants. We successfully generated a first generation of transgenic plants (SxPv1.0) producing mainly Z11-16OH. Homozygous SxPv1.0 lines maintained pheromone production up to the T_3 generation. It should also be noted that basal levels of Z11-16Ald and Z11-16OAc were detected in SxPv1.0, probably produced by endogenous enzymes, since no oxidase was included in this first version of the pathway, and the third enzyme of the route, *EaDAct*, was truncated. The disruption of the *EaDAct* gene in different transgenic lines may be explained by a tendency to recombine with plasmid DNA in the bacterial host. This seems to be the case based on the observation that a small fragment of plasmid origin was found interrupting the coding sequence in the truncated construct. In addition, the distal position of *EaDAct* with respect to the selection marker in SxPv1.0 could have made it more likely that rearrangements in this gene went unnoticed, as they did not affect regeneration on selective media. Although a relatively lower number of regenerants was obtained for SxPv1.1 and SxPv1.2 (8 and 5, respectively), compared to SxPv1.0 (11), this difference is most likely due to contingent factors such as chance, contamination, and even limited access to experimental facilities during the Covid-19 pandemic. The recovery of a single plant producing a blend of Z11-16OH and Z11-16OAc may have been aided by closely linking the previously truncated gene with selection markers to increase the probability of associating positive selection with an intact *EaDAct* gene. With the only exception of the above mentioned SxPv1.2 plant, all SxPv1.1 and SxPv1.2 recovered plants effectively integrated the intact construct, but failed to produce

measurable levels of pheromone compounds, probably due to silencing or positional effects. This seems to indicate that only certain levels/ratios of the two compounds are compatible with viable plant regeneration and biomass accumulation. Pheromone production in this new single line (now in the T_2 generation) is also very stable and maintains remarkably homogeneous levels of production. The establishment of SxPv1.0 and SxPv1.2 stable plants has allowed us to study in detail the production levels of the different pheromone components, their relative abundance, and their volatility, together with an in-depth characterization of the accompanying phenotype.

As results of our analysis, two main bottlenecks were identified: the associated growth penalty and the poor release rates of the pheromones to the environment. As highlighted also by Reynolds et al. (2017) and later by Xia et al. (2020), one of the most significant downsides to the constitutive overexpression of medium-chain fatty acid biosynthesis pathways in plants is the associated developmental abnormalities. These may result from an imbalance caused by diverting metabolic resources from fatty acid metabolism towards the products of interest, and possibly from the toxicity of the end-products. Such toxic effects can hamper plant viability and result in a negative selection pressure against the genotypes with higher pheromone production levels. Interestingly, whereas Xia et al. (2020) found strong deleterious effects associated with the production of *(E)*-11-tetradecenoic acid, the same authors regenerated normal plants that accumulated Z11-16CoA, the direct precursor of the volatile pheromones produced here. The fact that the simple addition of a desaturase activity leads to deleterious effects may indicate that Z11-16OH itself is responsible for the toxic effects observed when accumulated in leaves. Furthermore, this toxicity seems partially alleviated when a fraction of Z11-16OH is converted to Z11-16OAc, leading to higher biomass in the case of SxPv1.2.

Understanding the changes imposed on the leaf volatilome can shed light on the associated phenotypic changes and the possible imbalances produced by the introduction of the recombinant pheromone pathway. We show here that each SxP version has a distinctive volatile profile, that differs from wild type plants primarily by the presence of the pheromones themselves and a few related fatty-acid derived compounds, which apparently result from endogenous enzyme activities operating on new-to-plant molecules. This seems to be the case for Z11-

16Ald (itself a common component of moth pheromone blends), and also for the differential accumulation of other shorter chain fatty acid derivatives such as 1-pentadecene and hexenal. A close look at the clustered analysis shows that wild type adult *N. benthamiana* tends to produce more monoterpenes (e.g. linalool) and phenolic VOCs (e.g. phenylalanine derivatives) than younger plants. However, this tendency is reduced in SxP plants in general and is even more severe in SxPv1.0 plants. The observed downregulation of the normal volatile components in adult plants could reflect a reduced ability to set up defense mechanisms. The fact that *N. benthamiana* is considered as a generally immune-suppressed species (Bally et al., 2015; Goodin et al., 2008), could explain the premature senescence and the early collapse observed in many SxPv1.0 soon after flowering. The reasons behind the changes in the volatile profiles of the different plant lines may depend on a general reduction of plant fitness imposed by the expression of the heterologous pathway or may be due to specific changes affecting development and regulatory mechanisms. Insight into these imbalances may be fruitfully gained by transcriptomic analysis of the different genotypes. A strategy to alleviate deleterious effects would require disconnecting plant growth from pheromone production. This could be done by employing agronomically-compatible inducible expression systems for the activation of the pathway, taking advantage of the increasing number of Synthetic Biology tools made available for plants and particularly for *Nicotiana* species (Bernabé-Orts et al., 2020; Cai et al., 2020b; Molina-Hidalgo et al., 2020). Alternatively, the use of a different plant chassis displaying specialized structures, such as glandular trichomes to store potentially toxic pheromone compounds could be advantageous. Glandular trichomes serve as natural biofactories for VOC biosynthesis and release, e.g. in aromatic plant species (Huchelmann et al., 2017). A suggested roadmap showing the subsequent SxP version and the improvements they should incorporate in light of the problems encountered in SxPv1 is presented in Figure 7.

The quantification of pheromone tissue accumulation and environmental release in SxPv1.2 leads to interesting considerations. The maximum pheromone accumulation levels measured in SxPv1.2 reached 174.5 µg g^{-1} FW (totaling both alcohol and acetate forms). This is about half of the levels of the precursors reported by Ding et al. (2014) in transient experiments (381 µg g^{-1}) or by Xia et al. (2020) in stable plants (335 µg g^{-1}) and may indicate a partial conversion into

biologically active forms, or an upper limit for toxicity, especially in the case of Z11-16OH. However, only a small portion of the plant pheromone content can be detected in the environment after a 72h incubation. Typically, mating disruption strategies require daily release rates between 20 and 500 mg Ha^{-1} day^{-1} (Alfaro et al., 2009; Gavara et al., 2020). Our data indicates that the maximum release rates per biomass unit are around 20 µg Kg $plant^{-1}$ day^{-1}, therefore it would require between 1,000 Kg and 25,000 Kg of pheromone-producing intercropping biomass per Ha for effective mate disruption. This is obviously not viable for dwarf SxPv1.2 plants, whose average fresh weight is 9.35 g (aerial parts), and it would be still challenging even if plant species with large biomasses are used as bio-emitters. Therefore, it is concluded that the improvement in the release rates is an important objective to focus on. In leaves, VOCs are synthesized in mesophyll cells and release takes place through the stomata or cuticle (Loreto and Schnitzler, 2010). Emission rates of endogenous VOCs are highly variable and depend on the chemical properties of each molecule. Furthermore, volatility is temperature-dependent, with higher temperatures leading to a more rapid transition from the liquid to the gas phase (Mofikoya et al., 2019 and references therein). C16 fatty acid derivatives are indeed semi-volatile compounds and, in the absence of specialized structures (like the glandular trichomes described above), active transport may play an important role in their release from mesophyll cells. Active transporters of the adenosine triphosphate-binding cassette (ABC) class are known to be required for the release of at least some volatile components of flower scent in petunia (Adebesin et al., 2017). Pheromone binding proteins (PBPs) play important roles in binding pheromones and bringing them in contact with receptor complexes in the antennae (Zhou, 2010). Interesting biotechnological approaches have shown that fusing odorant binding proteins with transit peptides allows them to efficiently cross lipid membranes, thus moving odorants to the desired compartments (Gonçalves et al., 2018). The use of engineered PBPs or transporters to facilitate pheromone release needs further exploration (Figure 7). The availability of a first version of a live pheromone bio-dispenser will facilitate the study of transporters and permeability intermediaries and serves as the basis for new design-build-test iterations towards the deployment of efficient SxPs as new components of integrated pest management strategies.

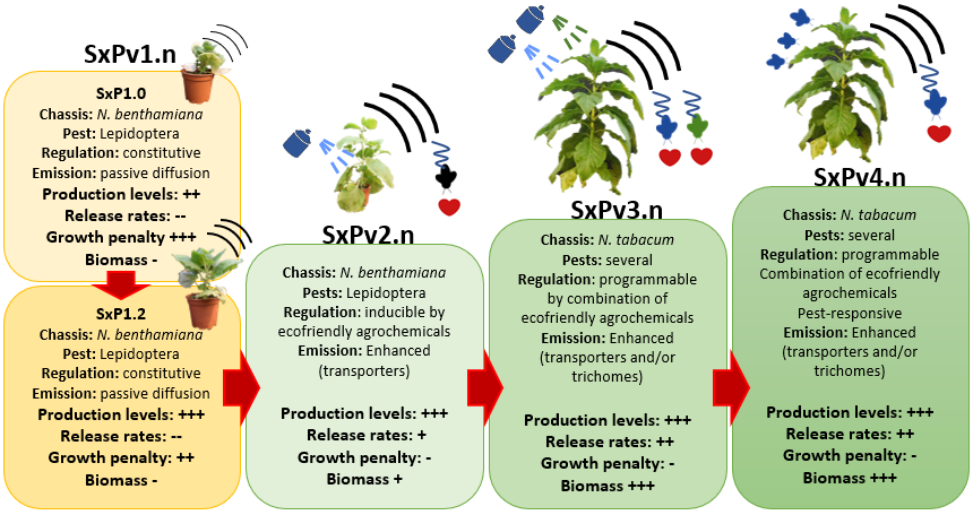

Figure 7. Roadmap for future SxP versions. The bottlenecks identified in SxPv1.n serve as guidance for future iterations in the development of pheromone biofactories. Key improvements in a second generation (SxPv2.n) should include inducible expression of the pheromone pathway to circumvent growth penalties, ideally triggered by environmentally friendly agrochemicals. Additionally, it should increase emission rates e.g., by co-expressing carrier proteins. Progress towards a third generation (SxPv3.n) would require the transfer of SxPv2.n tools to a related chassis with higher biomass, probably *N. tabacum*. Other improvements would involve the ability to produce different pheromone "programs" in the same plant, each one triggered by different chemicals, and the selective accumulation of pheromones in glandular trichomes to facilitate their release. Ideally, subsequent iterations (SxPv4.n) should incorporate, among others, the ability to respond directly to the presence of the target pest, as well as additional improvements in the chassis itself that facilitate its use as biosafe emitters in the field (e.g., non-flowering).

MATERIALS AND METHODS

DNA assembly and cloning

The basic DNA elements (promoters, coding regions, terminators) employed for the assembly of multigene constructs (Level 0 parts) were designed, synthesized and cloned using the GoldenBraid (GB) domestication strategy described by Sarrion-Perdigones et al. (2013). Once cloned into a pUPD2 vector, these new DNA elements were verified by enzymatic digestion and by sequencing. Transcriptional units (Level 1 parts) were then assembled via multipartite BsaI restriction-ligation reactions from level 0 parts, while level >1 modules were produced via binary BsaI

or BsmBI restriction–ligation. All level ≥1 parts were confirmed by restriction enzyme analysis. All GB constructs created and/or employed in this study are reported in Table S1 and their sequences are publicly accessible at https://gbcloning.upv.es/search/features. All constructs were cloned using the *Escherichia coli* TOP 10 strain. Transformation was performed using the Mix & Go kit (Zymo Research) following the manufacturer's instructions. The final expression vectors were transformed into electrocompetent *Agrobacterium tumefaciens* GV3101 C58 or LBA4404 for transient or stable transformations, respectively.

Transient expression assays in *Nicotiana benthamiana*

Agrobacterium tumefaciens GV3101 cultures harboring the constructs of interest were grown from glycerol stocks for 2 days to saturation, then refreshed by diluting them 1:1000 in LB liquid medium supplemented with the appropriate antibiotics. After being grown overnight, cells were pelleted and resuspended in agroinfiltration buffer (10 mM MES, pH 5.6, 10 mM $MgCl_2$ and 200 µM acetosyringone), incubated for 2 hours in the dark, and adjusted to an OD_{600} of 0.1. Equal volumes of each culture were mixed when needed for co-infiltration. A P19 silencing suppressor was included in the mixes to reduce post-transcriptional gene silencing (Zheng et al., 2009). Agroinfiltration was carried out with a 1 mL needleless syringe through the abaxial surface of the three youngest fully expanded leaves of 4-5 weeks-old plants grown at 24 °C (light)/20 °C (darkness) with a 16:8 h light:darkness photoperiod. Samples were collected 5 days post-infiltration using a Ø 1.5-2 cm corkborer and snap frozen in liquid nitrogen.

Nicotiana benthamiana stable transformation

Stable transgenic lines were generated following the transformation protocol of Clemente (2006), using *Agrobacterium tumefaciens* LBA4404 cultures with the corresponding plasmids. Briefly, leaves from 4-5 -week-old *N. benthamiana* plants grown at 24 °C (light)/20 °C (darkness) with a 16:8 h light:darkness photoperiod were sterilized by washing in a 2.5% sodium hypochlorite solution for 15 minutes, then rinsed in 70% ethanol for 10 seconds and washed 3 times in sterile distilled water for 15 minutes. Leaf discs were then cut using a Ø 0.8-1.2cm corkborer and transferred to a co-culture medium (MS medium supplemented with vitamins,

enriched with 1 mg L^{-1} 6-benzylaminopurine and 0.1 mg L^{-1} naphthalene acetic acid). After 24h on this medium, discs were incubated for 15 minutes in an *Agrobacterium* culture grown overnight to an OD_{600} of 0.2 in TY medium (10 g L^{-1} tryptone, 5 g L^{-1} yeast extract and 10 g L^{-1} NaCl, pH=5.6) supplemented with 2mM $MgSO_4 \cdot 7H_2O$, 200µM acetosyringone and the appropriate antibiotics. After incubation, discs were transferred back to the co-culture medium and incubated for 48h in the dark. Shoots were then induced by transferring to a MS medium supplemented with vitamins, 1 mg L^{-1} 6-benzylaminopurine, 0.1 mg L^{-1} naphthalene acetic acid and 100 mg L^{-1} kanamycin for selection of transformants. After 2-3 weeks of growth with weekly transfers to fresh media, shoots developing from the calli were isolated and transferred to root-inducing medium (MS supplemented with vitamins and 100 mg L^{-1} kanamycin). All in vitro growth was performed in a growth chamber (16:8 h light:darkness photoperiod, 24°C, 60%–70% humidity, 250 lmolm^{-2} s^{-1}). Rooted shoots were finally transferred to soil and grown in a greenhouse at 24:20°C (light:darkness) with a 16:8 h light:darkness photoperiod.

Plant growth and sampling

Transgenic SxP seeds were placed in a germination medium (MS with vitamins 4.9g L^{-1}, sucrose 30g L^{-1}, Phytoagar 9g L^{-1}, pH=5.7) supplemented with 100 mg L^{-1} kanamycin for positive transgene selection. Control WT plants were obtained similarly by placing seeds in a non-selective germination medium. WT and kanamycin-resistant seedlings were transferred to the greenhouse a week after germination, where they were grown at 24:20°C (light:darkness) with a 16:8 h light:darkness photoperiod.

Samples for targeted VOC analysis were collected from the 2nd and 3rd youngest and fully expanded leaves of each plant at the early flowering stage. All samples were collected between 4 and 6 pm, frozen in liquid nitrogen immediately after collection, and ground afterwards. Plant size was also estimated at this stage using a 1-10 scale. WT plants grown in parallel with each batch of transgenic plants were taken as a reference and given a score of 10.

For the comparative study of the SxPv1.0 and SxPv1.2 lines, seeds from SxPv1.0 5_1_7_X (T_2), SxPv1.2 4_X (T_0) and WT *N. benthamiana* plants were all sown simultaneously on selective and non-selective MS medium, then transferred to

soil and grown in the conditions described above. Leaf samples and pictures were taken at 4 weeks and 7 weeks after transplant, which corresponds to the young and early flowering stages (hereafter, adults), respectively. Roots were collected at the adult stage. All samples were snap-frozen in liquid nitrogen and ground. All samples were analyzed according to the same GC/MS protocol, as described below.

VOC analysis

50 mg of frozen, ground leaf samples were weighed in a 10mL headspace screw-cap vial and stabilized by adding 1 mL of 5M $CaCl_2$ and 150µL of 500mM EDTA (pH=7.5), after which they were sonicated for 5 minutes. Volatile compounds were captured by means of headspace solid phase microextraction (HS-SPME) with a 65 µm polydimethylsiloxane/divinylbenzene (PDMS/DVB) SPME fiber (Supelco, Bellefonte, PA, USA). Volatile extraction was performed automatically by means of a CombiPAL autosampler (CTC Analytics). Vials were first incubated at 80°C for 3 minutes with 500 rpm agitation. The fiber was then exposed to the headspace of the vial for 20 min under the same conditions of temperature and agitation. Desorption was performed at 250 °C for 1 minute (splitless mode) in the injection port of a 6890N gas chromatograph (Agilent Technologies). After desorption, the fiber was cleaned in a SPME fiber conditioning station (CTC Analytics) at 250°C for 5 min under a helium flow. Chromatography was performed on a DB5ms (60 m, 0.25 mm, 1 µm) capillary column (J&W) with helium as the carrier gas at a constant flow of 1.2 mL min^{-1}. For an initial identification of the pheromone peaks, oven programming conditions were 40°C for 2 min, 5°C min^{-1} ramp until reaching 280°C, and a final hold at 280°C for 5 min. Once the target peaks were identified, the oven conditions were changed to an initial temperature of 160°C for 2 min, 7°C min^{-1} ramp until 280°C, and a final hold at 280°C for 6 minutes to reduce the overall running time without losing resolution of the desired compounds. Identification of compounds was performed by the comparison of both retention time and mass spectrum with pure standards (for pheromones) or by comparison between the mass spectrum for each compound with those of the NIST 2017 Mass Spectral library (Supplementary File 1). All pheromone values were divided by the Total Ion Count (TIC) of the corresponding sample for normalization (Wu and Li, 2016).

The quantification of pheromone compounds emitted by plants was carried out by volatile collection in dynamic conditions. Individual plants were placed inside 5 L glass reactors (25 cm high × 17.5 cm diameter flask) with a 10 cm open mouth and a ground glass flange to fit the cover with a clamp. The cover had a 29/32 neck on top to fit the head of a gas washing bottle and to connect a glass Pasteur pipette downstream to trap effluents in 400 mg of Porapak-Q (Supelco Inc., Torrance, CA, USA) adsorbent. Samples were collected continuously for 72 h by using an ultrapurified-air stream, provided by an air compressor (Jun-air Intl. A/S, Norresundby, Denmark) coupled with an AZ 2020 air purifier system (Claind Srl, Lenno, Italy) to provide ultrapure air (amount of total hydrocarbons <0.1 ppm). In front of each glass reactor, an ELL-FLOW digital flowmeter (Bronkhorst High-Tech BV, Ruurlo, The Netherlands) was fitted to provide an air push flow of 150 mL min^{-1} during sampling. Trapped volatiles were then extracted with 5 mL pentane (Chromasolv, Sigma-Aldrich, Madrid, Spain), and extracts were concentrated to 200 µL under a nitrogen stream. Twenty microliters of an internal standard solution (TFN, 100 µg/ml in hexane) were added to the resulting extract prior to the chromatographic analysis for pheromone quantification.

Statistical analysis

For the untargeted volatilome analysis, data pre-processing was performed with Metalign (Lommen, 2009). Peak intensities were calculated for each compound for the SxP and WT samples and for blanks (mock $CaCl_2$ + EDTA samples), and compounds were included in the analysis if the sample:blank ratio was ≥2 for at least one of the categories (SxPv1.0, SxPv1.2 or WT). Principal Component Analysis and hierarchical clustering were performed with MetaboAnalyst 5.0 (https://www.metaboanalyst.ca/). After generalized logarithm transformation, data scaling was performed by mean-centering and dividing by the square root of the standard deviation of each variable. Hierarchical clustering was done using Ward clustering algorithm and Euclidean distance measure. Plant size values were analyzed with the non-parametric Kruskal-Wallis test using the Past3 software to determine the significance of plant size differences.

Plant solvent extraction

The total quantity of pheromone compounds accumulated in each plant was extracted with toluene (TLN). Plant samples (ca. 3 g), mixed with fine washed sand (1:1, plant:sand, w/w), were manually ground with a mortar to aid in tissue breakdown and facilitate the extraction. The resulting material was then transferred to 50 mL centrifuge tubes with 10 mL TLN. The extraction process was assisted by magnetic agitation for 12 h and finally by ultrasound in a Sonorex ultrasonic bath (Bandelin electronic, Berlin, Germany) for 30 min. A 1 mL sample of the resulting extract was filtered through a PTFE syringe filter (0.25 μm). Two-hundred microliters of an internal standard solution (TFN, 100 μg/ml in hexane) were added to the sample prior to the chromatographic analysis for pheromone quantification.

Synthetic pheromone samples and internal standard synthesis

A synthetic sample of 1g of Z11-16OH was obtained following the method described by Zarbin et al. (2007). The sample was carefully purified by column chromatography using silica gel and a mixture of hexane:Et_2O (9:1 to 8:2) as eluent. Evaporation of the solvent of the corresponding fraction generated a sample of 96 % purity by GC-FID.

A standard acetylation of Z11-16OH was carried out using acetic anhydride (1.2 eq) and trimethylamine (1.3 eq) as a base in dichloromethane (DCM), generating the corresponding acetate in 95 % yield, whose spectroscopical data was fully coincident with that described in the literature (Zarbin et al., 2007). Oxidation with pyridinium chlorocromate of a 100 mg sample of Z11-16OH was carried out following the method described by Zakrzewski et al. (2007) generating 62 mg (60 %) of Z11-16Ald, whose spectroscopical data was fully coincident with that described in the literature (Zakrzewski et al., 2007).

Due to the abundance of compounds structurally related to the pheromone in the biological samples, a straight chain fluorinated hydrocarbon ester (heptyl 4,4,5,5,6,6,7,7,8,8,9,9,9-tridecafluorononanoate; TFN) was selected as the internal standard to improve both sensitivity and selectivity for MS/MS method optimization. TFN was synthesized as follows: to a solution of 4,4,5,5,6,6,7,7,8,8,9,9,9-tridecafluorononanoic acid (500 mg, 1.3 mmol) in DCM,

oxalyl chloride was added. After 60 min of continuous stirring, the solvent was removed under vacuum. The residue was re-dissolved in dry DCM (15 ml) and 1-heptanol (0.26 mL, 1.5 mmol), followed by addition of triethyl amine (0.31 ml, 3 mmol) at room temperature, and the resultant solution was refluxed for 24 h. After this period, 15 ml of DCM were added and the solution was successively washed with HCl (1M, 20 ml), $NaHCO_3$ (sat., 20 mL), brine (15 ml) and dried with anhydrous $MgSO_4$. The solution was filtered and the residue was purified by column chromatography (silica gel; eluent: 1 % Et_2O/Hexane) to yield heptyl 4,4,5,5,6,6,7,7,8,8,9,9,9-tridecafluorononanoate (281 mg, 45 %), as a colorless oil of 95 % of purity estimated by GC-FID. MS (70 eV, m/z): 393 (10%), 375 (40%), 373 (5%), 132 (10%), 98 (30%), 83 (15%), 70 (100%), 69 (70%), 57 (90%) and 56 (90%).

Plant extract preparation for biosynthetic pheromone characterization

120 g of a pool of 10 T_1 SxPv1.2 plants (whole aerial portion of the plant) were mixed with fine washed sand (1:1, plant:sand, w/w) and were manually ground with a mortar to aid tissue breakdown and facilitate the extraction. The resulting material was then transferred to a 1 L Erlenmeyer flask and 400 mL of hexane were added. The extraction process was assisted by magnetic agitation for 12 h. After this time, the mixture was filtered and the filtrated was concentrated in a rotary evaporator. The residue (ca. 2 g) was chromatographed in a gravity column (30 cm X 1.5 cm) using silica gel (50 g) as the stationary phase and a mixture of Hexane:Et_2O (9:1) as the solvent. 60 fractions of ca. 3 mL were collected and analyzed by thin layer chromatography and GC/MS. Those fractions containing biosynthetic Z11-16OH were selected and those containing mainly biosynthetic Z11-16OH where mixed, and the solvent was rotary evaporated, generating 2 mg of material. The ^{1}H and ^{13}C NMR spectrum of the isolated biosynthetic Z11-16OH was recorded by a Bruker 600 Ultrashield Plus spectrometer (Bruker, Billerica, MA) at a frequency of 600 MHz, using $CDCl_3$ as the solvent and tetramethylsilane (TMS) as the internal standard.

Pheromone quantification

The quantification of the pheromone compounds was carried out by gas chromatography coupled to mass spectrometry (GC/MS/MS) using a TSQ 8000 Evo triple quadrupole MS/MS instrument operating in SRM (selected reaction

monitoring) mode using electron ionization (EI +), coupled with a Thermo Scientific TRACE 1300 gas chromatograph (GC). The GC was equipped with a ZB-5MS fused silica capillary column (30 m × 0.25 mm i.d. × 0.25 µm; Phenomenex Inc., Torrance, CA). The oven was held at 60 °C for 1 min then was raised by 10 °C min^{-1} up to 110 °C, maintained for 5 min, raised by 10 °C min^{-1} up to 150 °C, maintained for 3 min and finally raised by 10 °C min^{-1} up to 300 °C held for 1 min. The carrier gas was helium at 1 mL min^{-1}. For each compound, pheromone components (Z11-16OH and Z11-16Oac) and the internal standard (TFN), the MS/MS method was optimized by selecting the precursor ion and the product ions that provided the most selective and sensitive determinations (Table S2).

The amount of pheromone and the corresponding chromatographic areas were connected by fitting a linear regression model, y = a + bx, where y is the ratio between pheromone and TFN areas and x is the amount of pheromone.

Plant extract fractionation for electroantennography assays

10 g of T_1 SxPv1.2 plants (whole aerial portion of the plant) were mixed with fine washed sand (1:1, plant:sand, w/w) and were manually ground with a mortar to aid tissue breakdown and facilitate the extraction. The resulting material was then transferred to 50 mL centrifuge tubes with 40 mL TLN. The extraction process was assisted by magnetic agitation for 12 h and finally by ultrasounds in a Sonorex ultrasonic bath (Bandelin electronic, Berlin, Germany) for 60 min. After this time, the mixture was filtered off and the filtrated was concentrated in a rotary evaporator. The residue (ca. 0.2 g) was chromatographed in a gravity column (17 cm X 1 cm) using silica gel (15 g) as a stationary phase and a mixture Hexane:Et_2O (9:1) as solvent. Twenty-five fractions of ca. 2 ml were collected and analyzed by thin layer chromatography and GC/MS. Fractions 17-20 containing biosynthetic Z11-16OH were selected and combined for electroantennography assays.

Electroantennography assays for evaluating moth response to biosynthetic pheromone

Starter specimens of *Sesamia nonagrioides* (Lefèbvre) (Lepidoptera: Noctuidae) were collected from infested rice (*Oryza sativa*) plants in paddy fields located in Valencia (Spain). These were maintained on the stems until pupae were obtained and the progeny of the resulting adults was reared on an artificial diet (Eizaguirre

et al., 1994). Pupae were sexed using a stereomicroscope and males were kept separated from females in different chambers under an L16:D8 regime at 25±2 °C and 60% relative humidity.

The electrophysiological response of *S. Nonagrioides* males to the biosynthetic Z11-16OH was tested by gas chromatography coupled to mass spectrometry and electroantennography detectors (GC/MS-EAD). For this purpose, 2-3-day-old males were individually placed into test tubes in an ice bath to excise their antenna. Between two and five terminal segments of the antenna were also removed with a scalpel. The antenna was mounted between silver wire electrodes impregnated with conductive electrode gel (Spectra 360, Parker Laboratories, Inc., Fairfield, NJ, USA), to increase the electrical contact. A humidified and carbon-filtered airflow (50 ml/min) was directed continuously over the antenna preparation through a glass L-tube placed at less than 2 cm distance. The flow was delivered by a Syntech CS-55 stimulus controller (Ockenfels Syntech GmbH, Kirchzarten, Germany). A pore-sized opening in the elbow part of the L-tube allowed the introduction of the distal part of a fused-silica restrictor connected to the GC apparatus (Clarus 600 GC/MS, Perkin Elmer Inc., Wellesley, PA). The effluent of the GC column (ZB-5MS fused silica capillary column (30 m × 0.25 mm i.d. × 0.25 µm; Phenomenex Inc., Torrance, CA) was split 1:40 for simultaneous detection between the MS and the EAD apparatus. A Swafer S splitter (Perkin Elmer Inc., Wellesley, PA) was employed for this purpose. The GC/MS-EAD run was performed with the SxPv1.2 extract fraction containing the biosynthetic Z11-16OH obtained as described above. The GC oven temperature was programmed at 120 °C for 2 min, then raised to 200 °C at 10 °C/min and finally from 200 °C to 280 °C (held for 10 min) at 5 °C/min. The EAG responses were recorded with a Syntech IDAC 2 acquisition controller and the GC-EAD 32 (v. 4.3) software was employed for data recording and acquisition (Ockenfels Syntech GmbH, Kirchzarten, Germany).

SUPPLEMENTARY MATERIAL

Table S1. GoldenBraid Phytobricks created and used in this study.

GB ID	Name	Description
GB1018	HarFAR CDS	CDS of *Helicoverpa armigera* farnesyl reductase (accession number JF709978).
GB1019	AtrΔ11 CDS	CDS of *Amyelois transitella* Δ11-desaturase (accession number JX964774)
GB1020	EaDAct CDS	CDS of the *Euonymus alatus* acetyltransferase (accession number GU594061)
GB1021	P35S:HarFAR:T35S	TU for the constitutive expression of *Helicoverpa armigera* farnesyl reductase
GB1022	P35S:EaDAct:T35S	TU for the constitutive expression of *Euonymus alatus* acetyltransferase
GB1023	P35S:AtrΔ11:T35S	TU for the constitutive expression of *Amyelois transitella* Δ11-desaturase
GB1024	P35S:AtrΔ11:T35S-P35S:HarFAR:T35S	Module for the constitutive expression of *Amyelois transitella* Δ11-desaturase and *Helicoverpa armigera* farnesyl reductase
GB1025	P35S:AtrΔ11:T35S-P35S:HarFAR:T35S-SF-P35S:EaDAct:T35S	Module for the constitutive expression of *Amyelois transitella* Δ11-desaturase, *Helicoverpa armigera* farnesyl reductase and *Euonymus alatus* acetyltransferase
GB1491	Tnos:NptII:Pnos-P35S:DsRed:Tnos-P35S:AtrΔ11:T35S-P35S:HarFAR:T35S-P35S:EaDAct:T35S	Module for the constitutive expression of *Amyelois transitella* Δ11-desaturase, *Helicoverpa armigera* farnesyl reductase and *Euonymus alatus* acetyltransferase, together with NptII and DsRed marker genes
GB3534	Omega1_AtrD11-HarFAR-EaDAct-SF	Module for constitutive expression of the Sexy Plant enzymes
GB3535	Omega2_DsRed-nptII	Module for constitutive expression of DsRed and nptII selection genes
GB3536	Alpha1_AtrD11-HarFAR-EaDAct-SF- DsRed-nptII	Module for stable transformation of Sexy Plant genes
GB3537	Omega1_DsRed-SF	Construct made to have the DsRed selection gene in an omega plasmid
GB3538	Omega2_AtrD11-HarFAR-EaDAct-nptII	Module for constitutive expression of the Sexy Plant genes and the nptII selection marker
GB3539	Alpha1_DsRed-SF-AtrD11-HarFAR-EaDAct-nptII	Module for stable transformation of Sexy Plant genes, flanked by selection markers at both sides

Table S2. Optimized values of the MS/MS parameters for each target compound.

Compound	Transition[1]	Precursor ion (*m/z*)	Production (*m/z*)	Collision energy (eV)
TFN	1*	393	375	5
	2	375	263	10
	1	82	67	5
Z-11-C16:OH	2	95	67	10
Z-11-C16:Oac	3*	96	54	10
	4	96	81	5

[1] Transitions denoted with (*) were the ones employed to obtain the corresponding chromatographic areas. The others were monitored for confirmatory purposes to have increased selectivity when several peaks appear near to each peak retention time.

Table S3. Primers created and used in this study for testing the integrity of the *EaDAct* gene in SxPv1.0 plants.

Primer pair name	**Primer sequences (Fw; Rv)**	**Amplicon fragment size**
Full	TGCTTCGGCTTCTTTCACTT; GCGATAATGGCAGGGAAGTA	637 bp
CDS	TTGTCTCCCCATAACAATTA; CATGACAACAATATATCACG	200 bp
CHI	CCGGATAGGAATTGGCTAAGATCAT; TGCATTTCACATGCTTGAGTTGACC	1400 bp

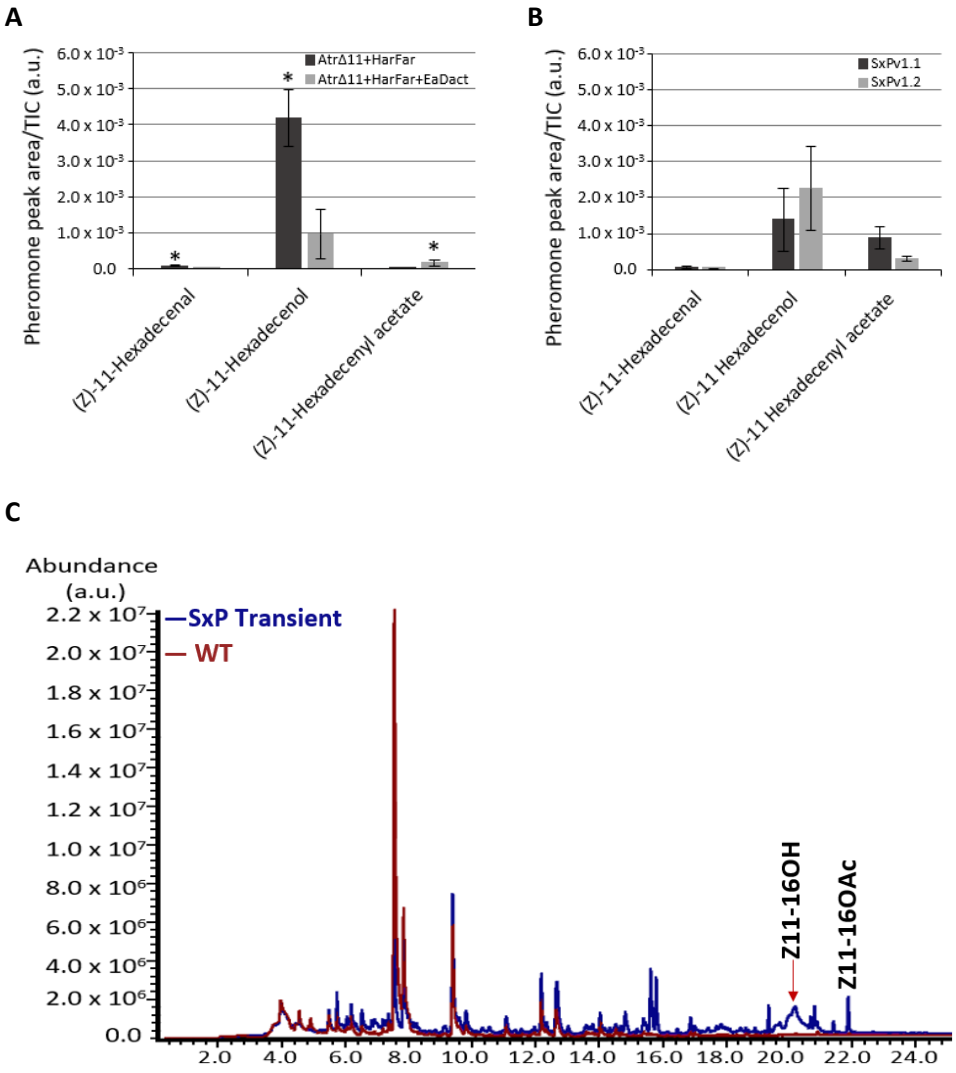

Figure S1. Transient expression in *Nicotiana benthamiana* of the moth pheromone synthetic pathway. (A) GC/MS quantification of the three pheromones when the three enzymes were transiently expressed, compared to the expression of only the first two enzymes (AtrΔ11, HarFAR). A 40x increase in acetate levels was observed when *EaDAct* was present, followed by a 4x decrease in the alcohol levels and a 3x decrease of aldehyde levels (T-test, α=0.05). (B) Pheromone levels obtained transiently with the SxPv1.1 and SxPv1.2 constructs. Error bars represent the ± SE of the measurements of three different leaf samples. (C) A representative chromatogram of a *Nicotiana benthamiana* plant agroinfiltrated with the SxPv1.2 construct (blue line) and a WT plant (red line).

A

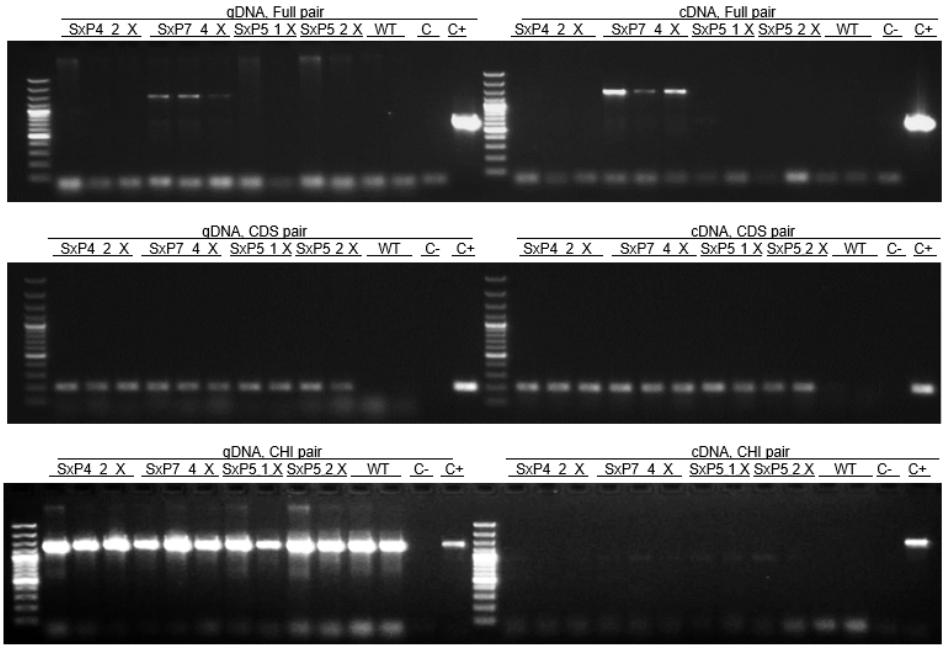

B

GGACGGTATGGCATTATGATCGCAACTTTGATATCAGCTCATTCATCTTATCAAGTATAACGGGATTTTTTCTAGCTTGGCTTACCACCTTT
AAGGTCATTAGCTTTGCATTCGATCAAGGCCCATTATACCCATTACCTCAGAATCTTCTTCATTTTATCTCAATTGCTTGTCTCCCCATAACA
ATTAAAAGAAATCCAAGCCCAAAATTGAAATCTACAACTAATCCATCACCAATCAGTCATCTTCTTAAAAAAGCCTTTATGAGTTTTCCATC
CAAGGTGCTATTCCATTGGGTTATCGCTCATCTGTACCAATACAAAAAATATATGGACCCGAACGTTGTGCTCGTGATATATTGTTGTCAT
GTTTACGTGGGTGATGCTGCCAACTTACTGATTTAGTGTATGATGGTGTTTTTGAGGTGCTCCAGTGGCTTCTGTTTCTATCAGCTGTCCCT
CCTGTTCAGCTACTGACGGGGTGGTGCGTAACGGCAAAAGCACCGCCGGACATCAGCGCTATCTCTGCTCTCACTGCCGTAAAACATGGC
AACTGCAGTTCACTTACACCGCTTCTCAACCCGGTACGCACCAGAAAATCATTGATATGGCCATGAATGGCGTTGGATGCCGGGCAACAG
CCCGCATTATGGGCGTTGGCCTCAACACGATTTTACGTCACTTAAAAAACTCAGGCCGCAGTCGGTAACCTCGCGCATACAGCCGGGCAG
TGACGTCATCGTCTGCGCGGAAATGGACGAACAGTGGGGCTATGTCGGGGCTAAATCGCGCCAGCGCTGGCTGTTTTACGCGTATGACA
GTCTCCGGAAGACGGTTGTTGCGCACGTATTCGGTGAACGCACTATGGCGACGCTGGGGCGTCTTATGAGCCTGCTGTCACCCTTTGACG
TGGTGATATGGATGACGGATGGCTGGCCGCTGTATGAATCCCGCCTGAAGGGAAAGCTGCACGTAATCAGCAAGCGATATACGCAGCGA
ATTGAGCGGCATAACCTGAATCTGAGGCAGCACCTGGCACGGCTGGGACGGAAGTCGCTGTCGTTCTCAAATCGTGGGAGCTGCATGAC
AAAGTCATCGGGCATTATCTGAACATAAAAACACTATCATAGTGGAGTCATTACCCGTTTACGTGATGTGAATATCAGTTGGAGTCTTTGC
GCCACTTTAGCAGAGTTCCTTTGTGGTTTTGATGTTGATCCTCAGTTCAAGGAACCATATTTAGCCACTTCTTTGCAGGACTTCTGGGGACG
GAGGTGGAACATTATAGTCTCTTCAGTCTTGAGGTCTACTGTTTATGCACCGACGCGTAACATCGCTCAACTCTTCGTCCGTTTTT

Figure S2. **Molecular characterization of *EaDAct* gene in SxPv1.0 plants.** (A) Gel electrophoresis of the PCR results with gDNA and cDNA from SxPv1.0 T_2 plants of the lines SxP4_2_X, SxP7_4_X and two representative plants for SxP5_1_X and SxP5_2_X. (B) Sequence obtained from the 1.5kb band observed in SxP7_4 samples for the Full primer pair. Highlighted is the unknown sequence found in the middle of the *EaDAct* coding sequence. Blast results suggest this sequence could be due to T-DNA re-organizations (data not shown).

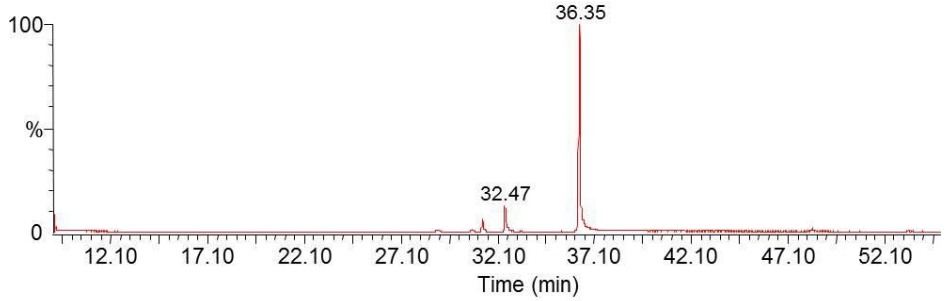

Figure S3. GC/MS of biosynthetic Z11-16OH.

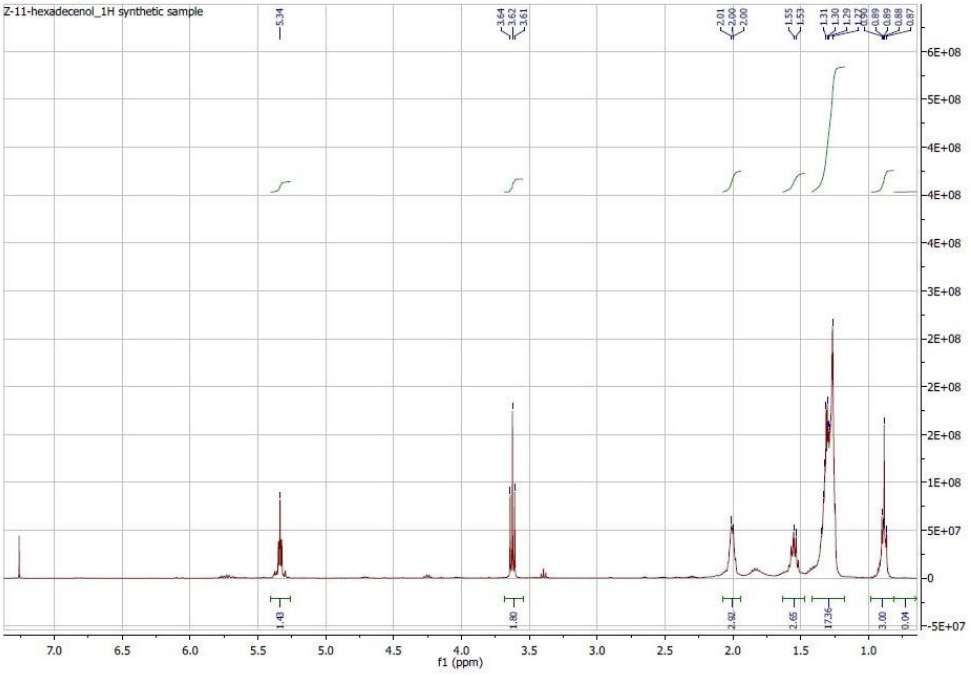

Figure S4. ^{1}H NMR of biosynthetic Z11-16OH. Despite our observation that spectroscopical data were fully consistent with those reported by Zarbin et al. [49], some ^{13}C signal described were wrongly assigned or duplicated in the original paper, so we list here a corrected version. Spectroscopical data for Z11-16OH: ^{1}H NMR (400 MHz, CDCl3) δ: 0.89 (t, J=6.8 Hz, 3H); 1.22–1.35 (m, 18H); 1.48–1.60 (m, 2H); 1.95–2.05 (m, 4H); 3.62 (t, J=6.8, 2H); 5.30–5.38 (m, 2H).

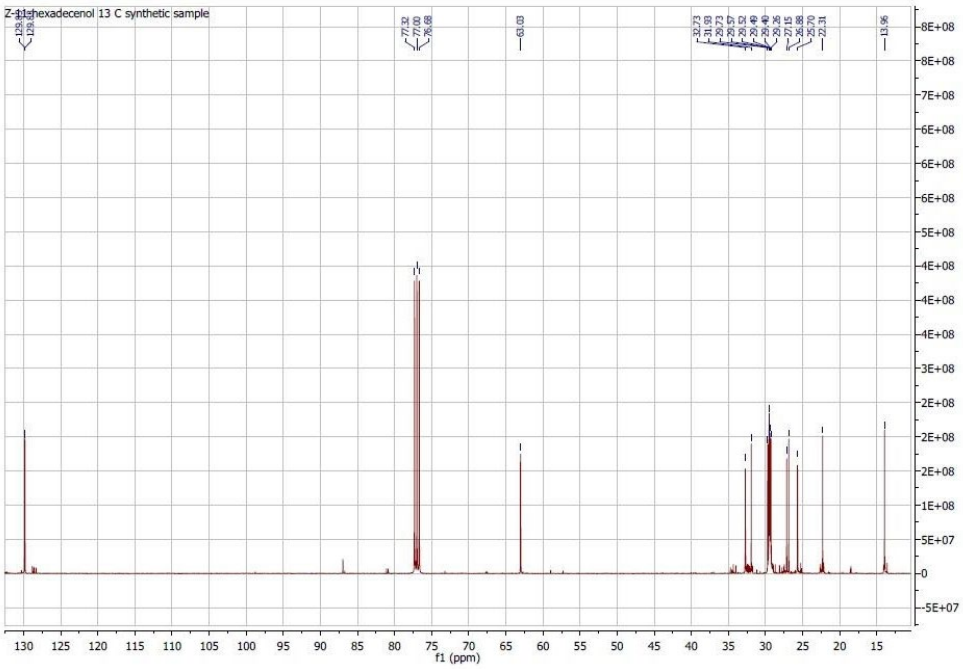

Figure S5. **^{13}C NMR of biosynthetic Z11-16OH**. Despite our observation that spectroscopical data were fully consistent with those reported by Zarbin et al. [49], some ^{13}C signal described were wrongly assigned or duplicated in the original paper, so we list here a corrected version. ^{13}C NMR (100 MHz, CDCl3) δ: 13.96, 22.31, 25.70, 26.88, 27.15, 29.26, 29.40, 29.49, 29.52, 29.57, 29.73, 31.93, 32.73, 63.03, 129.85 (2C). MS (70 eV, m/z): 222 (M^+, 3%), 152 (1%), 137 (4%), 123 (9%), 109 (18%), 96 (48%), 82 (63%), 67 (54%), 55 (100%).

CHAPTER II

CHAPTER II

GB_SynP: a modular dCas9-regulated synthetic promoter collection for fine-tuned recombinant gene expression in plants

***Elena Moreno-Giménez**, Sara Selma García, Camilo Calvache and Diego Orzáez.*

ACS Synthetic Biology, 2022. DOI: 10.1021/acssynbio.2c00238

My contribution to this work was essential for its publication. I contributed to most of the analysis performed and a major part of the manuscript writing. The entire manuscript is presented.

ABSTRACT

Programable transcriptional factors based on the CRISPR architecture are becoming commonly used in plants for endogenous gene regulation. In plants, a potent CRISPR tool for gene induction is the so-called dCasEV2.1 activation system, which has shown remarkable genome-wide specificity combined with a strong activation capacity. To explore the ability of dCasEV2.1 to act as a transactivator for orthogonal synthetic promoters, a collection of DNA parts was created (GB_SynP) for combinatorial synthetic promoter building. The collection includes (i) minimal promoter parts with the TATA box and 5'UTR regions, (ii) proximal parts containing single or multiple copies of the target sequence for the gRNA, thus functioning as regulatory cis boxes, and (iii) sequence-randomized distal parts that ensure the adequate length of the resulting promoter. A total of 35 promoters were assembled using the GB_SynP collection, showing in all cases minimal background and predictable activation levels depending on the proximal parts used. GB_SynP was also employed in a combinatorial expression analysis of an auto-luminescence pathway in *Nicotiana benthamiana*, showing the value of this tool in extracting important biological information such as the determination of the limiting steps in an enzymatic pathway.

INTRODUCTION

Plant synthetic biology is evolving fast, as high-throughput omics tools provide us with high-quality and precise knowledge about gene expression networks, providing clues for successful engineering interventions. However, there is a shortage of tools capable of controlling the expression of genes in the same precise way as occurs in nature. Many studies still rely on conventional genetic manipulation strategies such as gene knock-out or overexpression driven by constitutive promoters like the *Cauliflower mosaic virus* (CaMV*) 35S* promoter, which could easily cause pleiotropic or even detrimental effects in the transformed organism due to interferences with essential process during their development. To reach its full potential, plant genetic engineering is thus in need of tools for orthogonal and fine-tuned expression of genes. Synthetic promoters are strong allies, not only as tools for gene regulation but also for designing tailor-made metabolic pathways by controlling multiple genes simultaneously.

Plant synthetic promoters typically comprise a minimal promoter and a 5´ regulatory region where cis-regulatory elements are inserted. Regulatory DNA elements are often recruited from the binding sites of natural transcription factors (TFs). The dual architecture of many TFs allows the generation of synthetic TFs that combine their DNA-binding domains with the transcriptional regulatory domains of a different TF and vice versa, creating multiple functional combinations. Moreover, the availability of modular and interchangeable DNA parts greatly expands the possibilities of promoter design. In this regard, modular cloning methods such as MoClo (Engler et al., 2014; Weber et al., 2011), GoldenBraid (Sarrion-Perdigones et al., 2011), Mobius Assembly (Andreou and Nakayama, 2018) or Loop (Pollak et al., 2019) facilitate combinatorial rearrangement of promoter elements. GoldenBraid (GB) was conceived as an easy and modular assembly platform based on type IIS restriction enzymes, which makes use of the Phytobricks common syntax (Cai et al., 2020a; Patron et al., 2015) to facilitate the exchangeability of parts. The GB system also proposed a standard measurement using Luciferase/Renilla transient assay to estimate relative expression levels of promoter elements (Vazquez-Vilar et al., 2017).

A limitation of this classical approach lies in the hardwired DNA binding specificities of natural TFs, which imposes cis-regulatory elements in a fixed DNA

sequence, thus precluding free design, reducing combinatorial power, and comprising full orthogonality. These limitations could be overcome by employing programable transcriptional factors based on CRISPR/Cas9 architecture. The so-called CRISPR activation (CRISPRa) tools, based on the nuclease-deactivated Cas9 protein (dCas9), are becoming commonly used in plants for endogenous gene regulation (Chavez et al., 2015; Z. Li et al., 2017; Lowder et al., 2018; Pan et al., 2021). The main advantage of CRISPRa tools lays in its programable DNA binding activity, which is encoded in its custom-designed 20-nucleotides guide RNA (gRNA). Another remarkable feature of these tools is their multiplexing capacity, which enables several gRNAs to be directed to the same target gene to ensure higher activation levels, or to target different genes simultaneously to obtain a cascade of activation (Lowder et al., 2018; Pan et al., 2021; Vazquez-Vilar et al., 2016). CRISPRa tools reported in plants include different protein-fusion strategies, such as SunTag (Papikian et al., 2019) and dCas9-TV (Xiong et al., 2021), and strategies that make use of modified gRNA scaffolds to anchor additional activator domains (Konermann et al., 2015; Mali et al., 2013). In this last category falls the recently created dCasEV2.1, which makes use of a modified gRNA scaffold (called gRNA2.1) that includes two aptamer loops at the end of its sequence to allow the attachment of the viral MS2 protein. The use of this gRNA2.1 thus allows the combination of two activation domains in dCasEV2.1 system, firstly the EDLL plant motif fused to the dCas9 protein, and secondly the VPR (VP64, p65 and Rta) complex fused to MS2 protein. This system showed a strong activation level for endogenous genes that even surpassed those of their natural activation factors (Selma et al., 2019). Interestingly, the transcriptional activation achieved with dCasEV2.1 in *Nicotiana benthamiana* results in remarkable genome-wide specificity. When the promoter region of the endogenous dihydroflavonol-4-reductase (*NbDFR*) gene were targeted for activation in *N. benthamiana* leaves, transcriptomic analysis showed that only the two *NbDFR* homeologous genes were significantly activated, with negligible changes in the rest of the transcriptome. Similar genome-wide specificity was shown for another dCas9-based activation systems (Polstein et al., 2015), pointing towards dCasEV2.1 as the ideal system for creating orthogonal synthetic promoters.

In this work, we decided to explore the ability of dCasEV2.1 to transactivate plant genes as a strategy to build a comprehensive collection of orthogonal synthetic

promoters. To this end, we chose the 2Kb DNA 5´ regulatory region of tomato *SlDFR* gene promoter (p*SlDFR*) as a "model" promoter, given its remarkable inducibility using dCasEV2.1 (Selma et al., 2019). The strongest activation of p*SlDFR* occurred when targeted at a 20-nucleotides sequence at position -150 from its transcriptional start site (TSS). Taking the p*SlDFR* structure as a prototype, and randomizing most of its sequence, we created a set of synthetic DNA parts comprising distal, proximal and minimal promoter parts (Figure 1A), which, once assembled, produce full orthogonal promoter regions regulated by dCasEV2.1. The promoters in this so-called GB_SynP collection showed negligible basal expression in the presence of unrelated gRNAs, and a wide range of tunable transcriptional activities. Furthermore, the GB_SynP approach provides a general strategy to generate a virtually endless number of new promoters using interchangeable parts. Such tool can be used for designing large synthetic regulatory cascades where a number of downstream genes (e.g., a whole metabolic pathway) are controlled at custom expression levels by a single programable TF, avoiding repetitive promoter usage. To demonstrate this, we employed GB_SynP promoters in a combinatorial expression analysis of an auto-luminescence pathway in *N. benthamiana* leaves (Khakhar et al., 2020), extracting valuable information on the limiting steps of the pathway.

RESULTS

Design of dCasEV2.1-responsive synthetic promoters using the pSlDFR prototype

Previously, we showed in transient transactivation studies *N. benthamiana* that dCasEV2.1 led to a strong transcriptional activation of a firefly luciferase reporter gene (Fluc) driven by the 2Kb 5´regulatory region of the *SlDFR* promoter (herewith referred to as p*SlDFR*) (Selma et al., 2019). The responsiveness of p*SlDFR* was also confirmed in stably transformed reporter plant lines carrying the pSlDFR:Luc construct, which outperformed other reporter lines employing other promoters. Here, by performing a non-saturated scan of possible target sites in different regions of the p*SlDFR* fragment, we located a 20-nucleotides target box located at position -150 relative to the TSS, named gRNA1, yielding maximum transcriptional

activation in transient analysis (Figure 1B). Owing to its proven responsiveness to dCasEV2.1, and especially the low basal expression levels observed in repeated experiments, we decided to use the p*SlDFR* structure as the basis for the design of a new set of dCasEV2.1-regulated synthetic promoters (Figure 1C). A "minimal promoter" element was designed by selecting the region comprising the 5'UTR and the TATA box from the *SlDFR* gene (named mDFR) as previously reported by Garcia-Perez et al. (2022). This element was assigned a standard A3(-B2) position, according to the Phytobrick syntax, thus being flanked by TCCC and AATG overhangs (Figure 1A). Next to it, several "proximal promoter" parts, assigned to the A2 syntax category, were created. A2 proximal promoters consisted of single or multiple copies of the target sequence for gRNA1 functioning as cis-regulatory boxes, flanked by randomly generated DNA sequences (A2 parts sequences are collected and aligned in Figure S1A). The gRNA1 target in the synthetic parts was maintained at position -150 relative to the TSS, mimicking the structure of the native p*SlDFR*. We hereby defined a series of gRNA target positions or sites, named with lower case letters to differentiate them from the capital letters used in Phytobrick syntax. This target position of -150 from TSS was therefore named "a site" as being the first explored for this promoter collection. To expand the availability of unique A2 parts and avoid repetitions in promoter choice, six different A2 parts were initially designed (named G1a.1 to G1a.6). These A2 parts contain a single gRNA1 target site at this "a site" (position -150) and each one has a different random background sequence. For convenience, the target sequence of a different gRNA (named gRNA2), was also included in all G1a.N parts at position -210 from the TSS (referred to as "b site"). Later, the collection was further expanded with a second series of five new A2 parts (G1ab.1 to G1ab.5 parts), where a repetition of the gRNA1 box was inserted at the "b site" (position -210). Finally, a third group of five A2 sequences (G1abc.1 to G1abc.5) was created containing the target sequence three times, with the third copy located at position -100 (referred as the "c site") from the TSS (G1abc.1 to G1abc.5). To finalize the promoter design, an A1 "distal promoter" part (named R1) consisting of 1240 nucleotides of random DNA sequence was designed to mimic the length of the native p*SlDFR*. All randomly designed A1 and A2 sequences were analyzed with the TSSP software (http://www.softberry.com/berry) to ensure the absence of spurious cis-regulatory elements.

Promoter parts were next assembled to generate a total of 16 synthetic promoters, which were subsequently combined with the Fluc coding sequence and the CaMV35S terminator. All the resulting transcriptional units were further combined with renilla luciferase (Rluc) under CaMV35S promoter for normalization (as required for the standard Luciferase/Renilla transient assay) and the *P19* silencing suppressor and subsequently assayed in transient transactivation experiments in *N. benthamiana* leaves. All promoters showed negligible basal expression levels when co-transformed with a dCasEV2.1 loaded with a gRNA (named gRNA3) which target sequence is not present in the sequences of the promoters. On the contrary, co-transformation with gRNA1 led to substantial transcriptional activation in all promoters assayed, yielding a range of activation levels that increased with the number of copies for the gRNA target present in the A2 element (Figure 1C). Promoters that included the target sequence for gRNA1 once (G1a.N series) showed luciferase levels similar to those obtained with a *NOS* promoter used for normalization and set at a value of 1.0 relative promoter units (RPUs) (Vazquez-Vilar et al., 2017, 2016). Promoters with the target sequence present three times (G1abc.N series) reached activation levels of around 50 RPUs on average. The G1ab.N promoter series showed intermediate transcription levels, similar to those obtained with CaMV35S promoter, when activated with dCasEV2.1.

Expanding the combinatorial GB_SynP collection with additional configurations of the synthetic cis-regulatory region

The proposed modular GB_SynP structure allows, in principle, a limitless extension of the gRNA1-responsive promoter collection by the addition of new distal (using A1 syntax) and minimal promoter (with A3-B2 syntax) parts. To test this, two new A1 distal elements (R2 and R3) with random DNA sequences different to R1 were designed. These new parts were assayed in combination with A2 proximal promoters described above having one (G1a.1), two (G1ab.1) or three (G1abc.1) repetitions of the target sequence for gRNA1 (Figure 2A). As observed in Figure 2B, random distal promoter sequences had no significant influence on the transcriptional levels obtained with GB_SynP promoters. For all promoters assayed, the only relevant factor strongly determining the luciferase activity was

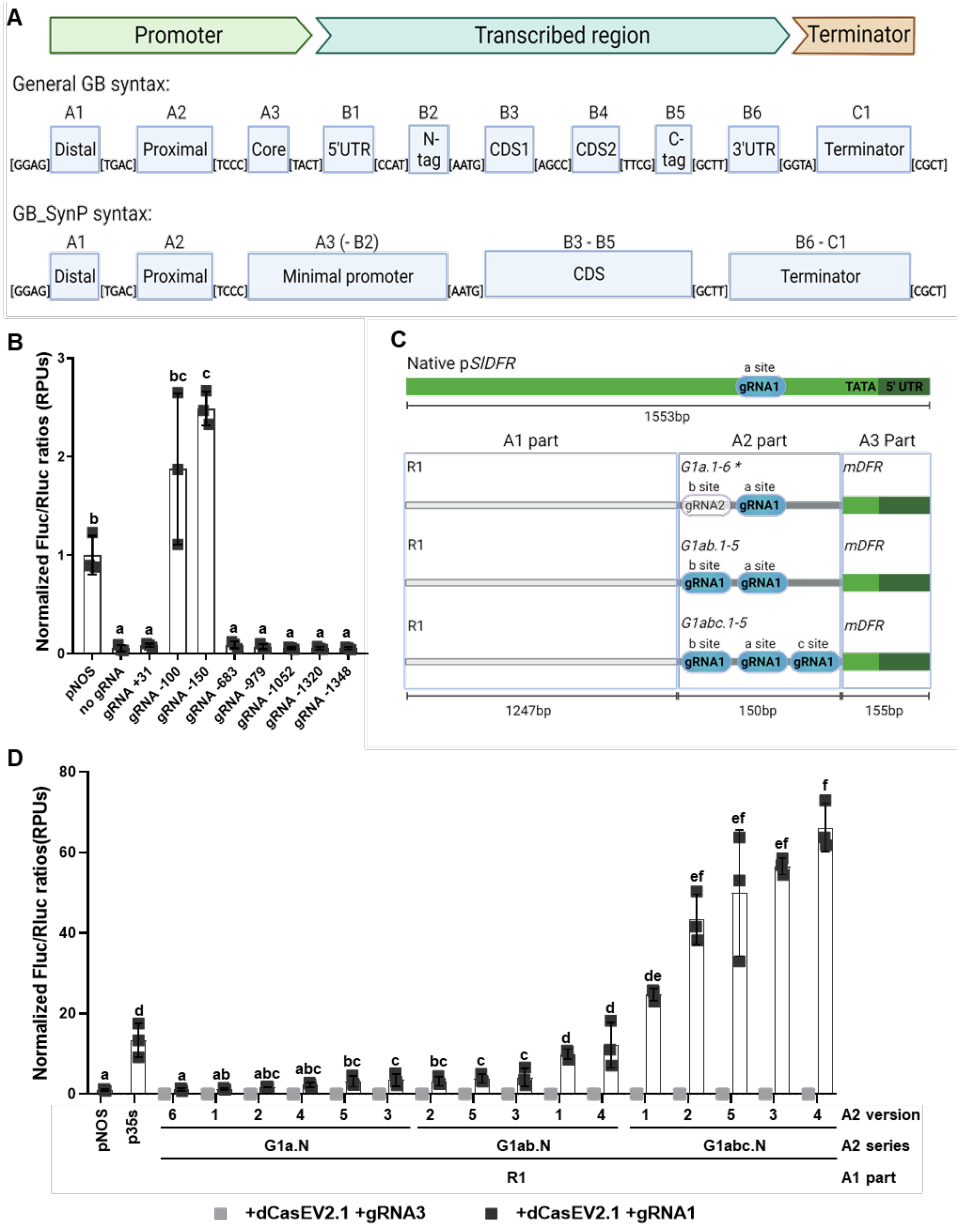

Figure 1. Design and expression range of dCasEV2.1-responsive GB_SynP promoter parts collection. (A) Schematic representation of GoldenBraid (GB) general syntax (A1 to C1 parts), and the specific syntax applied to the GB_SynP collection for A1 distal parts, A2 proximal parts, and A3(-B2) minimal promoter elements. Overhang sequences flanking each part are indicated between brackets. (B) Normalized (FLuc/RLuc) expression levels of *Nicotiana benthamiana* leaves transiently expressing a luciferase reporter gene (FLuc) under *SlDFR* promoter, co-infiltrated with dCasEV2.1

and different gRNAs targeting different positions at the *SlDFR* promoter. Luciferase under *NOS* promoter (p*NOS*) was included as a reference control. (C) Schematic representation of the *SlDFR* promoter (p*SlDFR*) used as a reference for the GB_SynP collection, and the promoter parts designed as A1 distal part (R1), A2 proximal part series containing one (G1a.1-6) two (G1ab.1-5) or three (G1abc.1-5) copies of the target sequence for the gRNA1, and as A3 minimal promoter part (mDFR). Positions of the gRNA target sequences in A2 parts are named with lower case letters, starting from "a site" to "c site" in this A2 part series. Parts in grey indicate the random DNA regions of A1 (light grey) and A2 parts (dark grey). (D) Normalized (FLuc/RLuc) expression levels of *N. benthamiana* leaves transiently expressing FLuc under the regulation of GB_SynP promoters containing R1 and mDFR parts assembled together with the different G1a.N, G1ab.N and G1abc.N A2 parts. Luciferase under *NOS*, CaMV35S and Sl*DFR* promoters (p*NOS*, p*35S* and p*SlDFR*, respectively) were included as reference controls. Letters denote statistically significance between (activated) promoters in a one-way ANOVA (Tukey's multiple comparisons test, $p \leq 0.05$) performed on the log-transformed data. Error bars represent the average values ± SD (n=3). Figure includes images created with Biorender (biorender.com).

*For convenience, the gRNA2 target was included in "b site" position in A2 parts G1a.1 to G1a.6, the full name of such parts are G1aG2b.1 to G1aG2b.6.

the number of cis gRNA1 elements present in the proximal promoter region, proving the orthogonality of distal promoter parts in the GB_SynP design.

Next, new A3 minimal promoter parts were also added to the collection and functionally assayed. Minimal promoter elements were designed based on the sequences of different strongly-regulated and/or tissue-specific genes from *Solanum lycopersicum, Nicotiana tabacum* and *Arabidopsis thaliana*. In addition, two minimal promoters based on fungal sequences were also created. Table S1 summarizes the genomic regions selected as A3 parts. All minimal promoters were assembled upstream with R1 and G1abc.1 (3xgRNA1-target) parts, downstream with the Luc/Ren reporter, and tested functionally. As shown in Figure 2C, minimal promoters had a stronger influence than A1 distal parts in determining the final transcriptional activity. We observed significant differences (up to 4-fold on average) among the plant promoters assayed. Maximum activation levels corresponded to the mPCPS2 A3 element. Fungal mGPDA showed almost no activity in *N. benthamiana*, however fungal mPAF A3 part promoted high transcriptional levels, similar to other promoter regions obtained from plants.

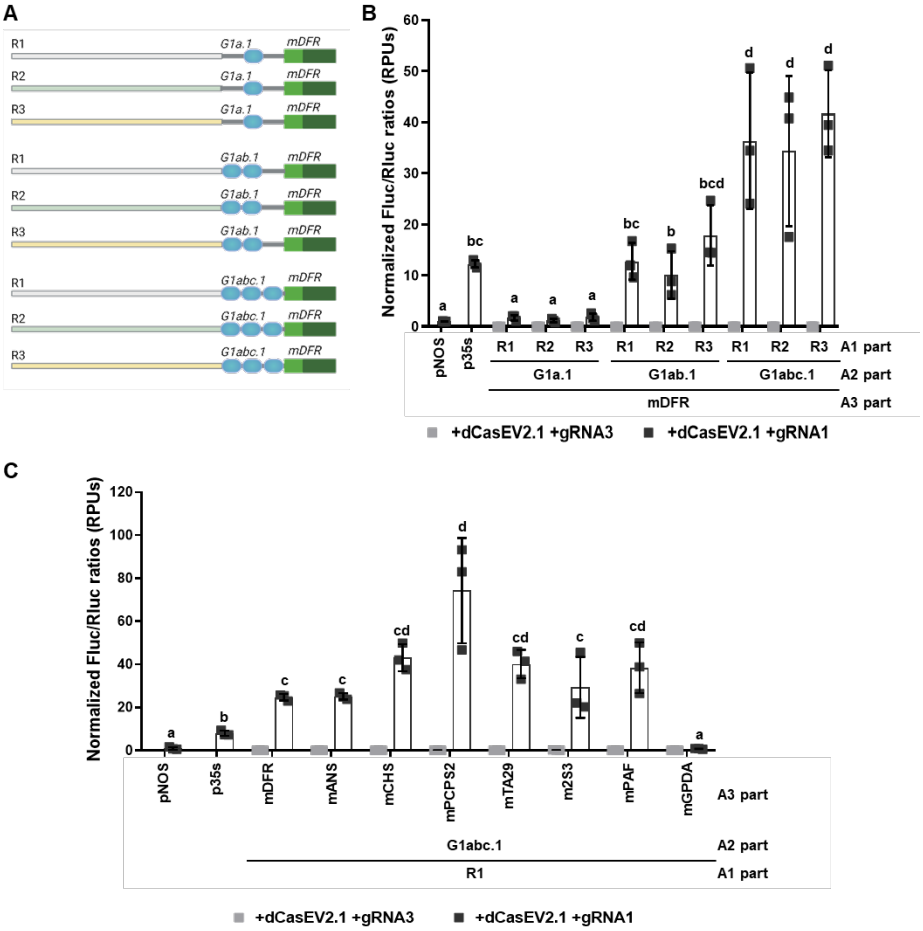

Figure 2. Addition and testing of new A1 distal sequences and A3 minimal promoter parts for the GB_SynP collection. (A) Schematic representation of the GB_SynP promoter series assembled to test the A1 distal parts R1, R2 and R3. A1 parts were combined with A3 mDFR and three different A2 proximal parts containing one (G1a.1) two (G1ab.1) or three (G1abc.1) copies of the gRNA1 target sequence (blue dots). (B) Normalized (FLuc/RLuc) expression levels of *Nicotiana benthamiana* leaves transiently expressing a luciferase reporter gene (FLuc) under the regulation of GB_SynP promoters combining the different A1 distal parts (R1, R2 or R3) with R1 part and different A2 parts including different repetitions of the gRNA1 target. (C) Normalized (FLuc/RLuc) expression levels of *Nicotiana benthamiana* leaves transiently expressing FLuc under the regulation of different GB_SynP promoters assembled with R1 and G1abc.1 parts in combination with different A3 minimal promoter elements. Luciferase under *NOS*, CaMV35S and Sl*DFR* promoters (*pNOS, p35S* and pSlDFR, respectively) were included as reference controls. Letters denote statistically significance between (activated) promoters in a one-way ANOVA (Tukey's multiple comparisons test, $p \leq 0.05$) performed on the log-transformed data. Error bars represent the average values ± SD (n=3). Figure includes images created with Biorender (biorender.com).

Despite the expression differences found employing different minimal promoters in the GB_SynP design, the A2 proximal region carrying the dCasEV2.1 cis protospacer elements concentrates most of the regulatory activity. Therefore, it was interesting to investigate modifications in its structure that could accommodate additional regulatory features. Accordingly, we first analyzed the influence of the relative position of the cis gRNA1 target to the TSS. New A2 proximal parts were thus designed which included the target for gRNA1 at positions -120 (named “d site”), -150 (“a site”), -210 (“b site”) and -320 (named “e site”) upstream of the TSS (named G1d.1, G1a.7, G1b.1 and G1e.1, respectively, see Figure 3A). As observed in Figure 3B, the transcriptional levels peaked when the gRNA1 target was at positions -120 and -150 from TSS, without statistical differences between these two positions, while the expression decreased when the target was positioned further away from the TSS. For G1e.1 part, which contained the target at “e site” (-320 from TSS), the activated expression levels were ten times lower than the *NOS* promoter used as reference, reaching values of 0.04 RPUs.

Next to the position of the target sequence, we analyzed the inclusion of new cis-regulatory elements other than gRNA1. For this, we chose the target sequence of gRNA3 as a new cis element, which is natively present at position -161 in the *NOS* promoter. This was previously shown to produce high activation of the *NOS* promoter when targeted with dCasEV2.1 (Selma et al., 2019). We then designed a new proximal element with the exact same sequence as G1a.7 but replacing the gRNA1 target by gRNA3 target (see Figure 3C, A2 parts sequences are collected and aligned in Figure S1B). In both G3a.1 and G1a.7 parts, the target sequence for the gRNA2 at the “b site” (position -210bp) was also present (thus renamed as G1aG2b.7 and G3aG2b.1, respectively). This target sequence is found at position 376 upstream of the TSS in the *SlDFR* promoter and showed low activation in the native promoter (Selma et al., 2019), which could be due to its distance from the TSS. The new A2 parts were then combined with R1 and mDFR parts (Figure 3C), and the resulting full promoters were assayed using single guide or double guide combinations (gRNA1+gRNA2 for G1aG2b.7 promoter, and gRNA3+gRNA2 for G3aG2b.1 promoter). Figure 3D shows that gRNA2 alone triggered a lower response when compared with gRNA1 in G1aG2b.7 or gRNA3 in G3aG2b.1, but still reaching transcriptional values close to a standard *NOS* promoter. gRNA3 and

gRNA1 showed similar activation levels when used alone to activate each (4.04 RPUs for gRNA1 in G1aG2b.7 and 2.68 RPUs gRNA3 in G3aG2b.1), while double activation using gRNA2+gRNA1 for G1aG2b.7 and gRNA2+gRNA3 for G3aG2b.1 resulted in higher activation levels (10.63 and 10.05 RPUs, respectively) when compared to using each gRNA individually.

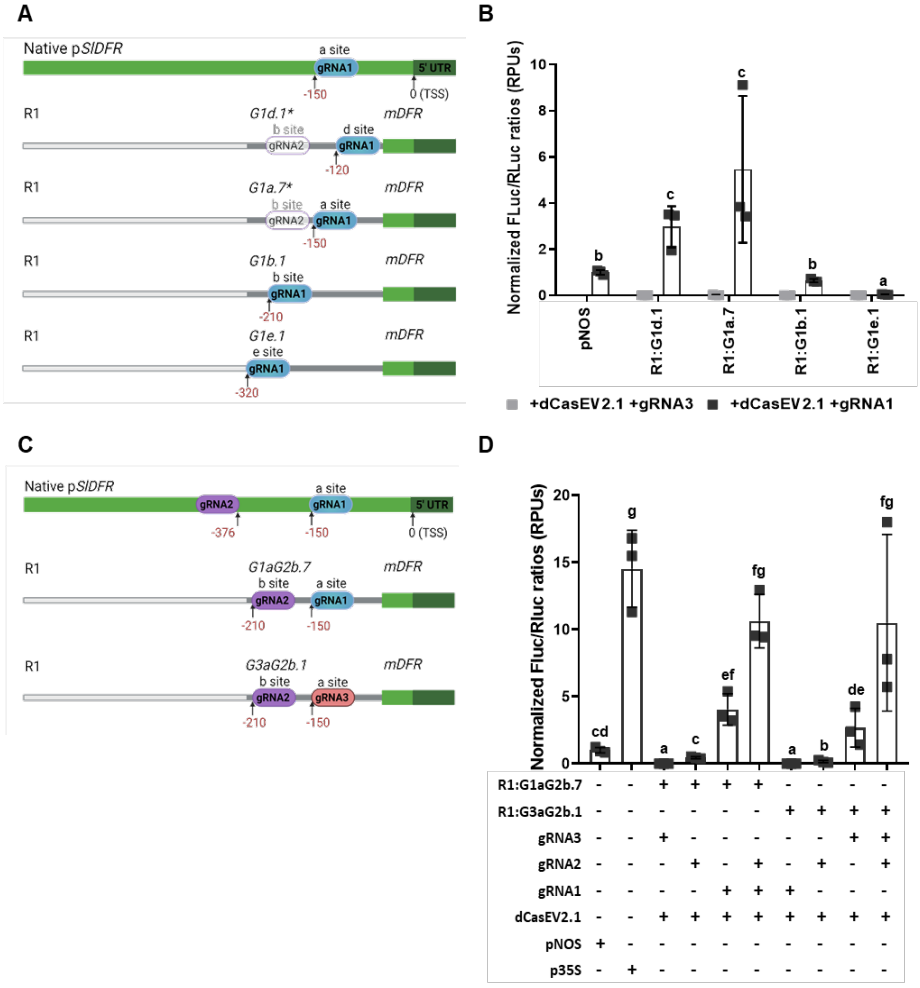

Figure 3. Variation of the cis-regulatory boxes within the A2 proximal parts of the GB_SynP collection. (A) Schematic design of the GB_SynP promoter series containing the target sequence for gRNA1 at position -120 ("d site"), -150 ("a site"), -210 ("b site") or -320 ("e site") from the Transcriptional Start Site (TSS). (B) Normalized (FLuc/RLuc) expression levels of *Nicotiana benthamiana* leaves transiently expressing a luciferase reporter gene (FLuc) under the regulation of GB_SynP promoters containing R1 and mDFR parts, in combination with A2 parts including the gRNA1 target sequence in different positions (G1d.1, G1a.7, G1b.1 and G1e.1). Luciferase under *NOS*

promoter (p*NOS*) was included as reference. (C) Schematic design of the GB_SynP promoters including the A2 parts G3aG2b.1 and G3aG2b.1. These two A2 parts contain the same sequence except for the gRNA target at position -150 from the TSS ("a site") which in G1aG2b.7 corresponds to gRNA1 target sequence and G3aG2b.1 part corresponds to gRNA3 target sequence. Arrows in the native pSlDFR promoter indicates the position of the nucleotide next to the PAM site for the target sequence of gRNA1 (localized in the reverse strand) and gRNA2 (localized in the forward strand). (D) Normalized (FLuc/RLuc) expression levels of *N. benthamiana* leaves transiently expressing FLuc under the regulation of GB_SynP promoters assembled with R1 and mDFR parts, in combination with the A2 part G1aG2b.7 or G3aG2b.1. Luciferase under *NOS* and CaMV35S promoters (p*NOS* and p*35S*, respectively) were included as references. Letters denote statistically significance between signals in a one-way ANOVA (Tukey's multiple comparisons test, $p \leq 0.05$) performed on the log-transformed data. Error bars represent the average values ± SD (n=3). Figure includes images created with Biorender (biorender.com).

*For convenience, the gRNA2 target was included in "b site" position in A2 parts G1d.1 and G1a.7, the full name of such parts will be G1dG2b.1 and G1aG2b.7, respectively.

Combining additional activation domains with dCas9 to activate synthetic promoters

The dCasEV2.1 system is considered to be a second-generation CRISPRa tool (Pan et al., 2021) as it combines the use of two proteins, dCas9 and MS2, to which two activation domains are fused (EDLL and VPR, respectively). This modular architecture can be exploited as an additional source of variability in the system, incorporating different activation domains (e.g., non-viral domains) to the dCas9 and MS2 modules, thus expanding the range of trans-activators for GB_SynP promoters. In addition, other dCas9-based transactivation strategies, such as the SunTag system can be also incorporated. In the SunTag approach, activation domains are fused to a single-chain variable fragment (ScFv) antibody, which in turn binds to a SunTag multiepitope peptide fused to dCas9 protein. To explore these additional expansions of the system, we assayed the two activation domains, ERF2 and EDLL, in four different combinations with dCas9 and MS2 modules, as well as the dCas9:SunTag system with EDLL, ERF2 or VPR fused to the ScFv antibody. All these dCas9-based TFs were co-infiltrated with the reporter R1:G1abc.1:mDFR: FLuc and transiently assayed (Figure 4). Significant activation levels were obtained compared to the background levels in all cases except for those in which ERF2 acted as the main activation domain. The higher activation

levels were obtained with the combination dCas:EDLL-MS2:ERF2 and dCas:SunTag-ScFv:VPR, which showed activations of 40-fold and 10-fold respectively, reaching activation levels of 0.75 and 0.14 relative promoter units (RPUs). In all new combinations, the expression levels were similar or lower than the standard p*NOS* signal. The original dCas:EDLL-MS2:VPR (dCasEV2.1) was the only combination that reached expression levels comparable to the CaMV35S promoter, thus confirming the unique characteristics of this activation tool in plants.

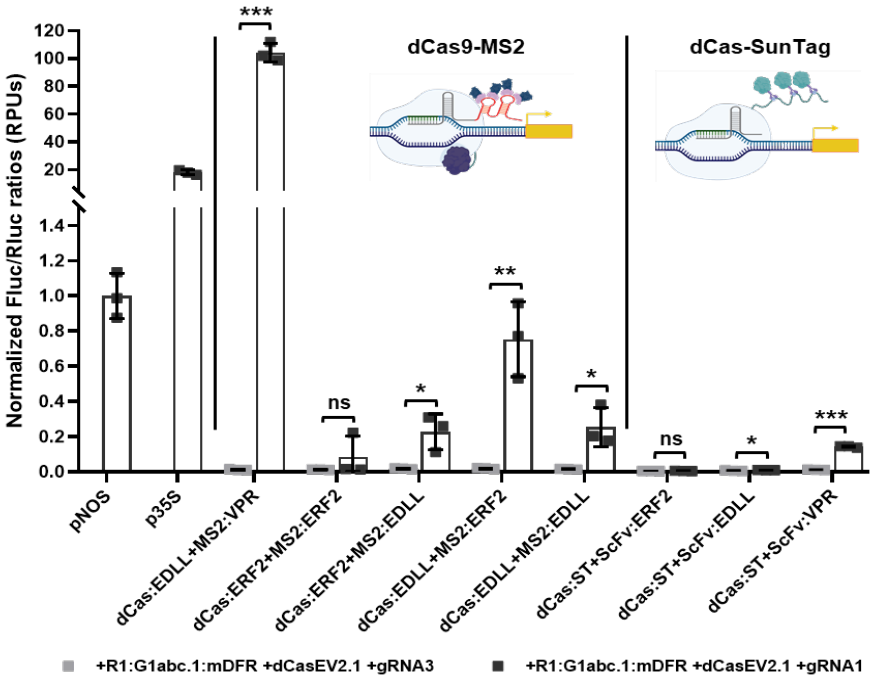

Figure 4. Transactivation of GB_SynP promoters with different CRISPRa strategies. Normalized (FLuc/RLuc) expression levels of *Nicotiana benthamiana* leaves transiently expressing a luciferase reporter gene (FLuc) under the regulation of a GB_SynP promoter containing the A1 part R1, A2 part G1abc.1 and A3 part mDFR (R1:G1abc.1:mDFR), co-infiltrated with dCas9-SunTag or dCas9-MS2 systems harboring different activation domains. Luciferase under *NOS* and CaMV35S promoters (p*NOS* and p*35S*, respectively) were included as references. Asterisks denote statistical significance between activated and basal expression levels, following APA's standards (Student's t-test, ns = $p <$ 0.05, * = $p \leq 0.05$, ** = $p \leq 0.01$ and *** = $P \leq 0.001$). Error bars represent the average values ± SD (n=3). Figure includes images created with Biorender (biorender.com).

Fine-tuning the expression of an auto-luminescence pathway

The fungal auto-luminescence pathway LUZ, described previously by Kotlobay et al. (2018), was recently adapted to plants (Khakhar et al., 2020; Mitiouchkina et al., 2020). The LUZ pathway has as major advantage that uses the plant's endogenous caffeic acid as a substrate to produce luciferin, thus avoiding the need for exogenous addition of luciferin substrate. Moreover, the self-sustainable luminescence emission implies that non-destructive assays can be performed, allowing for instance the visualization of time-course kinetics. The pathway comprises four genes, named *HispS* (hispidin synthase), *H3H* (hispidin-3 hydroxylase), *Luz* (luciferase) and *CPH* (caffeylpyruvate hydrolase). *HispS* encodes for the larger enzyme of the pathway which catalyzes three consecutive reactions to convert caffeic acid into hispidin, which is then turned into luciferin by a reaction catalyzed by *H3H* enzyme. Finally, luciferin is used by *LUZ* enzyme as a substrate to create a high energy intermediate that emits light upon its degradation to caffeylpyruvic acid. The fourth enzyme of the pathway, *CPH*, is included to recycle this degradation product back to caffeic acid, thus closing the cycle (Figure 5A).

Adapting the LUZ pathway as a reporter for gene expression analysis in plants requires identifying which genes in the pathway act as limiting steps, so that changes in their transcriptional levels are directly translated into changes in light intensity. Therefore, to understand the limiting steps governing the expression of this pathway in *N. benthamiana*, we took advantage of the combinatorial power and the wide expression range of the GB_SynP tool and created a series of assemblies to differentially regulate the expression of the *Luz*, *H3H* and *HispS* genes. We used three different GB_SynP promoters having either one (R3:G1a.1:mDFR, 1x gRNA-target), two (R2:G1ab.1:m2S3, 2x gRNA-target) or three targets (R1:G1abc.1:mPCPS2, 3x gRNA-target) for the gRNA1 (Figure 5B, see Figure S2 for the strength of each promoter). The *CPH* recycling enzyme was kept under the constitutive CaMV35S promoter in all genetic constructs to reduce the complexity of the analysis. An enhanced GFP protein (eGFP) under the CaMV35S promoter was also included in each construct to serve as internal reference for normalization. The normalized luminescence values of the resulting 27 pathway combinations co-infiltrated with dCasEV2.1 and gRNA1 are depicted in Figure 5C. The figure shows a time-course from day 1 to day 7 for each synthetic pathway,

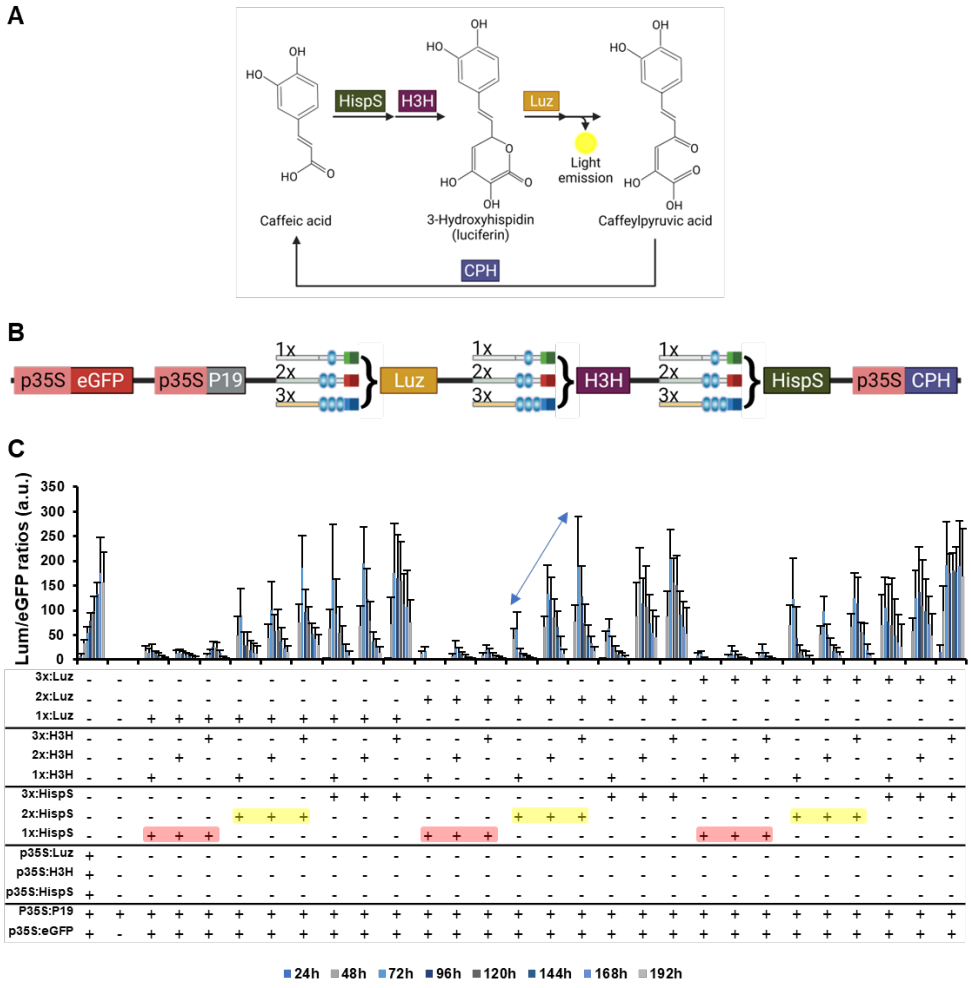

Figure 5. Transient expression of the auto-luminescence LUZ pathway under the regulation of GB_SynP promoters in *Nicotiana benthamiana* leaves. (A) Schematic representation of the LUZ pathway described by Kotlobay et al. (2018). The pathway consists of three genes (*HispS*, *H3H* and *Luz*) that converts caffeic acid into caffeylpyruvic acid with the emission of light, and a fourth gene (*CPH*) that turns caffeylpyruvic acid back to caffeic acid. (B) Schematic view of the genetic constructs assembled for expressing the LUZ pathway under the regulation of GB_SynP promoters. *Luz*, *H3H* and *HispS* genes were assembled in combination with synthetic promoters having one (1x, corresponds to promoter R3:G1a.1:mDFR), two (2x, corresponds to promoter R2:G1ab.1:m2S3) or three (3x, corresponds to promoter R1:G1abc.1:mPCPS2) targets for *gRNA1*. The fourth gene of the pathway, *CPH,* was constitutively expressed in all combinations under a CaMV35S promoter (p*35S*). The constructs included a constitutively expressed enhanced GFP protein (p35S:eGFP) for normalization of the luminescence values, and the P19 silencing suppressor (p35S:P19). (C) Time-course expression of the 27 constructs expressing the LUZ pathway transiently in *N. benthamiana*

leaves under the regulation of 1x, 2x or 3x GB_SynP promoters, co-infiltrated with dCasEV2.1 system and gRNA1. A constitutive control was included with all four genes of the LUZ pathway expressed under p*35S*. A negative control was also included by infiltration of P19 silencing suppressor (p35S:P19). Luminescence (Lum) values were normalized using fluorescence values produced by the constitutively expressed eGFP (p35S:eGFP) included in all the constructs as an internal control. Red boxes indicate combinations highlighted in the text where *HispS* is under regulation of 1x (gRNA-target) promoter, while yellow boxes indicate combinations where it is expressed under 2x (gRNA-target) promoter. The arrow highlights the three combinations where *HispS* and *Luz* are under regulation of 2x (gRNA-target) promoter, being *H3H* the only gene regulated by a different promoter in each of those three combinations. Error bars represent the average values ± SD (n=12). Figure includes images created with Biorender (biorender.com).

taking advantage of non-destructive auto-luminescence measurements. As expected, the highest luminescence values, comparable to those obtained when all three enzymes are controlled by the constitutive CaMV*35S* promoter, were reached when all three genes in the pathway were regulated by 3x gRNA-target promoters, while the lowest transcriptional levels were found when the three genes were under 1x gRNA-target promoter. Almost no luminescence was observed for any of the 27 combinations when co-infiltrated with dCasEV2.1 and an irrelevant gRNA (gRNA3, see Figure S3).

The analysis of the remaining pathway combinations served as guidance to understand the regulation of the synthetic pathway. In all combinations where *HispS* was driven by 1x gRNA-target promoters, the resulting normalized luminescence values remained at basal levels regardless of the synthetic promoters used to regulate the remaining genes (see red boxes in Figure 5C), thus indicating that *HispS* expression acts as a limiting factor. Raising *HispS* levels to those provided by dCasEV2.1-activated 2x gRNA-target promoters was sufficient to prove the effects of the regulation of the remaining genes (see yellow boxes in Figure 5C). Particularly promoters regulate both *Luz* and *HispS* (see arrow in Figure 5C). Using this conformation, the modifications in the promoter strength driving *H3H* are readily reflected in luminescence levels following a positive linear trend with no signs of saturation. Considering that activated 2x gRNA-type promoter show expression levels in the range of a *NOS* promoter, this indicates a reporter system with an appropriate dynamic range could consist in a pathway where *Luz* and *HispS* are regulated by constitutive *NOS* promoter and *H3H* is set under a variable-strength promoters for e.g., transactivation studies.

DISCUSSION

The synthetic promoters whose expression is regulated via CRISPRa systems are promising orthogonal tools for synthetic biology. CRISPRa-based synthetic promoters have been previously reported in bacteria (Dong et al., 2018), yeast (Farzadfard et al., 2013) and human cells (Farzadfard et al., 2013; Nissim et al., 2014), and now GB_SynP is one of the first collections reported in plants, together with the work recently published by Kar et al. (2022). In contrast to the commonly used activation systems based on transcription activator-like effectors (TALEs) or the zinc finger proteins, which require re-engineering of the DNA-binding motifs for each target sequence (Morbitzer et al., 2010; Urnov et al., 2010), GB_SynP allows the creation of promoters with completely different cis-boxes by simply creating new A2-type cis-regulatory parts, and its corresponding gRNA transcriptional unit, both elements being only a few hundred base pairs long. Here, we also demonstrated that two completely different gRNAs (gRNA1 and gRNA3) can reach similar activation levels when positioned in the same position within the GB_SynP synthetic promoter, implying that potentially any 20-nucleotides sequence can be used as a cis-regulatory box. Specificity of the transcriptional activation signaling GB_SynP promoters was also demonstrated, since co-expression of dCasEV2.1 with an unrelated gRNA led to negligible basal expression in all assays. These results position the GB_SynP collection as a promising tool for the regulation of complex multigene circuits with different gRNAs present in the cis-regulatory boxes of each promoter, thus creating logic gates that could be useful to further explore different metabolic fluxes within biosynthetic pathways. Moreover, other studies reported the successful expression of gRNAs under pol-II promoters, which in turn could be regulated by different inducers (García-Pérez et al., 2022; Kar et al., 2022), thus allowing customizable control of each gRNA with different stimuli to further direct the multigene circuits in different ways.

While we reported here the assembly and behavior of 35 synthetic promoters, the GB_SynP collection includes to date 32 promoter parts, compiled in Table S2, that can be used to assemble more than 500 different promoters without the need for creating any new sequence, standing out as one of the CRISPRa-based synthetic expression tools currently available for plants with the highest diversity and

combinatorial strength. Moreover, plant synthetic promoters created so far mostly rely on the well-characterized CaMV35S minimal promoter (Dey et al., 2015; Kar et al., 2022), which might lead to higher basal expression in comparison with other minimal promoters like mDFR (García-Pérez et al., 2022). To overcome this limitation, GB_SynP includes newly designed minimal promoter parts, for which negligible basal expression was shown in all cases, as well as a range of activation levels. The total length of the synthetic promoter should also be considered, as short sequences could easily be interfered with by other nearby promoters once they are introduced into the plant genome, especially considering the preference for T-DNA to be inserted into transcriptionally active regions (Ingelbrecht et al., 1991; Schneeberger et al., 2005). In this regard, different A1 random parts were also included in the GB_SynP collection to allow easy modulation of the length of the resulting promoter, while adding an extra source of sequence variation.

Although dCasEV2.1 remains as the most optimal system to regulate GB_SynP synthetic promoters, here we demonstrated that their activation can also be triggered by combining dCas9 and MS2 proteins with other activation domains, or by using other CRISPRa strategies, such as those based on dCas9:SunTag fusion. Among the combinations tested, the VPR activation domain showed the highest activation levels for both systems, which correlates with what was previously observed by Chavez et al. (2015) where VPR reached the highest fluorescence values out of the 22 different activation domains tested, including the commonly used VP64. VPR is in fact a combination of the activation domains VP64, P65 and Rta, of which VP64 is in turn comprised of four tetrameric repetitions of the herpes simplex virus VP16 protein. Depending on the intended application of GB_SynP promoters, concerns may arise from the use of viral proteins for the regulation of GB_SynP promoters. In this regard, as an alternative, we propose the combination of dCas9 and MS2 proteins with the EDLL and ERF2 activation domains, respectively, which triggered a considerable activation that led to a signal comparable to a NOS promoter level. Nevertheless, better-performing CRISPRa tools are continuously being developed (Pan et al., 2021) which could also be used in combination with different activation domains to increase the expression levels of GB_SynP promoters developed here.

The combinatorial power and the wide range of expression levels provided by the GB_SynP collection were further exploited in the optimization of a multigene bioluminescence pathway. The new synthetic promoters were shown to regulate the expression three genes in the pathway in a predictable and reliable way, with the lowest pathway output levels (luminescence) obtained when all three genes were under the regulation of the weakest promoter, and the highest expression reached when the three genes were driven by the strongest promoters. In this case, we showed that the GB_SynP system was also useful to further characterize the regulatory requirements of the synthetic pathway. We found that, unlike the rest of the genes, low HispS expression limits the flux in the pathway, rendering the regulation of the remaining steps useless. Such behavior is in line with previous observations described by Mitiouchkina et al. (2020), where they reported that the addition of caffeic acid to *N. benthamiana* leaves expressing the auto-luminescence pathway resulted in the development of lower and slower luminescence than the addition of hispidin or luciferin.

Lucks et al. (2008) defined five fundamental characteristics for efficient and predictable genetic engineering, which are independence, orthogonality, reliability, tunability and composability. Our GB_SynP system described here is a modular and composable system that has shown to be highly gRNA-specific and whose orthogonality is ensured by the negligible basal expression of the synthetic promoters generated when used in combination with the genome-wide specific dCasEV2.1 system (Selma et al., 2019). We further demonstrated that the GB_SynP system works in a reliable way for expressing the bioluminescence pathway and includes a range of expression levels that can be further modulated by the use of inducible pol-II driven gRNAs. All in all, the GB_SynP system constitutes a promising tool for the easy design and optimization of multigenic circuits in the field of plant genetic engineering.

MATERIALS AND METHODS

Construction and assembly of DNA parts

All plasmids used in this work were assembled using GoldenBraid (GB) cloning (Sarrion-Perdigones et al., 2013). The DNA sequences of the constructs generated

in this work are available at gbcloning.upv.es/search/features by entering the IDs provided in Table S3. Random DNA sequences were generated at www.bioinformatics.org/sms2/random_dna (Stothard, 2000) and each promoter part designed was ordered as gBlocks (IDT) and assembled following GoldenBraid (GB) domestication strategy. Briefly, DNA parts were first cloned into the pUPD2 entry vector and verified by digestion and sequencing. Transcriptional units were then generated via restriction-ligation reactions with the different DNA parts contained in pUPD2 vectors, and combined with binary assemblies into multigenic constructs via restriction-ligation with T4 ligase and BsaI or BsmBI. All constructs were cloned into *Escherichia coli* TOP 10 strain using Mix&Go kit (Zymo Research) as indicated by the manufacturer. All assemblies were confirmed by digestion.

Plant inoculation and transient expression assays

Transient expression assays were performed by agroinfiltration of 4-5-week-old *N. benthamiana* plants grown at 24°C/20°C (light/darkness) with a 16h:8h photoperiod. Expression vectors were transferred to *Agrobacterium tumefaciens* GV3101 by electroporation. Cultures were grown overnight in liquid LB medium supplemented with rifampicin and the corresponding antibiotic for plasmid selection. Cells were then pelleted and resuspended in agroinfiltration buffer (10 mM MES at pH 5.6, 10 mM $MgCl_2$ and 200 µM acetosyringone), incubated for 2 hours in the dark, and adjusted to an OD_{600} of 0.1. For co-infiltration, cultures were mixed at equal volumes, maintaining a final OD of 0.1. The silencing suppressor P19 was included in all tested constructs. Agroinfiltration was carried out using 1 mL needleless syringe through the abaxial surface of the three youngest fully expanded leaves of each plant.

In vitro Luciferase/Renilla assay

Agroinfiltrated samples were collected 5 days post-infiltration using a Ø 8 mm corkborer to extract a disc per each agroinfiltrated leaf, and snap frozen in liquid nitrogen. Expression of firefly luciferase (FLuc) and renilla luciferase (RLuc) were determined with the Dual-Glo® Luciferase Assay System (Promega) following manufacturer's instruction with some modifications. Frozen leaf samples were first homogenized and extracted with 180µl Passive Lysis Buffer, followed by a centrifugation (14,000×g) at 4 °C for 10 minutes. 10 µl of working plant extract

(supernatant) was then transferred to a 96 wellplate, where 40 µl LARII buffer was added to measure Fluc signal in a GloMax 96 Microplate Luminometer (Promega) with a 2-s delay and a 10-s measurement. RLuc signal was measured afterwards by adding 40 µl Stop&Glow reagent and measuring in the same way.

FLuc/RLuc ratios were determined as the mean value of three independent agroinfiltrated leaves of the same plant and were normalized to the FLuc/RLuc ratio obtained from a sample agroinfiltrated with a reference construct (GB1398) where Luciferase is driven by *NOS* promoter (p*NOS*) and Renilla is under CaMV35S promoter (p*35S*). Reference FLuc/RLuc ratios are arbitrarily set as 1.0 relative promoter units (RPUs). Differences between the FLuc/RLuc ratios were analyzed with one-way ANOVA followed by the post-hoc multiple comparisons Tukey's test ($p \leq 0.05$) using GraphPad Prism 8.0.1 software. As residuals of FLuc/RLuc ratios did not follow a normal distribution according to Anderson-Darling, D'Agostino-Pearson omnibus, Shapiro-Wilk and Kolmogorov-Smirnov tests, a logarithmic transformation of the data (Y=log(Y)) was performed previously to the statistical analysis to properly fit the ANOVA assumptions.

In vivo Luciferase/eGFP assay

Agroinfiltrated leaf discs were collected 24h post-infiltration using a Ø 6 mm corkborer to extract a disc per each agroinfiltrated leaf, and placed directly in white 96 wellplates containing 200 µL/well of solid MS medium (4.9 g/L MS+vitamins, 8 g/L agar pH=5.7). Plates were measured once per day for 8 days in a GloMax 96 Microplate Luminometer (Promega), first for luminescence and immediately after for fluorescence. For luminescence, a 2-s delay and 10-s measurement parameters were used as previously described for in vitro Luciferase/Renilla assays. For eGFP measurement, an optical kit was used with an excitation peak at 490nm and emission at 510-570 nm.

SUPPLEMENTARY MATERIAL

Table S1. Sequences of the A3 minimal promoters designed in this study for the GB_SynP collection. Highlighted in bold are the predicted TATA boxes of each promoter sequence. Underlined sequences correspond to predicted 5' UTR regions.

GB CODE	PART NAME	ORGANISM	SEQUENCE (TATA BOX IN BOLD, 5' UTR UNDERLINED)
GB3408	mCHS	*Solanum lycopersicum*	atctctagctaccattctttttctttttggacttca**tatataaa**tatatagttcatacaacc cccatgcaacaaaaatacaccaagacaattatcactctttcattcacgtagtcctaaac acaaaaaaacctagcatatccaccatttttttccggcgaaa
GB3409	mANS	*Solanum lycopersicum*	tatcttgtatgagataaatttcaagtgc**tataaa**tatacctaacgaaaagttatagtta gcagtactgaaaaaaacgagataaac
GB3410	mTA29	*Nicotiana tabacum*	ttttgcaagttgttgtgtatgtcttgtgctc**tatata**tgcccttgtggtgcaagtgtaaca gtacaacatcatcactcaaatcaaagtttttacttaaagaaattagctaaa
GB3412	mPCPS2	*Nicotiana tabacum*	tttaatatttgcccttcatcaagaggcaata**tataaa**taagcctgcgccattgcaacaa ctcaaaccatttccaatattgcctcacaagtcagtagtgccttttcctctctcaaacgttc attgtctttatctcccttccccaattctcattggaagaataaaacaaaaattaaattaga a
GB3411	m2S3	*Arabidopsis thaliana*	gcatgcatgcattcttacacgtgattgccatgcaaatctccttttctcacc**tataaa**taca aaccaaccccttcactacactcttccactcaaaccaaaacaagaaaacatacacaaata gcaaaac
GB3413	mPAF	*Penicillium chrysogenum*	tgtcacctttcacacagagctcatgatctggtt**tataa**aggcggcttcatgaccctcaa ttccatatagtatcactcccatcacagcatttcgatatcttcaaccactttaaccttctcc agaggatcatcatctcaagcccttcata
GB3414	mGPDA	*Aspergillus nidulans*	tttgttgcca**tattttc**ctgctctctccccaccagctgctcttttctttttctctttctttttcccat cttcagtatattcatcttcccatccaagaacctttaa

Table S2. Summary of all DNA parts included to date in the GB_SynP collection.

GB_SynP A1 parts (distal promoters)	GB_SynP A2 parts (proximal promoters)					GB_SynP A3 parts (minimal promoters)
	1x target for gRNA1	2x target for gRNA1	3x target for gRNA1	1 target for gRNA2	1 target for gRNA3	
R1	G1aG2b.1	G1ab.1	G1abc.1	G1aG2b.1	G3aG2b.1	mDFR
R2	G1aG2b.2	G1ab.2	G1abc.2	G1aG2b.2		mANS
R3	G1aG2b.3	G1ab.3	G1abc.3	G1aG2b.3		mCHS
	G1aG2b.4	G1ab.4	G1abc.4	G1aG2b.4		mPCPS2
	G1aG2b.5	G1ab.5	G1abc.5	G1aG2b.5		mTA29
	G1aG2b.6			G1aG2b.6		m2S3
	G1aG2b.7			G1aG2b.7		mPAF
	G1dG2b.1			G1dG2b.1		mGPDA
	G1b.1					
	G1e.1					

Table S3. DNA parts and assemblies created and/or used in this study.

GB Code	Part Name	Description
GB1119	pEGB 35S:Luciferase:TNos-SF-35S:Renilla:TNos-35S:P19:TNos	Module for the expression of the Firefly luciferase, the Renilla luciferasa and the P19 silencing suppressor genes driven by the 35S promoter and the nos terminator.
GB1160	pEGB SlDFR:Luc:TNos-SF-35S:Renilla:TNos-35S:P19:TNos	Module for the expression of the Firefly luciferase gene driven by the S.lycopersicum DFR promoter and terminator, the Renilla luciferase gene and the silencing suppressor P19 driven by the 35S promoter and the Nos terminator.
GB1190	pEGB 35S:dCas9-EDLL:tNOS	TU for the expression of the dCas9 with the activation domain EDLL as a CT fusion.
GB1398	pEGB3alpha2 Pnos:luc:Tnos-SF-35S:Ren:Tnos-35S:P19:Tnos-SF	Module for the expression of the Firefly Luciferase under the regulation of the Nos promoter, and the Renilla Luciferase and the P19 silencing suppressor under the regulation of the 35S promoter.
GB1603	35S:dCas9-SunTag:Tnos	TU for the expression of the dCas9 fused to the SunTag epitope.
GB1724	Alpha1 gRNA-Pnos:2.1 (gRNA3)	GB-cassette for the expression of guide RNA3 targeting the NOS promoter.
GB1738	Alpha2: 35S_MS2:EDLL_Tnos	TU for the constitutive expression of the MS2 coat protein fused on Ct to the activation domain EDLL.
GB1824	Alpha2_35S-dCas9:ERF2-Tnos	TU for the constitutive expression of dCas9 fused to the transcriptional activation domain ERF2.
GB1833	Alpha2_35S-MS2:ERF2-Tnos	TU for the constitutive expression of the MS2 coat protein fused on Ct to the transactivation domain of ERF2.
GB1838	Alpha1 1gRNA-DFR 2.1 (gRNA1)	GB-cassette for the expression of guide RNA1 targeting the DFR promoter in −150 position.
GB1839	Alpha1 5gRNA-DFR 2.1 (gRNA2)	GB-cassette for the expression of guide RNA2 targeting the DFR promoter in −376 position.
GB1867	Alpha2_35S-ScFv:VPR-Tnos	TU for constitutive expression of ScFv antibody fused to VPR activation.
GB1869	Alpha2_35S-ScFv:ERF2-Tnos	TU for constitutive expression of ScFv antibody fused to ERF2 activation domain.
GB2033	Alpha1:1gRNA SlDFR	Multiplex construct to target SlDFR in −100 position.
GB2034	Alpha1: 2gRNA SlDFR	Multiplex construct to target SlDFR in +31 position.
GB2035	Alpha1: 3gRNA SlDFR	Multiplex construct to target SlDFR in -1320 position.
GB2036	Alpha1: 4gRNA SlDFR	Multiplex construct to target SlDFR in -1052 position.
GB2037	Alpha1:5gRNA SlDFR	Multiplex construct to target SlDFR in -979 position.
GB2038	Alpha1:6gRNA SlDFR	Multiplex construct to target SlDFR in -683 position.
GB2039	Alpha1:7gRNA SlDFR	Multiplex construct to target SlDFR in -1348 position.
GB2085	Omega1_35S-Ms2:VPR-Tnos-35S-dCas9:EDLL-Tnos	Module for the expression of Ms2 protein fused to VPR and dCas9 fused to EDLL.

GB Code	Part Name	Description
GB2566	pUPD2_miniDFR	Minimal promoter of SlDFR gene containing 62bp upstream the transcription start site and the 5'UTR region.
GB2815	pUPD2_GB_SynP (A1) Random Sequence R1	Random sequence R1 of 1240 bp for A1 distal promoter position.
GB2878	pUPD2_GB_SynP (A2) G1aG2b.1	A2 Proximal promoter sequence consisting of the target sequences for the gRNA-1 DFR (gRNA1) and gRNA-5 DFR (gRNA2) flanked by random sequences.
GB2879	pUPD2_GB_SynP (A2) G1aG2b.5	A2 Proximal promoter sequence consisting of the target sequences for the gRNA-1 DFR (gRNA1) and gRNA-5 DFR (gRNA2) flanked by random sequences.
GB2880	pUPD2_GB_SynP (A2) G1aG2b.6	A2 Proximal promoter sequence consisting of the target sequences for the gRNA-1 DFR (gRNA1) and gRNA-5 DFR (gRNA2) flanked by random sequences.
GB2881	pUPD2_GB_SynP (A2) G1aG2b.2	A2 Proximal promoter sequence consisting of the target sequences for the gRNA-1 DFR (gRNA1) and gRNA-5 DFR (gRNA2) flanked by random sequences.
GB2882	pUPD2_GB_SynP (A2) G1aG2b.3	A2 Proximal promoter sequence consisting of the target sequences for the gRNA-1 DFR (gRNA1) and gRNA-5 DFR (gRNA2) flanked by random sequences.
GB2883	pUPD2_GB_SynP (A2) G1aG2b.4	A2 Proximal promoter sequence consisting of the target sequences for the gRNA-1 DFR (gRNA1) and gRNA-5 DFR (gRNA2) flanked by random sequences.
GB2884	pUPD2_GB_SynP (A2) G1ab.2	A2 Proximal promoter sequence consisting of two times the target sequence for the gRNA-1 DFR (gRNA1) flanked by random sequences.
GB2885	pUPD2_GB_SynP (A2) G1ab.1	A2 Proximal promoter sequence consisting of two times the target sequence for the gRNA-1 DFR (gRNA1) flanked by random sequences.
GB2886	pUPD2_GB_SynP (A2) G1ab.3	A2 Proximal promoter sequence consisting of two times the target sequence for the gRNA-1 DFR (gRNA1) flanked by random sequences.
GB2887	pUPD2_GB_SynP (A2) G1ab.6	A2 Proximal promoter sequence consisting of two times the target sequence for the gRNA-1 DFR (gRNA1) flanked by random sequences.
GB2888	pUPD2_GB_SynP (A2) G1ab.4	A2 Proximal promoter sequence consisting of two times the target sequence for the gRNA-1 DFR (gRNA1) flanked by random sequences.
GB2889	pUPD2_GB_SynP (A2) G1ab.5	A2 Proximal promoter sequence consisting of two times the target sequence for the gRNA-1 DFR (gRNA1) flanked by random sequences.
GB2890	pUPD2_GB_SynP (A2) G1dG2b.1	A2 Proximal promoter sequence consisting of the target sequence for the gRNA-1 DFR (gRNA1, at "d site" positioned at -120 from TSS) and gRNA-5 DFR (gRNA2) flanked by random sequences.

GB Code	Part Name	Description
GB2891	pUPD2_GB_SynP (A2) G1abc.1	A2 Proximal promoter sequence consisting of three times the target sequence for the gRNA-1 DFR (gRNA1) flanked by random sequences.
GB2894	Alpha1_R1:G1aG2b.1:mDFR:luc:t35S	TU for the expression of firefly luciferase driven by a GB_SynP promoter with A1 R1 and A3 mSlDFR parts, and an A2 part containing a target for the gRNA-1DFR (gRNA1) and gRNA-5 DFR (gRNA2).
GB2895	Alpha1_R1:G1aG2b.5:mDFR:luc:t35S	TU for the expression of firefly luciferase driven by a GB_SynP promoter with A1 R1 and A3 mSlDFR parts, and an A2 part containing a target for the gRNA-1DFR (gRNA1) and gRNA-5 DFR (gRNA2).
GB2896	Alpha1_R1:G1aG2b.6:mDFR:luc:t35S	TU for the expression of firefly luciferase driven by a GB_SynP promoter with A1 R1 and A3 mSlDFR parts, and an A2 part containing a target for the gRNA-1DFR (gRNA1) and gRNA-5 DFR (gRNA2).
GB2897	Alpha1_R1:G1aG2b.2:mDFR:luc:t35S	TU for the expression of firefly luciferase driven by a GB_SynP promoter with A1 R1 and A3 mSlDFR parts, and an A2 part containing a target for the gRNA-1DFR (gRNA1) and gRNA-5 DFR (gRNA2).
GB2898	Alpha1_R1:G1aG2b.3:mDFR:luc:t35S	TU for the expression of firefly luciferase driven by a GB_SynP promoter with A1 R1 and A3 mSlDFR parts, and an A2 part containing a target for the gRNA-1DFR (gRNA1) and gRNA-5 DFR (gRNA2).
GB2899	Alpha1_R1:G1aG2b.4:mDFR:luc:t35S	TU for the expression of firefly luciferase driven by a GB_SynP promoter with A1 R1 and A3 mSlDFR parts, and an A2 part containing a target for the gRNA-1DFR (gRNA1) and gRNA-5 DFR (gRNA2).
GB2900	Alpha1_R1:G1ab.2:mDFR:luc:t35S	TU for the expression of firefly luciferase driven by a GB_SynP promoter with A1 R1 and A3 mSlDFR parts, and an A2 part containing the target for the gRNA-1DFR (gRNA1) twice.
GB2901	Alpha1_R1:G1ab.1:mDFR:luc:t35S	TU for the expression of firefly luciferase driven by a GB_SynP promoter with A1 R1 and A3 mSlDFR parts, and an A2 part containing the target for the gRNA-1DFR (gRNA1) twice.
GB2902	Alpha1_R1:G1ab.3:mDFR:luc:t35S	TU for the expression of firefly luciferase driven by a GB_SynP promoter with A1 R1 and A3 mSlDFR parts, and an A2 part containing the target for the gRNA-1DFR (gRNA1) twice.
GB2904	Alpha1_R1:G1ab.4:mDFR:luc:t35S	TU for the expression of firefly luciferase driven by a GB_SynP promoter with A1 R1 and A3 mSlDFR parts, and an A2 part containing the target for the gRNA-1DFR (gRNA1) twice.
GB2905	Alpha1_R1:G1ab.5:mDFR:luc:t35S	TU for the expression of firefly luciferase driven by a GB_SynP promoter with A1 R1 and A3 mSlDFR parts, and an A2 part containing the target for the gRNA-1DFR (gRNA1) twice.

GB Code	Part Name	Description
GB2906	Alpha1_R1:G1dG2b.1:mDFR:luc:t35S	TU for the expression of firefly luciferase driven by a GB_SynP promoter with A1 R1 and A3 mSlDFR parts, and an A2 part containing a target for the gRNA-1DFR (gRNA1, at "d site") and gRNA-5 DFR (gRNA2).
GB2907	Alpha1_R1:G1abc.1:mDFR:luc:t35S	TU for the expression of firefly luciferase driven by a GB_SynP promoter with A1 R1 and A3 mSlDFR parts, and an A2 part containing three times the gRNA-1DFR (gRNA1) target sequence.
GB2909	Omega1_R1:G1aG2b.1:mDFR:luc:t35S +P19(TU) +Renilla(TU)	Module for the expression of luciferase driven by a GB_SynP promoter with A1 R1, A3 mSlDFR, and an A2 part containing a target for gRNA1 and gRNA2, and for the constitutive expression of renilla and P19.
GB2910	Omega1_R1:G1aG2b.5:mDFR:luc:t35S +P19(TU) +Renilla(TU)	Module for the expression of luciferase driven by a GB_SynP promoter with A1 R1, A3 mSlDFR, and an A2 part containing a target for gRNA1 and gRNA2, and for the constitutive expression of renilla and P19.
GB2912	Omega1_R1:G1aG2b.2:mDFR:luc:t35S +P19(TU) +Renilla(TU)	Module for the expression of luciferase driven by a GB_SynP promoter with A1 R1, A3 mSlDFR, and an A2 part containing a target for gRNA1 and gRNA2, and for the constitutive expression of renilla and P19.
GB2913	Omega1_R1:G1aG2b.3:mDFR:luc:t35S +P19(TU) +Renilla(TU)	Module for the expression of luciferase driven by a GB_SynP promoter with A1 R1, A3 mSlDFR, and an A2 part containing a target for gRNA1 and gRNA2, and for the constitutive expression of renilla and P19.
GB2914	Omega1_R1:G1aG2b.4:mDFR:luc:t35S +P19(TU) +Renilla(TU)	Module for the expression of luciferase driven by a GB_SynP promoter with A1 R1, A3 mSlDFR, and an A2 part containing a target for gRNA1 and gRNA2, and for the constitutive expression of renilla and P19.
GB2915	Omega1_R1:G1ab.2:mDFR:luc:t35S +P19(TU) +Renilla(TU)	Module for the expression of luciferase driven by a GB_SynP promoter with A1 R1, A3 mSlDFR, and an A2 part with the target for gRNA1 twice, and the constitutive expression of renilla and P19.
GB2916	Omega1_R1:G1ab.1:mDFR:luc:t35S +P19(TU) +Renilla(TU)	Module for the expression of luciferase driven by a GB_SynP promoter with A1 R1, A3 mSlDFR, and an A2 part with the target for gRNA1 twice, and the constitutive expression of renilla and P19.
GB2917	Omega1_R1:G1ab.3:mDFR:luc:t35S +P19(TU) +Renilla(TU)	Module for the expression of luciferase driven by a GB_SynP promoter with A1 R1, A3 mSlDFR, and an A2 part with the target for gRNA1 twice, and the constitutive expression of renilla and P19.
GB2919	Omega1_R1:G1ab.4:mDFR:luc:t35S +P19(TU) +Renilla(TU)	Module for the expression of luciferase driven by a GB_SynP promoter with A1 R1, A3 mSlDFR, and an A2 part with the target for gRNA1 twice, and the constitutive expression of renilla and P19.
GB2920	Omega1_R1:G1ab.5:mDFR:luc:t35S +P19(TU) +Renilla(TU)	Module for the expression of luciferase driven by a GB_SynP promoter with A1 R1, A3 mSlDFR, and an A2 part with the target for gRNA1 twice, and the constitutive expression of renilla and P19.

GB Code	Part Name	Description
GB2921	Omega1_R1:G1dG2b.1:mDFR:luc:t35S +P19(TU) +Renilla(TU)	Module for the expression of luciferase driven by a GB_SynP promoter with A1 R1, A3 mSlDFR, and an A2 part containing a target for gRNA1 (d site) and gRNA2, and for the constitutive expression of renilla and P19.
GB2922	Omega1_R1:G1abc.1:mDFR:luc:t35S +P19(TU) +Renilla(TU)	Module for the expression of luciferase driven by a GB_SynP promoter with A1 R1, A3 mSlDFR, and an A2 part with three times the target for gRNA1, and the constitutive expression of renilla and P19.
GB3269	pUPD2_GB_SynP (A1) Random Sequence R2	Random sequence R2 of 1240 bp for A1 distal promoter position.
GB3270	pUPD2_GB_SynP (A1) Random Sequence R3	Random sequence R3 of 1240 bp for A1 distal promoter position.
GB3271	pUPD2_GB_SynP (A2) G1aG2b.7	A2 Proximal promoter sequence consisting of the target sequence for the gRNA-1 DFR (gRNA1) and gRNA-5 DFR (gRNA2) flanked by random sequences.
GB3272	pUPD2_GB_SynP (A2) G1b.1	A2 Proximal promoter sequence consisting of the target sequence for the gRNA-1 DFR (gRNA1) at "b site" (-210 from TSS).
GB3273	pUPD2_GB_SynP (A2) G1e.1	A2 Proximal promoter sequence consisting of the target sequence for the gRNA-1 DFR (gRNA1) at "e site" (-320 from TSS).
GB3274	pUPD2_GB_SynP (A2) G3aG2b.1	A2 Proximal promoter sequence consisting of the target sequences for the gRNA-4 NOS (gRNA3) and gRNA-5 DFR (gRNA2) flanked by random sequences.
GB3275	pUPD2_GB_SynP (A2) G1abc.2	A2 Proximal promoter sequence consisting of three times the target sequence for the gRNA-1 DFR (gRNA1) flanked by random sequences.
GB3276	pUPD2_GB_SynP (A2) G1abc.3	A2 Proximal promoter sequence consisting of three times the target sequence for the gRNA-1 DFR (gRNA1) flanked by random sequences.
GB3277	pUPD2_GB_SynP (A2) G1abc.4	A2 Proximal promoter sequence consisting of three times the target sequence for the gRNA-1 DFR (gRNA1) flanked by random sequences.
GB3278	pUPD2_GB_SynP (A2) G1abc.5	A2 Proximal promoter sequence consisting of three times the target sequence for the gRNA-1 DFR (gRNA1) flanked by random sequences.
GB3279	Alpha1_R2:G1aG2b.1:mDFR:luc:t35S	TU for the expression of firefly luciferase driven by a GB_SynP promoter with A1 R2 and A3 mSlDFR parts, and an A2 part containing a target for the gRNA-1DFR (gRNA1) and gRNA-5 DFR (gRNA2).
GB3280	Alpha1_R2:G1ab.1:mDFR:luc:t35S	TU for the expression of firefly luciferase driven by a GB_SynP promoter with A1 R2 and A3 mSlDFR parts, and an A2 part containing the target for the gRNA-1DFR (gRNA1) twice.
GB3281	Alpha1_R2:G1abc:mDFR:luc:t35S	TU for the expression of firefly luciferase driven by a GB_SynP promoter with A1 R2 and A3 mSlDFR parts, and an A2 part containing three times the gRNA-1DFR (gRNA1) target sequence.

GB Code	Part Name	Description
GB3282	Alpha1_R3:G1aG2b.1:mDFR:luc:t35S	TU for the expression of firefly luciferase driven by a GB_SynP promoter with A1 R3 and A3 mSlDFR parts, and an A2 part containing a target for the gRNA-1DFR (gRNA1) and gRNA-5 DFR (gRNA2).
GB3283	Alpha1_R3:G1ab.1:mDFR:luc:t35S	TU for the expression of firefly luciferase driven by a GB_SynP promoter with A1 R3 and A3 mSlDFR parts, and an A2 part containing the target for the gRNA-1DFR (gRNA1) twice.
GB3284	Alpha1_R3:G1abc:mDFR:luc:t35S	TU for the expression of firefly luciferase driven by a GB_SynP promoter with A1 R3 and A3 mSlDFR parts, and an A2 part containing three times the gRNA-1DFR (gRNA1) target sequence.
GB3285	Omega1_R2:G1aG2b.1:mDFR:luc:t35S +P19(TU) +Renilla(TU)	Module for the expression of luciferase driven by a GB_SynP promoter with A1 R2, A3 mSlDFR, and an A2 part containing a target for gRNA1 and gRNA2, and for the constitutive expression of renilla and P19.
GB3286	Omega1_R2:G1ab.1:mDFR:luc:t35S +P19(TU) +Renilla(TU)	Module for the expression of luciferase driven by a GB_SynP promoter with A1 R2, A3 mSlDFR, and an A2 part with the target for gRNA1 twice, and the constitutive expression of renilla and P19.
GB3287	Omega1_R2:G1abc:mDFR:luc:t35S +P19(TU) +Renilla(TU)	Module for the expression of luciferase driven by a GB_SynP promoter with A1 R2, A3 mSlDFR, and an A2 part with three times the target for gRNA1, and the constitutive expression of renilla and P19.
GB3288	Omega1_R3:G1aG2b.1:mDFR:luc:t35S +P19(TU) +Renilla(TU)	Module for the expression of luciferase driven by a GB_SynP promoter with A1 R3, A3 mSlDFR, and an A2 part containing a target for gRNA1 and gRNA2, and for the constitutive expression of renilla and P19.
GB3289	Omega1_R3:G1ab.1:mDFR:luc:t35S +P19(TU) +Renilla(TU)	Module for the expression of luciferase driven by a GB_SynP promoter with A1 R3, A3 mSlDFR, and an A2 part with the target for gRNA1 twice, and the constitutive expression of renilla and P19.
GB3290	Omega1_R3:G1abc:mDFR:luc:t35S +P19(TU) +Renilla(TU)	Module for the expression of luciferase driven by a GB_SynP promoter with A1 R3, A3 mSlDFR, and an A2 part with three times the target for gRNA1, and the constitutive expression of renilla and P19.
GB3317	Alpha1_R1:G1aG2b.7:mDFR:luc:t35S	TU for the expression of firefly luciferase driven by a GB_SynP promoter with A1 R1 and A3 mSlDFR parts, and an A2 part containing a target for the gRNA-1DFR (gRNA1) and gRNA-5 DFR (gRNA2).
GB3318	Alpha1_R1:G1b.1:mDFR:luc:t35S	TU for the expression of firefly luciferase driven by a GB_SynP promoter with A1 R1 and A3 mSlDFR parts, and an A2 part containing a target for the gRNA-1DFR (gRNA1, at "b site").
GB3319	Alpha1_R1:G1e.1:mDFR:luc:t35S	TU for the expression of firefly luciferase driven by a GB_SynP promoter with A1 R1 and A3 mSlDFR parts, and an A2 part containing a target for the gRNA-1DFR (gRNA1, at "e site").

GB Code	Part Name	Description
GB3320	Alpha1_R1:G3aG2b.1:mDFR:luc:t35S	TU for the expression of firefly luciferase driven by a GB_SynP promoter with A1 R1 and A3 mSlDFR parts, and an A2 part containing a target for the gRNA-4 NOS (gRNA3) and gRNA-5 DFR (gRNA2).
GB3321	Alpha1_R1:G1abc.2:mDFR:luc:t35S	TU for the expression of luciferase driven by a GB_SynP promoter with A1 R1 and A3 mSlDFR, and an A2 part with three times the gRNA1-DFR (gRNA1) target sequence.
GB3322	Alpha1_R1:G1abc.3:mDFR:luc:t35S	TU for the expression of luciferase driven by a GB_SynP promoter with A1 R1 and A3 mSlDFR, and an A2 part with three times the gRNA1-DFR (gRNA1) target sequence.
GB3323	Alpha1_R1:G1abc.4:mDFR:luc:t35S	TU for the expression of luciferase driven by a GB_SynP promoter with A1 R1 and A3 mSlDFR, and an A2 part with three times the gRNA1-DFR (gRNA1) target sequence.
GB3324	Alpha1_R1:G1abc.5:mDFR:luc:t35S	TU for the expression of luciferase driven by a GB_SynP promoter with A1 R1 and A3 mSlDFR, and an A2 part with three times the gRNA1-DFR (gRNA1) target sequence.
GB3325	Omega1_R1:G1aG2b.7:mDFR:luc:t35S +P19(TU) +Renilla(TU)	Module for the expression of luciferase driven by a GB_SynP promoter with A1 R1, A3 mSlDFR, and an A2 part containing a target for gRNA1 and gRNA2, and for the constitutive expression of renilla and P19.
GB3326	Omega1_R1:G1b.1:mDFR:luc:t35S +P19(TU) +Renilla(TU)	Module for the expression of luciferase driven by a GB_SynP promoter with A1 R1, A3 mSlDFR, and an A2 part containing a target for gRNA1 (b site) and gRNA2, and for the constitutive expression of renilla and P19.
GB3327	Omega1_R1:G1e.1:mDFR:luc:t35S +P19(TU) +Renilla(TU)	Module for the expression of luciferase driven by a GB_SynP promoter with A1 R1, A3 mSlDFR, and an A2 part containing a target for gRNA1 (e site) and gRNA2, and for the constitutive expression of renilla and P19.
GB3328	Omega1_R1:G3aG2b.1:mDFR:luc:t35S +P19(TU) +Renilla(TU)	Module for the expression of luciferase driven by a GB_SynP promoter with A1 R1, A3 mSlDFR, and an A2 part containing a target for gRNA3 and gRNA2, and for the constitutive expression of renilla and P19.
GB3329	Omega1_R1:G1abc.2:mDFR:luc:t35S +P19(TU) +Renilla(TU)	Module for the expression of luciferase driven by a GB_SynP promoter with A1 R1, A3 mSlDFR, and an A2 part with three times the target for gRNA1, and the constitutive expression of renilla and P19.
GB3330	Omega1_R1:G1abc.3:mDFR:luc:t35S +P19(TU) +Renilla(TU)	Module for the expression of luciferase driven by a GB_SynP promoter with A1 R1, A3 mSlDFR, and an A2 part with three times the target for gRNA1, and the constitutive expression of renilla and P19.

GB Code	Part Name	Description
GB3331	Omega1_R1:G1abc.4:mDFR:luc:t35S +P19(TU) +Renilla(TU)	Module for the expression of luciferase driven by a GB_SynP promoter with A1 R1, A3 mSlDFR, and an A2 part with three times the target for gRNA1, and the constitutive expression of renilla and P19.
GB3332	Omega1_R1:G1abc.5:mDFR:luc:t35S +P19(TU) +Renilla(TU)	Module for the expression of luciferase driven by a GB_SynP promoter with A1 R1, A3 mSlDFR, and an A2 part with three times the target for gRNA1, and the constitutive expression of renilla and P19.
GB3408	pUPD2_mSlCHS	Minimal promoter of slCHS1 gene (Solyc09g091510) containing 62bp upstream the transcription start site and the 5'UTR region.
GB3409	pUPD2_mSlANS	Minimal promoter of slANS gene (Solyc10g076660) containing 62bp upstream the transcription start site and the 5'UTR region.
GB3410	pUPD2_mNtTA29	Minimal promoter of NtTA29 gene containing 62bp upstream the transcription start site and the 5'UTR region (from GB1477 sequence).
GB3411	pUPD2_mAt2S3	Minimal promoter of At2S3 gene containing 84bp upstream the transcription start site and the 5'UTR region (from GB0029 sequence).
GB3412	pUPD2_mNtPCPS2	Minimal promoter of NtPCPS2 gene containing 62bp upstream the transcription start site and the 5'UTR region (from GB1027 sequence).
GB3413	pUPD2_mPcPAF	Minimal promoter of PcPAF gene containing 62bp upstream the transcription start site and the 5'UTR region (from FB029 sequence).
GB3414	pUPD2_mAnGPDA	Minimal promoter of AnGPDA gene containing 62bp upstream the transcription start site and the 5'UTR region (from FB007 sequence).
GB3520	Alpha1_R1:G1abc.1:mSlCHS:luc:t35S	TU for the expression of firefly luciferase driven by a GB_SynP promoter with A1 R1 and A3 mSlCS parts, and an A2 part containing three times the gRNA-1DFR (gRNA1) target sequence.
GB3521	Alpha1_R1:G1abc.1:mSlANS:luc:t35S	TU for the expression of luciferase driven by a GB_SynP promoter with A1 R1, A3 mSlANS, and an A2 part containing three times the gRNA-1DFR (gRNA1) target sequence.
GB3522	Alpha1_R1:G1abc.1:mNtTA29:luc:t35S	TU for the expression of luciferase driven by a GB_SynP promoter with A1 R1, A3 mNtTA29, and an A2 part containing three times the gRNA-1DFR (gRNA1) target sequence.
GB3523	Alpha1_R1:G1abc.1:mAt2S3:luc:t35S	TU for the expression of luciferase driven by a GB_SynP promoter with A1 R1, A3 mAt2S3, and an A2 part containing three times the gRNA-1DFR (gRNA1) target sequence.
GB3524	Alpha1_R1:G1abc.1:mNtPCPS2:luc:t35S	TU for the expression of luciferase driven by a GB_SynP promoter with A1 R1, A3 mNtPCPS2, and an A2 part containing three times the gRNA-1DFR (gRNA1) target sequence.

GB Code	Part Name	Description
GB3525	Alpha1_R1:G1abc.1:mPcPAF:luc:t35S	TU for the expression of luciferase driven by a GB_SynP promoter with A1 R1, A3 mPcPAF, and an A2 part containing three times the gRNA-1DFR (gRNA1) target sequence.
GB3526	Alpha1_R1:G1abc.1:mAnGPDA:luc:t35S	TU for the expression of luciferase driven by a GB_SynP promoter with A1 R1, A3 mAnGPDA, and an A2 part containing three times the gRNA-1DFR (gRNA1) target sequence.
GB3527	Omega1_R1:G1abc.1:mSlCHS:luc:t35S +P19(TU) +Renilla(TU)	Module for the expression of luciferase driven by a GB_SynP promoter with A1 R1, A3 mSlCHS, and an A2 part with three times the target for gRNA1, and the constitutive expression of renilla and P19.
GB3528	Omega1_R1:G1abc.1:mSlANS:luc:t35S +P19(TU) +Renilla(TU)	Module for the expression of luciferase driven by a GB_SynP promoter with A1 R1, A3 mSlANS, and an A2 part with three times the target for gRNA1, and the constitutive expression of renilla and P19.
GB3529	Omega1_R1:G1abc.1:mNtTA29:luc:t35S +P19(TU) +Renilla(TU)	Module for the expression of luciferase driven by a GB_SynP promoter with A1 R1, A3 mNtTA29, and an A2 part with three times the target for gRNA1, and the constitutive expression of renilla and P19.
GB3530	Omega1_R1:G1abc.1:mAt2S3:luc:t35S +P19(TU) +Renilla(TU)	Module for the expression of luciferase driven by a GB_SynP promoter with A1 R1, A3 mAt2S3, and an A2 part with three times the target for gRNA1, and the constitutive expression of renilla and P19.
GB3531	Omega1_R1:G1abc.1:mNtPCPS2:luc: t35S +P19(TU) +Renilla(TU)	Module for the expression of luciferase driven by a GB_SynP promoter with A1 R1, A3 mNtPCPS2, and an A2 part with three times the target for gRNA1, and the constitutive expression of renilla and P19.
GB3532	Omega1_R1:G1abc.1:mPcPAF:luc: t35S +P19(TU) +Renilla(TU)	Module for the expression of luciferase driven by a GB_SynP promoter with A1 R1, A3 mPcPAF, and an A2 part with three times the target for gRNA1, and the constitutive expression of renilla and P19.
GB3533	Omega1_R1:G1abc.1:mAnGPDA:luc: t35S +P19(TU) +Renilla(TU)	Module for the expression of luciferase driven by a GB_SynP promoter with A1 R1, A3 mAnGPDA, and an A2 part with three times the target for gRNA1, and the constitutive expression of renilla and P19.
GB4435	Alpha1_R2:G1ab.1:min2S3:luc:t35S	TU for the expression of firefly luciferase driven by a GB_SynP promoter with A1 R2 and A3 mAt2S3 parts, and an A2 part containing the target for the gRNA-1DFR (gRNA1) twice.
GB4436	Omega1_R2:G1ab.1:min2S3:luc:t35S +P19(TU) +Renilla(TU)	Module for the expression of luciferase driven by a GB_SynP promoter with A1 R2, A3 mAt2S3, and an A2 part with the target for gRNA1 twice, and the constitutive expression of renilla and P19.
GB4437	Alpha1_p35S:HispS:t35S	TU for constitutive expression of HispS enzyme
GB4438	Alpha1_p35S:Luz:t35S	TU for constitutive expression of Luz enzyme
GB4439	Alpha2_p35S:H3H:t35S	TU for constitutive expression of H3H enzyme

GB Code	Part Name	Description
GB4440	Alpha1_R1:G1abc.1:minPCPS2:HispS:t35S	TU for inducible expression of HispS enzyme, using a GB_SynP promoter with one copy of the target sequence for gRNA1 (1x).
GB4441	Alpha1_R1:G1abc.1:minPCPS2:Luz:t35S	TU for inducible expression of Luz enzyme, using a dCasEV-regulated synthetic promoter with one copy of the target sequence for gRNA1DFR (1x).
GB4442	Alpha2_R1:G1abc.1:minPCPS2:H3H:t35S	TU for inducible expression of H3H enzyme, using a dCasEV-regulated synthetic promoter with one copy of the target sequence for gRNA1DFR (1x).
GB4443	Alpha1_R2:G1ab.1:min2S3:HispS:t35S	TU for inducible expression of HispS enzyme, using a dCasEV-regulated synthetic promoter with two copies of the target sequence for gRNA1DFR (2x).
GB4444	Alpha1_R2:G1ab.1:min2S3:Luz:t35S	TU for inducible expression of Luz enzyme, using a dCasEV-regulated synthetic promoter with two copies of the target sequence for gRNA1DFR (2x).
GB4445	Alpha2_R2:G1ab.1:min2S3:H3H:t35S	TU for inducible expression of H3H enzyme, using a dCasEV-regulated synthetic promoter with two copies of the target sequence for gRNA1DFR (2x).
GB4446	Alpha1_R3:G1aG2b.1:minDFR:HispS:t35S	TU for inducible expression of HispS enzyme, using a dCasEV-regulated synthetic promoter with three copies of the target sequence for gRNA1DFR (3x).
GB4447	Alpha1_R3:G1aG2b.1:minDFR:Luz:t35S	TU for inducible expression of Luz enzyme, using a dCasEV-regulated synthetic promoter with three copies of the target sequence for gRNA1DFR (3x).
GB4448	Alpha2_R3:G1aG2b.1:minDFR:H3H:t35S	TU for inducible expression of H3H enzyme, using a dCasEV-regulated synthetic promoter with three copies of the target sequence for gRNA1DFR (3x).
GB4449	Omega1_35S:Luz:t35S+35S:H3H:t35S	Module for the constitutive expression of Luz and H3H enzymes
GB4450	Omega2_35S:HispS:t35S+35S:CPH:tNOS	Module for the constitutive expression of HispS and CPH enzymes
GB4451	Omega1_1x:Luz+1x:H3H	Module for the inducible expression of (1x)Luz and (1x)H3H enzymes
GB4452	Omega1_1x:Luz+2x:H3H	Module for the inducible expression of (1x)Luz and (2x)H3H enzymes
GB4453	Omega1_1x:Luz+3x:H3H	Module for the inducible expression of (1x)Luz and (3x)H3H enzymes
GB4454	Omega1_2x:Luz+1x:H3H	Module for the inducible expression of (2x)Luz and (1x)H3H enzymes
GB4455	Omega1_2x:Luz+2x:H3H	Module for the inducible expression of (2x)Luz and (2x)H3H enzymes
GB4456	Omega1_2x:Luz+3x:H3H	Module for the inducible expression of (2x)Luz and (3x)H3H enzymes
GB4457	Omega1_3x:Luz+1x:H3H	Module for the inducible expression of (3x)Luz and (1x)H3H enzymes
GB4458	Omega1_3x:Luz+2x:H3H	Module for the inducible expression of (3x)Luz and (2x)H3H enzymes

GB Code	Part Name	Description
GB4459	Omega1_3x:Luz+3x:H3H	Module for the inducible expression of (3x)Luz and (3x)H3H enzymes
GB4460	Omega2_1x:HispS+35S:CPH	Module for the inducible expression of (1x)HispS and the constitutive expression of CPH
GB4461	Omega2_2x:HispS+35S:CPH	Module for the inducible expression of (2x)HispS and the constitutive expression of CPH
GB4462	Omega2_3x:HispS+35S:CPH	Module for the inducible expression of (3x)HispS and the constitutive expression of CPH
GB4497	Alpha2_35S:Luz.t35S+35S:H3H:t35S +35S:HispS:t35S+35S:CPH:tNOS	Module for the constitutive expression of Luz, H3H, HispS and CPH enzymes
GB4498	Alpha2_1x:Luz+1x:H3H+1x:HispS +35SCPH	Module for the inducible expression of (1x)Luz, (1x)H3H and (1x)HispS enzymes, and the constitutive expression of CPH
GB4499	Alpha2_1x:Luz+2x:H3H+1x:HispS +35S:CPH	Module for the inducible expression of (1x)Luz, (2x)H3H and (1x)HispS enzymes, and the constitutive expression of CPH
GB4500	Alpha2_1x:Luz+3x:H3H+1x:HispS +35S:CPH	Module for the inducible expression of (1x)Luz, (3x)H3H and (1x)HispS enzymes, and the constitutive expression of CPH
GB4501	Alpha2_2x:Luz+1x:H3H+1x:HispS +35S:CPH	Module for the inducible expression of (2x)Luz, (1x)H3H and (1x)HispS enzymes, and the constitutive expression of CPH
GB4502	Alpha2_2x:Luz+2x:H3H+1x:HispS +35S:CPH	Module for the inducible expression of (2x)Luz, (2x)H3H and (1x)HispS enzymes, and the constitutive expression of CPH
GB4503	Alpha2_2x:Luz+3x:H3H+1x:HispS +35S:CPH	Module for the inducible expression of (2x)Luz, (3x)H3H and (1x)HispS enzymes, and the constitutive expression of CPH
GB4504	Alpha2_3x:Luz+1x:H3H+1x:HispS +35S:CPH	Module for the inducible expression of (3x)Luz, (1x)H3H and (1x)HispS enzymes, and the constitutive expression of CPH
GB4505	Alpha2_3x:Luz+2x:H3H+1x:HispS +35S:CPH	Module for the inducible expression of (3x)Luz, (2x)H3H and (1x)HispS enzymes, and the constitutive expression of CPH
GB4506	Alpha2_3x:Luz+3x:H3H+1x:HispS +35S:CPH	Module for the inducible expression of (3x)Luz, (3x)H3H and (1x)HispS enzymes, and the constitutive expression of CPH
GB4507	Alpha2_1x:Luz+1x:H3H+2x:HispS +35S:CPH	Module for the inducible expression of (1x)Luz, (1x)H3H and (2x)HispS enzymes, and the constitutive expression of CPH
GB4508	Alpha2_1x:Luz+2x:H3H+2x:HispS +35S:CPH	Module for the inducible expression of (1x)Luz, (2x)H3H and (2x)HispS enzymes, and the constitutive expression of CPH
GB4509	Alpha2_1x:Luz+3x:H3H+2x:HispS +35S:CPH	Module for the inducible expression of (1x)Luz, (3x)H3H and (2x)HispS enzymes, and the constitutive expression of CPH

GB Code	Part Name	Description
GB4510	Alpha2_2x:Luz+1x:H3H+2x:HispS +35S:CPH	Module for the inducible expression of (2x)Luz, (1x)H3H and (2x)HispS enzymes, and the constitutive expression of CPH
GB4511	Alpha2_2x:Luz+2x:H3H+2x:HispS +35S:CPH	Module for the inducible expression of (2x)Luz, (2x)H3H and (2x)HispS enzymes, and the constitutive expression of CPH
GB4512	Alpha2_2x:Luz+3x:H3H+2x:HispS +35S:CPH	Module for the inducible expression of (2x)Luz, (3x)H3H and (2x)HispS enzymes, and the constitutive expression of CPH
GB4513	Alpha2_3x:Luz+1x:H3H+2x:HispS +35S:CPH	Module for the inducible expression of (3x)Luz, (1x)H3H and (2x)HispS enzymes, and the constitutive expression of CPH
GB4514	Alpha2_3x:Luz+2x:H3H+2x:HispS +35S:CPH	Module for the inducible expression of (3x)Luz, (2x)H3H and (2x)HispS enzymes, and the constitutive expression of CPH
GB4515	Alpha2_3x:Luz+3x:H3H+2x:HispS +35S:CPH	Module for the inducible expression of (3x)Luz, (3x)H3H and (2x)HispS enzymes, and the constitutive expression of CPH
GB4516	Alpha2_1x:Luz+1x:H3H+3x:HispS +35S:CPH	Module for the inducible expression of (1x)Luz, (1x)H3H and (3x)HispS enzymes, and the constitutive expression of CPH
GB4517	Alpha2_1x:Luz+2x:H3H+3x:HispS +35S:CPH	Module for the inducible expression of (1x)Luz, (2x)H3H and (3x)HispS enzymes, and the constitutive expression of CPH
GB4518	Alpha2_1x:Luz+3x:H3H+3x:HispS +35S:CPH	Module for the inducible expression of (1x)Luz, (3x)H3H and (3x)HispS enzymes, and the constitutive expression of CPH
GB4519	Alpha2_2x:Luz+1x:H3H+3x:HispS +35S:CPH	Module for the inducible expression of (2x)Luz, (1x)H3H and (3x)HispS enzymes, and the constitutive expression of CPH
GB4520	Alpha2_2x:Luz+2x:H3H+3x:HispS +35S:CPH	Module for the inducible expression of (2x)Luz, (2x)H3H and (3x)HispS enzymes, and the constitutive expression of CPH
GB4521	Alpha2_2x:Luz+3x:H3H+3x:HispS +35S:CPH	Module for the inducible expression of (2x)Luz, (3x)H3H and (3x)HispS enzymes, and the constitutive expression of CPH
GB4522	Alpha2_3x:Luz+1x:H3H+3x:HispS +35S:CPH	Module for the inducible expression of (3x)Luz, (1x)H3H and (3x)HispS enzymes, and the constitutive expression of CPH
GB4523	Alpha2_3x:Luz+2x:H3H+3x:HispS +35S:CPH	Module for the inducible expression of (3x)Luz, (2x)H3H and (3x)HispS enzymes, and the constitutive expression of CPH
GB4524	Alpha2_3x:Luz+3x:H3H+3x:HispS +35S:CPH	Module for the inducible expression of (3x)Luz, (3x)H3H and (3x)HispS enzymes, and the constitutive expression of CPH
GB4558	Omega2_eGFP+P19+35S:Luz+ 35S:H3H:t35S+35S:HispS:t35S+ 35S:CPH:tNOS	Module for the constitutive expression of Luz, H3H, HispS, CPH eGFP and P19 proteins

GB Code	Part Name	Description
GB4559	Omega2_eGFP+P19+1x:Luz+1x:H3H +1x:HispS+35S:CPH	Module for the inducible expression of (1x)Luz, (1x)H3H and (1x)HispS enzymes, and the constitutive expression of CPH, eGFP and P19
GB4560	Omega2_eGFP+P19+1x:Luz+2x:H3H +1x:HispS+35S:CPH	Module for the inducible expression of (1x)Luz, (2x)H3H and (1x)HispS enzymes, and the constitutive expression of CPH, eGFP and P19
GB4561	Omega2_eGFP+P19+1x:Luz+3x:H3H +1x:HispS+35S:CPH	Module for the inducible expression of (1x)Luz, (3x)H3H and (1x)HispS enzymes, and the constitutive expression of CPH, eGFP and P19
GB4562	Omega2_eGFP+P19+2x:Luz+1x:H3H +1x:HispS+35S:CPH	Module for the inducible expression of (2x)Luz, (1x)H3H and (1x)HispS enzymes, and the constitutive expression of CPH, eGFP and P19
GB4563	Omega2_eGFP+P19+2x:Luz+2x:H3H +1x:HispS+35S:CPH	Module for the inducible expression of (2x)Luz, (2x)H3H and (1x)HispS enzymes, and the constitutive expression of CPH, eGFP and P19
GB4564	Omega2_eGFP+P19+2x:Luz+3x:H3H +1x:HispS+35S:CPH	Module for the inducible expression of (2x)Luz, (3x)H3H and (1x)HispS enzymes, and the constitutive expression of CPH, eGFP and P19
GB4565	Omega2_eGFP+P19+3x:Luz+1x:H3H +1x:HispS+35S:CPH	Module for the inducible expression of (3x)Luz, (1x)H3H and (1x)HispS enzymes, and the constitutive expression of CPH, eGFP and P19
GB4566	Omega2_eGFP+P19+3x:Luz+2x:H3H +1x:HispS+35S:CPH	Module for the inducible expression of (3x)Luz, (2x)H3H and (1x)HispS enzymes, and the constitutive expression of CPH, eGFP and P19
GB4567	Omega2_eGFP+P19+3x:Luz+3x:H3H +1x:HispS+35S:CPH	Module for the inducible expression of (3x)Luz, (3x)H3H and (1x)HispS enzymes, and the constitutive expression of CPH, eGFP and P19
GB4568	Omega2_eGFP+P19+1x:Luz+1x:H3H +2x:HispS+35S:CPH	Module for the inducible expression of (1x)Luz, (1x)H3H and (2x)HispS enzymes, and the constitutive expression of CPH, eGFP and P19
GB4569	Omega2_eGFP+P19+1x:Luz+2x:H3H +2x:HispS+35S:CPH	Module for the inducible expression of (1x)Luz, (2x)H3H and (2x)HispS enzymes, and the constitutive expression of CPH, eGFP and P19
GB4570	Omega2_eGFP+P19+1x:Luz+3x:H3H +2x:HispS+35S:CPH	Module for the inducible expression of (1x)Luz, (3x)H3H and (2x)HispS enzymes, and the constitutive expression of CPH, eGFP and P19
GB4571	Omega2_eGFP+P19+2x:Luz+1x:H3H +2x:HispS+35S:CPH	Module for the inducible expression of (2x)Luz, (1x)H3H and (2x)HispS enzymes, and the constitutive expression of CPH, eGFP and P19
GB4572	Omega2_eGFP+P19+2x:Luz+2x:H3H +2x:HispS+35S:CPH	Module for the inducible expression of (2x)Luz, (2x)H3H and (2x)HispS enzymes, and the constitutive expression of CPH, eGFP and P19
GB4573	Omega2_eGFP+P19+2x:Luz+3x:H3H +2x:HispS+35S:CPH	Module for the inducible expression of (2x)Luz, (3x)H3H and (2x)HispS enzymes, and the constitutive expression of CPH, eGFP and P19
GB4574	Omega2_eGFP+P19+3x:Luz+1x:H3H +2x:HispS+35S:CPH	Module for the inducible expression of (3x)Luz, (1x)H3H and (2x)HispS enzymes, and the constitutive expression of CPH, eGFP and P19

GB Code	Part Name	Description
GB4575	Omega2_eGFP+P19+3x:Luz+2x:H3H +2x:HispS+35S:CPH	Module for the inducible expression of (3x)Luz, (2x)H3H and (2x)HispS enzymes, and the constitutive expression of CPH, eGFP and P19
GB4576	Omega2_eGFP+P19+3x:Luz+3x:H3H +2x:HispS+35S:CPH	Module for the inducible expression of (3x)Luz, (3x)H3H and (2x)HispS enzymes, and the constitutive expression of CPH, eGFP and P19
GB4577	Omega2_eGFP+P19+1x:Luz+1x:H3H +3x:HispS+35S:CPH	Module for the inducible expression of (1x)Luz, (1x)H3H and (3x)HispS enzymes, and the constitutive expression of CPH, eGFP and P19
GB4578	Omega2_eGFP+P19+1x:Luz+2x:H3H +3x:HispS+35S:CPH	Module for the inducible expression of (1x)Luz, (2x)H3H and (3x)HispS enzymes, and the constitutive expression of CPH, eGFP and P19
GB4579	Omega2_eGFP+P19+1x:Luz+3x:H3H +3x:HispS+35S:CPH	Module for the inducible expression of (1x)Luz, (3x)H3H and (3x)HispS enzymes, and the constitutive expression of CPH, eGFP and P19
GB4580	Omega2_eGFP+P19+2x:Luz+1x:H3H +3x:HispS+35S:CPH	Module for the inducible expression of (2x)Luz, (1x)H3H and (3x)HispS enzymes, and the constitutive expression of CPH, eGFP and P19
GB4581	Omega2_eGFP+P19+2x:Luz+2x:H3H +3x:HispS+35S:CPH	Module for the inducible expression of (2x)Luz, (2x)H3H and (3x)HispS enzymes, and the constitutive expression of CPH, eGFP and P19
GB4582	Omega2_eGFP+P19+2x:Luz+3x:H3H +3x:HispS+35S:CPH	Module for the inducible expression of (2x)Luz, (3x)H3H and (3x)HispS enzymes, and the constitutive expression of CPH, eGFP and P19
GB4583	Omega2_eGFP+P19+3x:Luz+1x:H3H +3x:HispS+35S:CPH	Module for the inducible expression of (3x)Luz, (1x)H3H and (3x)HispS enzymes, and the constitutive expression of CPH, eGFP and P19
GB4584	Omega2_eGFP+P19+3x:Luz+2x:H3H +3x:HispS+35S:CPH	Module for the inducible expression of (3x)Luz, (2x)H3H and (3x)HispS enzymes, and the constitutive expression of CPH, eGFP and P19
GB4585	Omega2_eGFP+P19+3x:Luz+3x:H3H +3x:HispS+35S:CPH	Module for the inducible expression of (3x)Luz, (3x)H3H and (3x)HispS enzymes, and the constitutive expression of CPH, eGFP and P19

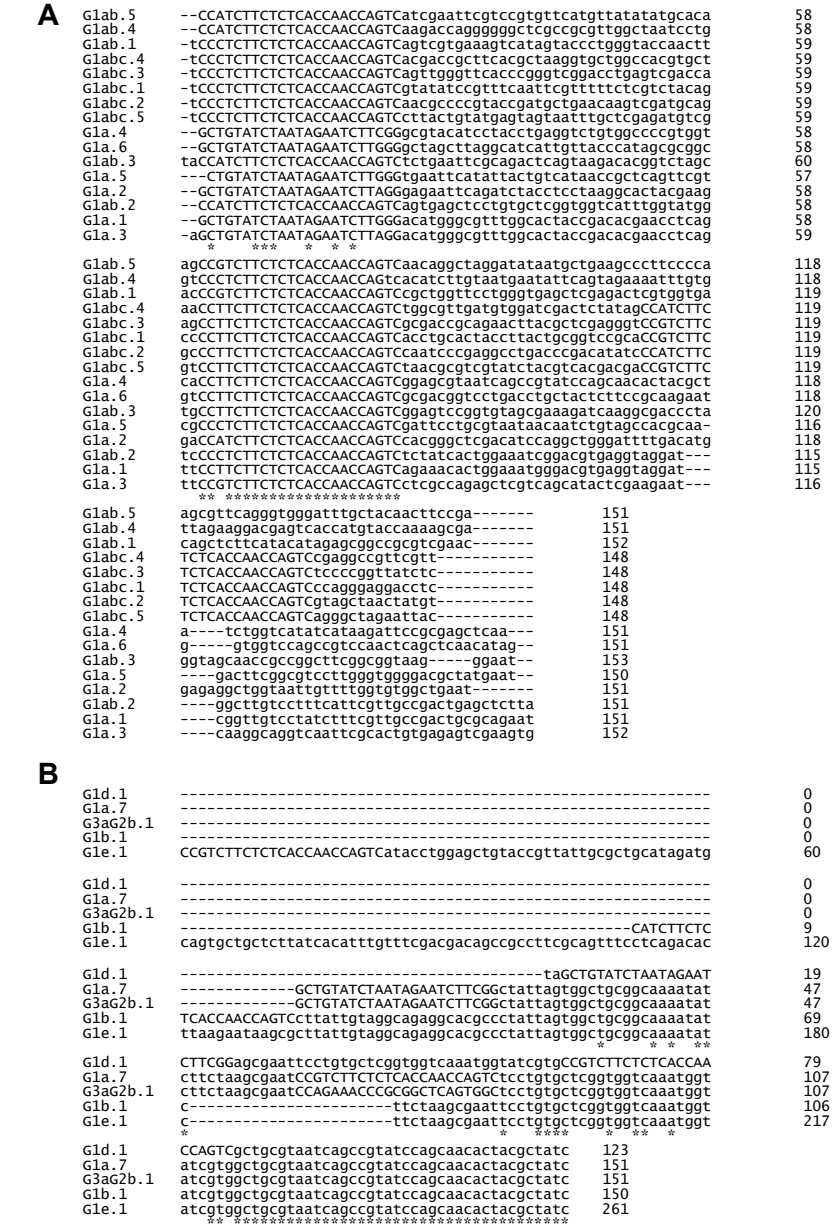

Figure S1. Alignment of A2 parts sequences included in the GB_SynP collection. (A) Alignment of the three A2 parts series including different repetitions of the gRNA1 target (G1a.N, G1ab,N and G1abc.N). (B) Alignment of the A2 part series including the target for gRNA1 at different positions (G1d.1, G1a.7, G1b.1 and G1e.1) and the G3a.1 part that contains the same sequence as G1a.7 but replacing the gRNA1 target by gRNA3 target. Alignments were performed using CLUSTAL-Omega (v1.2.4). Capital letters denote the target sequences for the different gRNAs.

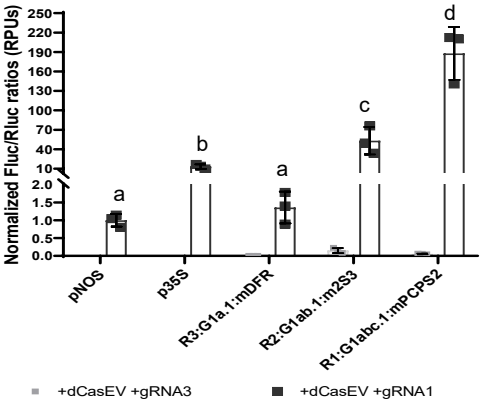

Figure S2. Expression range of the GB_SynP promoters used for regulation of LUZ pathway. Normalized (Fluc/Rluc) expression levels of Nicotiana benthamiana leaves transiently expressing a luciferase reporter gene (Fluc) under the regulation of promoter R3:G1a.1:mDFR (1x gRNA-target), R2:G1ab.1:m2S3 (2x gRNA-target) or R1:G1abc.1:mPCPS2 (3x gRNA-target). Luciferase under *NOS* and CaMV35S promoters (p*NOS* and p*35S*, respectively) were included as references. Letters denote statistically significance between (activated) promoters in a one-way ANOVA (Tukey's multiple comparisons test, $p \leq 0.05$) performed on the log-transformed data. Error bars represent the average values ± SD (n=3).

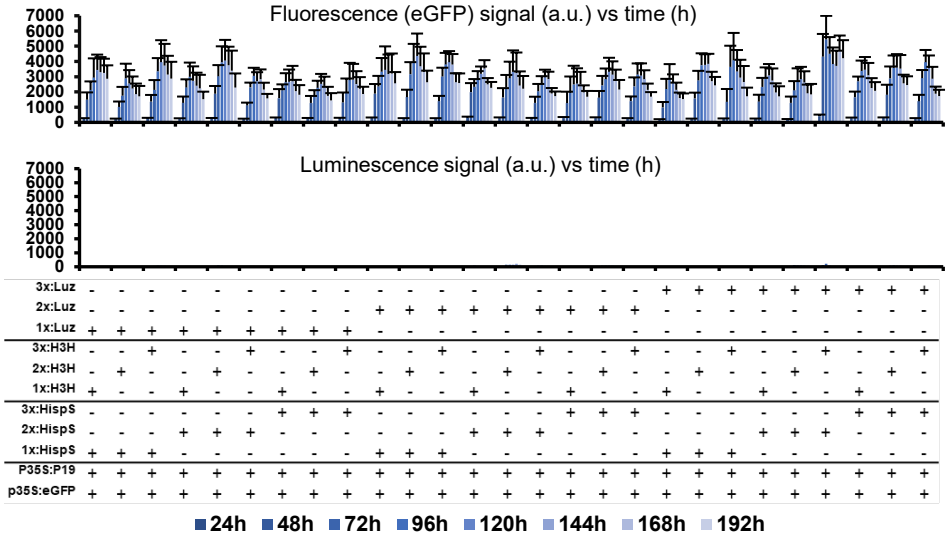

Figure S3. Basal expression of the Time-course experiment including the 27 constructs expressing the LUZ pathway transiently in *Nicotiana benthamiana* leaves under the regulation of 1x, 2x or 3x GB_SynP promoters. Fluorescence and luminescence signals correspond to the co-infiltration in *Nicotiana benthamiana* leaves of each LUZ pathway construct with dCasEV2.1 and an irrelevant gRNA (gRNA3). Error bars represent the average values ± SD (n=12).

CHAPTER III

CHAPTER III

Tunable control of insect pheromone biosynthesis in Nicotiana benthamiana

Kalyani Kallam, **Elena Moreno-Giménez***, Rubén Mateos-Fernández, Connor Tansley, Silvia Gianoglio, Diego Orzáez and Nicola Patron.*

Plant Biotechnology Journal, 2023. DOI: 10.1111/pbi.14048

*These authors contributed equally to this work.

My contribution to this work was essential for its publication. I performed most of the experiments related to transient expression analysis, stable transformations, and the characterization of plants expressing the copper sensing dCasEV2.1 module. I also contributed significantly to manuscript writing. This chapter contains an adapted extract of the published article, focusing on my contribution.

ABSTRACT

Previous work has demonstrated that plants can be used as production platforms for molecules used in health, medicine, and agriculture. Production has been exemplified in both stable transgenic plants and using transient expression strategies. In particular, species of *Nicotiana* have been engineered to produce a range of useful molecules, including insect sex pheromones, which are valued for species-specific control of agricultural pests. To date, most studies have relied on strong constitutive expression of all pathway genes. However, work in microbes has demonstrated that yields can be improved by controlling and balancing gene expression. Synthetic regulatory elements that provide control over the timing and levels of gene expression are therefore useful for maximizing yields from heterologous biosynthetic pathways. In this study, we demonstrate the use of pathway engineering and synthetic genetic elements for controlling the timing and levels of production of Lepidopteran sex pheromones in *Nicotiana benthamiana*. We demonstrate that copper can be used as a low-cost molecule for tightly regulated inducible expression. Further, we show how construct architecture influences relative gene expression and, consequently, product yields in multigene constructs. We compare a number of synthetic orthogonal regulatory elements and demonstrate maximal yields from constructs in which expression is mediated by dCas9-based synthetic transcriptional activators. The approaches demonstrated here provide new insights into the heterologous reconstruction of metabolic pathways in plants.

INTRODUCTION

The reconstruction of biosynthetic pathways in heterologous organisms has become an established route for the production of valuable biomolecules. While recombinant DNA technologies have been in use for decades, recent advances in metabolic engineering and synthetic biology have expanded the breadth and complexity of molecules produced by heterologous biosynthesis (Keating and Young, 2019; Romero-Suarez et al., 2022). Indeed, a major advantage of biological manufacturing is the ability to produce complex molecules, including those for which chemical synthesis has proven difficult or commercially non-viable due to the requirement of multiple stereoselective steps (Cravens et al., 2019). For example, there is growing interest in the biological production of insect sex pheromones for the control of agricultural pests.

The use of chemical formulations to control insect pests in food crops has a long history but the increasing use of synthetic pesticides in the twentieth century led to concerns about the deterioration of biodiversity in agricultural landscapes, as well as risks to farmworkers and consumers (Köhler and Triebskorn, 2013). One alternative is to expand the use of insect sex pheromones, volatile molecules typically produced by females to attract a mate, of which even minute quantities from alternative sources can disrupt breeding and behavior (Mateos-Fernández et al., 2022). However, while the pheromones of some species can be cheaply manufactured by synthetic chemistry, the pheromones of many insect species have complex structures requiring stereoselective steps making them difficult and expensive to produce (Petkevicius et al., 2020). Consequently, there has been increasing interest in the biological synthesis of these molecules (Ding et al., 2014; Holkenbrink et al., 2020; Mateos-Fernández et al., 2022, 2021; Xia et al., 2021).

Most progress in the heterologous biosynthesis of natural products, including pheromones, has been achieved by the engineering of industrially established microbes. However, plant and algal production systems are becoming more widely used (Brodie et al., 2017; Burnett and Burnett, 2020; Stephenson et al., 2020). The use of photosynthetic hosts negates the requirement for sugar feedstocks required by some microorganisms, which, depending on the sources from which they are derived, can raise new issues of sustainability (Dammer et al., 2019; Matthews et al., 2019). Plants can express, fold and post-translationally

modify most eukaryotic proteins. They also produce many metabolic precursors and cofactors allowing the facile reconstruction of metabolic pathways often without the need to engineer host genes and pathways (Patron, 2020; Stephenson et al., 2020).

Tobacco (*Nicotiana tabacum*) and other species in the *Nicotiana* genus are highly amenable to *Agrobacterium*-mediated transformation and, consequently, have become widely used both as model plants for studying gene function and for biotechnology (Bally et al., 2018; Lein et al., 2008; Molina-Hidalgo et al., 2020). *N. benthamiana*, a non-cultivated species native to Australia, has a comparatively short life cycle and does not accumulate much biomass in field conditions. However, it is particularly amenable to *Agrobacterium*-mediated transient expression (agroinfiltration), which has been exploited for the large-scale production of recombinant proteins, including the production of an approved COVID-19 vaccine in Canada (Chen et al., 2013; Hager et al., 2022; Stephenson et al., 2020). In recent years, this method has been applied to the reconstruction of many metabolic pathways, including the production of preparative quantities (Molina-Hidalgo et al., 2020; Reed et al., 2017; Stephenson et al., 2020; van Herpen et al., 2010). Transient production offers many advantages, including a short timeline (less than two weeks) allowing updated construct designs to be rapidly implemented (Chen et al., 2013; Hager et al., 2022; Stephenson et al., 2020). Agroinfiltration also results in the delivery of multiple copies of the synthetic assembly per cell, enabling high yields. While it is possible to produce high levels of recombinant proteins in transplastomic plants, leveraging the multiple nature of plastid genomes, metabolites must be produced in the cellular compartments in which the required precursors are available. Therefore, transgenic approaches to metabolite biosynthesis are mainly limited to the nuclear genome where, to avoid gene silencing, single copy events are preferable. Another advantage of agroinfiltration is that it takes place within contained facilities meaning the lengthy and expensive regulatory processes required for field release of transgenic plants are not required. However, large-scale agroinfiltration has higher energy demands and requires an initial investment in infrastructure. In contrast, transgenic seeds can be easily and cheaply stored and distributed, and transgenic plant lines can be used to produce biomass on an agricultural scale. In particular, *N. tabacum* has been bred for leaf production and

accumulates considerable biomass; it has been estimated that field-grown transgenic tobacco are several-fold more cost-effective than cell culture methods for the production of some recombinant proteins (Conley et al., 2011; Schmidt et al., 2019). However, the identification and assessment of high-yielding, stable transgenic lines can be laborious, and regulatory barriers to field cultivation can add substantial costs. The complex advantages and disadvantages of transient and transgenic approaches make it challenging to determine which strategy will be most cost-effective for large-scale production of a given molecule.

Previous studies have demonstrated proof-of principle for plant production of Lepidopteran sex pheromones. Ding et al. (2014) used transient agroinfiltration of *N. benthamiana* to produce the sex pheromones of small ermine moths, *Yponomeuta evonymella* and *Y. padella*. They were able to detect the major sex pheromone components, *(Z)*-11-hexadecenyl acetate (Z11-16OAc) and *(Z)*-11-hexadecenol (Z11-16OH) and showed that moths were attracted to baits containing the plant-produced molecules. However, they noted that the ratio of pheromone components was not optimal and that adjusting these remained a challenge (Ding et al., 2016a). The ability to tune the relative expression of genes within heterologous pathways might provide the ability to balance metabolic pathways, for example, to control the relative yields of pheromone components, the ratio of which is known to differ between moth species (Zavada et al., 2011). Xia et al., (2022) also used transient agroinfiltration of *N. benthamiana* to produce Z11-16OH and Z11-16OAc, as well as *(Z)*-11-hexadecenal (Z11-16Ald), a component of the pheromone blends of around 200 lepidopteran species. To explore the potential of using plants to disperse pheromones directly into the environment, they also investigated the use of trichome-specific promoters, observing that this led to higher amounts of pheromone components being released from leaves (Xia et al., 2022). Production in stable transgenics has also been demonstrated, with the pheromone biosynthetic pathway encoded on a single T-DNA (Mateos-Fernández et al., 2021). The resulting transgenics accumulated Z11-16OH, Z11-16OAc, and Z11-16Ald, however, plant growth was compromised in transgenic lines producing the highest yields. A subsequent analysis of transcriptional changes revealed stress-like responses, including the downregulation of photosynthesis-related genes (Juteršek et al., 2022). Recent

studies have also investigated the production of sex pheromone precursors in field-grown transgenic *Camelina sativa* (false flax) (Wang et al., 2022).

To date, most efforts to express new pathways in plants have used strong constitutive expression of all pathway genes. However, the use of orthogonal synthetic elements reduces the possibility of unpredictable expression resulting from inadvertent interactions with host machinery (Brophy and Voigt, 2014; Meyer et al., 2019). Further, work in microbial systems has demonstrated that balancing the expression of pathway genes can influence the accumulation of pathway intermediates and precursors and lead to increases in yields (Jones et al., 2015). The availability of characterized regulatory elements and design rules that allow control over expression levels of heterologous pathways is, therefore, highly desirable. For example, impacts on growth and development might be overcome by improvements to construct design that allow the timing and levels of expression to be tuned. Tightly controlled inducible regulatory systems are particularly useful tools. However, to reach the scales required for cost-effective production, any agents used to induce expression must be low-cost and, ideally, usable in open-field systems. In previous work, we showed that synthetic transcriptional activators comprised of translational fusions of the yeast protein, CUP2, which binds to cognate DNA sequences in the presence of copper (Buchman et al., 1989), and the yeast transcriptional activator, Gal4, (Ma and Ptashne, 1987) resulted in strong, copper-inducible activation of minimal synthetic promoters containing CUP2 binding sites (CBSs) (García-Pérez et al., 2022).

Building multigene constructs has been facilitated by parallel assembly methods and toolkits such as Golden Braid (Sarrion-Perdigones et al., 2013; Vazquez-Vilar et al., 2017). However, it remains difficult to design large constructs that behave as desired as genetic context can affect the behavior of synthetic regulatory elements in ways that are poorly understood (Brophy and Voigt, 2014). Further, it has long been known that the repetition of some genetic elements within constructs as well as the insertion of T-DNA as tandem repeats can trigger gene silencing (Stam et al., 1997; Vaucheret et al., 1998). This presents a challenge for designing synthetic circuits in which coordinated expression of multiple genes in response to a single signal is desirable. For transient expression, it is possible to avoid co-assembly onto a single T-DNA by the co-delivery of multiple strains of *A.*

tumefaciens. However, it is unknown what proportion of cells receive all strains and if this affects maximum yields. Further, when producing stable transgenic lines, it is desirable that pathway genes are co-assembled to enable integration into a single genomic locus, preventing segregation in the progeny.

In this study, we prototype synthetic genetic elements and construct designs for the control of metabolite production in plant systems demonstrating their use in the production of Lepidopteran pheromones. We demonstrate and compare synthetic regulatory elements assessing their suitability for pheromone production, simultaneously evaluating if transgenic or transient production methods are likely to provide the best net yields. We show that expression systems inducible by copper (García-Pérez et al., 2022), a relatively low-cost molecule that is readily taken up by plants and registered for field use (Kumar et al., 2021; Mett et al., 1993; Saijo and Nagasawa, 2014) result in tight control of expression but that highest yields are obtained from a dCas9-based system (dCasEV2.1; Selma et al., 2019) using transient agroinfiltration. We also demonstrate that construct architectures affect the expression levels of co-assembled synthetic genes in a sequence-dependent manner. We leverage the positional effects on gene expression in multigene constructs to tune the relative levels of the major pheromone components. In addition, we demonstrate that these positional effects are not observed when production is controlled by copper-inducible dCas9-mediated regulatory elements.

RESULTS

Copper inducible expression of Lepidopteran pheromones

Control over gene expression allows production to be limited to mature plants close to the intended harvest time, limiting effects on plant growth. We therefore tested copper-inducible accumulation of pheromone components, reasoning that copper sulfate is low-cost and already used in agriculture. To do this, we assembled the coding sequences of *AtrΔ11* desaturase from *Amyelois transitella, HarFAR* fatty acid reductase from *Helicoverpa armigera* and *SpATF1-2* diacylglycerol acetyltransferase from *Saccharomyces pastorianus*, all with a minimal 35S promoter preceded by four copies of the CBS (Figure 1A). These three

synthetic genes were then co-assembled with a synthetic gene in which the *A. tumefaciens* nopaline synthase promoter (p*NOS*) was fused to CUP2:GAL4 for moderate constitutive expression (Figure 1A). The resulting multigene construct (construct 678) was agroinfiltrated into *N. benthamiana* leaves in a 1 : 1 ratio with an *Agrobacterium* strain carrying a plasmid encoding the P19 suppressor of silencing (Garabagi et al., 2012). Three days post-infiltration, leaves were sprayed with either water or 2.5 mM copper sulfate ($CuSO_4$), previously identified as the optimal concentration (García-Pérez et al., 2022). The total volatile organic compound (VOC) composition of all samples was analyzed five days post-infiltration by gas chromatography/mass spectrometry (GC/MS). GC peaks corresponding to the pheromone compounds Z11-16OH and Z11-16OAc were detected in samples treated with $CuSO_4$, but not in untreated samples or in control samples infiltrated with P19 alone (Figure 1B). The best yields were obtained from construct 678, estimated at 12.4 µg Z11-16OH g^{-1} fresh weight (FW) and 4.5 µg Z11-16OAc g^{-1} FW.

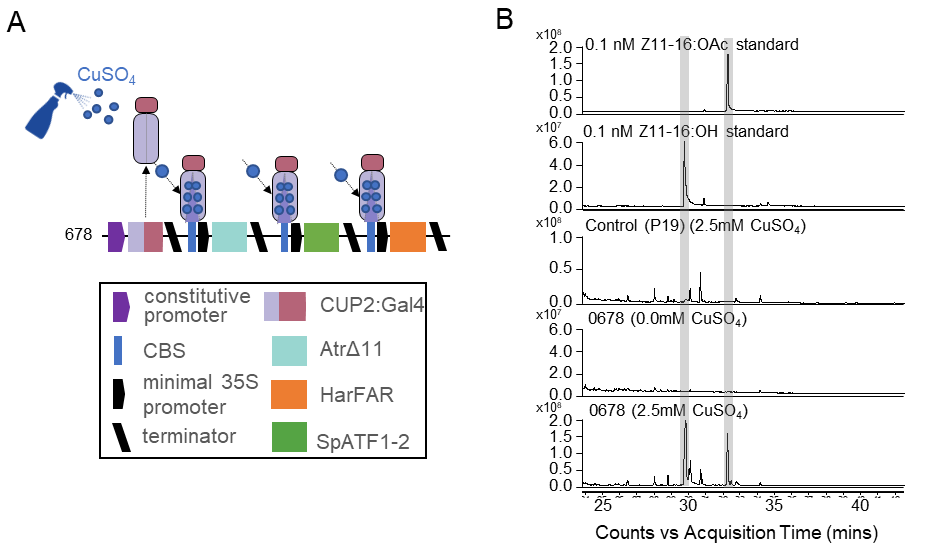

Figure 1. Copper inducible expression of Lepidopteran pheromones. (A) Schematic of a plant expression construct containing synthetic genes encoding the copper-responsive transcription factor CUP2 in translational fusion with the Gal4 activation domain and the coding sequences of *AtrΔ11*, *HarFAR* and *SpATF1*-2 under control of a minimal 35S promoter preceded by four copies of the CUP2 binding site (CBS). (B) Total ion chromatogram showing the accumulation of Z11-16:OH and Z11-16:Oac in leaves of *N. benthamiana* co-infiltrated with *Agrobacterium* strains containing the expression construct (678) and a construct expressing the P19 suppressor of silencing only after application of 2.5 mM copper sulfate ($CuSO_4$).

Construct architecture influences expression and product yield

To determine if and how expression levels of synthetic genes are affected by co-assembly in a multigene construct, we first compared expression in single and multigene assemblies. Initially, we compared the relative expression levels from two luciferase reporters driven by CaMV35S promoters in single and multi-gene configurations (Figure 2A). In multigene configurations, transcription units were assembled on the same strand; constructs in which the two genes were assembled on opposing strands were unstable. We observed that co-infiltration of separate constructs expectedly resulted in equal quantities of each reporter, however, the relative expression within multi-gene constructs was affected by the position of the gene in the assembly, with relatively more expression from the first gene (Figure 2A). To investigate if the same effect is seen with copper-inducible regulatory promoters, we performed equivalent assays with two versions of copper-inducible synthetic promoters. The first version used a minimal 35S promoter preceded by four copies of the CBS. In the second version, the minimal 35S promoter was replaced with a minimal promoter of the *Solanum lycopersicum* NADPH-dependent dihydroflavonol reductase (SlDFR) (García-Pérez et al., 2022). In both cases, luminescence was greater in leaves treated with $CuSO_4$, however, while background expression in the absence of $CuSO_4$ was somewhat lower with the minimal DFR, higher expression was obtained with the minimal 35S promoter (Figure S1). Although less pronounced than with the CaMV35S promoters, expression levels obtained from copper inducible genes were also affected by co-assembly into multigene constructs (Figure 2A). This data demonstrates that relative expression levels measured for individual synthetic genes are not always maintained in multigene constructs, and that the effects are sequence dependent.

From these results, we reasoned that construct architecture would affect yield and product ratios. We therefore investigated if altering the relative position of genes in constructs encoding the pheromone biosynthesis pathway would affect relative expression and thus alter the accumulation of total and relative quantities of Z11-16OH and Z11-16OAc. To do this, we assembled and compared three copper-inducible constructs within which we varied the relative positions of each gene (Figure 2B). Consistent with our observation of reporter genes, we observed variations in both the overall yields and the relative ratios of Z11-16OH and Z11-

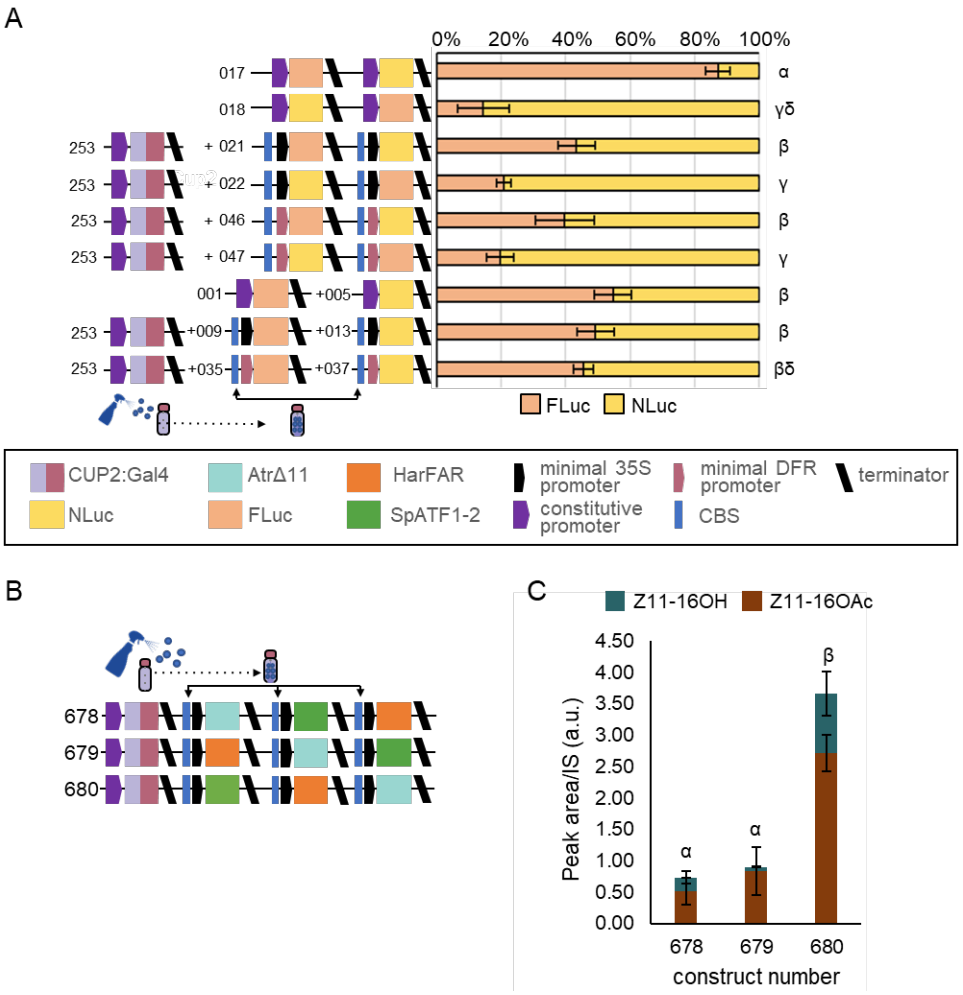

Figure 2. Construct architecture influences expression and product yield. (A) The level of expression of firefly luciferase (Fluc) and nanoluciferase (Nluc) in a multigene construct is dependent on the position in which the gene is assembled. Values shown are the mean and standard error of n=6 biological replicates (independent infiltrations) and differences were analyzed using a Kruskal-Wallis test followed by pairwise Wilcoxon rank sum test with Benjamini-Hochberg correction. Bars annotated with a common Greek letter (α, β, γ, δ) are not significantly different. (B) Schematics of plant expression constructs containing synthetic genes for copper-inducible expression of lepidopteran sex pheromones. (C) The relative positions of pathway genes influenced the overall yield and the relative ratios of pheromone products. Values shown are the mean and standard error of n=3 biological replicates (independent infiltrations). Means annotated with common Greek letters (α, β) are not significantly different by a one-way ANOVA followed by Post-hoc Tukey test at the 5% level of significance.

16Oac components (Figure 2C). The construct configuration with *AtrΔ11* in the last position (construct 680) improved yields threefold.

Copper inducible CRISPR-mediated control of gene expression

The CUP2:GAL4 transcriptional activation system was previously used to control expression of a CRISPR-based programmable activator, enabling tightly-regulated control of the expression of both synthetic and endogenous genes (García-Pérez et al., 2022). In recent years several orthogonal synthetic activators have been demonstrated in plants but have not been directly compared. To determine which synthetic promoters might provide the best levels of activation and background expression levels when combined with copper-inducibility, we compared three previously reported synthetic promoters activated by (i) a transcription activator-like effector (TALE) (Cai et al., 2020b), (ii) a Gal4:ΦC31 fusion protein (Bernabé-Orts et al., 2020; Cai et al., 2020b), and (iii) the dCasEV2.1, which consists of dCas9 fused to the EDLL transcriptional activation domain (Cas9:EDLL), the MS2 phage coat protein fused to a synthetic VPR transcriptional activation domain (MS2:VPR), and a guide RNA (gRNA) that guides the complex to a recognition sequence in the promoter (Selma et al., 2019). Expression of all protein-coding elements was controlled by a copper inducible promoter, except the gRNA, which was controlled by the RNA polymerase III dependent Arabidopsis promoter, U6-26, previously demonstrated to function in *N. benthamiana* (Castel et al., 2019; García-Pérez et al., 2022). All systems were functional with expression increasing with the application of $CuSO_4$ and with the number of binding sites in the synthetic promoter (Figure 3A-C). However, although the maximal expression levels obtained from the TALE and dCasEV2.1 system were similar (Figure 3B and 3C), the expression levels from the TALE system in the absence of copper were considerable and only the dCasEV2.1 system retained low levels of background expression in the absence of copper (Figure 3C).

To investigate if this copper-sensing dCasEV2.1 system would enable control over pheromone biosynthesis, we assembled the coding sequence of each pathway enzyme with a synthetic promoter activated by the dCasEV2.1 system. To reduce the amount of sequence repeated within each transcriptional unit, and therefore minimize the potential for gene silencing, pathway genes were each assembled

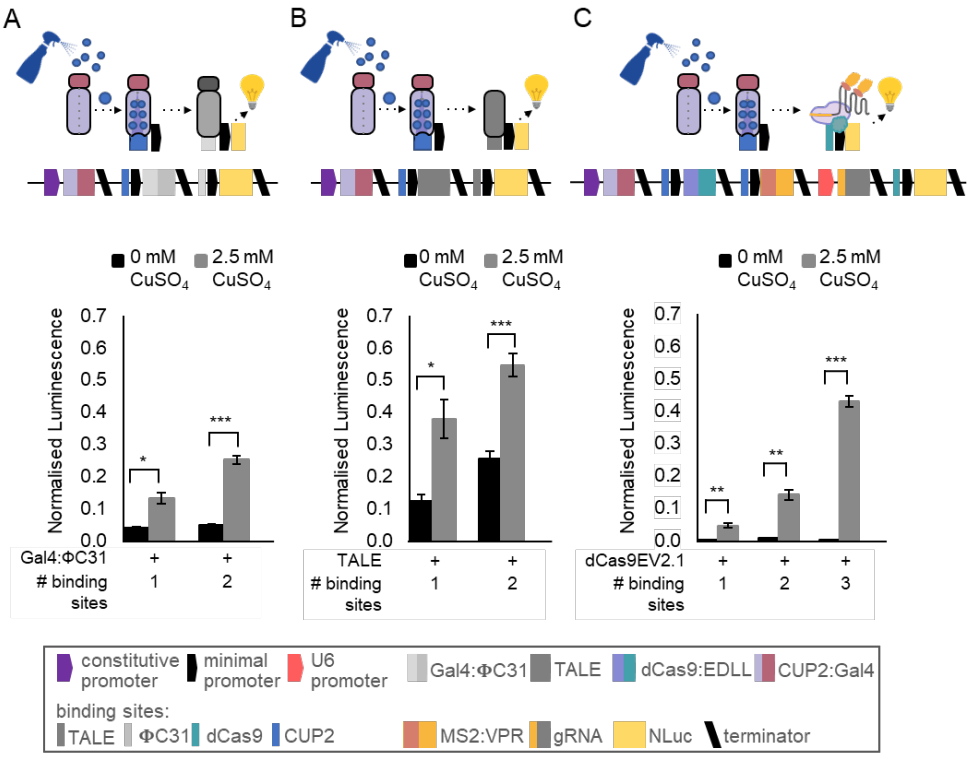

Figure 3. Comparison of synthetic transcriptional activators. Normalized luminescence from reporter constructs activated by copper-inducible (A) GAL4:ΦC31 (B) activator-like effector (TALE) and (C) dCasEV2.1 synthetic transcriptional activators. In all systems, expression levels increase with copper and with the number of transcriptional activator binding sites in the promoter. Copper inducible expression of dCasEV2.1 maintains tight control (low background) of gene expression. Values shown are the mean and standard error of n=3 biological replicates (independent infiltrations). P-values were calculated using Welch two sample t-*test: *P ≤ 0.05, **P ≤ 0.01, ***P ≤ 0.001*.

with synthetic promoters that had minimal sequence similarity (Moreno-Giménez et al., 2022). Each promoter consisted of three parts: a distal region consisting of random sequence unique to each promoter and lacking any known transcription factor binding sites (parts GB2815, GB3269 and GB3270); a proximal region containing three copies of the gRNA recognition site flanked by random sequence (parts GB3275, GB3276 and GB3277); and a constant minimal DFR core region (part GB2566). This design minimized sequence repetition within the multigene

assembly while maintaining activation by a single transcriptional activator. As previously, three assemblies were produced, altering the relative position of each pathway gene (Figure 4A). These constructs were co-infiltrated with the copper-sensing dCasEV2.1 module (GB4070). In contrast to direct copper activation, in which yields were affected by construct architecture (Figure 2C), all constructs produced similar ratios of pheromone components, with slightly more Z11-16OH than Z11-16OAc (Figure 4B), indicating that these regulatory elements might be less affected by co-assembly. Yields obtained using the copper-sensing dCasEV2.1 were estimated to reach 32.7 µg Z11-16OH g^{-1} FW and 25 µg Z11-16OAc g^{-1} FW. We also repeated the entire experiment replacing SpATF1-2 with another acetyltransferase from the yeast *Saccharomyces cerevisiae* (ScATF1), with similar results (Figure S2).

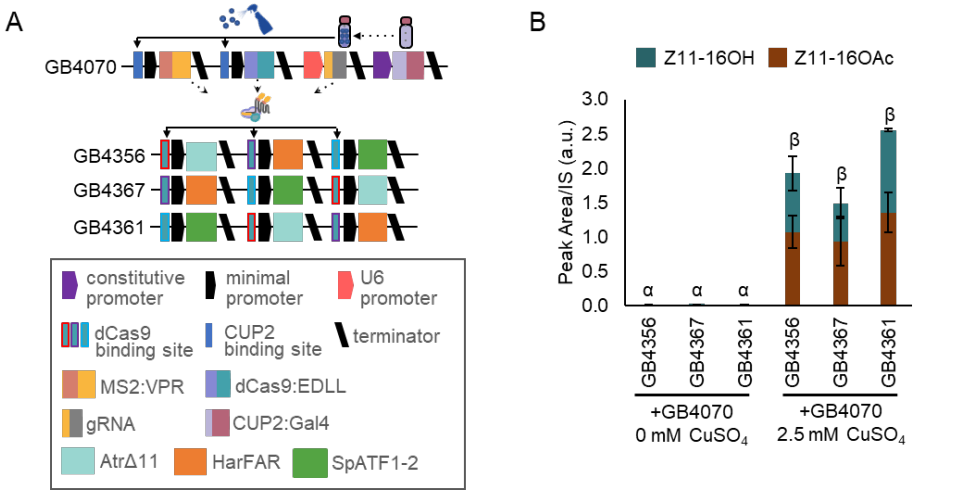

Figure 4. Copper inducible, CRISPR/Cas9-mediated control of pheromone biosynthesis. (A) Schematic of plant expression constructs containing elements for copper inducible expression of the dCasEV2.1 transcriptional activator (above) and multigene constructs containing coding sequences for AtrΔ11, HarFAR and SpATF1-2. The latter are assembled with a promoter consisting of a minimal DFR core promoter fused to unique sequences containing the conserved gRNA target sites. (B) Application of $CuSO_4$ results in dCasEV2.1 mediated production of the pheromone components (Z11-16OH and Z11-16OAc). Values shown are the mean and standard error of n=3 biological replicates (independent infiltrations). Means followed by a common Greek letter (α, β) are not significantly different (one-way ANOVA with post-hoc Tukey HSD at the 5% level of significance).

Copper-inducible expression in stable transgenics

The above transient experiments indicate that copper inducible synthetic elements enable tight control of heterologous pathway genes. This would enable expression to be induced after the accumulation of biomass, potentially limiting effects on plant growth. However, expression levels and pheromone yields obtained from copper-inducible promoters were observed to be reduced as compared to those achieved from constitutive promoters. As the copy number and, therefore, yield is also expected to be reduced in stable transgenics, it is important to quantify potential expression levels in such lines. To investigate expression levels from the copper sensing dCasEV2.1 system in stable transgenics, we produced plants expressing the regulatory components dCas9:EDLL and MS2:VPR under the control of copper-inducible promoters, and the CUP2:GAL4 transcriptional activator under the control of the constitutive nopaline synthase (*NOS*) promoter (Figure 5A). The resulting plant lines provide a modular, reusable resource that could be crossed with lines expressing synthetic pathways driven by orthogonal promoters with binding sites for one or more co-expressed single guide RNAs (gRNA). To identify high-performing lines, we infiltrated ten independent T_0 plants with constructs encoding firefly luciferase (Fluc) under the control of the previously tested synthetic promoter with three recognition sites for the gRNA and the gRNA, together with a constitutively expressed Renilla luciferase (RLuc) calibrator gene. Three leaves of each plant were infiltrated and 0.0 mM $CuSO_4$ or 2.5 mM $CuSO_4$ were applied to each side of the midrib. Protein was extracted and dual luciferase assays were used to quantify expression. Expression was compared to non-transgenic lines in which all components were transiently expressed (Figure 5B). One line, CBS:dCas4, was identified in which 2.5 mM $CuSO_4$ resulted in a significant increase in expression. Expression from stable transgenics was considerably less (~85 fold) than from plants in which all constructs were transiently expressed, presumably due to the reduced availability of dCasEV2.1 components (Figure 5B). To confirm this, T1 seed from three lines were collected and RNA was extracted from plants treated with 0.0 mM $CuSO_4$ or 2.5 mM $CuSO_4$. The expression levels of dCas9:EDLL and MS2:VPR were quantified by qRT-PCR, finding that mRNA levels correlated with luminescence (Figure S3). These data indicate that, while the copper-sensing dCasEV2.1 system is functional

when integrated into the plant genome, stable transgenic lines are unlikely to produce useful levels of pheromones.

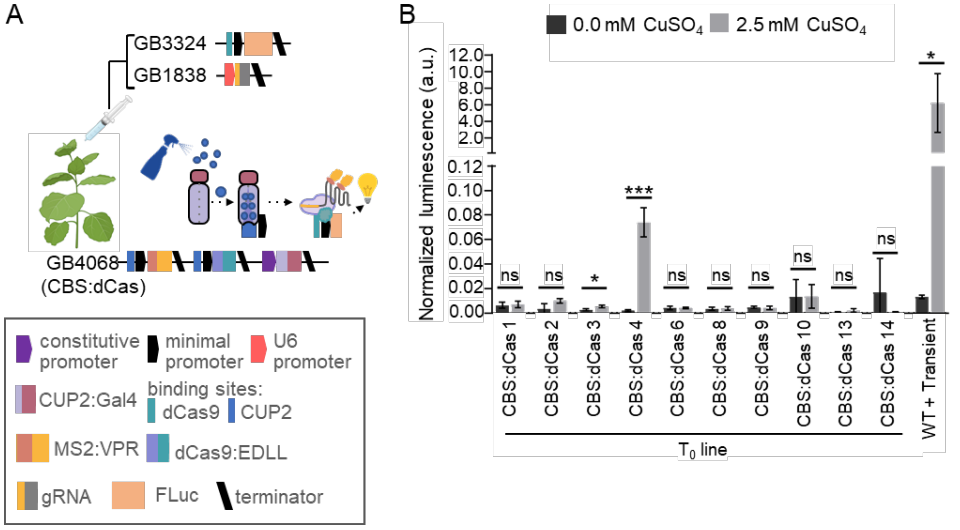

Figure 5. Functionality of the copper sensing dCasEV2.1 module in stable *Nicotiana benthamiana* transgenics. (A) Transgenic plants expressing the CBS:dCasEV2.1 (construct GB4068) were agroinfiltrated with a luciferase reporter module (construct GB3324) and gRNA module (construct 1838). (B) Normalized expression levels of luciferase in T_0 CBS:dCas transgenic plants after copper induction. Values are the mean and standard deviation of n=3 independent infiltrations. P-values were calculated using Student's t-*test; * P ≤ 0.05, *** P ≤ 0.001*; ns= not significant. The figure includes images from Biorender (117ortune117r.com).

DISCUSSION

Plants, particularly species of *Nicotiana*, are emerging as useful platforms for heterologous production of a range of small molecules for health, industry and agriculture (Brückner and Tissier, 2013; Dudley et al., 2022; Mateos-Fernández et al., 2021; Mikkelsen et al., 2010; Reed et al., 2017; Schultz et al., 2019; Stephenson et al., 2020; van Herpen et al., 2010). Metabolic engineering in microbial systems has demonstrated that optimization of expression constructs to balance pathways and engineering host metabolism can strongly influence yields, (Jensen and Keasling, 2014; Jones et al., 2015). In particular, the use of orthogonal synthetic elements improves the predictability of engineered circuits (Brophy and Voigt,

2014; Meyer et al., 2019). Such elements also provide the ability to control the timing and levels of expression to limit impacts on growth and development, as well as the ability to tune the relative expression of genes within heterologous pathways to enable pathway balancing. However, to date, heterologous pathway reconstruction in plants has largely been limited to constitutive overexpression.

In this study we used a number of synthetic genetic regulatory elements to control the production of moth sex pheromones. Several studies have reported the production of Lepidopteran sex pheromones in heterologous systems including yeast (Hagström et al., 2013; Holkenbrink et al., 2020; Konrad et al., 2017; Petkevicius et al., 2020) and *N. benthamiana* (Ding et al., 2014; Mateos-Fernández et al., 2021; Xia et al., 2022, 2020). To produce the Z11-16OAc component, previous studies have used acetyl transferases from either plants (Ding et al., 2014; Mateos-Fernández et al., 2021) or yeast (Ding et al., 2016ª; Xia et al., 2022). Here we studied the use of yeast enzymes for pathway reconstruction with a number of different regulatory elements to enable transient and transgenic expression in *N. benthamiana*.

Both transient and transgenic approaches have been demonstrated for expressing heterologous molecules. Both strategies are, in principle, capable of being scaled for large-scale production. Large-scale transient expression requires more costly infrastructure than field-growth of transgenic lines and, being limited to young plants, cannot achieve high-biomass at low production cost. However, agroinfiltration has a short timeframe, high copy-number (and therefore yield per gram of biomass). In addition, there is no requirement to identify and characterize specific high-yielding lines, or for the expensive regulatory approval required for field growth. The economics of scaling-up production are likely to be different for different molecules and there is merit in comparing production methods. In previous experiments, we observed that the growth of transgenic lines of *N. benthamiana* producing the highest yields (per gram fresh weight) of moth pheromones was negatively affected and photosynthesis-related genes were downregulated (Juteršek et al., 2022; Mateos-Fernández et al., 2021). Inducible gene expression systems are essential tools commonly employed to switch metabolism from growth to production, enabling biomass to accumulate before energy is redirected into the biosynthesis of desired products. Many inducible

systems for controlling gene expression in plants use expensive molecules such as estradiol or dexamethasone, or require the application of stresses such as heat or wounding, which cannot easily be applied to large numbers of plants and may affect plant fitness (Corrado and Karali, 2009). Expression systems inducible by $CuSO_4$, a relatively low-cost molecule that is readily taken up by plants and registered for field use, have also been demonstrated (Kumar et al., 2021; Mett et al., 1993; Saijo and Nagasawa, 2014). In previous work, we optimized a copper-inducible system demonstrating that this enabled high levels of expression of reporter and endogenous genes in *N. benthamiana* and, in the absence of copper, very low background expression (García-Pérez et al., 2022). The range of concentrations at which copper is active as a signaling molecule is much lower than those employed for antifungal applications in field conditions, therefore the employment of copper sulfate as a trigger for recombinant gene expression could be compatible with the current reduction trend in copper-based antifungal formulations. Here, we demonstrate that this system is suitable for controlling the expression of biosynthetic pathways (Figure 1). As $CuSO_4$ is approved for agricultural use, it provides a possible tool for large-scale bioproduction systems.

Modular cloning systems have facilitated the design and assembly of multigene constructs (Pollak et al., 2019; Sarrion-Perdigones et al., 2011; Weber et al., 2011). However, only a few studies have sought to quantify how co-assembly affects the performance of synthetic genes. In mammalian systems it has been observed that the upstream genes in multigene constructs have dominant expression, a phenomenon proposed to be caused by positive supercoiling accumulating downstream and limiting RNA polymerase binding and initiation of the downstream gene (Johnstone and Galloway, 2022). It was also shown that the extent to which the expression levels of downstream genes are negatively impacted by co-assembly may correlate with strength of expression of the upstream gene (Patel et al., 2021). Using ratiometric reporter assays, we found that the position in which genes are located within multigene plant constructs also differentially affects their expression (Figure 2). The effects were similar to those observed in mammalian cells, with expression being reduced in the downstream gene and most obvious with strong constitutive promoters. In this study, rather than attempting to avoid the unequal expression from co-assembled, copper-inducible genes, we investigated whether the different levels of expression could

be used to alter the product profile obtained from our biosynthetic pathway. We found that changing the relative position of each pathway gene within the construct altered both overall yield and the relative quantities of the major pheromone components (Figure 2C).

We also coupled copper-inducible to a CRISPR-based programmable activator, dCasEV2.1, previously shown to enable tightly-regulated upregulation of endogenous genes (García-Pérez et al., 2022). Compared to TALE and PhiC3-based synthetic regulatory elements, dCasEV2.1 had low to undetectable background expression in the absence of copper (Figure 3). Further, the gRNA binding sites could be positioned within different unique promoter sequences to avoid repeating sequence elements within multigene constructs. The yield from these assemblies was comparable to copper-inducible promoters but were not affected by combinatorial rearrangements (Figure 4). This may be because expression from the copper sensing dCasEV2.1 system was low, however, we also considered if the lack of repetitive sequences could explain this. It has long been known that gene-silencing can reduce expression from transgenes and that some regulatory elements and construct architectures (e.g. the inclusion of inverted repeats) are more susceptible (Stam et al., 1997; Vaucheret et al., 1998). However, it is unclear why transcripts from a downstream gene would be preferentially silenced in constructs in which expression was affected by relative position. Another explanation may be that transcriptional readthrough from a strong promoter coupled to an insufficient terminator might have exacerbated supercoiling. Transcriptional readthrough has also been observed to cause the generation of small interfering RNAs (F de Felippes et al., 2020). However, it is unclear why only the dCasEV2.1 regulated constructs would be unaffected. Further studies with multiple different promoter and terminator combinations are required to investigate how genes in large and complex constructs behave and to determine the best construct architectures for multigene constructs. This will be especially important as more information emerges about the impact of different regulatory elements, including the effects of untranslated sequences and terminators on expression and post-transcriptional silencing (F de Felippes et al., 2020; Wang et al., 2020). It may also be possible to achieve more equal levels of expression by testing the efficacy of insulator sequences that have been used to reduce the

effects of genomic locations on transgene expression (Pérez-González and Caro, 2019).

In previous studies we observed that constitutive expression impacts biomass (Juteršek et al., 2022; Mateos-Fernández et al., 2021). Although yields obtained using copper sensing dCasEV2.1 system in transient infiltration were lower (estimated at 32.7 µg Z11-16OH g^{-1} FW and 25 µg Z11-16OAc g^{-1} FW), than those that we obtained using CaMV35S promoter (estimated at 116.6 µg Z11-16OH g^{-1} FW and 110.1 µg Z11-16OAc g^{-1} FW), a lower yield per unit of biomass might be compensated for by high biomass production. We therefore assessed how expression levels from copper inducible promoters in stable transgenics compared to transient agroinfiltration. We found that transgenic lines expressing the copper inducible elements had up to 85-fold reduction in expression (Figure 5). We do not consider these expression levels to be viable for pheromone production and conclude that alternative field-compatible, inducible expression systems must be tested or developed. Pheromone yields from alternative species in which production is limited to specific organs might also be tested. For example, precursors of Lepidopteran sex pheromones have recently been produced in the seeds of field-grown transgenic *Camelina sativa* (false flax) (Wang et al., 2022).

Following a comparison of the three orthogonal regulatory systems (Figure 3), in our lab we also tested pheromone production using constitutive dCasEV2.1 regulatory elements (see Kallam et al., 2023, the published version of this chapter, and Mateos-Fernández PhD dissertation). This resulted in the highest yields, estimated at 384.4 µg Z11-16OH/g FW and 175.8 µg Z11-16OAc/g FW in transient expression. These titers are in the same range as previously reported transient expression experiments (381 µg/g Z11-16OH FW by Ding et al. (2014); 335 µg/g Z11-16OH FW by Xia et al. (2020). However, we note that the titers in those studies were obtained using absolute quantification based on solvent extractions. Yields are, expectedly, greater than those reported from stable transgenics (164.9 µg Z11-16OH/g FW and 9.6 µg Z11-16OAc/g FW) (Mateos-Fernández et al., 2021). As noted above, the dCasEV2.1 system has the additional advantage of using unique promoter sequences while maintaining activation to a single transcriptional activator, which negates positional effects (Figure 4). Finally, it is worth mentioning that our lab also tested dCasEV2.1 activation of stable

transgenes to investigate if maintaining an abundance of transcriptional activators could maintain high yields. In these experiments (see Kallam et al., 2023 and Mateos-Fernández PhD dissertation), the maximum yields obtained from T1 lines were approximately reduced ~20-fold, suggesting that transgenic production may be viable if coupled with a system to enable high level, inducible expression of dCasEV2.1 elements.

The potential of plants as living bioemitters of pheromones has previously been discussed (Mateos-Fernández et al., 2022) and trichome-specific promoters have recently shown to increase the release of pheromones from leaves (Xia et al., 2022). However, pheromone components can be extracted from plant biomass for use in existing pheromone dispenser systems. Therefore, yield, sustainability, and cost of biosynthesis are the main considerations. From our experiments, we consider that dCasEV2.1 mediated transient agroinfiltration is currently the best method for plant-based metabolite production. This provides the highest yields and enables predictable and equal expression from genes within multigene constructs. Further, when coupled with the relatively short timeline for production and the ability to rapidly prototype and implement new construct designs, this provides great potential for biomanufacturing. Further, the gene regulatory systems demonstrated here and developed as modular genetic elements for facile reuse, are not limited to controlling pheromone biosynthesis, but are broadly useful to the design of constructs for plant metabolic engineering.

MATERIALS AND METHODS

Assembly of expression constructs

All constructs were assembled using the GoldenBraid (GB) cloning system (Sarrion-Perdigones et al., 2013; Vazquez-Vilar et al., 2017). Standardized DNA parts (promoters, coding sequences, and terminators) were cloned as Level 0 parts using the GoldenBraid (GB) domestication strategy described by Sarrion-Perdigones et al. (2013). Transcriptional units (Level 1) were then assembled in parallel, one-step restriction-ligation reactions and transformed into bacteria as previously described (Cai et al., 2020a). Hierarchical stepwise assembly of

transcriptional units into multigene constructs was achieved using binary assembly via BsaI or BsmBI-mediated restriction ligation as defined by the GB system. GB constructs employed in this study are provided in Supplementary Table S1 and have been deposited at Addgene. Details of GB constructs are also available at https://gbcloning.upv.es/.

Transient expression in *N. benthamiana*

N. benthamiana plants were grown in a controlled environment room with 16 hr light, 8 hr hours dark, 22℃, 80% humidity, ~200 µmol/m^2/s light intensity. Expression constructs were transformed into electrocompetent *Agrobacterium tumefaciens* GV3101. *A. tumefaciens* strains harboring the expression constructs were grown in LB medium supplemented with 50 µg/mL kanamycin or spectinomycin and 50 µg/mL rifampicin for 16 hours at 28℃/250 rpm. Overnight saturated cultures were centrifuged at 3,400 x *g* for 30 min at room temperature and cells were resuspended in infiltration medium (10 mM 2-(N-morpholino)ethanesulfonic acid (MES) pH 5.7, 10 mM $MgCl_2$, 200 µM 3',5'-Dimethoxy-4'-hydroxyacetophenone (acetosyringone)) and incubated at room temperature for 2-3 hours with slow shaking. Healthy plants (29-37 days old) with 3-4 fully expanded true leaves were infiltrated on the abaxial side of the leaf using a 1 mL needleless syringe and grown for five days in a growth chamber with 16 hr light, 8 hr hours dark at 22℃ and 120-180 µmol/m^2/s light intensity. Infiltrated leaves were treated with 2.5 mM copper sulfate by spray at three days post infiltration. The spray was applied to both the adaxial and abaxial surfaces of the leaf. All chemical compounds were purchased from Sigma-Aldrich (St. Louis, MO).

Production of transgenic *N. benthamiana*

Constructs were transformed into *A. tumefaciens* strain LBA4404. Cells were collected from saturated cultures grown from a single colony and grown overnight to OD600 of 0.2 in TY medium (10 g L^{-1} tryptone, 5 g L^{-1} yeast extract, and 10 g L^{-1} NaCl, pH 5.6) supplemented with 2 mM MgSO4·7H2O, 200 µM acetosyringone and the appropriate antibiotics (Horsch et al., 1985). Leaves were harvested from immature, non-flowering plants, and surface sterilized. Leaf discs were cut using a 0.8-1.2 cm cork borer and transferred to co-cultivation media (MS medium with Phytoagar 9 g L^{-1}, supplemented with vitamins enriched with 1 mg L^{-1} 6-

benzylaminopurine and 0.1 mg L^{-1} naphthalene acetic acid). After 24 hours, the discs were incubated within the *A. tumefaciens* culture for 15 minutes and placed abaxial side down back on co-cultivation media. After two days, explants were transferred to selection medium (MS pH 5.8 with Phytoagar 9 g L^{-1}, supplemented with Gamborg's B5 vitamins, 1 mg L^{-1} 6-benzylaminopurine, 0.1 mg L^{-1} naphthalene acetic acid, and 100 mg L^{-1} kanamycin). Explants were sub-cultured at 14-day intervals and shoots were transferred to rooting medium (MS salts and Phytoagar 9 g L^{-1}, supplemented with Gamborg's B5 vitamins and 100 mg L^{-1} kanamycin). Plantlets were transferred to soil and grown in a greenhouse (16 h light, 24 °C : 8 h dark, 20 °C).

Quantification of reporter gene expression

Luciferase expression was detected using the Nano-Glo® Dual-Luciferase® reporter assay system (Promega, Madison, WI, USA). Two 8 mm-diameter discs per infiltrated leaf were homogenized in180 µL passive lysis buffer (Promega) containing protease inhibitor (P9599, Sigma-Aldrich, Dorset, UK). Following incubation on ice for 15 min and centrifugation (100 × *g*, 2 min, 4°C), the supernatant was diluted to a 1:5 dilution. 10 µL of the dilution was mixed with 20 µL of passive buffer which was then mixed with 30 µL ONE-Glo™ EX Luciferase Assay Reagent (Promega) and incubated at room temperature for 10 min. Fluc luminescence was detected using either a GloMax 96 Microplate Luminometer (Promega) or a Clariostar microplate reader (BMG Labtech, Aylesbury, UK) with a 10 s read time and 1 s settling time. Nluc luminescence was detected from the same sample by adding 30 µL NanoDLR™ Stop & Glo® Reagent (Promega). After incubation for 10 min at room temperature, luminescence was detected as above. To calculate the proportion of expression from each reporter, luminescence from firefly luciferase (Fluc) was scaled to the nanoluciferase (Nluc) signal by an experimentally determined factor obtained from expression from single gene Nluc and Fluc constructs. Normalized (relative) expression levels of synthetic promoters were obtained as previously described (Cai et al., 2021) and are reported as the ratio of luminescence from the test promoter (Nluc) to the calibrator promoter (Fluc), normalized to the luminescence of an experiment control Nluc/Fluc expressed from calibrator promoters.

Metabolite extraction and quantification

Standards, extraction methods and analysis of pheromone compounds were as previously described (Mateos-Fernández et al., 2021). Briefly, synthetic samples of Z11-16OH were obtained as described by Zarbin et al. (2007) and purified by column chromatography using silica gel and a mixture of hexane : Et2O (9 : 1 to 8 : 2) as an eluent. Acetylation of Z11-16OH was carried out using acetic anhydride (1.2 eq) and trimethylamine (1.3 eq) as a base in dichloromethane (DCM). For biological samples, 8 mm leaf disks were snap frozen in liquid nitrogen and ground to a fine powder. 50 mg of frozen powder was transferred to 10 mL headspace vials and stabilized with 1 mL 5M $CaCl_2$ and 150 µL 500 mM EDTA (pH=7.5). Tridecane was added to a final concentration of 10 ppb for use as an internal standard and vials were bath-sonicated for 5 minutes. For volatile extraction, vials were incubated at 80°C for 3 minutes with 500 rpm agitation, after which the volatile compounds were captured by exposing a 65 µm polydimethylsiloxane/divinylbenzene (PDMS/DVB) SPME fiber (Supelco, Bellefonte, PA) to the headspace of the vial for 20 minutes. Volatile compounds were analyzed using a 6890 N gas chromatograph (Agilent Technologies, Santa Clara, CA) with a DB5ms (60 m, 0.25 mm, 1 µm) J&W GC capillary column (Agilent Technologies) with helium at a constant flow of 1.2 mL min^{-1}. Fiber was desorbed for 1 minute in the injection port at 250°C and chromatography was performed with an initial temperature of 160°C for 2 min, 7°C min^{-1} ramp until 280°C, and a final hold at 280°C for 6 minutes. All pheromone values were divided by the tridecane value of each sample for normalization.

SUPPLEMENTARY MATERIAL

Table S1. Constructs used in this study.

Plasmid Code	Contents	Addgene Code and Reference	Description
GB1203	35s:P19:NOS	#68214 (Sarrion-Perdigones et al., 2013)	Transcriptional unit for constitutive expression of the silencing suppressor P19 driven by the 35s promoter.
253 (pEPKKα1KN0253)	pNos+TMVΩ:CUP2: Gal4:35s	#187560 (this study)	Transcriptional unit for constitutive expression of CUP2:GAL4 driven by the NOS promoter.
021 (pEPCTΩSP0021)	CBS:Fluc (forward):35s + CBS:Nluc (forward)	#187561 (this study)	Module for copper-inducible expression of firefly luciferase and nanoluc luciferase driven by minimal synthetic promoters with binding sites for CUP2.
022 (pEPCTΩSP0022)	CBS:Nluc (forward):35s + CBS:Fluc:35s (forward)	#187562 (this study)	Module for copper-inducible expression of nanoluc luciferase and firefly luciferase driven by minimal synthetic promoters with binding sites for CUP2.
009 (pEPCTαKN009)	CBS:Fluc:35s	#187563 (this study)	Transcriptional unit for copper-inducible expression of firefly luciferase driven by a minimal synthetic promoter with binding sites for CUP2.
013 (pEPCTαKN013)	CBS:Nluc (forward):35s	#187564 (this study)	Transcriptional unit for copper-inducible expression of nanoluc luciferase driven by a minimal synthetic promoter with binding sites for CUP2.
017 (pEPCTΩSP0017)	35s:Fluc (forward):35s + 35s:Nluc (forward)	#187565 (this study)	Module for constitutive expression of firefly luciferase and nanoluc luciferase driven by 35s promoters.
018 (pEPCTΩSP0018)	35s:Nluc (forward):35s + 35s:Fluc (forward)	#187566 (this study)	Module for constitutive expression of nanoluc luciferase and firefly luciferase driven by 35s promoters.
019 (pEPCTΩSP0019)	35s:Fluc (forward):35s + 35s:Nluc (reverse)	#187567 (this study)	Module for constitutive expression of firefly luciferase and nanoluc luciferase driven by 35s promoters.
001 (pEPCTαKN001)	35S:Fluc:35S	#187568 (this study)	Transcriptional unit for constitutive expression of firefly luciferase driven by the 35s promoter.
005 (pEPCTαKN005)	35S:Nluc:35S	#187569 (this study)	Transcriptional unit for constitutive expression of nanoluc luciferase driven by the 35s promoter.

Plasmid Code	Contents	Addgene Code and Reference	Description
GB UA 114 A	35S:Gal4:PhiC31:35S	#187570 (Vazquez-Vilar et al., 2017)	Transcriptional unit for constitutive expression of Gal4:ΦC31 driven by the 35s promoter.
pEPKKα2KN0100	2xOpattB-min 35S:Nluc:g7	#154621 (Cai et al., 2020)	Transcriptional unit for Gal4:ΦC31-activated expression of nanoluciferase.
pEPKKα2KN0101	4xOpattBt-min 35S:Nluc:g7	#154622 (Cai et al., 2020)	Transcriptional unit for Gal4:ΦC31-activated expression of nanoluciferase.
pEPKKα2KN0102	6xOpattBt-min 35S:Nluc:g7	#154623 (Cai et al., 2020)	Transcriptional unit for Gal4:ΦC31-activated expression of nanoluciferase.
pEPKKα1RKN0115	pNos:TALE:35S	#187571 (Cai et al., 2020)	Transcriptional unit for constitutive expression of a TALE driven by the NOS promoter.
pEPKKα2KN0091	1xTALEbs-min 35S:Nlucc:g7	#154618 (Cai et al., 2020)	Transcriptional unit for TALE-activated expression of nanoluciferase.
pEPKKα2KN0092	2xTALEbs-min 35S:Nlucc:g7	#154619 (Cai et al., 2020)	Transcriptional unit for TALE-activated expression of nanoluciferase.
pEPKKα2KN0093	4xTALEbs-min 35S:Nlucc:g7	#154620 (Cai et al., 2020)	Transcriptional unit for TALE-activated expression of nanoluciferase.
GB2085	35s:Ms2VPR:nos + 35s:dCas9:EDLL:NOS	#160645 (Selma et al.,2019)	Module for the expression of dCas9 fused to EDLL and Ms2 protein fused to VPR.
GB1724	U626:gRNA4(pNOS)	#160621 (Selma et al., 2019)	Transcriptional unit for a gRNA targeting the NOS promoter with a MS2 recognition loop.
GB1838	U6-26-1gRNA(pDFR)	#160625 (Selma et al., 2019)	Transcriptional unit for the expression of a g RNA targeting the DFR promoter with two copies of the MS2 aptamer.
GB2513	35s:dCas9:EDLL:nos +35s:MS2:VPR:nos + U626:gRNA1 (pDFR)	#187803 (this study)	Module for constitutive expression of dCas9:EDLL, Ms2:VPR and a gRNA targeting the DFR promoter.
GB1024	35s:AtrΔ11:35s + 35s:HarFAR:35s	#187804 (this study)	Module for the constitutive expression of the Δ11 desaturase from *Amyelois transitella* and a fatty acid reductase from *Helicoverpa armigera*.
GB1022	35s:EaDAct:35s	#187805 (this study)	Transcriptional unit for expression of diacylglycerol acetyltransferase from *Euonymus alatus.*

Plasmid Code	Contents	Addgene Code and Reference	Description
GB3681	35s:ScATF1:35s	#187806 (this study)	Transcriptional unit for expression of alcohol O-acetyltransferase from *Saccharomyces cerevisiae* S288C, codon optimized for Nicotiana.
GB3682	35s:SpATF1-2:35s	#187807 (this study)	Transcriptional unit for expression of alcohol O-acetyltransferase from *Saccharomyces pastorianus* strain CBS 1483 chromosome SeVIII-SeXV, codon optimized for Nicotiana.
GB3683	35s:EfDAct:35s	#187808 (this study)	Transcriptional unit for expression of 1,2-diacyl-sn-glycerol:acetyl-CoA acetyltransferase from *Euonymus 128ortune*, codon optimized for Nicotiana.
678 (pEPKKΩ1SP0678)	35s:TMVΩ:CUP2:Gal4:nos + CBSmin35s:AatrΔ11:35s + CBSmin35s:ATF1-2:mas + CBSmin35s:HarFAR:g7	#187605 (this study)	Module for copper inducible expression of AtrD11, HarFAR and EaDAct.
GB3897	minDFR:ATF1:mtb + minDFRHarFAR:pds + minDFR:AtrΔ11:dfr+ U626:gRNA1 (pDFR)	#187809 (this study)	Module for dCasEV2.1 activated expression of AtrD11, HarFAR and ScATF1 plus gRNA-1DFR.
GB4068	nos:CUP2:GAL4:nos + CBS:dCas9:EDLL:nos + CBS: MS2:VPR;nos	#187810 (this study)	Module for the constitutive expression of CUP2:Gal4AD and copper-inducible expression of dCasEV2.1 (dCas9:EDLL and MS2:VPR).
GB4070	nos:CUP2:Gal4:nos + U626:gRNA (DFR) + CBS:dCas9:EDLL:nos + CBS:MS2:VPR:nos	#187811 (this study)	Module for the constitutive expression of CUP2:Gal4AD and gRNA-1 DFR, and the copper-inducible expression of dCasEV2.1 (dCas9:EDLL and MS2:VPR).
GB2815	pUPD2_GB_SynP (A1) Random Sequence R1	#193112 (Moreno-Giménez et al., 2022)	Random sequence R1 of 1240 bp for A1 distal promoter position.
GB3269	pUPD2_GB_SynP (A1) Random Sequence R2	#193113 (Moreno-Giménez et al., 2022)	Random sequence R2 of 1240 bp for A1 distal promoter position.
GB3270	pUPD2_GB_SynP (A1) Random Sequence R3	#193114 (Moreno-Giménez et al., 2022)	Random sequence R3 of 1240 bp for A1 distal promoter position.

Plasmid Code	Contents	Addgene Code and Reference	Description
GB3275	pUPD2_GB_SynP (A2) G1abc.2	#193129 (Moreno-Giménez et al., 2022)	A2 Proximal promoter sequence consisting of three times the target sequence for the gRNA-1 DFR (gRNA1) flanked by random sequences.
GB3276	pUPD2_GB_SynP (A2) G1abc.3	#193130 (Moreno-Giménez et al., 2022)	A2 Proximal promoter sequence consisting of three times the target sequence for the gRNA-1 DFR (gRNA1) flanked by random sequences.
GB3277	pUPD2_GB_SynP (A2) G1abc.4	#193131 (Moreno-Giménez et al., 2022)	A2 Proximal promoter sequence consisting of three times the target sequence for the gRNA-1 DFR (gRNA1) flanked by random sequences.
GB2566	pUPD2_miniDFR	#193104 (Moreno-Giménez et al., 2022)	Minimal promoter of SlDFR gene containing 62bp upstream the transcription start site and the 5'UTR region.
GB3898	minDFR:AtrΔ11:dfr + minDFR:HarFAR:pds + minDFR:ScATF1:mtb	#187812 (this study)	Module for dCasEV2.1 activated expression of AtrΔ11, HarFAR and ScATF1.
GB4356	minDFR:AtrΔ11:dfr + minDFR:HarFAR:pds + minDFR:SpATF1-2:mtb	#187813 (this study)	Module for dCasEV2.1 activated expression of AtrΔ11, HarFAR and SpATF1-2.
GB4360	minDFR:ScATF1:mtb + minDFR:AtrΔ11:dfr + minDFR:HarFAR	#187814 (this study)	Module for dCasEV2.1 activated expression of ATF1, AtrΔ11 and HarFAR.
GB4361	minDFR:SpATF1-2:mtb + minDFR:AtrΔ11:dfr + minDFR:HarFAR:pds	#187815 (this study)	Module for dCasEV2.1 activated expression of ATF1-2, HarFAR and AtrΔ11.
GB4366	minDFR:HarFAR:pds + minDFR:ScATF1:mtb + minDFR:AtrΔ11:dfr	#187816 (this study)	Module for dCasEV2.1 activated expression of HarFAR, ATF1 and AtrΔ11.
GB4367	minDFR:HarFAR:pds + minDFR:SpATF1-2:mtb + minDFR:AtrΔ11:dfr	#187817 (this study)	Module for dCasEV2.1 activated expression of HarFAR, ATF1-2 and AtrΔ11.

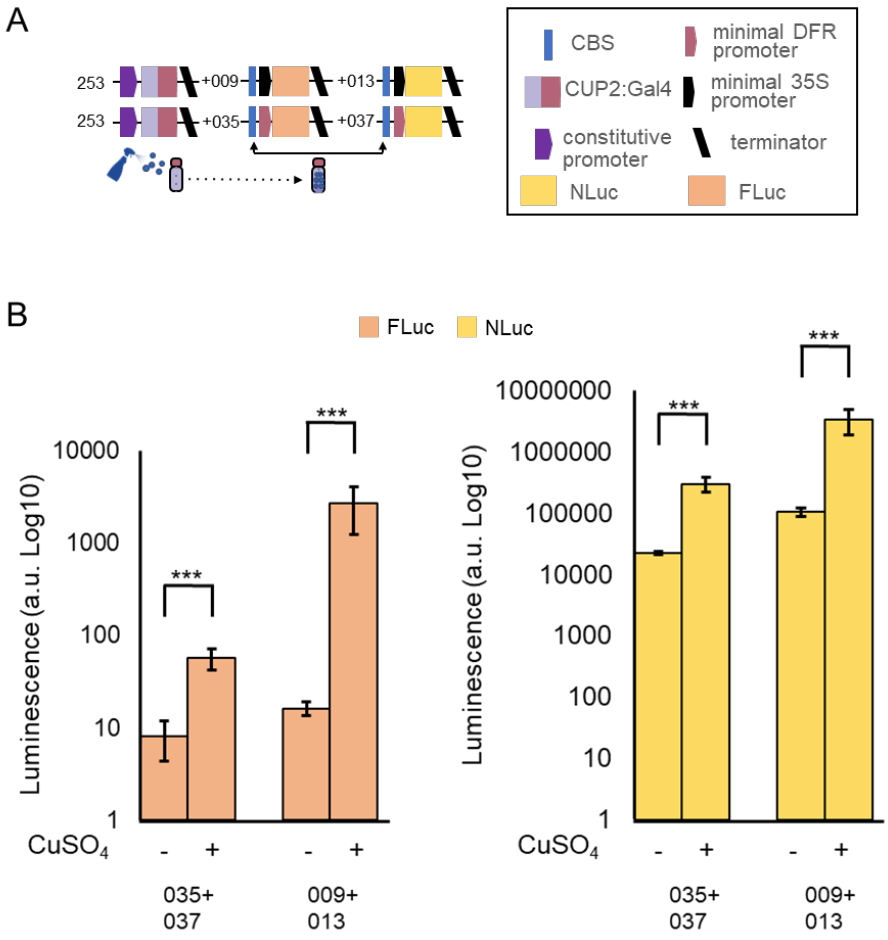

Figure S1. Copper sulfate can induce Copper inducible promoters with minimal DFR or minimal 35S. (A) Schematics of plant expression constructs containing synthetic genes for copper inducible expression of firefly luciferase (Fluc) and nanoluciferase (Nluc). (B) Copper inducible promoters with minimal 35S or minimal DFR can be induced with copper sulfate (2.5 mM). Values shown are the mean and standard error of n=10 biological replicates (independent infiltrations) and differences were analyzed using pairwise Wilcoxon rank sum test with Benjamini-Hochberg correction (***P ≤ 0.001).

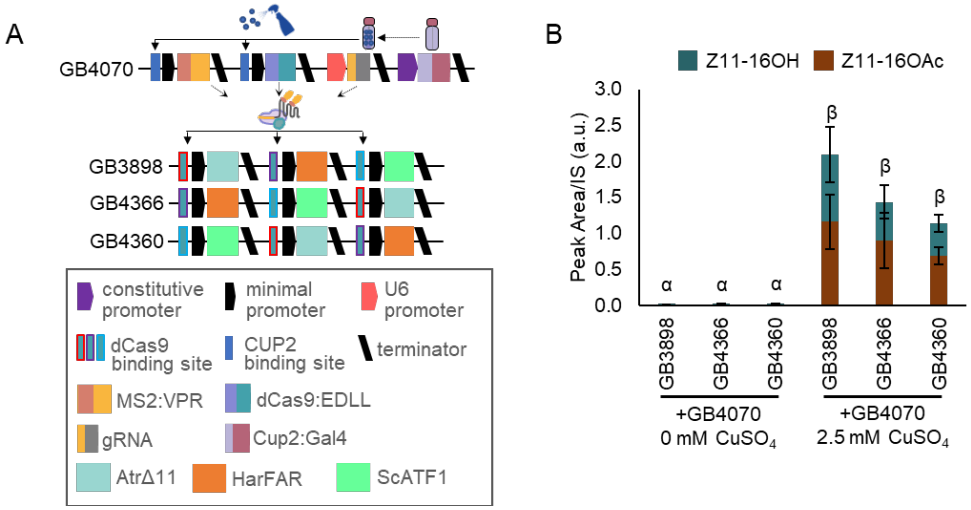

Figure S2. Copper inducible, CRISPR/Cas9-mediated control of pheromone biosynthesis. (A) Schematic of plant expression constructs containing elements for copper inducible expression of the dCasEV2.1 transcriptional activator (above) and multigene constructs containing coding sequences for AtrΔ11, HarFAR and ScATF1. The latter are assembled with a promoter consisting of a minimal DFR core promoter fused to one of three unique sequences containing the conserved gRNA target sites. (B) Application of $CuSO_4$ results in dCasEV2.1 mediated production of the pheromone components (Z11-16OH and Z11-16OAc). Values shown are the mean and standard error of n=3 biological replicates (independent infiltrations). Means followed by a common Greek letter (α, β) are not significantly different (one-way ANOVA with post-hoc Tukey HSD at the 5% level of significance).

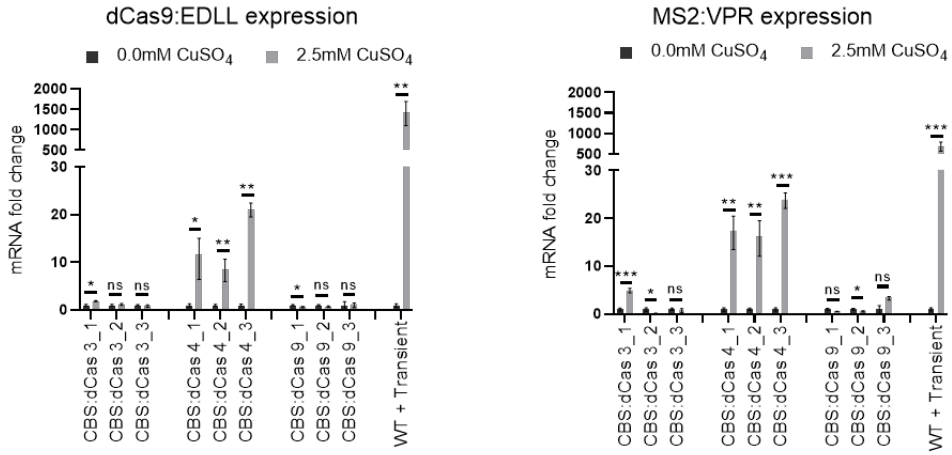

Figure S3. Transcription of dCas9:EDLL and MS2:VPR in T_1 CBS:dCas transgenic plants. Three leaves from each of three transgenic progeny (T_1) of three independent transgenic T0 lines were selected and 0.0mM $CuSO_4$ or 2.5mM $CuSO_4$ applied each side of the midrib. Samples were collected from each plant 2 days after the induction (5dpi for the transient constructs). mRNA levels, relative to expression of the F-BOX gene (ΔCt) and the ΔΔCt used to calculate fold change between copper concentrations. A WT plant infiltrated with the CBS:dCas module was included as a control. Error bars represents SD (n = 3). *P*-values were calculated using Student's t-test; **P* ≤ 0.05, ***P* ≤ 0.01, ****P* ≤ 0.001; ns= not significant.

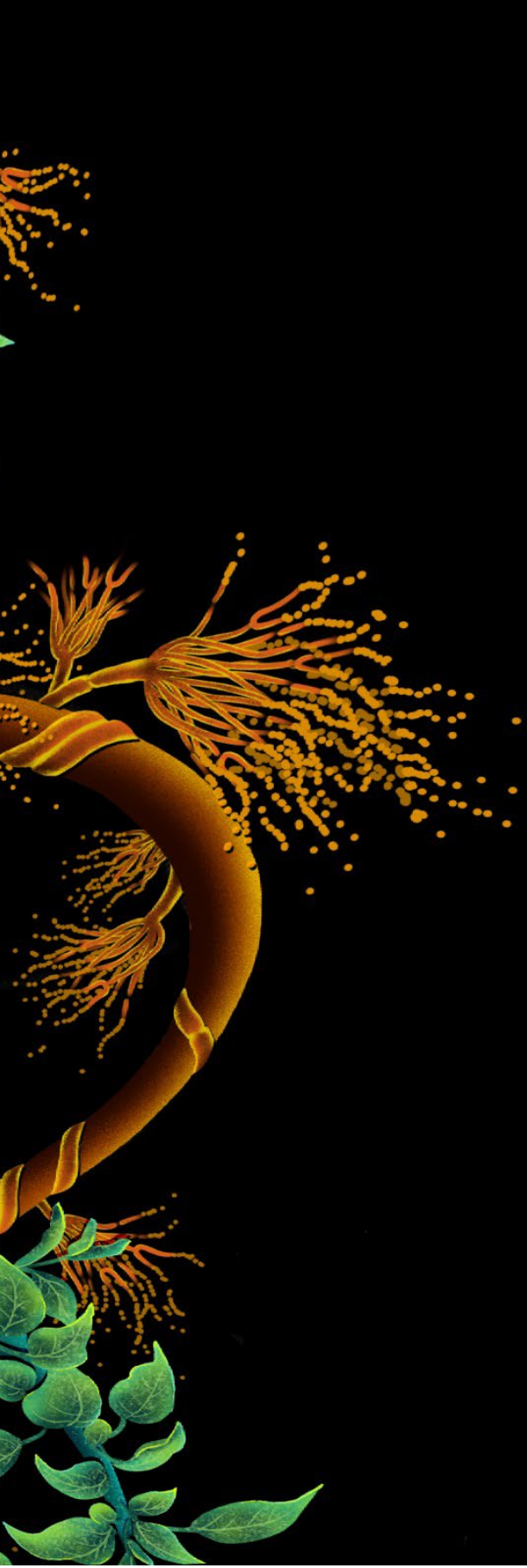

CHAPTER IV

CHAPTER IV

FungalBraid 2.0: expanding the synthetic biology toolbox for the biotechnological exploitation of filamentous fungi

***Elena Moreno-Giménez**, Mónica Gandía, Zara Sáez, Paloma Manzanares, Lynne Yenush, Diego Orzáez, Jose F. Marcos and Sandra Garrigues.*

Frontiers in Bioengineering and Biotechnology, 2023. DOI: 10.3389/fbioe.2023.1222812

My contribution to this work was essential for its publication. I performed the validation of promoters using the normalized luciferase reporter system, and the implementation of the dCas9-regulated GB_SynP synthetic promoters. I also contributed to the characterization antibiotic resistance markers and to a major part of the manuscript writing. The entire manuscript is presented for clarity.

ABSTRACT

Fungal synthetic biology is a rapidly expanding field that aims to optimize the biotechnological exploitation of fungi through the generation of standard, ready-to-use genetic elements and universal syntax and rules for contributory use by the fungal research community. Recently, an increasing number of synthetic biology toolkits have been developed and applied to filamentous fungi, which highlights the relevance of these organisms in the biotechnology field. The FungalBraid (FB) modular cloning platform enables interchangeability of DNA parts with the GoldenBraid (GB) platform designed for plants and other systems compatible with the standard Golden Gate cloning and syntax, and uses binary pCAMBIA-derived vectors to allow *Agrobacterium tumefaciens*-mediated transformation of a wide range of fungal species. In this study, we have expanded the original FB catalog by adding 27 new DNA parts that we have functionally validated *in vivo*. Among these are the resistance selection markers for the antibiotics phleomycin and terbinafine, as well as the uridine auxotrophy marker *pyr4.* We also used a normalized luciferase reporter system to validate several promoters, namely P*pkiA,* P7760*,* P*ef1α,* P*afpB* constitutive promoters, and the P*glaA*, P*amyB* and P*xlnA* inducible promoters. Additionally, the recently developed dCas9-regulated GB_SynP synthetic promoter collection for orthogonal CRISPR activation (CRISPRa) in plants has been adapted to fungi through the FB system. In general, the expansion of the FB catalog is of great interest for the scientific community since it expands the number of possible modular and interchangeable DNA assemblies, exponentially increasing the possibilities of studying, developing and exploiting filamentous fungi.

INTRODUCTION

Filamentous fungi have acquired a great biotechnological relevance as biofactories for the sustainable production of organic acids, proteins, enzymes and metabolites with applications in the agri-food, chemical, pharmaceutical, textile, paper and biofuel industries (Meyer et al., 2016). Their ability to grow on many distinct -and economic- substrates and plant residues, and their high secretory capacity justify the biotechnological interest of these microorganisms, which have become essential contributors to the so-called circular bio-economy (Meyer et al., 2020). Enzymes produced by fungi currently make up more than half of the enzymes used in industry (de Vries et al., 2020). Additionally, fungal genomes contain a large number of biosynthetic gene clusters encoding potentially useful biomolecules to be exploited (Robey et al., 2021), reflecting the relevance of filamentous fungi as cell factories. However, there are still aspects that need to be improved, since the conditions and levels of production of the different biomolecules are highly variable, and some of them are difficult to produce in a cost-efficient manner.

Synthetic biology (SynBio) is an ever-expanding scientific field that has revolutionized genetic and metabolic engineering. SynBio provides new tools for the generation of ready-to-use, standardized, modular genetic elements to obtain microbial strains with optimized properties either by the production of specific proteins, or by fine-tuning the expression of specific metabolic pathway-related genes (Benner and Sismour, 2005). In this context, fungal SynBio is rapidly evolving. Our group has adapted the GoldenBraid (GB) modular cloning platform originally developed for plants (Sarrion-Perdigones et al., 2013) to filamentous fungi, a variant called FungalBraid (FB) (https://gbcloning.upv.es/fungal/). This modular cloning method is based on type IIS restriction enzymes and pCAMBIA-derived binary vectors for *Agrobacterium tumefaciens*-mediated transformation (ATMT), with the main advantages of the full reusability of its DNA parts and their interchangeability between plants and fungi as long as they are functionally compatible (Hernanz-Koers et al., 2018; Vazquez-Vilar et al., 2020). The domestication or incorporation of new DNA parts into the FB system is achieved by cloning them into level 0 pUPD2 vectors, and Transcriptional Units (TUs) are then formed by combining different level 0 parts in a multipartite assembly into

level 1 pDGB3α vectors. The GB and FB systems allow the combination of different TUs contained in two compatible pDGB3α vectors in a bipartite assembly into level 2 pDGB3Ω vectors, which can then be combined in the same way back into pDGB3α vectors, allowing the indefinite expansion of the multigene construct and designs of increased complexity.

Since the development of the FB system, an increasing number of SynBio-based applications in fungi have been reported (Dahlmann et al., 2021; Mózsik et al., 2022, 2021), which highlights the need for a boost in the SynBio toolkit for these organisms. However, there is still a shortage of tools for orthogonal and fine-tuned expression of genes applied to filamentous fungi. In this sense, an increase in the repertoire of promoters is required. Promoters with different expression levels, or which are inducible and/or cell-specific would increase the flexibility and the ability to optimize expression systems, especially for proteins which can be toxic. These promoters may come from different organisms or may be created using synthetic designs. Whereas constitutive and inducible promoters are commonly used among the scientific community, synthetic promoters have been less exploited. These promoters are often comprised of a core or minimal promoter and an upstream region in which cis-regulatory elements are incorporated (Martins-Santana et al., 2018). These cis-regulatory elements are typically obtained from the binding sites of transcriptional regulators which activate or inactivate gene expression. While natural transcriptional regulators limit the freedom in the design of cis-regulatory elements, the use of CRISPR activation (CRISPRa) strategies allows the use of virtually any 20 base pair (bp) sequence as a cis-regulatory box in the development of synthetic promoters (Moreno-Giménez et al., 2022). In this regard, the collection of nuclease-deactivated Cas9 (dCas9)-regulated synthetic promoters GB_SynP that has been recently developed for plants (Moreno-Giménez et al., 2022) could easily be adapted to fungi given the interchangeability of DNA parts between GB and FB systems. Additionally, the GB/FB systems provide a standard measurement using a Luciferase/Renilla transient assay to estimate relative expression levels of promoters, including the synthetic ones (Gandía et al., 2022; Vazquez-Vilar et al., 2017).

In this study, we have incorporated 27 new genetic parts into the FB system (Table 1), which include native strong and inducible fungal promoters, synthetic

promoters, terminators, and selection markers. All these components have been validated *in vivo* in two economically-relevant fungi: the non-model postharvest pathogen of citrus *Penicillium digitatum* (Palou, 2014), and in the well-known fungus with Generally Recognized as Safe (GRAS) status and a long record of industrial use *Penicillium chrysogenum* (Fierro et al., 2022). The strength of the constitutive promoters has been characterized and compared in a nanoluciferase-normalized luciferase-based reporter system; the induction levels of the inducible promoters have also been quantified, and the activation of the synthetic promoters has been studied using programmable transcriptional factors based on CRISPRa (Mózsik et al., 2021). Overall, the expansion of the FB toolkit will be of great interest for the scientific community to further aid the exploitation of fungal workhorses and accelerate the discovery and production of (novel) bioactive molecules for multiple biotechnological applications.

Table 1. **FB parts reported in this study**. DNA parts are grouped according to the purpose for which they were used.

Selection markers				
Auxotrophy				
Code	**Name**	**Plasmid**	**Description**	**Reference**
FB271*	P*pyr4*	pUPD2	Promoter of *pyr4* gene from *T. reesei.*	This study
FB272*	*pyr4*	pUPD2	Coding sequence of *pyr4* gene from *T. reesei*.	This study
FB273*	T*pyr4*	pUPD2	Terminator of *pyr4* gene from *T. reesei.*	This study
FB293*	TU_*pyr4*	pDGB3α2	Assembly of the transcriptional unit for the auxotrophy marker *pyr4* from *T. reseei*.	This study
FB359*	5' upstream Pdig *pyrG*	pUPD2	5' upstream region of *pyrG* gene in *P. digitatum*.	This study
FB361*	3' downstream Pdig *pyrG*	pUPD2	3' downstream region of *pyrG* gene in *P. digitatum*.	This study
FB372*	FB359+FB361	pDGB3α1	Assembly for *pyrG* deletion in *P. digitatum*.	This study
Resistances				
Code	**Name**	**Plasmid**	**Description**	**Reference**
FB413*	*ble*	pUPD2	Coding sequence for phleomycin resistance.	This study
FB414*	*ergA*	pUPD2	Coding sequence for terbinafine resistance.	This study
FB411*	P*pcbC*	pUPD2	Promoter of Isopenicillin N synthase from *P. rubens.*	This study
FB416*	T*amdS*	pUPD2	Terminator of acetamidase-encoding gene *amdS* from *A. nidulans*	This study
FB430*	P*pcbc:ble:*T*amdS*	pDGB3α2	TU for the expression of phleomycin resistance.	This study
FB431*	P*gpdA:ergA:*T*amdS*	pDGB3α2	TU for the expression of terbinafine resistance.	This study

Constitutive/Inducible promoters				
Code	**Name**	**Plasmid**	**Description**	**Reference**
FB007	P*gpdA*	pUPD2	Promoter of glyceraldehyde-3-phosphate dehydrogenase from *A. nidulans.*	(Hernanz-Koers et al., 2018)
FB291*	P*xlnA*	pUPD2	Promoter of the endo-1,4-beta-xylanase A gene from *A. nidulans*, xylose-inducible.	This study
FB389*	P*pkiA*	pUPD2	Promoter of the highly-expressed pyruvate kinase gene from *A. niger.*	This study
FB404*	P*afpB*	pUPD2	Promoter of antifungal protein *afpB* gene from *P. digitatum.*	This study
FB405*	P*glaA*	pUPD2	Promoter of the glucoamylase gene from *A. niger,* maltose/starch-inducible.	This study
FB406*	P*amyB*	pUPD2	Promoter of the TAKA-amylase A gene from *A. oryzae,* maltose/starch-inducible.	This study
FB407*	P*ef1α*	pUPD2	Promoter of the elongation factor 1-α gene from *P. digitatum* (PDIG_59570).	This study
FB408*	P07760	pUPD2	Promoter of the ubiquitin ligase gene from *P. digitatum* (PDIG_07760).	This study
GB0096	Luciferase (FLuc)	pUPD	Coding sequence for the firefly luciferase protein.	(Sarrion-Perdigones et a 2013)
FB001	P*trpC*	pUPD2	Promoter of the multifunctional tryptophan biosynthesis protein coding gene *trpC* from *A. nidulans*.	(Hernanz-Koers et al., 2018)
FB002	T*tub*	pUPD2	Terminator of tubulin-encoding gene from *N. crassa.*	(Hernanz-Koers et al., 2018)
FB008	T*trpC*	pUPD2	Terminator of *trpC* gene from *A. nidulans*.	(Hernanz-Koers et al., 2018)
FB009	P*trpC*:*nptII*:T*tub*	pDGB3α2	TU for the expression of geneticin resistance.	(Hernanz-Koers et al., 2018)
FB312	P*gpdA*:Nluc:T*tub*	pDGB3α1R	TU for the expression of nanoluciferase (Nluc) under the P*gpdA*	(Gandía et al., 2022)
FB323	P*gpdA*:Nluc:T*tub::*P*trpC:nptII:*T*tub::Ppaf*:Luc*:Ttub*	pDGB3α1	Module for the expression of geneticin resistance and nanoluciferase, and the expression of firefly luciferase under the P*paf*	(Gandía et al., 2022)
FB367*	P*gpdA*:Nluc:T*tub::*P*trpC:nptII:*T*tub*	pDGB3α1	Module for the expression of geneticin resistance and nanoluciferase.	This study
FB417	P*afpB*:FLuc:T*trpC*	pDGB3α2	TU for the expression of luciferase under P*afpB*.	This study
FB418	P*glaA*:FLuc:T*trpC*	pDGB3α2	TU for the expression of luciferase under P*glaA*.	This study
FB419	P*amyB*:FLuc:T*trpC*	pDGB3α2	TU for the expression of luciferase under P*amyB*.	This study

Code	Name	Plasmid	Description	Reference
FB420	P*ef1α*:FLuc:T*trpC*	pDGB3α2	TU for the expression of luciferase under P*ef1α*.	This study
FB421	P07760:FLuc:T*trpC*	pDGB3α2	TU for the expression of luciferase under P07760.	This study
FB423	P*gpdA*:FLuc:T*trpC*	pDGB3α2	TU for the expression of luciferase under P*gpdA*.	This study
FB424	P*xlnA*:FLuc:T*trpC*	pDGB3α2	TU for the expression of luciferase under P*xlnA*.	This study
FB426	P*pkiA*:FLuc:T*trpC*	pDGB3α2	TU for the expression of luciferase under P*pkiA.*	This study
FB432	FB367+FB417	pDGB3Ω1	Module for the expression of geneticin resistance, Nluc under P*gpdA* promoter and luciferase under P*afpB*.	This study
FB433	FB367+FB418	pDGB3Ω1	Module for the expression of geneticin resistance, Nluc under P*gpdA* promoter and luciferase under P*glaA*.	This study
FB434	FB367+FB419	pDGB3Ω1	Module for the expression of geneticin resistance, Nluc under P*gpdA* promoter and luciferase under P*amyB*.	This study
FB435	FB367+FB420	pDGB3Ω1	Module for the expression of geneticin resistance, Nluc under P*gpdA* promoter and luciferase under P*ef1α.*	This study
FB436	FB367+FB421	pDGB3Ω1	Module for the expression of geneticin resistance, Nluc under P*gpdA* promoter and luciferase under P07760.	This study
FB438	FB367+FB423	pDGB3Ω1	Module for the expression of geneticin resistance, Nluc under P*gpdA* promoter and luciferase under P*gpdA*.	This study
FB439	FB367+FB424	pDGB3Ω1	Module for the expression of geneticin resistance, Nluc under P*gpdA* promoter and luciferase under P*xlnA*.	This study
FB441	FB367+FB426	pDGB3Ω1	Module for the expression of geneticin resistance, Nluc under P*gpdA* promoter and luciferase under P*pkiA*.	This study

dCas9-activated Synthetic Promoters

Code	Name	Plasmid	Description	Reference
GB2815	RandomSequence R1	pUPD2	Random sequence R1 of 1240 bp for A1 distal promoter position.	(Moreno-Giménez et al., 2022)
GB2878	G1aG2b.1	pUPD2	A2 Proximal promoter sequence containing the target sequence for the gRNA1 flanked by random sequences.	(Moreno-Giménez et al., 2022)
GB2885	G1ab.1	pUPD2	A2 Proximal promoter sequence consisting of two times the target sequence for the gRNA1 flanked by random sequences.	(Moreno-Giménez et al., 2022)

Code	Name	Plasmid	Description	Reference
GB3276	G1abc.3	pUPD2	A2 Proximal promoter sequence consisting of three times the target sequence for the gRNA1 flanked by random sequences.	(Moreno-Giménez et al., 2022)
GB3413	m*PAF*	pUPD2	Minimal promoter of *paf* gene from *P. chrysogenum*, containing 62 bp upstream the transcription start site and the 5' UTR region.	(Moreno-Giménez et al., 2022)
FB395*	R1:G1aG2b.1:m*PAF*:FLuc:T*trpc*	pDGB3α2	TU for the expression of luciferase under a synthetic promoter containing the target sequence for gRNA1 (1xLuc).	This study
FB396*	R1:G1ab.1:m*PAF*:FLuc:T*trpc*	pDGB3α2	TU for the expression of luciferase under a synthetic promoter containing two times the target sequence for gRNA1 (2xLuc).	This study
FB397*	R1:G1abc.3:m*PAF*:FLuc:T*trpc*	pDGB3α2	TU for the expression of luciferase under a synthetic promoter containing three times the target sequence for gRNA1 (3xLuc).	This study
FB398*	FB367+FB395	pDGB3Ω1	Module for the expression of geneticin resistance, Nluc under P*gpdA* promoter and luciferase under a synthetic promoter containing the target sequence for gRNA1.	This study
FB399*	FB367+FB396	pDGB3Ω1	Module for the expression of geneticin resistance, Nluc under P*gpdA* promoter and luciferase under a synthetic promoter containing two times the target sequence for gRNA1 (2xLuc).	This study
FB400*	FB367+FB397	pDGB3Ω1	Module for the expression of geneticin resistance, Nluc under P*gpdA* promoter and luciferase under a synthetic promoter containing three times the target sequence for gRNA1 (3xLuc).	This study
FB403	pAMA18.0_gRNA1	pAMA18.0	Expression plasmid for dCas9 activation system and the (GB_SynP) gRNA1.	This study

* DNA parts deposited in Addgene.

RESULTS

Selection markers for antibiotic resistance

The FB platform already contains some commonly used positive fungal selection markers based on antibiotic resistance such as *hph* (hygromycin^R, FB003) or *nptII* (geneticin^R, FB009) (Hernanz-Koers et al., 2018). However, in the case of integrative approaches, multiple genetic modifications often depend on the availability of different antibiotic resistance genes for transformant selection,

which can be a bottleneck for the exploitation of filamentous fungi. In this study, we expand the range of selection markers available in the FB platform by including two alternative antibiotic resistance-inducing genes, the *ble* resistance gene from the bacterial transposon Tn5 and the squalene epoxidase *ergA* gene from *P. chrysogenum*. The expression of the *ble* gene provides selection for the antibiotic phleomycin (Austin et al., 1990), whereas the expression of the *ergA* gene provides resistance against the antibiotic terbinafine in a broad range of filamentous fungi (Austin et al., 1990; Sigl et al., 2010).

In order to include the *ble* resistance in the FB platform, a functional TU was generated. For this, we assembled the *ble* coding sequence (FB413), together with the promoter of Isopenicillin N synthase (P*pcbC*) from *Penicillium rubens* (FB411) (Polli et al., 2016) and the terminator from the acetamidase (T*amds*) from *Aspergillus nidulans* (FB416) (Kelly and Hynes, 1985) into the pDGB3α2 vector to obtain FB430 (Table 1, Figure 1A) via restriction-ligation reactions. To functionally validate the resulting construct, we transformed *P. chrysogenum* and *P. digitatum* wild-type strains with the same FB430 via ATMT for the ectopic integration of the *ble* TU. *P. chrysogenum* transformants grown in the presence of 25 µg/mL phleomycin were selected and analyzed by PCR for the presence of the *ble* cassette (Figure 1B). The positive transformants PCEM43053 and PCEM43062 showed growth on phleomycin-containing plates compared to the parental ATCC 10002 (Figure 1C), further demonstrating the functionality of FB430. In parallel, FB430 was also validated in *P. digitatum* (Figure 1D-G). *P. digitatum* transformants grown in the presence of 35 µg/mL phleomycin were selected and confirmed by PCR (Figure 1D). The positive transformants PDZS43023, PDZS43041 and PDZS43051 were able to grow on phleomycin-containing plates (Figure 1E) and showed the same pathogenicity as the parental CECT 20796 in orange fruits (Figure 1F-G).

Similarly, to incorporate the terbinafine resistance-inducing gene in the FB platform, a functional TU for *ergA* was generated and validated in *P. chrysogenum* (Figure 2). We assembled the *ergA* coding sequence (FB414), together with the P*gpdA* promoter (FB007) and the T*amds* terminator (FB416) into the pDGB3α2 vector to obtain the FB431 construct (Table 1, Figure 2A). *P. chrysogenum* transformants grown on 0.5 µg/mL terbinafine were chosen and confirmed by PCR

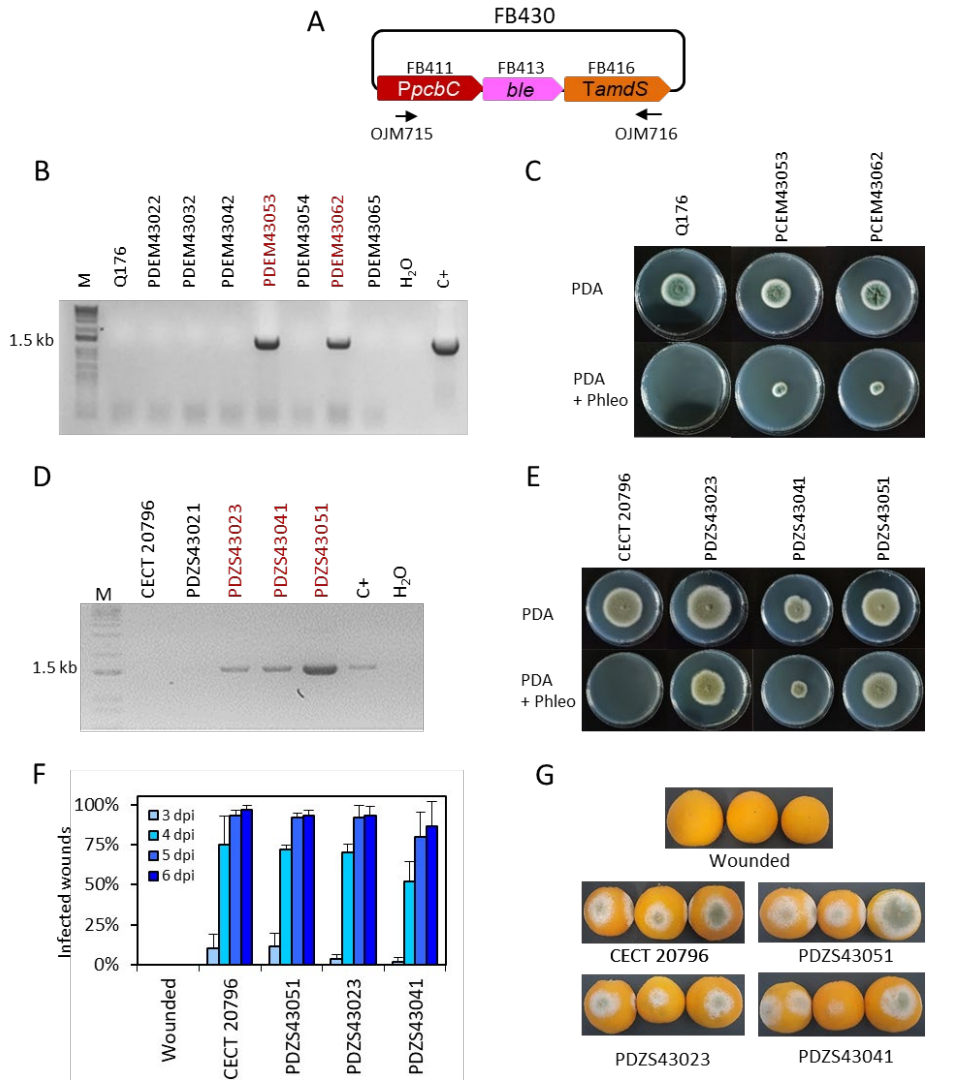

Figure 1: Functional validation of *ble* TU. (A) Plasmid pDGB3α2 FB430 for the ectopic integration of *ble* TU through ATMT to generate phleomycin resistance (Phleo^R). Primers OJM715 and OJM716 were used for the molecular characterization of the Phleo^R *P. digitatum* and *P. chrysogenum* strains. (B) Molecular characterization of *P. chrysogenum* transformants. The 1.5 kb band corresponds to the complete *ble* TU. Selected strains are highlighted in red. (C) Growth profile of *P. chrysogenum* selected Phleo^R transformants after 7 days of growth in the presence of the antibiotic (25 µg/mL) at 25 ºC. (D) Molecular characterization of *P. digitatum* transformants. The 1.5 kb band corresponds to the complete *ble* TU as in (B). Selected strains are highlighted in red. (E) Growth profile of *P. digitatum* Phleo^R transformants after 7 days of growth in the presence of the antibiotic (35 µg/mL) at 25 ºC. (F) Fruit infection assays of Phleo^R mutants on oranges. Data indicate the % of infected

wounds (mean ± SD) at each day post-inoculation (dpi). No statistical difference was found between the parental CECT 20796 and the mutants at each dpi (*t* test, $p < 0.05$). (E) Representative images of oranges infected by the indicated strains at 6 dpi.

(Figure 2B). The positive transformants PDZS43122, PDZS43131 and PDZS43142 could grow on phleomycin-containing PDA plates in contrast to the parental ATCC 10002 (Figure 2C), demonstrating the functionality of FB431.

Overall, both resistances were transformed ectopically to avoid any bias regarding the targeting of specific loci, and these experiments validate the use of FB430 and FB431 as standardized TUs for conferring positive selection in transformation of different fungal species, expanding the antibiotic resistance selection markers currently available in the FB system.

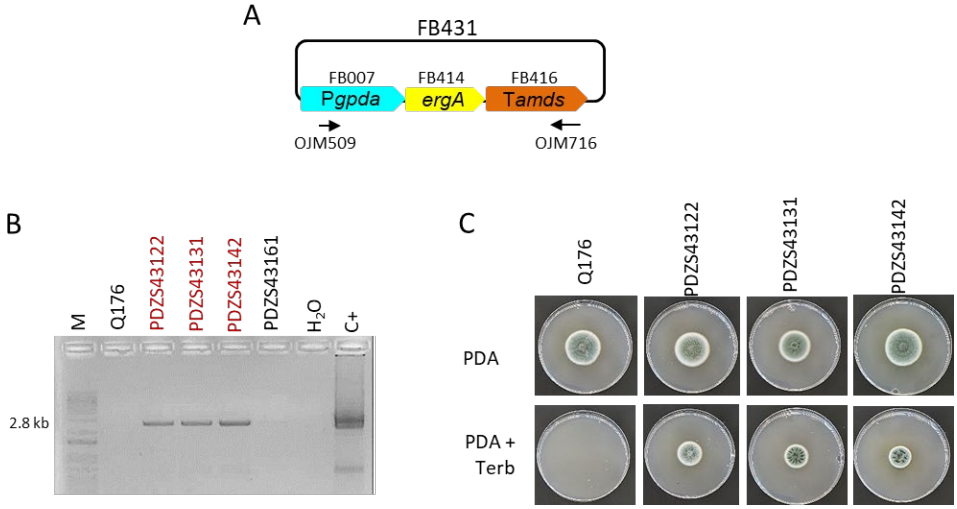

Figure 2: **Functional validation of *ergA* TU in *P. chrysogenum*.** (A) Plasmid pDGB3α2 FB431 for the ectopic integration of *ergA* TU through ATMT to generate terbinafine resistance (Terb^R). Primers OJM509 and OJM716 were used for the molecular characterization of the Terb^R strains shown in (B). The 2.8 kb bands correspond to the complete *ergA* TU. Selected strains are highlighted in red. (C) Growth profile of selected Terb^R transformants after 7 days of growth in the presence of the antibiotic (0.5 µg/mL) at 25 °C.

Selection markers based on fungal auxotrophy

To date, no auxotrophic markers have been included in the FB platform, despite the fact that they are sustainable alternatives to the use of antibiotics for transformant selection. The orotidine 5'-phosphate decarboxylase *pyr4* gene from *T. reesei* is widely used as an auxotrophic selection marker that can be counter-selected using 5-FOA or fully supplemented using uridine (Derntl et al., 2015; Díez et al., 1987). In this study, we set up several experiments to design, test and validate *pyr4* as selection marker in *pyr4/pyrG*-deficient fungal strains. As a first step, uridine-auxotrophic *P. digitatum* Δ*pyrG* mutants were generated through ATMT using FB372 as template for homologous recombination at the *pyrG* locus (Table 1, Figure S4). Transformants were selected on PDA plates supplemented with 1.22 g/L uridine and 1.25 g/L 5-FOA and were molecularly and phenotypically characterized (Figure S4). Growth profiles showed that after *pyrG* deletion*, P. digitatum* mutants could no longer grow on PDA plates unless supplemented with uridine, confirming their auxotrophic condition. Additionally, these mutants could also grow in the presence of uridine and 5-FOA in contrast to the parental CECT 20796, further confirming *pyrG* deletion. Finally, infection assays on orange fruits revealed that *P. digitatum* Δ*pyrG* mutants showed highly reduced pathogenesis compared to the control (Figure S4). Once the *pyrG* deletion mutants were obtained, a functional TU for *T. reesei pyr4* gene was generated. For this, we assembled the *Penicillium* codon-optimized and extensively domesticated *pyr4* coding sequence (FB272), promoter (FB271) and terminator (FB276) into the pDGB3α2 vector to obtain FB293 (Table 1, Figure 3A) via restriction-ligation reactions. To functionally validate the resulting construct FB293, we transformed *P. digitatum* Δ*pyrG* mutant PDSG37213 with FB293 via ATMT for the ectopic integration of the *pyr4* TU. Transformants grown on PDA plates were assessed by PCR (Figure 3B) and phenotypically analyzed to confirm *pyrG:pyr4* complementation and, therefore, the absence of the auxotrophy. As shown in Figure 3C, complemented mutants PDSG29312, PDSG29321 and PDSG29333 were all able to grow on PDA plates without uridine, in contrast to the auxotrophic parental PDSG37213. Remarkably, *P. digitatum* complemented mutants fully recovered their original pathogenicity (Figure 3D-E), which validates *pyr4* as an auxotrophic selectable marker also for (phyto)pathogenic fungi, in which the deletion of *pyrG* orthologs has been demonstrated to decrease pathogenicity and

virulence in the corresponding fungi (Higashimura et al., 2022; Zameitat et al., 2007).

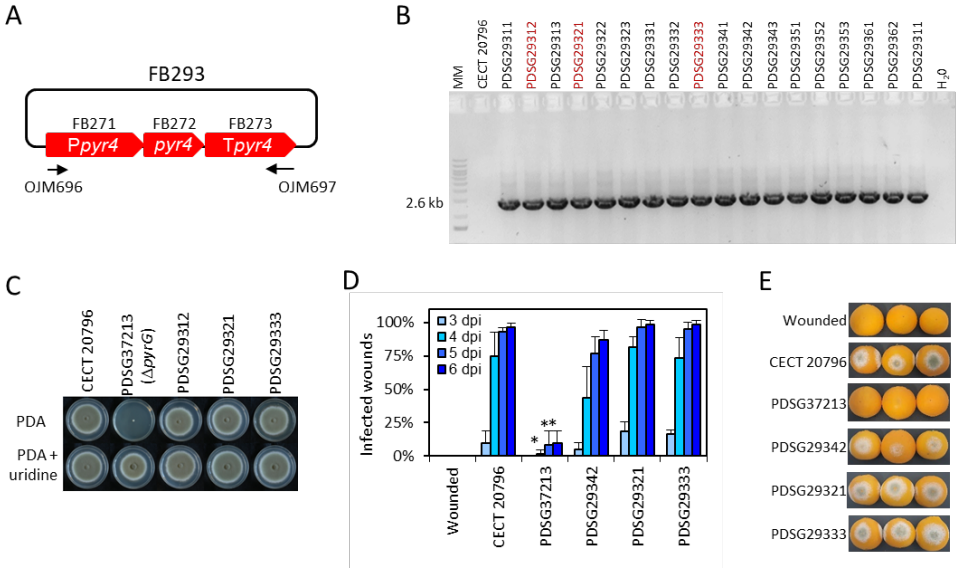

Figure 3: **Functional validation of *T. reesei pyr4* TU in *P. digitatum*.** (A) Plasmid pDGB3α2 FB293 for the ectopic integration of *pyr4* TU through ATMT to restore uridine auxotrophy. Primers OJM696 and OJM697 were used for the molecular characterization of the non-auxotrophic *P. digitatum* strains shown in (B). The 2.6 kb bands correspond to the complete *pyr4* TU. Selected strains are highlighted in red. (C) Growth profile of selected Δ*pyrG:pyr4* transformants grown on PDA plates supplemented with 1.22 g/L uridine. Note that PDSG372013 was used as parental for transformation with FB293. (D) Fruit infection assays of Δ*pyrG:pyr4* mutants on orange fruits. Data indicate the % of infected wounds (mean ± SD) at each day post-inoculation (dpi). (*) shows statistical significance between each sample compared to the control CECT 20796 at each dpi (*t* test, $p < 0.05$). (E) Representative images of oranges infected by the indicated strains at 6 dpi.

Constitutive and inducible promoters

In order to further expand and characterize the promoter catalog available in the FB platform, a series of promoters from different fungal species were included in the collection (Table 1) and functionally validated using a luciferase reporter system previously described (Gandía et al., 2022). This reporter consists of two TUs, the nanoluciferase coding sequence (Nluc, FB310) under the regulation of the P*gpdA* promoter that serves as an internal standard for normalization, and the firefly luciferase sequence (FLuc, GB0096) under the regulation of the promoter

to be tested. Promoter strength is expressed as the ratio of FLuc signal divided by the Nluc internal standard. The promoters to be evaluated included the previously characterized strong pyruvate kinase gene promoter (P*pkiA*) from *Aspergillus niger* (FB389) (de Graaff et al., 1992). Novel promoters from *P. digitatum* included the antifungal protein AfpB gene promoter P*afpB* (FB404) (Garrigues et al., 2017) and two promoters with high expression levels reported in a previous transcriptomic study: the elongation factor 1α gene promoter (P*ef1*α) (FB407) and the ubiquitin ligase PDIG_07760 gene promoter (P07760) (FB408) (Ropero-Pérez et al., 2023). Among the inducible promoters included in this study are the endo-1,4-β-xylanase A gene promoter (P*xlnA*) from *A. nidulans* (FB291, xylose-responsive) (Orejas et al., 1999), the glucoamylase gene promoter (P*glaA*) from *A. niger,* and the TAKA-amylase A gene promoter (P*amyB*) from *Aspergillus oryzae* (FB405 and FB406, respectively, both maltose/starch-responsive) (Fowler et al., 1990; Tsuchiya et al., 1992b). The widely used glyceraldehyde-3-phosphate dehydrogenase promoter P*gpdA* from *A. nidulans*, which was already available in the FB collection (FB007) (Hernanz-Koers et al., 2018), was also included in the analysis, as well as the luciferase reporter construct for *P. chrysogenum* antifungal protein PAF promoter (P*paf*) from previously published data (FB323) (Gandía et al., 2022) to serve as references. To facilitate the cloning of the new luciferase reporter constructs, the nanoluciferase reference gene and the *nptII* resistance gene were cloned into a pDGB3α1 vector (FB367), to be combined in a single reaction with the luciferase TUs cloned into pDGB3α2 vectors that included the promoters to be tested (Figure 4A). Due to the requirements of the FB binary assembly, an insulator sequence (GB3458) was also included at the 3' end of the FB367 vector, which also helps to prevent interaction between Nluc and FLuc TUs. The luciferase reporter constructs for each of the assayed promoters (FB432 to FB441) showed different normalized luciferase expression levels in *P. digitatum* after 2 days of growth in PDB (Figure 4B). The lowest expression levels were observed for the inducible promoters P*xlnA*, P*amyB* and P*glaA,* in this order, due to the lack of inducers in this medium. Their expression levels, together with that driven by P*afpB,* were slightly above the basal signal observed in the control strain, but these were not statistically significant. The expression driven by P*pkiA*, P*gpdA* and the new P*ef1*α were similar to those observed for P*paf*, while P07760 showed intermediate expression values between these and the inducible promoters.

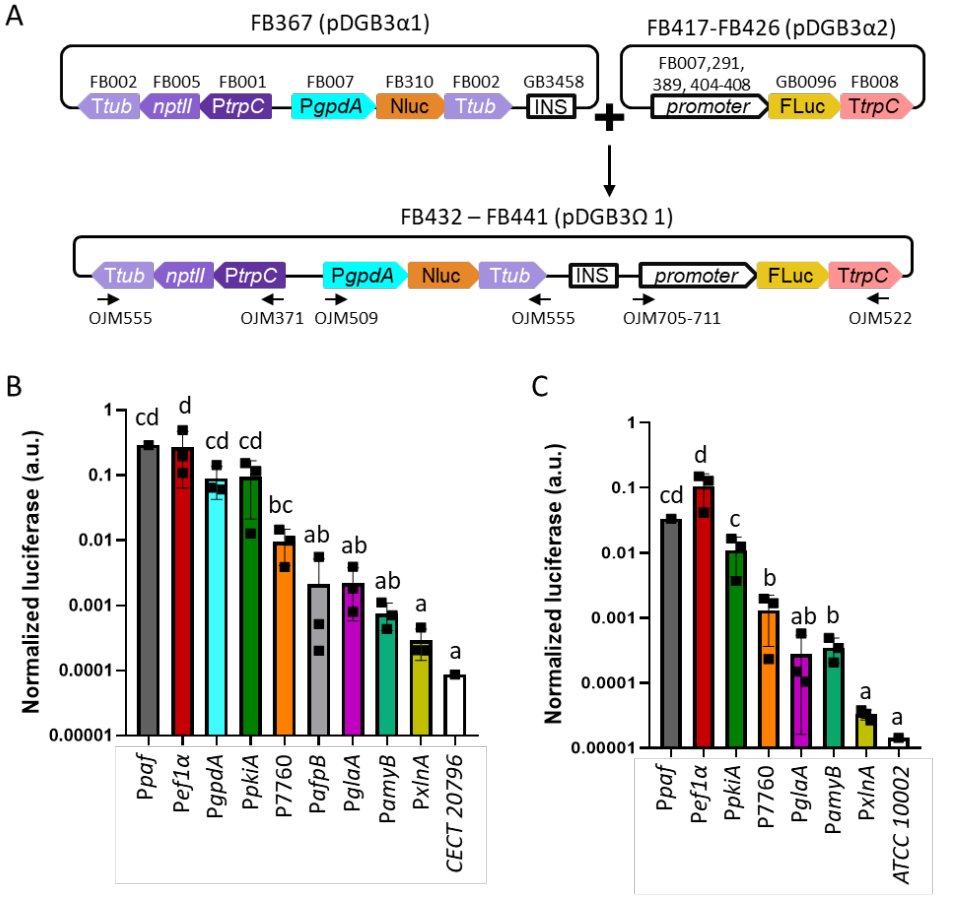

Figure 4: Functional promoter validation via luciferase assay in *P. digitatum* and *P. chrysogenum*. (A) Scheme of the assembly architecture used to express the luciferase reporter system. The different promoters were tested using luciferase as a reporter, and the constitutive expression of nanoluciferase under the P*gpdA* promoter was used as a reference for normalization. All constructs included a geneticin resistance gene (*nptII*) for selection of the positive transformants. An insulator sequence was introduced between the nanoluciferase and luciferase genes to allow the binary assembly of the plasmids. Primers used for the molecular characterization of transformants are indicated with arrows. (B) Normalized luciferase expression for each promoter in *P. digitatum* transformants grown in PBD for 2 days. (C) Normalized luciferase expression for each promoter in *P. chrysogenum* transformants grown in PBD for 2 days. Constitutive expression of luciferase under P*paf* promoter was included as a reference. Letters denote statistical significance between values in a one-way ANOVA (Tukey's multiple comparisons test, $p \leq 0.05$). Error bars represent the average values ± SD (n=9). Squares represent the mean value of each of the three biological replicates (transformants) measured twice. Note that Y-axis is represented in logarithmic scale.

The selected constructs carrying P*xlnA*, P*pkiA*, P*glaA*, P*amyB*, P*ef1*α and P07760 were also transformed into *P. chrysogenum*, in which the luciferase expression level was about 10 times lower than the overall levels observed in *P. digitatum* (Figure 4C), except for P*ef1*α and P*amyB*, which showed a similar signal in both fungal chassis (0.27 and 0.1 for P*ef1*α in *P. digitatum* and *P. chrysogenum*, respectively, and 0.0007 and 0.0004 for P*amyB*). Unlike *P. digitatum,* the signal driven by P*amyB* was above the basal signal in *P. chrysogenum* and showed similar expression levels to that of the P7760 promoter. Relative expression levels amongst the other promoters were nevertheless maintained in both fungi, with P*pkiA* and P*ef1*α signals similar to that of the P*paf* reference promoter and with P*xlnA*-, P*glaA*- and P*amyB*-driven signals similar to that of the control strains.

Induction of P*glaA*, P*amyB* and P*xlnA* promoters

In order to further characterize the inducible promoters included in this study, we analyzed the induction of luciferase expression directed by P*glaA*, P*amyB* and P*xlnA* promoters in *P. digitatum* (Figure 5A) and *P. chrysogenum* strains (Figure 5B) after 4 days of growth in Minimal Medium (PdMM for *P. digitatum* and PcMM for *P. chrysogenum*) using the different inducers as the sole carbon source (2% maltose for P*glaA* and P*amyB*, and 2% xylose for P*xlnA*). When the fungi were grown in the presence of the inducer, the expression levels driven by all three promoters were significantly higher than the expression observed in the reference media with 2% glucose, increasing by 8x, 4x and 10x for P*glaA,* P*amyB* and P*xlnA*, respectively, in *P. digitatum* (Figure 5A); and by 2x, 9x and 8x in *P. chrysogenum* (Figure 5B). Signals observed for P*xlnA* promoter in the reference media (MM + glucose) were similar to the basal signal of the reference strains in both fungi, while P*amyB* and P*glaA* promoters showed higher basal expression in the same media, especially in *P. chrysogenum.* Remarkably, expression levels in the reference P*paf* promoter were found to increase significantly in *P. chrysogenum* when grown in the PcMM supplemented with maltose or xylose (0.22 a.u. on average) when compared to the medium supplemented with glucose (0.015 a.u. on average, 15 times lower). The same was observed, but to a lesser extent, in *P. digitatum* when P*paf* was expressed in PdMM glucose (average values of 0.6 a.u.) compared to its expression in PdMM xylose (0.15 a.u. average values, 4 times higher).

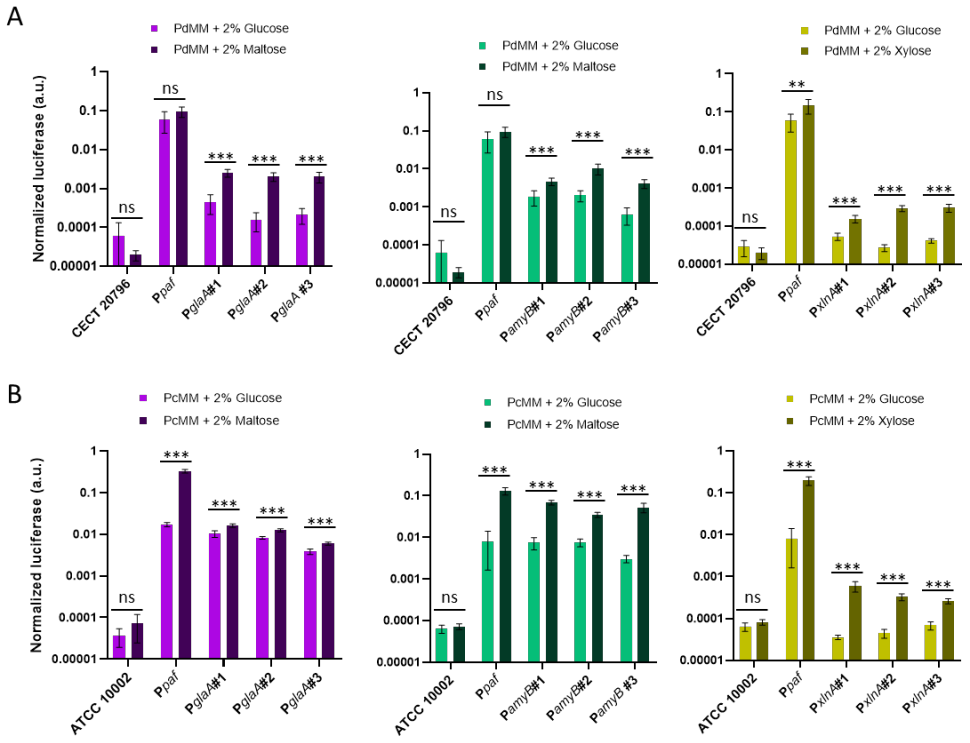

Figure 5: Activation of inducible promoters P*glaA*, P*amyB* and P*xlnA* in *P. digitatum* (A) and *P. chrysogenum* (B). Expression was measured after 4 days of growth in Minimal Medium (MM), replacing glucose with maltose as the carbon source for P*amyB* and P*glaA* transformants, and with xylose for P*xlnA* transformants. The expression of luciferase under P*paf* promoter was also included as a reference. Asterisks represent statistical significance (Student's *t* test, ns = $p \geq 0.05$, *$p < 0.05$, **$p < 0.01$, and ***$p < 0.001$) between the expression levels of each individual transformant in MM with maltose/xylose and those observed in the reference MM with glucose. Error bars represent the average values ± SD (n=6). Note that Y-axis is represented in logarithmic scale.

dCas9-activated synthetic promoters

Finally, we tested the recently developed GB_SynP (Moreno-Giménez et al., 2022) in our fungal chassis in combination with the pAMA18.0_gRNA1 plasmid, which delivers the CRISPRa system necessary to activate GB_SynP promoters in a non-integrative manner(Mózsik et al., 2021). To this end, we developed luciferase reporter constructs following the same procedure as for the natural promoters (Figure 6A). In these constructs, luciferase expression was regulated by synthetic promoters consisting of an A1 distal promoter part formed by random

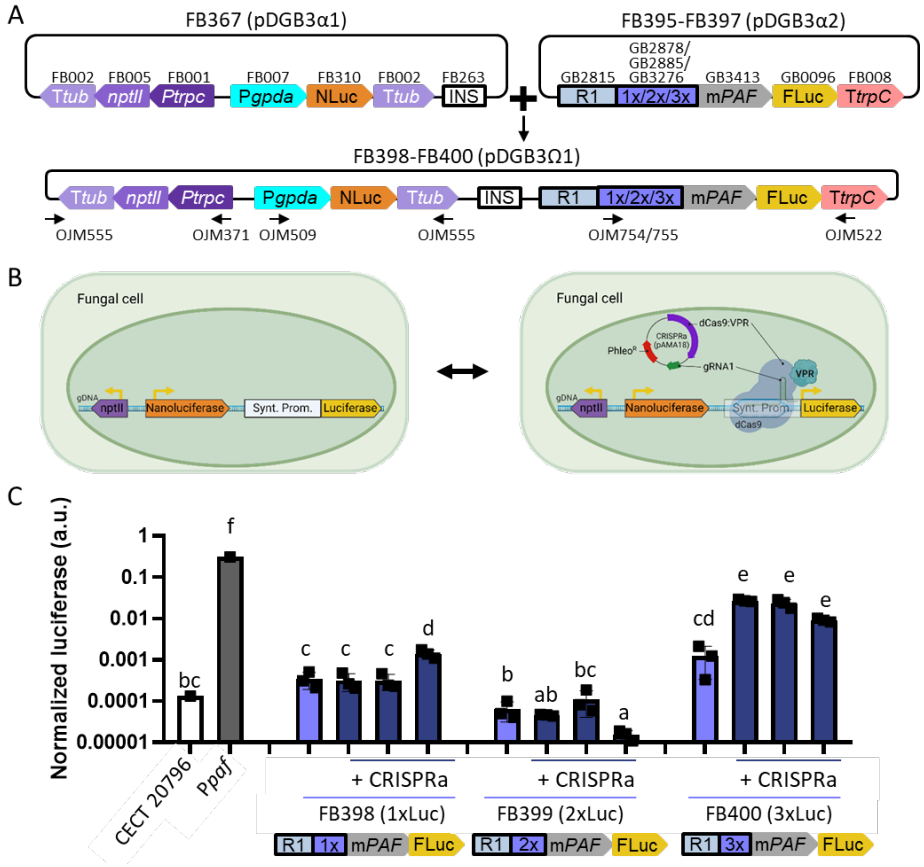

Figure 6: Functional validation of GB_SynP in *P. digitatum*. (A) Scheme of the construct architecture used to constitutively express the luciferase reporter system using the dCas9-regulated synthetic promoters with low (1xLuc, FB398), medium (2xLuc, FB399) or high (3xLuc, FB400) promoter strength. The constructs included the constitutive expression of nanoluciferase under the P*gpdA* promoter as a reference for normalization, geneticin resistance for selection of the transformants and an insulator sequence to allow the binary assembly of the plasmids. Oligos used for the molecular characterization of transformants are indicated with arrows. (B) Schematic representation of the dCas9-activated luciferase reporter system. Expression of geneticin resistance and nanoluciferase is constant, while the expression of luciferase is only achieved in the presence of the dCas9-based activation system (CRISPRa) contained in pAMA18-derived plasmid. (C) Expression of positive transformants for FB398 (1xLuc), FB399 (2xLuc) or FB400 (3xLuc) in the presence (+ CRISPRa) or absence of the pAMA18.0_gRNA1 plasmid. Constitutive expression of luciferase under P*paf* promoter was included as a reference. Squares represent the mean value of each of the three biological replicates (transformants) measured twice. Letters denote statistical significance between values in a one-way ANOVA (Tukey's multiple comparisons test, $p \leq 0.05$). Error bars represent the average values ± SD (n=6). Note that y-axis is represented in logarithmic scale. Figure includes images created with Biorender (biorender.com).

sequence (GB2815), and an A2 proximal promoter part including the target sequence for gRNA1 repeated once (GB2878), twice (GB2885), or three times (GB3276), and the minimal promoter m*PAF* (GB3423) derived from the native P*paf* from the fungus *P. chrysogenum* which, interestingly, was previously found to drive a strong induction when exposed to the dCasEV2.1 system loaded with the gRNA1 in plants (Moreno-Giménez et al., 2022). The resulting constructs containing one gRNA1 target (FB395, 1xLuc), two targets (FB396, 2xLuc), or three targets (FB397, 3xLuc) were stably transformed into *P. digitatum* via ATMT. Protoplasts obtained from these strains were re-transformed with the CRISPRa expression vector pAMA18.0_gRNA1 (Figure 6B). The expression levels of 1xLuc and 2xLuc constructs were not significantly higher than the basal signal of the control strain despite the presence of pAMA18.0_gRNA1, except for one of the 1xLuc re-transformants, which showed a low, but statistically significant increase in the luciferase expression when compared to the same strain in the absence of the CRISPRa system. A higher and significant increase of about 16 times on average in the luciferase signal was observed for the 3xLuc construct (Figure 6C) in all tested re-transformants. Although the expression driven by this promoter was around 10 times lower than that observed with the reference P*paf* promoter*,* it is comparable to that achieved with P*glaA* and P*amyB***,** showing the functionality of these dCas9-activated synthetic promoters in fungi.

DISCUSSION

The FB cloning platform allows for the open exchange of standardized, ready-to-use DNA parts among the fungal research community (Hernanz-Koers et al., 2018). Moreover, if functionally compatible and validated, it also allows the exchange of parts between plants and fungi, as occurred with the yellow fluorescent protein (YFP) or the hygromycin selection marker reported previously (Hernanz-Koers et al., 2018) or the GB_SynP synthetic promoters reported here. However, the number of validated genetic elements present in the FB platform was very limited to date, which hindered the biotechnological exploitation of filamentous fungi. In this study, we have expanded the available genetic elements in the FB platforms by incorporating one auxotrophic selection marker (*pyr4*)*,* two additional

antibiotic resistance markers (*ergA* and *ble*), two strong promoters (P*pkiA,* and P*ef1α*), two intermediate promoters (P*afpB* and P7760), three inducible promoters (P*glaA,* P*amyB,* and P*xlnA*), and three versions of the dCas9-regulated GB_SynP synthetic promoters. Even though the validation of these new parts has been performed in *Penicillium* species, the FB system has been demonstrated to allow the expression of the same construct in different fungal genera. Such is the case, for instance, of the FB027 construct for the expression of YFP, which has been functionally validated in *P. digitatum, Penicillium expansum* and *Aspergillus niger* (Hernanz-Koers et al., 2018; Vazquez-Vilar et al., 2020). Therefore, the FB system, and subsequently the new FB parts described here, are expected to be of use in a wide range of fungal species of different genera.

Since the FB release, there has been an increasing number of SynBio-based genetic toolkits developed for filamentous fungi (Dahlmann et al., 2021; Mózsik et al., 2022, 2021). In this sense, FB, which derives from the GB cloning framework, shares most of the codes and type IIS restriction enzymes with these alternative SynBio collections (Weber et al., 2011), making it possible to combine code-compatible level 0 plasmids between these systems to assemble TUs into level 1 plasmids. However, these Golden Gate-based collections alternative to FB use plasmids derived from pAMA1 or pEHN8, which are introduced into fungal cells via protoplast transformation. In contrast, the FB collection is based on pCAMBIA-derived vectors and can be applied to a broad spectrum of fungal species that are compatible with ATMT (de Groot et al., 1998), which is considered a more advantageous transformation method than protoplasts, as spores can be used directly for genetic transformation and transformation efficiencies are generally higher (D. Li et al., 2017 and references therein). Moreover, unlike these other Golden Gate cloning systems, the FB/GB systems allow for the indefinite expansion of multigenic constructs via bipartite assemblies between pDG3α and pDGB3Ω vectors (Sarrion-Perdigones et al., 2011). To date, the FB/GB system has allowed the assembly of up to 10 TUs (GB3243) (Selma et al., 2022b) and inserts as large as 20 kb (GB4559-GB4585) (Moreno-Giménez et al., 2022), yet the transformation and propagation of larger constructs into *E. coli* might be hampered by the limitations of this host (Weber et al., 2011). On this regard, the adaptation of other ATMT-compatible vectors into FB/GB could be considered, such as the binary-BAC (BIBAC) vector reported by Hamilton (1997), which can

carry >100 kb and has already been used to transform *Fusarium, Aspergillus* or *Ustilago* species (Ali and Bakkeren, 2011; Takken et al., 2004).

Among the new genetic elements in the FB system, we included three commonly used fungal selection markers, two of them based on antibiotic resistance (*ble* and *ergA*, which confer resistance to phleomycin and terbinafine, respectively), and one based on fungal auxotrophy (*pyr4*), further expanding the possibilities for fungal transformation and mutant selection within the frame of the FB platform. Although antibiotic resistance markers are among the most widely used approaches for positive transformant selection, auxotrophic markers are more sustainable alternatives to the use of antibiotics, which can have undesired side effects on the fitness of the organism under study or cause unwanted spontaneous resistance. The orotidine 5'-phosphate decarboxylase-encoding gene *pyr4* from *T. reesei*, which is an ortholog of the *Aspergillus* and *Penicillium pyrA*/*pyrG* gene, is widely applied as a strong auxotrophic selection marker that can be counter-selected using 5-FOA or fully supplemented using uracil or uridine (Derntl et al., 2015; Díez et al., 1987). Interchangeability of these two orthologs has already been demonstrated between fungi from different phylogenetic classes, from Sordariomycetes to Ascomycetes and vice versa (Ballance and Turner, 1985; Díez et al., 1987; Gruber et al., 1990). Therefore, the FB-adapted *pyr4* TU is expected to restore uridine/uracil auxotrophy in a broad range of fungal species. In the case of fungal (plant) pathogens, for which *pyr* disruption has been reported to reduce pathogenicity and virulence (Higashimura et al., 2022; Zameitat et al., 2007), and as also demonstrated here for *P. digitatum* Δ*pyrG* for the first time (Figure S4), *pyr4* complementation completely restored pathogenicity, thus demonstrating the suitability of this genetic element as an auxotrophic selectable marker also for (phyto)pathogenic fungi.

The luciferase reporter system has allowed us to functionally validate and characterize 7 distinct promoters that have been incorporated as standard DNA parts to the FB toolbox. Among these are novel promoter sequences for which their functionality had never been validated before (P*afpB*, P7760 and P*ef1*α). These promoters were selected either for their interesting behavior in a *P. digitatum*-based transcriptome analysis (Ropero-Pérez et al., 2023), or because they are well-known promoters, such as the strong P*pkiA* or the maltose-

responsive P*glaA* and *PamyB,* all of which have been extensively used in *Aspergillus* species (Oliveira et al., 2008; Song et al., 2018; Storms et al., 2005). Among the inducible promoters included in this study, P*glaA* and P*xlnA* have already been implemented in alternative Golden Gate-compatible collections (Mózsik et al., 2021; Polli et al., 2016), yet validation of either basal or induced states has not been described in *Penicillium* species. Here, a wide expression range was found for all tested promoters, from the highly expressed P*pkiA* and P*ef1*α promoters, with levels similar to those of the well-known P*paf* and P*gpdA,* to lower -or almost no- expressed ones, such as P07760 and P*afpB*. The expression levels of almost all these promoters were reduced in *P. chrysogenum* compared to *P. digitatum*, except for the newly characterized P*ef1*α promoter from *P. digitatum*, which showed similar values in both fungal backgrounds. This likely reflects a greater orthogonality in this promoter, which may be of preferable use to ensure strong expression in other fungal chassis. Inducibility of P*glaA*, P*amyB* and P*xlnA* was also validated using the luciferase reporter system in both *Penicillium* species, showing different expression ranges both in the presence and absence of the inducer. This allows for multiple options for the custom design of future experiments, allowing the choice of promoters with lower background expression, such as P*xlnA*, when basal expression needs to be almost completely avoided, or to prioritize activation over background expression with promoters such as P*amyB*. Interestingly, P*amyB* induction in *P. chrysogenum* was similar to that shown in the industrial workhorse *Aspergillus oryzae* using β-glucuronidase as reporter. The expression of this promoter was reported to increase 10 times in a maltose-containing medium compared to glucose (Ozeki et al., 1996). This expression was slightly higher (1250 U/mg) (Tada et al., 1991) than that reported for P*glaA* (903 mg U/mg) (Hata et al., 1992), which correlates with our results shown in Figure 5B. Both P*glaA* and P*amyB* promoters are commonly applied for the production of different proteins of interest such as human tissue plasminogen (Wiebe et al., 2001), bovine chymosin (Ohno et al., 2011) or synthetic human lysozyme (Tsuchiya et al., 1992a), which further shows their relevance in the field of fungal biotechnology. On the other hand, the use of P*xlnA* promoter is much limited to date, being its ortholog, P*xylP* from *P. chrysogenum,* more extensively used (Yap et al., 2022). Here, we demonstrate the possibility of implementing this promoter in the *Penicillium* genus, with more modest induction levels than those

of P*glaA* and P*amyB* but with lack of basal expression in the absence of the inducer.

Unexpectedly, the P*paf* expression was found to significantly increase in the presence of maltose in *P. chrysogenum* and xylose in both *P. chrysogenum* and *P. digitatum.* This would suggest that (i) maltose and xylose themselves or any of the maltose/xylose catabolic intermediates serve as inducers for P*paf* or (ii) P*paf* expression is partially repressed by glucose, which can be attributed to the presence of carbon catabolite repression CREA motifs in the P*paf* sequence, as previously described (Marx et al., 1995). This repression is nevertheless almost completely lost when P*paf* is expressed in a different fungal chassis, such as *P. digitatum,* suggesting different regulatory mechanisms between both fungal species despite their phylogenetic proximity.

The activation of GB_SynP promoters in *P. digitatum* was addressed using the luciferase reporter system and the CRISPRa system included in the pAMA18.0_gRNA1 vector (Mózsik et al., 2020). The non-integrative nature of this pAMA1-based plasmid makes it possible to revert promoter activation upon plasmid loss in the absence of selection pressure (Garrigues et al., 2022). Additionally, this CRISPRa system provides a method to easily assay expression variations within the same background strain, either by testing different activation domains or inducible systems, or by analyzing the induction level in different culture conditions. The activation of 1xLuc and 2xLuc constructs, however, was not achieved in *P. digitatum* using the pAMA18.0_gRNA1 vector, as signals of all but one 1xLuc re-transformant were on the same range as the basal signal of the reference strain. The expression of 1xLuc was, however, not different from the expression observed in 3xLuc strains in the absence of the CRISPRa system, which could mean that this expression is within the range of basal expression of the synthetic promoters. On the other hand, in the case of the 3xLuc construct, we did observe an increase of more than one order of magnitude in the presence of the CRISPRa system compared to the non-activation control for all 3xLuc re-transformants tested. These results indicates that activation of these promoters in fungi requires the presence of at least 3 repetitions of the gRNA target, which highly differ from what was observed in plants, where one repetition of the target sequence for gRNA1 was sufficient to drive a significant increase of the synthetic

promoter expression (Moreno-Giménez et al., 2022). The discrepancies in GB_SynP behavior between plants and fungi could be attributed to the differences in the CRISPRa systems used in each organism. While the pAMA18.0_gRNA1 used for activation in *P. digitatum* is comprised of the dCas9 protein fused to the VPR activation domain, the dCasEV2.1 complex used for activation in *Nicotiana benthamiana* plants includes a dCas9 protein fused to a EDLL activation domain and an extra MS2 protein fused to the VPR domain able to recognize and bind the modified gRNA scaffold (Selma et al., 2019). Although VPR showed a major contribution in the activation as the expression levels dropped significantly when MS2 was fused to other activation domains (Moreno-Giménez et al., 2022), in fungi a second activation component might be required to reach higher activation levels. Another explanation for the low expression levels in fungi may reside in the gRNA1 used to trigger the activation of GB_SynP promoters, which was originally designed for plants. Although no off-targets were found for the gRNA1 in *P. digitatum* CECT 20796 genome, the efficiency of this gRNA may not be optimal for this chassis, and therefore a gRNA designed specifically for fungi might enhance the activated expression levels. Additionally, expression levels in fungi could also be enhanced by creating new A2 proximal promoter parts with more than three repetitions of the gRNA1 target sequence. Further optimization of GB_SynP promoters for filamentous fungi following these guidelines will be explored in the near future to better characterize this tool and its potentially wide range of expression for the design of customizable synthetic promoters in filamentous fungi.

MATERIALS AND METHODS

Strains, media and growth conditions

The fungal strains used in this study were *P. digitatum* CECT 20796 (isolate PHI26) (Marcet-Houben et al., 2012) and *P. chrysogenum* wild type ATCC 10002 (Q176) (Hegedüs et al., 2011). Fungi were routinely cultured on Potato Dextrose Agar (PDA, Difco-BD Diagnostics) plates for 7 days at 25°C. For transformation, vectors generated were amplified in the bacterium *Escherichia coli* JM109 grown in LB medium at 37°C with either 50 µg/mL chloramphenicol, 50 µg/mL kanamycin,

100 µg/mL spectinomycin or 100 µg/mL ampicillin depending on the vector. *Agrobacterium tumefaciens* AGL-1 was cultured in LB medium at 28°C with 20 µg/mL rifampicin and the corresponding antibiotic depending on the vector carried.

For growth profiles, 5 µL of conidial suspension (5×10^4 conidia/mL) were deposited on the center of PDA plates and colony morphology was assessed and compared daily by visual inspection.

Design, domestication and DNA assemblies of genetic elements

All the genetic elements that have been incorporated in the FB platform are listed in Table 1. New DNA parts were domesticated according to GB rules and tools (https://gbcloning.upv.es) and ordered from an external company as synthetic genes (gBlocks™, IDT). In the case of the coding sequence (CDS) of *pyr*4, the gene from *Trichoderma reesei* was codon-optimized according to optimal codon frequency of *Penicillium* genera, previous to the GB/FB domestication. Domesticated elements were ligated into the pUPD2 entry vector via the restriction-ligation protocol as previously described (Hernanz-Koers et al., 2018; Vazquez-Vilar et al., 2020). Positive *E. coli* clones were confirmed by routine PCR amplifications and Sanger sequencing using external specific primers OJM524 and OJM525 designed for pUPD2 vectors (Hernanz-Koers et al., 2018) (Table 2). Multiple assemblies into pDGB3α vectors of the DNA parts contained in pUPD2 vectors were carried out to obtain the different TUs, and binary assemblies were subsequently performed to combine the different TUs into multigenic constructs within these pDGB3α or pDGB3Ω vectors as previously described (Hernanz-Koers et al., 2018; Vazquez-Vilar et al., 2020).

The sequence of the single guide RNA 1 (gRNA1) required to activate GB_SynP promoters was checked for the absence of off-target mutations in the *P. digitatum* genome using Geneious Prime software (https://www.geneious.com/), and was cloned into the pAMA18.0 vector as described (Mózsik et al., 2020). Briefly, a primer pair was designed (OJM698 and OJM699, Table 2) which contained the target sequence of gRNA1, the hammerhead ribozyme, the inverted repetition of the 5'-end of the spacer sequence and the recognition sites of B*sa*I. The resulting PCR product was purified (Wizard SV Gel and PCR Clean-Up System, Promega) and

inserted into pAMA18.0 via restriction-ligation reaction with B*sa*I and T4 ligase. Correct assemblies of the resulting pAMA18.0_gRNA1 vector were confirmed by Sanger sequencing.

Fungal transformation and mutant confirmation

Transformation of *P. digitatum* CECT 20796 (PHI26) and *P. chrysogenum* ATTC 10002 (Q176) with the corresponding FB binary vectors described in Table 1 was performed through ATMT as previously described (Khang et al., 2006) with some modifications (Harries et al., 2015; Vazquez-Vilar et al., 2020).

In the case of *P. digitatum* uridine-auxotrophic Δ*pyrG* mutants, in which the *pyrG* gene (gene ID PDIG_38390) was deleted by homologous recombination without insertion of any positive selection marker, mutants were selected on PDA supplemented with 1.22 g/L uridine (Sigma Aldrich) and 1.25 g/L of 5-Fluoroorotic acid (5-FOA, Formedium). For the ectopically complemented *P. digitatum* Δ*pyrG:pyr4* strains, mutants were selected on PDA plates. *P. digitatum* and *P. chrysogenum* ectopic transformants containing *ble* TU (phleomycin^{R}) were selected on PDA plates supplemented with 35 µg/mL or 25 µg/mL phleomycin (InvivoGen), respectively. Finally, *P. chrysogenum* ectopic transformants carrying *ergA* TU (terbinafine^{R}) were selected on PDA plates supplemented with 0.5 µg/mL terbinafine hydrochloride (Sigma-Aldrich).

P. digitatum and *P. chrysogenum* transformants carrying the different luciferase reporter constructs to test the constitutive, inducible and GB_SynP promoters were selected on PDA plates containing 25 µg/mL geneticin (G418) (InvivoGen).

All transformants were molecularly confirmed by PCR reactions using NZYTaq II DNA polymerase (Nzytech) (Figures 1-3; Figures S1-S3) from genomic DNA isolated with NZY Tissue gDNA Isolation kit (Nzytech) and primers purchased from IDT (Table 2).

For the validation of the GB_SynP promoters, *P. digitatum* protoplasts from strains carrying the luciferase reporter vectors for each of the three synthetic promoters tested (FB398, FB399 and FB400) (Table 1) were transformed with the self-replicative AMA1-based dCas9-containing plasmid pAMA18.0_gRNA1 (Mózsik et al., 2020) as described (Garrigues et al., 2022). Transformants were selected on

PDA plates containing 0.95 M sucrose and 35 µg/mL phleomycin. To verify the reusability of the system, the loss of pAMA18.0_gRNA1 plasmid was confirmed after three consecutive streaks of the transformants in non-selective PDA plates, as previously described (Garrigues et al., 2022).

Luciferase/Nanoluciferase assays

P. digitatum and *P. chrysogenum* strains carrying the luciferase reporter vectors for each of the tested promoters (FB433, FB434, FB435, FB436, FB438, FB439 and FB441) and *P. digitatum* strains with the luciferase reporter for the GB_SynP synthetic promoters (FB398, FB399 and FB400), carrying or not the pAMA18.0_gRNA1, were grown in duplicate for 2 days in 100 mL flasks with 25 mL of liquid Potato Dextrose Broth (PDB, Difco-BD Diagnostics) at 25°C with shaking (150 rpm). For induction assays, transformants were grown in duplicate for 4 days in 100 mL flasks with 25 mL of either *P. digitatum* or *P. chrysogenum* minimal medium (PdMM or PcMM, respectively) (Sonderegger et al., 2016) using 2% D-glucose (Panreac), 2% maltose (Sigma-Aldrich) or 2% D-xylose (Sigma-Aldrich) as the sole carbon source. Grown mycelia were filtered and a sample of ~20 mg was collected and immediately frozen in liquid nitrogen. Luciferase and nanoluciferase measurements were performed with the Dual-Glo® Luciferase Assay System (Promega) as previously described (Gandía et al., 2022). Briefly, frozen samples were homogenized in 180 µL Passive Lysis Buffer with a pestle and centrifuged (12,000 ×*g*, 10 min at 4 °C). Ten µL of the supernatant were transferred to a white 96-well plate (Thermo Fisher Scientific) and mixed with 40 µL of Luciferase reagent to measure luciferase luminescence in a CLARIOStar microplate reader (BMG LABTECH GmbH) with a measurement of 10 s and a delay of 2 s. Nanoluciferase luminescence was quantified thereafter by adding 40 µL of Stop&Glow Reagent and measured in the same way.

The Luciferase/Nanoluciferase ratio was determined for each sample, and normalized luminescence was calculated as the mean value of the ratios obtained from each duplicate. Statistical analyses were performed with GraphPad Prism 8.0.1 software. Differences between the strains were analyzed using one-way ANOVA followed by the post hoc multiple comparisons Tukey's test ($p < 0.05$). For the induction experiments, we analyzed the differences in the growth of each

strain in the presence of the different carbon sources using Student's t test ($p < 0.05$).

Fruit infection assays

P. digitatum parental and mutant strains were inoculated on freshly harvested oranges (Citrus sinensis L. Osbeck cv Lane Late) as previously described (González-Candelas et al., 2010). Briefly, three replicates of five orange fruits were inoculated with 5 µL of fungal conidial suspension (10^4 conidia/mL) at four equidistant wounds around the equator. Control mock inoculations were performed with 5 µL of sterile Milli-Q H_2O. Once inoculated, fruits were maintained at 20°C and 90% relative humidity for up to 6 days. Each inoculated wound was scored daily for infection symptoms on consecutive days post-inoculation (dpi). We repeated the experiments twice. Differences in the % of infection for each strain compared to the control CECT 20796 were analyzed using Student's *t* test ($p < 0.05$) for each individual dpi.

Table 2. Primers used in this study.

ID	Use*	Sequence 5'-3' **	Tm (ºC)	Origin	Purpose	Reference
OJM371	F	ATAGATCTAACTGATATTGAAGGAGCA	52	P*trpC*	Molecular characterization	This study
OJM509	F	GCGCCGTCTCGCTCGGGAGTGGCGCATGCGGACAGACGG	64	P*gpdA*	Molecular characterization	(Hernanz-Koers et al., 2018)
OJM522	R	GCGCCGTCTCGCTCAAGCGCATGTCTCAGACGGTCGATG	62	T*trpC*	Molecular characterization	(Hernanz-Koers et al., 2018)
OJM524	F	GCTTTCGCTAAGGATGATTTCTGG	70	pUPD2	Molecular characterization	(Hernanz-Koers et al., 2018)
OJM525	R	CAGGGTGGTGACACCTTGCC	66	pUPD2	Molecular characterization	(Hernanz-Koers et al., 2018)
OJM555	R	TCATCATGCAACATGCATGTA	58	T*tub*	Molecular characterization	(Hernanz-Koers et al., 2018)
OJM655	R	CATCCATACTCCATCCTTCCC	60	pAMA18.0	Molecular characterization and sequencing	This study

ID	Use*	Sequence 5'-3' **	Tm (ºC)	Origin	Purpose	Reference
OJM656	F	CATTTTTGTCGTCATGTGCTGG	55	5' Pdig *pyrG*	Molecular characterization	This study
OJM657	R	GAAGGCTGAACTCACTGTGG	55	3' Pdig *pyrG*	Molecular characterization	This study
OJM662	F	GCTTTTGCTAACCATTTGGGACAC	52	GB B6 code	Cloning of FB372 into pDGB3α1	This study
OJM663	R	AGCGGTGTCCCAAATGGTTAGCAA	52	GB C1 code	Cloning of FB372 into pDGB3α1	This study
OJM696	F	TTGTCTCACTCTCTCTTTTCC	51	*pyr4*	Molecular characterization	This study
OJM697	R	ATTCCATGCTTCCAGATCC	51	*pyr4*	Molecular characterization	This study
OJM698	F	ATGGTCTCACCGACCAGTCCTGATGAGTCCGTGAGGACGAAACGAG	60	pAMA18.0	Cloning of gRNA1 into pAMA18.0	This study
OJM699	R	ATGGTCTCTAAACTCTTCTCTCACCAACCAGTCGACGAGCTTACTCGTTTCGTCCTCACGGACTCA	60	pAMA18.0	Cloning of gRNA1 into pAMA18.0	This study
OJM705	F	TCCTGGAAGTGCGTTGATCA	51	P*xlnA*	Molecular characterization	This study
OJM706	F	GGAAGAGAAAACCTCCGAGTAC	54	P*pkiA*	Molecular characterization	This study
OJM707	F	ATGAATTCCACCGAATGCAC	53	P*afpB*	Molecular characterization	This study
OJM708	F	TGCCATTGGCGGAGGGGTCC	53	P*glaA*	Molecular characterization	This study
OJM709	F	TCAACTGATTAAAGGTGCCG	53	P*amyB*	Molecular characterization	This study
OJM710	F	GTGAAAAAACGGATGGGGAC	53	P*ef1α*	Molecular characterization	This study
OJM711	F	GATAATGGTGATTCGGCGCG	53	P07760	Molecular characterization	This study
OJM715	F	GTATCTGCATGTTGCATCGG	53	P*pcbC*	Molecular characterization	This study
OJM716	R	TACCGCTCGTACCATGGGTT	53	T*amds*	Molecular characterization	This study

* F: forward; R: reverse.

** gRNA1 sequence is underlined.

SUPPLEMENTARY MATERIAL

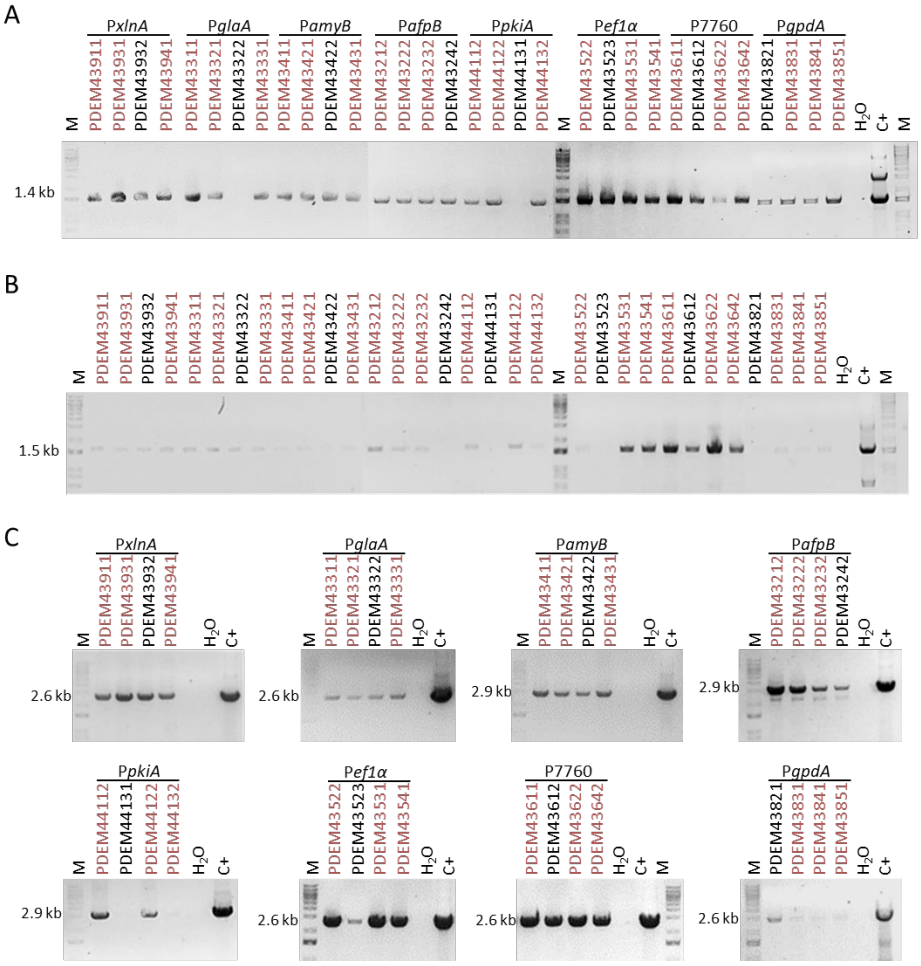

Figure S1. Molecular characterization of *P. digitatum* strains transformed with luciferase reporter system for each of the assayed promoters. (A) Amplification of the *nptII* geneticin resistance TU (1.4 kb) using primers OJM371 and OJM555. (B) Amplification of nanoluciferase TU (1.5 kb) using primers OJM509 and OJM555. (C) Amplification of luciferase TUs for each construct using the reverse primer OJM522 and the corresponding forward primer for each promoter (OJM509 for P*gpdA*, OJM705 for P*xlnA*, OJM706 for P*pkiA*, OJM707 for P*afpB*, OJM708 for P*glaA*, OJM709 for P*amyB*, OJM710 for P*ef1α*, and OJM711 for P7760). The 2.6 kb bands correspond to the complete luciferase TU when expressed under the promoter P*xlnA,* P*glaA*, P*gpdA*, P7760 or P*ef1α*, and the 2.9 kb bands correspond to the luciferase TU under P*amyB*, P*kiA* or P*afpB*. A total of 4 transformants for each construct were analyzed. Names in red correspond to the validated transformants that were selected for the luciferase assay.

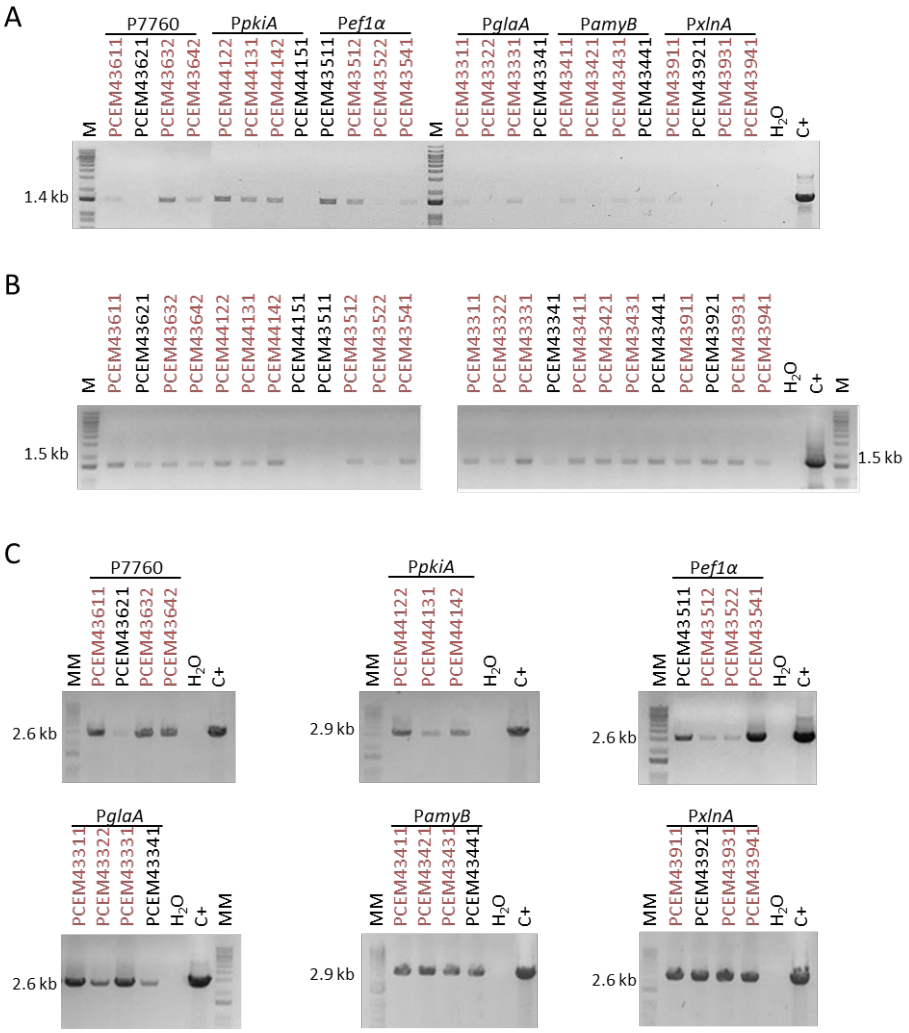

Figure S2. Molecular characterization of *P. chrysogenum* strains transformed with luciferase reporter system for each of the assayed promoters. (A) Amplification of the *nptII* geneticin resistance TU (1.4 kb) using primers OJM371 and OJM555. (B) Amplification of nanoluciferase TU (1.5 kb) using primers OJM509 and OJM555. (C) Amplification of luciferase TUs for each construct using the reverse primer OJM522 and the corresponding forward primer for each promoter (OJM705 for P*xlnA*, OJM706 for P*pkiA*, OJM708 for P*glaA*, OJM709 for P*amyB*, OJM710 for P*ef1α*, and OJM711 for P7760). The 2.6 kb bands correspond to the complete luciferase TU expressed under the promoter P*xlnA* (FB439), P*glaA* (FB433), P7760 (FB436) or P*ef1α* (FB435), and the 2.9 kb bands correspond to the luciferase TU under P*amyB* or P*pkiA*. Names in red correspond to the validated transformants that were selected for the luciferase assay.

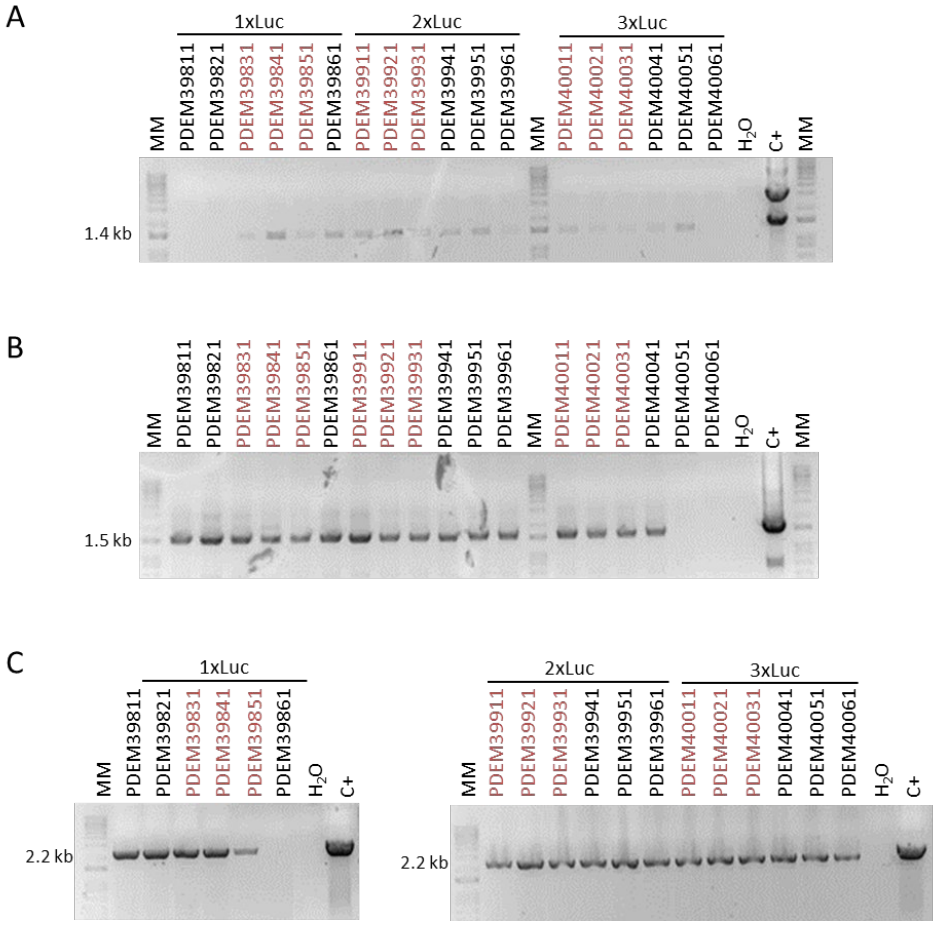

Figure S3. Molecular characterization of *P. digitatum* strains transformed with luciferase reporter system under the regulation of GB_SynP synthetic promoters. (A) Amplification of the geneticin resistance *nptII* TU (1.4 kb) using primers OJM371 and OJM555. Transformant names correspond to the construct carried, which contained the luciferase under the regulation of the synthetic promoter with one repetition of the gRNA1 target sequence (1xLuc, FB398 construct, PDEM398XX transformants), two repetitions (2xLuc, FB399, PDEM399XX) or three repetitions (3xLuc, FB400, PDEM400XX). (B) Amplification of nanoluciferase TU (1.5 kb) using primers OJM509 and OJM555. (C) Amplification of luciferase TU (2.2 kb) in each construct using the primers OJM522 and OJM754 for 1xLuc and the primers OJM522 and OJM755 for 2xLuc and 3xLuc. Names in red correspond to the validated transformants that were selected for the luciferase assay.

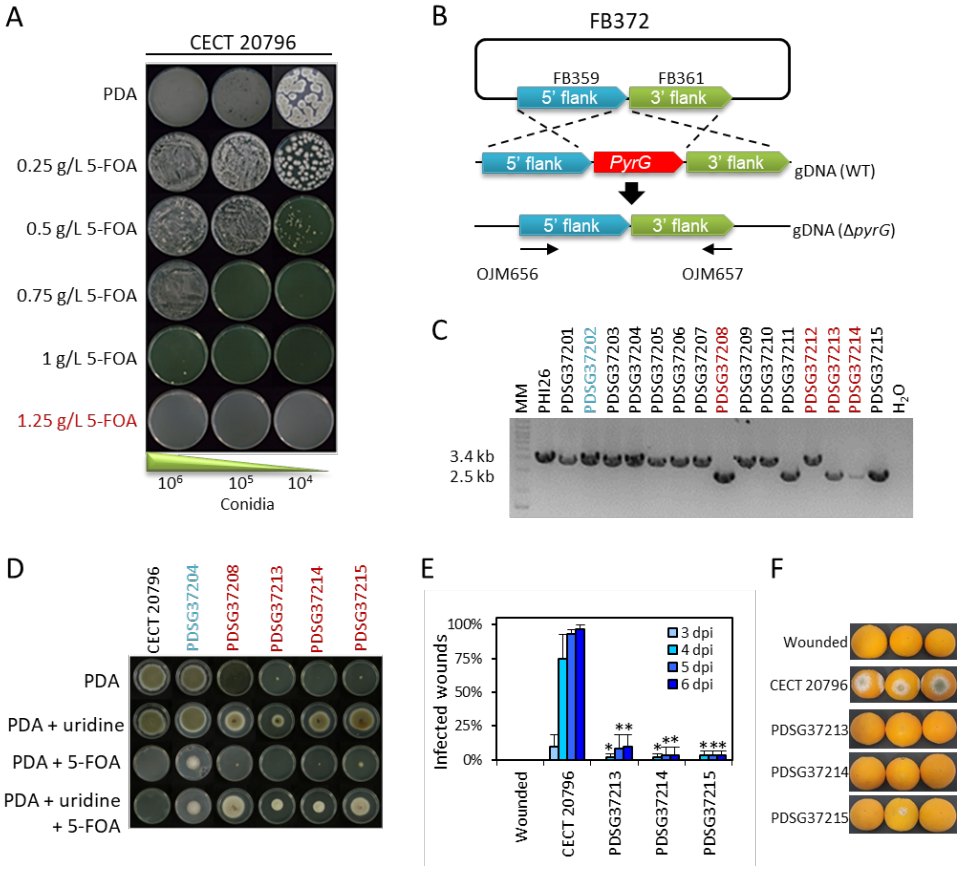

Figure S4: Generation of *P. digitatum* Δ*pyrG* mutants. (A) Minimum Inhibitory Concentration (MIC) analysis of *P. digitatum* CECT 20796 in the presence of increasing concentrations of 5-Fluoroorotic acid (5-FOA). A concentration of 1.25 g/L was chosen for *pyrG* deletant selection (in red). (B) Plasmid pDGB3α1 FB372 meant for the deletion of *pyrG* gene in *P. digitatum* by ATMT and homologous recombination. Note that no marker was included for positive selection. Primers OJM656 and OJM657 were used for the molecular characterization of the 5-FOA resistant transformants shown in (C). The 3.4 kb band corresponds to the *pyrG* gene whereas 2.5 bands correspond to expected amplicon size after *pyrG* deletion. Selected transformants are highlighted in red. (D) Growth profile of positive Δ*pyrG* transformants. PDSG37024 was included as a control of a spontaneous 5-FOA resistant strain that did not have *pyrG* deleted as shown in (C) (in blue). (E) Fruit infection assays of Δ*pyrG* mutants on oranges. Data indicate the percentage of infected wounds (mean ± SD) at each day post-inoculation (dpi). (*) shows statistical significance between each sample compared to the control CECT 20796 at each dpi (*t* test, $p < 0.05$). (F) Representative images of oranges infected by the indicated strains at 6 dpi.

GENERAL DISCUSSION

GENERAL DISCUSSION

Pheromone production in different biological platforms

The bio-based production of pheromones is still in the early phases of development, yet the increasing number of publications highlights the considerable interest in this sustainable solution for pest control. So far, work has been mainly done in yeast and model plants. Although microbial fermentation is well-established and generally preferred for the production of many biomolecules in industry, plant-based production might be better adapted for this purpose as plants have evolved to use and take advantage of this communication system to attract pollinators and natural enemies of pests. In this regard, the transient expression strategy in *N. benthamiana* has allowed for the fast production of high amounts of lepidopteran pheromones (Ding et al., 2014; Xia et al., 2022, 2020). The transient nature of this expression system, however, cannot provide field-grown advantages, nor can be envisioned as biodispenser comparable to stable transgenics. Stable transgenic *N. tabacum* plants could be grown in the field and provide potentially higher production yields than its smaller relative, *N. benthamiana*.

Although work so far has focused on the use of model plants, the exploitation of more specialised species for biomanufacturing pheromones should also be explored. Regarding pheromone emission, enhanced volatilization could be achieved by employing aromatic plants, although biotechnological tools are much more limited in these species and entails additional difficulties for their transformation and *in vitro* growth (Shelepova et al., 2022). Regarding the lipidic nature of type I lepidopteran pheromones, the employment of oil crops like *Camelina sativa* for their production could result in higher yields, although it may generate concerns about competition with food crops (Löfstedt and Xia, 2021; Ortiz et al., 2020; Wang et al., 2022). As an alternative to plants, the use of filamentous fungi could also be of interest for the industrial-scale production of pheromones due to their reduced complexity in terms of production and extraction processes. In fact, lipid-rich fungal platforms are already available, and they could be engineered to produce these type I lepidopteran pheromones (Rivaldi et al., 2017).

Regardless of the platform, pheromone yields need to be increased to be industrially feasible, reaching hundreds of kg Ha^{-1} for plants or above 1g/L for bioreactors (Löfstedt and Xia, 2021). For the biodispenser goal, emissions of at least 20 mg Ha^{-1} day^{-1} are required (Alfaro et al., 2009; Gavara et al., 2020). In order to efficiently engineer biological platforms to achieve these production goals, a better understanding of the metabolic impact and assessment of production strategies are still required.

Assessment of plant biofactories for the production of insect pheromones

In Chapter I, we provide a comprehensive analysis of the constitutive production of two lepidopteran sex pheromones, Z-11:16OH and Z-11:16OAc, using the well-established *N. benthamiana* model plant to further identify the drawbacks and issues associated with the production of these fatty acid-derived molecules in a plant chassis. The transgenic plants (SxPs) generated in this study were extensively examined for their physiology and volatilome, which was later complemented with an extensive analysis of their transcriptome (Juteršek et al., 2022). The results showed that SxPs were able to stably produce and emit modest amounts of both pheromones for several generations, yet pheromone production was strongly linked to growth deficiencies, as high producer plants were small and prone to diseases and senescence. This growth penalty was consistent with previous studies that reported similar phenotypes in plants expressing fatty acid-derived molecules (Reynolds et al., 2017; Xia et al., 2020). Moreover, pheromone production had a significant impact on the plant's volatilome, leading to a general increase in fatty acid-derived compounds and a marked reduction in phenolics and monoterpenoids. The photosynthetic activity was also adversely affected, along with the activation of numerous stress responses. Interestingly, higher production of Z-11:OAc with respect to Z-11:OH seemed to partially alleviate the metabolic burden, suggesting that the accumulation of Z-11:OH pheromone might also be toxic to the plant. In summary, this chapter concludes that constitutive production of lepidopteran type I pheromones in plants results in a substantial diversion of metabolic flux towards lipid biosynthesis, thereby reducing the resources available for normal plant development and defense. To optimize plant pheromone biofactories, it is crucial to reduce the impact of pheromone

production and accumulation on plant fitness, which could also be partially achieved by enhancing the volatilization and emission of the pheromone molecules.

The use of tissue-specific promoters could be effective for both reducing the pheromone toxicity and for enhancing their release into the environment. In this regard, Xia et al. (2022) reported a significant increase in both pheromone accumulation and volatilization by expressing the diacylglycerol acetyltransferase *ATF1* gene, the last enzyme of the pathway, under a trichome-specific promoter. This improvement may be further enhanced with the use of active transporters such as ATP-binding cassette (ABC) transporters to increase the pheromone transport outside the cell. Another complementary approach may include the use of pheromone/odorant binding proteins to alleviate the toxicity caused by accumulation. Regulation of stomatal opening or leaf cuticular composition might improve production and emission ratios as well. Nevertheless, these approaches pose challenges and uncertainties as the mechanisms underlying the transport of volatiles in plant leaves remain largely unknown (Escobar-Bravo et al., 2023). On the other hand, extensive knowledge on genetic regulation is currently available for the design of tightly regulated promoters that could effectively separate plant growth from pheromone production and accumulation by limiting their synthesis both spatially and temporally. In this thesis we decided to focus on this latter approach and develop synthetic biology tools to enable precise and timely regulation of pheromone production.

Combination of GB_SynP promoters with the dCasEV2.1 activation system for transgene expression in plants

In Chapter II, dCasEV2.1 versatility was harnessed to develop a set of robust, predictable and orthogonal synthetic promoters. The so-called GB_SynP demonstrated tight and predictable regulation of transgene expression, reaching levels similar to the widely used *NOS* and CaMV35S constitutive promoters. GB_SynP were envisioned as fully customizable tools where any 20-nucleotide sequence could act as a cis-regulatory element without affecting the performance of the designed promoter. Their modular nature further consolidates this design flexibility to fit any application, while facilitating the avoidance of repetitions in multigene constructs that could lead to unpredictable rearrangements and

expression issues (Stam et al., 1997; Vaucheret et al., 1998). In fact, the expression of pheromone pathway enzymes under copper-sensing promoters was found to be affected by the multigenic architecture in Chapter III. Interestingly, we were able to greatly reduce this effect when the enzymes were expressed under GB_SynP promoters coupled to copper-sensing dCasEV2.1. This represents one of the important contributions of this doctoral thesis to the field of plant synthetic biology, as it provides a steppingstone for designs with more precise control of transgene expression.

In Chapter III, we present a comparison between three powerful regulatory systems transiently expressed in *N. benthamiana* based on TALE, ΦC31 integrase, or this dCasEV2.1-GB_SynP system. This comparison positioned dCasEV2.1-GB_SynP as the most tightly regulated of the three, with the lowest expression detected in the absence of the inducer, while reaching similar expression levels upon activation. The expression of this system, however, was greatly reduced in stable transformation and proved insufficient to enable the detection of pheromone production (data not shown). Improvement of the system is still necessary to allow for the further development of the transgenic SxPv2 plants described in Chapter I. In fact, recent work by our research group, building on the work presented here, showed that the stable transformation of the pheromone pathway under the control of GB_SynP combined with the transient expression of the dCasEV2.1 system can reach yields of around 400 µg Z11-16OH g^{-1} FW and 200 µg Z11-16OAc g^{-1} FW (Kallam et al., 2023), which are comparable to those reported by other groups (Ding et al., 2014; Xia et al., 2020) and even higher than those reported for stable SxPv1.2 (164.9 µg Z11-16OH g^{-1} FW and 9.6 µg Z11-16OAc g^{-1} FW).

Regarding dCasEV2.1 components, dCas9:VPR and MS2:EDLL fusion proteins are likely more limiting in terms of abundance than the gRNA itself. If this is the case, the constitutive expression of these proteins in combination with the inducible expression of the gRNA could be a suitable approach to achieve effective regulation of the system, while reaching sufficiently high expression in the activated state. Such an approach has been already explored by our research group by expressing the gRNA under the control of pol-II promoters, which enables the application of copper-sensing and other well-described regulatory

systems in plants for the expression of gRNAs (García-Pérez et al., 2022). Alternatively, the expression of either gRNA or CRISPRa proteins can be enhanced by using viral expression vectors, which could also be easily delivered into plant cells by spraying (Selma et al., 2022a). The use of alternative inducers should also be considered. Although most plant studies have employed inducible systems based on expensive compounds (dexamethasone) or physical stresses (heat, wounding) that may hamper plant fitness, novel approaches are emerging to provide new agronomically-friendly inducible systems. Among these are optogenetic (light-inducible) systems (Müller et al., 2014; Ochoa-Fernandez et al., 2020) or even oxygen induction (Iacopino et al., 2019). Many of these options, however, could affect normal plant growth if applied during long periods of time. In this regard, the use of so-called memory switches could also be considered for pheromone production to further facilitate the handling of plants, since only a single treatment would be required to switch on pheromone production. Efforts in our research group have also been made towards this aim, resulting in the development of a memory switch based on the ΦC31 integrase (Bernabé-Orts et al., 2020).

Pheromone production in filamentous fungi as an alternative for their easy adaptation to industrial processes

The constitutive production of pheromones in filamentous fungi should also be considered, as any deleterious effects arising from pheromone accumulation can be avoided by taking advantage of the secretory system of these organisms. In addition, the interchangeability of GoldenBraid and FungalBraid parts can be employed to easily translate the biosynthetic pathways developed for plants to fungal expression constructs, which can then be transformed into many filamentous fungi species via ATMT. However, preliminary attempts made within the context of this thesis to produce the same lepidopteran pheromones constitutively in *Penicillium species* were unsuccessful (data not shown), likely due to limitations of precursors or to non-optimal growth conditions to produce these compounds. Both issues should be further investigated by testing different growth conditions and/or adding the precursors themselves to determine if the issue is a matter of resource scarcity.

In contrast to plants, the inducible systems available in filamentous fungi are extensively implemented in industry and commonly work with economic and environmentally friendly molecules, such as sugars or lignins, as inducers (Kluge et al., 2018). In Chapter IV, some of these well-characterized inducible promoters were included in our FB collection, together with other well-known constitutive promoters and some newly described ones. The inducible promoters included in this work were two maltose-responsive (P*glaA* and P*amyB*) and one lignin-responsive (P*xlnA*) promoter, all of which showed a significant increase in the expression of the target reporter gene in the presence of the inducer and so they could be tested for pheromone production in *Penicillium* species.

Chapter IV also provides the validation and characterization of these promoters in two *Penicillium* species. This was accomplished by adapting the normalized luciferase reporter system employed in Chapter II and III for the assessment and comparison of promoters in plants to filamentous fungi. This characterization was useful to observe variations between promoter strengths within and between fungal species, giving valuable insight for the selection of the most suitable promoter depending on the application and fungal species. In the same way, Chapter IV also expands the FB selection marker repertoire with the incorporation of phleomycin and terbinafine antibiotic resistances, and the *pyr4* uridine auxotrophy marker.

As discussed in Chapter III, the use of promoters with different strengths for each enzyme should also be considered as this could lead to an increase in pheromone production. In addition, we also showed that the use of different configurations affects transgene expression levels and should also be taken into consideration in future design strategies. In this regard, constitutive promoters such as P*ef1*α which showed strong expression similar to the widely used P*paf* promoter, or the intermediate P07760, could also be tested for pheromone production. Attention should also be given to the fungal chassis employed, as variations in promoter performance were observed between the two *Penicillium* species assayed under similar growth conditions. Finally, following Chapter III findings, a configuration where *Atr∆11* is positioned downstream of the other two enzymes should be tested, since this configuration was proven to be optimal for constitutive production in plants.

GB_SynP tool works in both plants and filamentous fungi

Chapter IV further explores the interchangeability of genetic parts between plants and filamentous fungi with the implementation of GB_SynP promoters in *Penicillium* species. The expression of GB_SynP promoters comprising the mPAF minimal promoter part and three repetitions of the gRNA1 target sequence was observed to significantly increase in all tested strains transformed with the pAMA18.0_gRNA1 vector. Important differences between plants and fungi were nevertheless observed, as activation of GB_SynP in fungi was only observed in the promoter containing three repetitions of the gRNA target, while in plants an activation of almost 900x (from an average value of 0.0023 RPUs to 2.16 RPUs when activated) was achieved with only one binding site for the gRNA in the promoter.

Moreover, additional GB_SynP promoters could be developed to include more than three repetitions of the gRNA target sequence. This can be optional in plants, but probably a must in fungi to ensure sufficient levels of activation. The incorporation of additional targets in future A2 designs should be done, paying special attention to the position in the promoter and the distance between cis-boxes. For the former, we further confirmed in Chapter II that the optimal window for activation is between -100 and -200 bp from the TSS in plants, as was previously reported by our group (Selma et al., 2019). Cis-boxes placed outside of these limits will therefore have a limited impact on transgene activation. Regarding the latter, the distance between boxes needs to be at least 20 bp to allow the fusion proteins to correctly bind the target promoter all at the same time.

Feasibility of the bioproduction of other insect pheromones

Although the work presented here has focused on the bioproduction of lepidopteran pheromones, the production of pheromones for other important species should also be studied. In this regard, pheromones of the Coccoidea family are of major interest due to their agronomical importance and their complex structure, elusive to chemical synthesis (Zou and Millar, 2015). Contrary to Lepidoptera, Coccoidea pheromones are terpenoid derivatives with many examples of irregular non-head-to-tail terpene alcohols and uncommon

cyclizations. However, the complexity of these structures has also hindered the elucidation of the genes involved in their biosynthesis, which are yet to be discovered (Juteršek et al., 2023). In this regard, recent work in our group has made use of plant genes to produce (R)-lavandulyl acetate, an active pheromone compound for different Coccoidea species, in *N. tabacum* plants (Mateos-Fernández et al., 2023).

In addition to direct production of pheromones, another interesting approach would be to produce central intermediate metabolites and precursors, to both provide sustainable starting materials and facilitate the development of new pheromone biofactories. Regarding type I pheromones, which comprise around 75% of the lepidopteran pheromones identified to date (Löfstedt and Xia, 2021), an interesting strain would be one able to produce (E)-11-tetradecenol, (Z)-11-tetradecenol, and (Z)-11-hexadecenol, as described in Ding et al. (2014). These compounds, as well as the corresponding acetates, can be used to attract more than 600 species of moths (El-Sayed, 2021). Apart from sex pheromones, systems designed for the production of other types of pheromones should also be translated to biodispensers, such as the production of (E)-β-farnesene in wheat, which could potentially deter many pest aphids (Beale et al., 2006; Bruce et al., 2015), or aggregation pheromones, such as those employed to attract natural predators of the targeted species (Kappers et al., 2005; Schnee et al., 2006).

Final remarks

This thesis presents the generation and characterization of initial versions of the SexyPlant biofactory for the stable production of lepidopteran pheromones. Based on these results, we present the design and characterization of GB_SynP synthetic promoters as a first step towards the development of a plant-based biodispenser to overcome the fitness issues associated with the production of these molecules. Future work will be focused on using alternative chassis more suitable for industrial implementation, such as *N. tabacum* to increase biomass and potentially reaching the attractive and cost-saving biodispenser goal. We also provided the adaptation of GB_SynP and other important constitutive and inducible promoters to *Penicillium* species for the tight regulation of gene expression in fungal platforms, which would be an interesting alternative for the production of pheromones, since these organisms are nowadays better adapted

to industrial processes. The results and SynBio tools obtained in this thesis thus pave the way for the efficient development and characterization of pheromone production pathways in both plants and filamentous fungi, facilitating the engineering of these chassis for the industrial production of these and other compounds.

CONCLUSIONS

CONCLUSIONS

1. The first two versions of pheromone-producing *N. benthamiana* plants were established and characterized. These new plant lines, named SxPv1.0 and SxPv1.2, showed constitutive production and detectable emission of the two lepidopteran pheromones Z-11-16OH and Z-11-16OAc throughout various generations. Their phenotypic characterization revealed deleterious effects on plant fitness and an impact on the composition of the plant´s volatilome as a consequence of the constitutive expression of lipid-based pheromones.

2. A collection of orthogonal synthetic promoters was developed and functionally characterized in combination with the programable transcriptional activator dCasEV2.1 based on the CRISPR/Cas9 architecture. Each promoter in the so-called GB_SynP collection results from the combinatorial assembly of three subsets of DNA elements: (i) a subset of randomized A1 distal DNA fragments that provide sequence variability, (ii) a second subset of A2 proximal DNA parts containing gRNA target sequences acting as cis-regulatory boxes, and (iii) a third subset of minimal promoter elements that ensure proper transcriptional initiation. GB_SynP has proven to be a powerful tool with neglectable basal expression for the coordinated expression of multigene pathways.

3. A comparison of the dCasEV2.1/GB_SynP system with two other synthetic activator strategies based on TALE, and ΦC31 architecture revealed that dCasEV2.1 is not only more versatile due to its programmable nature, but also yields higher gene activation levels and lower background than their activator counterparts.

4. The use of GB_SynP, in combination with a copper-regulated dCasEV2.1 activation system, allowed for the tight regulation of lepidopteran pheromone production in *N. benthamiana* plants, both in transient and stable expression systems, with higher pheromone yields observed in the transient expression strategy.

5. The normalized GB luciferase reporter system employed in plants was transferred to filamentous fungi and used to compare and validate different constitutive and inducible promoters included in the FungalBraid collection in two different *Penicillium* species. The tested promoters widen the expression range to choose from depending on the application, need for inducibility or fungal chassis. These additions expand the options available for the future production of pheromones and other biomolecules in fungal platforms.

6. The implementation of GB_SynP promoters in *Penicillium* species further confirmed the compatibility of the GB/FB systems and expanded the toolkit for synthetic biology in filamentous fungi, paving the way for easy, orthogonal and customizable regulation of transgenes in this chassis. The combination of GB_SynP with the non-integrative pAMA18-derived CRISPRa system also provides a testing method for dCas9-based inducible systems using the same background strain. Contrary to what was observed in plants, at least three copies of the gRNA target acting as the cis-regulatory box are required to obtain significant activation of GB_SynP using pAMA18-derived vectors.

REFERENCES

REFERENCES

Adebesin, F., Widhalm, J.R., Boachon, B., Lefèvre, F., Pierman, B., Lynch, J.H., Alam, I., Junqueira, B., Benke, R., Ray, S., Porter, J.A., Yanagisawa, M., Wetzstein, H.Y., Morgan, J.A., Boutry, M., Schuurink, R.C., Dudareva, N., 2017. Emission of volatile organic compounds from petunia flowers is facilitated by an ABC transporter. Science 356, 1386–1388. https://doi.org/10.1126/science.aan0826

Agricultural Pheromone Market report FBI100071, 2021. Fortune Business Insights, Global, 2021. https://www.fortunebusinessinsights.com/industry-reports/agricultural-pheromones-market-100071.

Aguilar, A., Twardowski, T., 2022. Bioeconomy in a changing word. EFB Bioeconomy J. 2, 100041. https://doi.org/10.1016/j.bioeco.2022.100041

Alfaro, C., Navarro-Llopis, V., Primo, J., 2009. Optimization of pheromone dispenser density for managing the rice striped stem borer, *Chilo suppressalis* (Walker), by mating disruption. Crop Prot. 28, 567–572. https://doi.org/10.1016/j.cropro.2009.02.006

Ali, S., Bakkeren, G., 2011. Introduction of large DNA inserts into the barley pathogenic fungus, Ustilago hordei, via recombined binary BAC vectors and Agrobacterium-mediated transformation. Curr. Genet. 57, 63–73. https://doi.org/10.1007/s00294-010-0324-0

Ando, T., 2021. List of sex pheromones, Ando Laboratory. URL https://lepipheromone.sakura.ne.jp/lepi_phero_list_eng.html

Andreou, A.I., Nakayama, N., 2018. Mobius Assembly: A versatile Golden-Gate framework towards universal DNA assembly. PLOS ONE 13, e0189892. https://doi.org/10.1371/journal.pone.0189892

Antonovsky, N., Gleizer, S., Noor, E., Zohar, Y., Herz, E., Barenholz, U., Zelcbuch, L., Amram, S., Wides, A., Tepper, N., Davidi, D., Bar-On, Y., Bareia, T., Wernick, D.G., Shani, I., Malitsky, S., Jona, G., Bar-Even, A., Milo, R., 2016. Sugar Synthesis from CO2 in Escherichia coli. Cell 166, 115–125. https://doi.org/10.1016/j.cell.2016.05.064

Appelhagen, I., Wulff-Vester, A.K., Wendell, M., Hvoslef-Eide, A.-K., Russell, J., Oertel, A., Martens, S., Mock, H.-P., Martin, C., Matros, A., 2018. Colour bio-factories: Towards scale-up production of anthocyanins in plant cell cultures. Metab. Eng. 48, 218–232. https://doi.org/10.1016/j.ymben.2018.06.004

Arnau, J., Yaver, D., Hjort, C.M., 2020. Strategies and Challenges for the Development of Industrial Enzymes Using Fungal Cell Factories, in: Nevalainen, H. (Ed.), Grand Challenges in Fungal Biotechnology, Grand Challenges in Biology and Biotechnology. Springer International Publishing, Cham, pp. 179–210. https://doi.org/10.1007/978-3-030-29541-7_7

Austin, B., Hall, R.M., Tyler, B.M., 1990. Optimized vectors and selection for transformation of Neurospora crassa and Aspergillus nidulans to bleomycin and phleomycin resistance. Gene 93, 157–162. https://doi.org/10.1016/0378-1119(90)90152-H

Ballance, D.J., Turner, G., 1985. Development of a high-frequency transforming vector for Aspergillus nidulans. Gene 36, 321–331. https://doi.org/10.1016/0378-1119(85)90187-8

Bally, J., Jung, H., Mortimer, C., Naim, F., Philips, J.G., Hellens, R., Bombarely, A., Goodin, M.M., Waterhouse, P.M., 2018. The Rise and Rise of *Nicotiana benthamiana* : A Plant for All Reasons. Annu. Rev. Phytopathol. 56, 405–426. https://doi.org/10.1146/annurev-phyto-080417-050141

Bally, J., Nakasugi, K., Jia, F., Jung, H., Ho, S.Y.W., Wong, M., Paul, C.M., Naim, F., Wood, C.C., Crowhurst, R.N., Hellens, R.P., Dale, J.L., Waterhouse, P.M., 2015. The extremophile *Nicotiana benthamiana* has traded viral defence for early vigour. Nat. Plants 1, 15165. https://doi.org/10.1038/nplants.2015.165

Bapat, V.A., Kavi Kishor, P.B., Jalaja, N., Jain, S.M., Penna, S., 2023. Plant Cell Cultures: Biofactories for the Production of Bioactive Compounds. Agronomy 13, 858. https://doi.org/10.3390/agronomy13030858

Bartlett, J.G., Smedley, M.A., Harwood, W.A., 2014. Analysis of T-DNA/Host-Plant DNA Junction Sequences in Single-Copy Transgenic Barley Lines. Biology 3, 39–55. https://doi.org/10.3390/biology3010039

Beal, J., Goñi-Moreno, A., Myers, C., Hecht, A., De Vicente, M.D.C., Parco, M., Schmidt, M., Timmis, K., Baldwin, G., Friedrichs, S., Freemont, P., Kiga, D., Ordozgoiti, E., Rennig, M., Rios, L., Tanner, K., De Lorenzo, V., Porcar, M., 2020. The long journey towards standards for engineering biosystems: Are the Molecular Biology and the Biotech communities ready to standardise? EMBO Rep. 21, e50521. https://doi.org/10.15252/embr.202050521

Beale, M.H., Birkett, M.A., Bruce, T.J.A., Chamberlain, K., Field, L.M., Huttly, A.K., Martin, J.L., Parker, R., Phillips, A.L., Pickett, J.A., Prosser, I.M., Shewry, P.R., Smart, L.E., Wadhams, L.J., Woodcock, C.M., Zhang, Y., 2006. Aphid alarm pheromone produced by transgenic plants affects aphid and parasitoid behavior. Proc. Natl. Acad. Sci. 103, 10509–10513. https://doi.org/10.1073/pnas.0603998103

Beaudoin, F., Sayanova, O., Haslam, R.P., Bancroft, I., Napier, J.A., 2014. Oleaginous crops as integrated production platforms for food, feed, fuel and renewable industrial feedstock: Manipulation of plant lipid composition via metabolic engineering and new opportunities from association genetics for crop improvement and valorisation of co-products. OCL 21, D606. https://doi.org/10.1051/ocl/2014042

Behera, B.C., 2020. Citric acid from *Aspergillus niger* : a comprehensive overview. Crit. Rev. Microbiol. 46, 727–749. https://doi.org/10.1080/1040841X.2020.1828815

Benelli, G., Lucchi, A., Thomson, D., Ioriatti, C., 2019. Sex Pheromone Aerosol Devices for Mating Disruption: Challenges for a Brighter Future. Insects 10, 308. https://doi.org/10.3390/insects10100308

Benner, S.A., Sismour, A.M., 2005. Synthetic biology. Nat. Rev. Genet. 6, 533–543. https://doi.org/10.1038/nrg1637

Bernabé-Orts, J.M., Quijano-Rubio, A., Vazquez-Vilar, M., Mancheño-Bonillo, J., Moles-Casas, V., Selma, S., Gianoglio, S., Granell, A., Orzaez, D., 2020. A memory switch for plant synthetic biology based on the phage φC31 integration system. Nucleic Acids Res. 48, 3379–3394. https://doi.org/10.1093/nar/gkaa104

Berovic, M., Legisa, M., 2007. Citric acid production, in: Biotechnology Annual Review. Elsevier, pp. 303–343. https://doi.org/10.1016/S1387-2656(07)13011-8

Bird, J.E., Marles-Wright, J., Giachino, A., 2022. A User's Guide to Golden Gate Cloning Methods and Standards. ACS Synth. Biol. 11, 3551–3563. https://doi.org/10.1021/acssynbio.2c00355

Bjostad, L.B., Roelofs, W.L., 1984. Biosynthesis of sex pheromone components and glycerolipid precursors from sodium [1-14C]acetate in redbanded leafroller moth. J. Chem. Ecol. 10, 681–691. https://doi.org/10.1007/BF00994228

Bjostad, L.B., Roelofs, W.L., 1983. Sex Pheromone Biosynthesis in *Trichoplusia ni* : Key Steps Involve Delta-11 Desaturation and Chain-Shortening. Science 220, 1387–1389. https://doi.org/10.1126/science.220.4604.1387

Brodie, J., Chan, C.X., De Clerck, O., Cock, J.M., Coelho, S.M., Gachon, C., Grossman, A.R., Mock, T., Raven, J.A., Smith, A.G., Yoon, H.S., Bhattacharya, D., 2017. The Algal Revolution. Trends Plant Sci. 22, 726–738. https://doi.org/10.1016/j.tplants.2017.05.005

Brophy, J.A.N., Voigt, C.A., 2014. Principles of genetic circuit design. Nat. Methods 11, 508–520. https://doi.org/10.1038/nmeth.2926

Bruce, T.J.A., Aradottir, G.I., Smart, L.E., Martin, J.L., Caulfield, J.C., Doherty, A., Sparks, C.A., Woodcock, C.M., Birkett, M.A., Napier, J.A., Jones, H.D., Pickett, J.A., 2015. The first crop plant genetically engineered to release an insect pheromone for defence. Sci. Rep. 5, 11183. https://doi.org/10.1038/srep11183

Brückner, K., Tissier, A., 2013. High-level diterpene production by transient expression in Nicotiana benthamiana. Plant Methods 9, 46. https://doi.org/10.1186/1746-4811-9-46

Buchman, C., Skroch, P., Welch, J., Fogel, S., Karin, M., 1989. The *CUP2* Gene Product, Regulator of Yeast Metallothionein Expression, Is a Copper-Activated DNA-Binding Protein. Mol. Cell. Biol. 9, 4091–4095. https://doi.org/10.1128/mcb.9.9.4091-4095.1989

Burnett, M.J.B., Burnett, A.C., 2020. Therapeutic recombinant protein production in plants: Challenges and opportunities. PLANTS PEOPLE PLANET 2, 121–132. https://doi.org/10.1002/ppp3.10073

Buyel, J.F., 2019. Plant Molecular Farming – Integration and Exploitation of Side Streams to Achieve Sustainable Biomanufacturing. Front. Plant Sci. 9, 1893. https://doi.org/10.3389/fpls.2018.01893

Cai, Y.-M., Carrasco Lopez, J.A., Patron, N.J., 2020a. Phytobricks: Manual and Automated Assembly of Constructs for Engineering Plants, in: Chandran, S., George, K.W. (Eds.), DNA Cloning and Assembly, Methods in Molecular Biology. Springer US, New York, NY, pp. 179–199. https://doi.org/10.1007/978-1-0716-0908-8_11

Cai, Y.-M., Kallam, K., Tidd, H., Gendarini, G., Salzman, A., Patron, N.J., 2020b. Rational design of minimal synthetic promoters for plants. Nucleic Acids Res. 48, 11845–11856. https://doi.org/10.1093/nar/gkaa682

Cardé, R.T., Minks, A.K., 1995. Control of Moth Pests by Mating Disruption: Successes and Constraints. Annu. Rev. Entomol. 40, 559–585. https://doi.org/10.1146/annurev.en.40.010195.003015

Castel, B., Tomlinson, L., Locci, F., Yang, Y., Jones, J.D.G., 2019. Optimization of T-DNA architecture for Cas9-mediated mutagenesis in Arabidopsis. PLOS ONE 14, e0204778. https://doi.org/10.1371/journal.pone.0204778

Chavez, A., Scheiman, J., Vora, S., Pruitt, B.W., Tuttle, M., P R Iyer, E., Lin, S., Kiani, S., Guzman, C.D., Wiegand, D.J., Ter-Ovanesyan, D., Braff, J.L., Davidsohn, N., Housden, B.E., Perrimon, N., Weiss, R., Aach, J., Collins, J.J., Church, G.M., 2015. Highly efficient Cas9-mediated transcriptional programming. Nat. Methods 12, 326–328. https://doi.org/10.1038/nmeth.3312

Chen, Q., Lai, H., Hurtado, J., Stahnke, J., Leuzinger, K., Dent, M., 2013. Agroinfiltration as an Effective and Scalable Strategy of Gene Delivery for Production of Pharmaceutical Proteins. Adv. Tech. Biol. Med. 01. https://doi.org/10.4172/atbm.1000103

Clarke, L., Kitney, R., 2020. Developing synthetic biology for industrial biotechnology applications. Biochem. Soc. Trans. 48, 113–122. https://doi.org/10.1042/BST20190349

Clarke, L.J., 2017. Synthetic biology UK: progress, paradigms and prospects. Eng. Biol. 1, 66–70. https://doi.org/10.1049/enb.2017.0022

Clemente, T., 2006. *Nicotiana* (*Nicotiana tabaccum*, *Nicotiana benthamiana*), in: Wang, K. (Ed.), Agrobacterium Protocols. Springer, pp. 143–154.

Clomburg, J.M., Crumbley, A.M., Gonzalez, R., 2017. Industrial biomanufacturing: The future of chemical production. Science 355, aag0804. https://doi.org/10.1126/science.aag0804

Conley, A.J., Zhu, H., Le, L.C., Jevnikar, A.M., Lee, B.H., Brandle, J.E., Menassa, R., 2011. Recombinant protein production in a variety of Nicotiana hosts: a comparative analysis: Protein production in various Nicotiana hosts. Plant Biotechnol. J. 9, 434–444. https://doi.org/10.1111/j.1467-7652.2010.00563.x

Cook, S.M., Khan, Z.R., Pickett, J.A., 2007. The Use of Push-Pull Strategies in Integrated Pest Management. Annu. Rev. Entomol. 52, 375–400. https://doi.org/10.1146/annurev.ento.52.110405.091407

Corrado, G., Karali, M., 2009. Inducible gene expression systems and plant biotechnology. Biotechnol. Adv. 27, 733–743. https://doi.org/10.1016/j.biotechadv.2009.05.006

Cravens, A., Payne, J., Smolke, C.D., 2019. Synthetic biology strategies for microbial biosynthesis of plant natural products. Nat. Commun. 10, 2142. https://doi.org/10.1038/s41467-019-09848-w

Dahlmann, T.A., Terfehr, D., Becker, K., Teichert, I., 2021. Golden Gate vectors for efficient gene fusion and gene deletion in diverse filamentous fungi. Curr. Genet. 67, 317–330. https://doi.org/10.1007/s00294-020-01143-2

Dammer, L., Carus, M., Piotrowski, D.S., 2019. Sugar as feedstock for the Chemical Industry.

de Graaff, L., Van Den Broeck, H., Visser, J., 1992. Isolation and characterization of the Aspergillus niger pyruvate kinase gene. Curr. Genet. 22, 21–27. https://doi.org/10.1007/BF00351737

de Groot, M.J.A., Bundock, P., Hooykaas, P.J.J., Beijersbergen, A.G.M., 1998. Agrobacterium tumefaciens-mediated transformation of filamentous fungi. Nat. Biotechnol. 16, 839–842. https://doi.org/10.1038/nbt0998-839

de Vries, R.P., Patyshakuliyeva, A., Garrigues, S., Agarwal-Jans, S., 2020. The Current Biotechnological Status and Potential of Plant and Algal Biomass Degrading/Modifying Enzymes from Ascomycete Fungi, in: Nevalainen, H. (Ed.), Grand Challenges in Fungal Biotechnology, Grand Challenges in Biology and Biotechnology. Springer International Publishing, Cham, pp. 81–120. https://doi.org/10.1007/978-3-030-29541-7_4

Demain, A.L., Adrio, J.L., 2008. Contributions of Microorganisms to Industrial Biology. Mol. Biotechnol. 38, 41–55. https://doi.org/10.1007/s12033-007-0035-z

Derntl, C., Kiesenhofer, D.P., Mach, R.L., Mach-Aigner, A.R., 2015. Novel Strategies for Genomic Manipulation of Trichoderma reesei with the Purpose of Strain Engineering. Appl. Environ. Microbiol. 81, 6314–6323. https://doi.org/10.1128/AEM.01545-15

Dey, N., Sarkar, S., Acharya, S., Maiti, I.B., 2015. Synthetic promoters in planta. Planta 242, 1077–1094. https://doi.org/10.1007/s00425-015-2377-2

Dhevagi, P., Ramya, A., Priyatharshini, S., Geetha Thanuja, K., Ambreetha, S., Nivetha, A., 2021. Industrially Important Fungal Enzymes: Productions and Applications, in: Yadav, A.N. (Ed.), Recent Trends in Mycological Research, Fungal Biology. Springer International Publishing, Cham, pp. 263–309. https://doi.org/10.1007/978-3-030-68260-6_11

Díez, B., Alvarez, E., Cantoral, J.M., Barredo, J.L., Martín, J.F., 1987. Selection and characterization of pyrG mutants of Penicillium chrysogenum lacking orotidine-5?-phosphate decarboxylase and complementation by the pyr4 gene of Neurospora crassaa. Curr. Genet. 12, 277–282. https://doi.org/10.1007/BF00435290

Ding, B.-J., Carraher, C., Löfstedt, C., 2016a. Sequence variation determining stereochemistry of a Δ11 desaturase active in moth sex pheromone biosynthesis. Insect Biochem. Mol. Biol. 74, 68–75. https://doi.org/10.1016/j.ibmb.2016.05.002

Ding, B.-J., Hofvander, P., Wang, H.-L., Durrett, T.P., Stymne, S., Löfstedt, C., 2014. A plant factory for moth pheromone production. Nat. Commun. 5, 3353. https://doi.org/10.1038/ncomms4353

Ding, B.-J., Lager, I., Bansal, S., Durrett, T.P., Stymne, S., Löfstedt, C., 2016b. The Yeast ATF1 Acetyltransferase Efficiently Acetylates Insect Pheromone Alcohols: Implications for

the Biological Production of Moth Pheromones. Lipids 51, 469–475. https://doi.org/10.1007/s11745-016-4122-4

Dominguez, A.A., Lim, W.A., Qi, L.S., 2016. Beyond editing: repurposing CRISPR–Cas9 for precision genome regulation and interrogation. Nat. Rev. Mol. Cell Biol. 17, 5–15. https://doi.org/10.1038/nrm.2015.2

Dong, C., Fontana, J., Patel, A., Carothers, J.M., Zalatan, J.G., 2018. Synthetic CRISPR-Cas gene activators for transcriptional reprogramming in bacteria. Nat. Commun. 9, 2489. https://doi.org/10.1038/s41467-018-04901-6

Dudley, Q.M., Jo, S., Guerrero, D.A.S., Chhetry, M., Smedley, M.A., Harwood, W.A., Sherden, N.H., O'Connor, S.E., Caputi, L., Patron, N.J., 2022. Reconstitution of monoterpene indole alkaloid biosynthesis in genome engineered Nicotiana benthamiana. Commun. Biol. 5, 949. https://doi.org/10.1038/s42003-022-03904-w

Dufossé, L., Fouillaud, M., Caro, Y., Mapari, S.A., Sutthiwong, N., 2014. Filamentous fungi are large-scale producers of pigments and colorants for the food industry. Curr. Opin. Biotechnol. 26, 56–61. https://doi.org/10.1016/j.copbio.2013.09.007

Eizaguirre, M., Lopez, C., Asín, L., Albajes, R., 1994. Thermoperiodism, Photoperiodism and Sensitive Stage in the Diapause Induction of *Sesamia nonagrioides* (Lepidoptera: Noctuidae). J. Insect Physiol. 40, 113–119. https://doi.org/doi.org/10.1016/0022-1910(94)90082-5

El-Enshasy, H.A., 2022. Fungal morphology: a challenge in bioprocess engineering industries for product development. Curr. Opin. Chem. Eng. 35, 100729. https://doi.org/10.1016/j.coche.2021.100729

El-Sayed, A.M., 2021. The Pherobase: Database of Pheromones and Semiochemicals. URL https://www.pherobase.com/

El-Sayed, A.M., Suckling, D.M., Byers, J.A., Jang, E.B., Wearing, C.H., 2009. Potential of "Lure and Kill" in Long-Term Pest Management and Eradication of Invasive Species. J. Econ. Entomol. 102, 815–835. https://doi.org/10.1603/029.102.0301

Endy, D., 2005. Foundations for engineering biology. Nature 438, 449–453. https://doi.org/10.1038/nature04342

Engler, C., Youles, M., Gruetzner, R., Ehnert, T.-M., Werner, S., Jones, J.D.G., Patron, N.J., Marillonnet, S., 2014. A Golden Gate Modular Cloning Toolbox for Plants. ACS Synth. Biol. 3, 839–843. https://doi.org/10.1021/sb4001504

Escobar-Bravo, R., Lin, P.-A., Waterman, J.M., Erb, M., 2023. Dynamic environmental interactions shaped by vegetative plant volatiles. Nat. Prod. Rep. 40, 840–865. https://doi.org/10.1039/D2NP00061J

Evenden, M., 2016. Mating Disruption of Moth Pests in Integrated Pest Management: A Mechanistic Approach, in: Allison, J.D., Cardé, R.T. (Eds.), Pheromone Communication in Moths. University of California Press, Berkeley, pp. 365–394.

F de Felippes, F., McHale, M., Doran, R.L., Roden, S., Eamens, A.L., Finnegan, E.J., Waterhouse, P.M., 2020. The key role of terminators on the expression and post-transcriptional gene silencing of transgenes. Plant J. 104, 96–112. https://doi.org/10.1111/tpj.14907

Farzadfard, F., Perli, S.D., Lu, T.K., 2013. Tunable and Multifunctional Eukaryotic Transcription Factors Based on CRISPR/Cas. ACS Synth. Biol. 2, 604–613. https://doi.org/10.1021/sb400081r

Ferreira, J.A., Varjani, S., Taherzadeh, M.J., 2020. A Critical Review on the Ubiquitous Role of Filamentous Fungi in Pollution Mitigation. Curr. Pollut. Rep. 6, 295–309. https://doi.org/10.1007/s40726-020-00156-2

Fierro, F., Vaca, I., Castillo, N.I., García-Rico, R.O., Chávez, R., 2022. Penicillium chrysogenum, a Vintage Model with a Cutting-Edge Profile in Biotechnology. Microorganisms 10, 573. https://doi.org/10.3390/microorganisms10030573

Forsbach, A., Schubert, D., Lechtenberg, B., Gils, M., Schmidt, R., 2003. A comprehensive characterization of single-copy T-DNA insertions in the *Arabidopsis thaliana* genome. Plant Mol. Biol. 52, 161–176. https://doi.org/doi:10.1023/A:1023929630687

Fowler, T., Berka, R.M., Ward, M., 1990. Regulation of the glaA gene of Aspergillus niger. Curr. Genet. 18, 537–545. https://doi.org/10.1007/BF00327025

Fulmer, E.I., 1930. The Chemical Approach to Problems of Fermentation. Ind. Eng. Chem. 22, 1148–1150. https://doi.org/10.1021/ie50251a009

Gandía, M., Moreno-Giménez, E., Giner-Llorca, M., Garrigues, S., Ropero-Pérez, C., Locascio, A., Martínez-Culebras, P.V., Marcos, J.F., Manzanares, P., 2022. Development of a FungalBraid *Penicillium expansum* -based expression system for the production of antifungal proteins in fungal biofactories. Microb. Biotechnol. 15, 630–647. https://doi.org/10.1111/1751-7915.14006

Garabagi, F., Gilbert, E., Loos, A., McLean, M.D., Hall, J.C., 2012. Utility of the P19 suppressor of gene-silencing protein for production of therapeutic antibodies in *Nicotiana* expression hosts. Plant Biotechnol. J. 10, 1118–1128. https://doi.org/10.1111/j.1467-7652.2012.00742.x

García-Pérez, E., Diego-Martin, B., Quijano-Rubio, A., Moreno-Giménez, E., Selma, S., Orzaez, D., Vazquez-Vilar, M., 2022. A copper switch for inducing CRISPR/Cas9-based transcriptional activation tightly regulates gene expression in Nicotiana benthamiana. BMC Biotechnol. 22, 12. https://doi.org/10.1186/s12896-022-00741-x

Garrigues, S., Gandía, M., Popa, C., Borics, A., Marx, F., Coca, M., Marcos, J.F., Manzanares, P., 2017. Efficient production and characterization of the novel and highly active antifungal protein AfpB from Penicillium digitatum. Sci. Rep. 7, 14663. https://doi.org/10.1038/s41598-017-15277-w

Garrigues, S., Manzanares, P., Marcos, J.F., 2022. Application of recyclable CRISPR/Cas9 tools for targeted genome editing in the postharvest pathogenic fungi Penicillium digitatum and Penicillium expansum. Curr. Genet. 68, 515–529. https://doi.org/10.1007/s00294-022-01236-0

Gavara, A., Vacas, S., Navarro, I., Primo, J., Navarro-Llopis, V., 2020. Airborne Pheromone Quantification in Treated Vineyards with Different Mating Disruption Dispensers against *Lobesia botrana*. Insects 11, 289. https://doi.org/10.3390/insects11050289

Gonçalves, F., Castro, T.G., Nogueira, E., Pires, R., Silva, C., Ribeiro, A., Cavaco-Paulo, A., 2018. OBP fused with cell-penetrating peptides promotes liposomal transduction. Colloids Surf. B Biointerfaces 161, 645–653. https://doi.org/10.1016/j.colsurfb.2017.11.026

González, A., Cruz, M., Losoya, C., Nobre, C., Loredo, A., Rodríguez, R., Contreras, J., Belmares, R., 2020. Edible mushrooms as a novel protein source for functional foods. Food Funct. 11, 7400–7414. https://doi.org/10.1039/D0FO01746A

González-Candelas, L., Alamar, S., Sanchez-Torres, P., Zacarias, L., Marcos, J.F., 2010. A transcriptomic approach highlights induction of secondary metabolism in citrus fruit in response to Penicillium digitatum infection. BMC Plant Biol. 10, 194. https://doi.org/10.1186/1471-2229-10-194

Goodin, M.M., Zaitlin, D., Naidu, R.A., Lommel, S.A., 2008. Nicotiana benthamiana: its history and future as a model for plant-pathogen interactions. Mol. Plant-Microbe Interact. MPMI 21, 1015–1026. https://doi.org/10.1094/MPMI-21-8-1015

Grand View Research, 2021. Recombinant Proteins Market Size & Growth Report, 2030. https://www.grandviewresearch.com/industry-analysis/recombinant-proteins-market-report. San Francisco, CA, USA.

Gregg, P.C., Del Socorro, A.P., Landolt, P.J., 2018. Advances in Attract-and-Kill for Agricultural Pests: Beyond Pheromones. Annu. Rev. Entomol. 63, 453–470. https://doi.org/10.1146/annurev-ento-031616-035040

Gruber, F., Visser, J., Kubicek, C.P., De Graaff, L.H., 1990. The development of a heterologous transformation system for the cellulolytic fungus Trichoderma reesei based on a pyrG-negative mutant strain. Curr. Genet. 18, 71–76. https://doi.org/10.1007/BF00321118

Hager, K.J., Pérez Marc, G., Gobeil, P., Diaz, R.S., Heizer, G., Llapur, C., Makarkov, A.I., Vasconcellos, E., Pillet, S., Riera, F., Saxena, P., Geller Wolff, P., Bhutada, K., Wallace, G., Aazami, H., Jones, C.E., Polack, F.P., Ferrara, L., Atkins, J., Boulay, I., Dhaliwall, J., Charland, N., Couture, M.M.J., Jiang-Wright, J., Landry, N., Lapointe, S., Lorin, A., Mahmood, A., Moulton, L.H., Pahmer, E., Parent, J., Séguin, A., Tran, L., Breuer, T., Ceregido, M.-A., Koutsoukos, M., Roman, F., Namba, J., D'Aoust, M.-A., Trepanier, S., Kimura, Y., Ward, B.J., 2022. Efficacy and Safety of a Recombinant Plant-Based Adjuvanted Covid-19 Vaccine. N. Engl. J. Med. 386, 2084–2096. https://doi.org/10.1056/NEJMoa2201300

Hagström, Å.K., Wang, H.-L., Liénard, M.A., Lassance, J.-M., Johansson, T., Löfstedt, C., 2013. A moth pheromone brewery: production of *(Z)*-11-hexadecenol by heterologous co-expression of two biosynthetic genes from a noctuid moth in a yeast cell factory. Microb. Cell Factories 12, 125. https://doi.org/10.1186/1475-2859-12-125

Hamilton, C.M., 1997. A binary-BAC system for plant transformation with high-molecular-weight DNA. Gene 200, 107–116. https://doi.org/10.1016/S0378-1119(97)00388-0

Harries, E., Gandía, M., Carmona, L., Marcos, J.F., 2015. The *Penicillium digitatum* protein *O* -mannosyltransferase Pmt2 is required for cell wall integrity, conidiogenesis, virulence and sensitivity to the antifungal peptide PAF26: *P. digitatum* protein glycosylation and virulence. Mol. Plant Pathol. 16, 748–761. https://doi.org/10.1111/mpp.12232

Hata, Y., Kitamoto, K., Gomi, K., Kumagai, C., Tamura, G., 1992. Functional elements of the promoter region of the Aspergillus oryzae glaA gene encoding glucoamylase. Curr. Genet. 22, 85–91. https://doi.org/10.1007/BF00351466

Hegedüs, N., Sigl, C., Zadra, I., Pócsi, I., Marx, F., 2011. The paf gene product modulates asexual development in Penicillium chrysogenum. J. Basic Microbiol. 51, 253–262. https://doi.org/10.1002/jobm.201000321

Hernanz-Koers, M., Gandía, M., Garrigues, S., Manzanares, P., Yenush, L., Orzaez, D., Marcos, J.F., 2018. FungalBraid: A GoldenBraid-based modular cloning platform for the assembly and exchange of DNA elements tailored to fungal synthetic biology. Fungal Genet. Biol. 116, 51–61. https://doi.org/10.1016/j.fgb.2018.04.010

Higashimura, N., Hamada, A., Ohara, T., Sakurai, S., Ito, H., Banba, S., 2022. The target site of the novel fungicide quinofumelin, *Pyricularia oryzae* class II dihydroorotate dehydrogenase. J. Pestic. Sci. 47, 190–196. https://doi.org/10.1584/jpestics.D22-027

Holkenbrink, C., Ding, B.-J., Wang, H.-L., Dam, M.I., Petkevicius, K., Kildegaard, K.R., Wenning, L., Sinkwitz, C., Lorántfy, B., Koutsoumpeli, E., França, L., Pires, M., Bernardi, C., Urrutia, W., Mafra-Neto, A., Ferreira, B.S., Raptopoulos, D., Konstantopoulou, M., Löfstedt, C., Borodina, I., 2020. Production of moth sex pheromones for pest control by yeast fermentation. Metab. Eng. 62, 312–321. https://doi.org/10.1016/j.ymben.2020.10.001

Horsch, R.B., Fry, J.E., Hoffmann, N.L., Wallroth, M., Eichholtz, D., Rogers, S.G., Fraley, R.T., 1985. A Simple and General Method for Transferring Genes into Plants. Science 227, 1229–1231. https://doi.org/10.1126/science.227.4691.1229

Hossain, M.S., Williams, D.G., Mansfield, C., Bartelt, R.J., Callinan, L., Il'ichev, A.L., 2006. An attract-and-kill system to control *Carpophilus* spp. in Australian stone fruit orchards. Entomol. Exp. Appl. 118, 11–19. https://doi.org/10.1111/j.1570-7458.2006.00354.x

Huchelmann, A., Boutry, M., Hachez, C., 2017. Plant Glandular Trichomes: Natural Cell Factories of High Biotechnological Interest. Plant Physiol. 175, 6–22. https://doi.org/10.1104/pp.17.00727

Iacopino, S., Jurinovich, S., Cupellini, L., Piccinini, L., Cardarelli, F., Perata, P., Mennucci, B., Giuntoli, B., Licausi, F., 2019. A Synthetic Oxygen Sensor for Plants Based on Animal Hypoxia Signaling. Plant Physiol. 179, 986–1000. https://doi.org/10.1104/pp.18.01003

Ingelbrecht, I., Breyne, P., Vancompernolle, K., Jacobs, A., Van Montagu, M., Depicker, A., 1991. Transcriptional interference in transgenic plants. Gene 109, 239–242. https://doi.org/10.1016/0378-1119(91)90614-H

Iskandarov, U., Kim, H.J., Cahoon, E.B., 2014. Camelina: An Emerging Oilseed Platform for Advanced Biofuels and Bio-Based Materials, in: McCann, M.C., Buckeridge, M.S., Carpita, N.C. (Eds.), Plants and BioEnergy. Springer New York, New York, NY, pp. 131–140. https://doi.org/10.1007/978-1-4614-9329-7_8

Jensen, M.K., Keasling, J.D., 2014. Recent applications of synthetic biology tools for yeast metabolic engineering. FEMS Yeast Res. n/a-n/a. https://doi.org/10.1111/1567-1364.12185

Jo, C., Zhang, J., Tam, J.M., Church, G.M., Khalil, A.S., Segrè, D., Tang, T.-C., 2023. Unlocking the magic in mycelium: Using synthetic biology to optimize filamentous fungi for biomanufacturing and sustainability. Mater. Today Bio 19, 100560. https://doi.org/10.1016/j.mtbio.2023.100560

Johnstone, C.P., Galloway, K.E., 2022. Supercoiling-mediated feedback rapidly couples and tunes transcription. Cell Rep. 41, 111492. https://doi.org/10.1016/j.celrep.2022.111492

Jones, J.A., Toparlak, Ö.D., Koffas, M.A., 2015. Metabolic pathway balancing and its role in the production of biofuels and chemicals. Curr. Opin. Biotechnol. 33, 52–59. https://doi.org/10.1016/j.copbio.2014.11.013

Jones, M., Gandia, A., John, S., Bismarck, A., 2020. Leather-like material biofabrication using fungi. Nat. Sustain. 4, 9–16. https://doi.org/10.1038/s41893-020-00606-1

Juteršek, M., Gerasymenko, I.M., Petek, M., Haumann, E., Vacas, S., Kallam, K., Gianoglio, S., Navarro-Llopis, V., Fuertes, I.N., Patron, N., Orzáez, D., Gruden, K., Warzecha, H., Baebler, Š., 2023. Identification and characterisation of *Planococcus citri cis* - and *trans* -isoprenyl diphosphate synthase genes, supported by short- and long-read transcriptome data. https://doi.org/10.1101/2023.06.09.544309

Juteršek, M., Petek, M., Ramšak, Ž., Moreno-Giménez, E., Gianoglio, S., Mateos-Fernández, R., Orzáez, D., Gruden, K., Baebler, Š., 2022. Transcriptional deregulation of stress-growth balance in Nicotiana benthamiana biofactories producing insect sex pheromones. Front. Plant Sci. 13, 941338. https://doi.org/10.3389/fpls.2022.941338

Kafle, A., Timilsina, A., Gautam, A., Adhikari, K., Bhattarai, A., Aryal, N., 2022. Phytoremediation: Mechanisms, plant selection and enhancement by natural and synthetic agents. Environ. Adv. 8, 100203. https://doi.org/10.1016/j.envadv.2022.100203

Kallam, K., Moreno-Giménez, E., Mateos-Fernández, R., Tansley, C., Gianoglio, S., Orzaez, D., Patron, N., 2023. Tunable control of insect pheromone biosynthesis in *Nicotiana benthamiana*. Plant Biotechnol. J. 21, 1440–1453. https://doi.org/10.1111/pbi.14048

Kalra, R., Conlan, X.A., Goel, M., 2020. Fungi as a Potential Source of Pigments: Harnessing Filamentous Fungi. Front. Chem. 8, 369. https://doi.org/10.3389/fchem.2020.00369

Kappers, I.F., Aharoni, A., Van Herpen, T.W.J.M., Luckerhoff, L.L.P., Dicke, M., Bouwmeester, H.J., 2005. Genetic Engineering of Terpenoid Metabolism Attracts Bodyguards to *Arabidopsis*. Science 309, 2070–2072. https://doi.org/10.1126/science.1116232

Kar, S., Bordiya, Y., Rodriguez, N., Kim, J., Gardner, E.C., Gollihar, J.D., Sung, S., Ellington, A.D., 2022. Orthogonal control of gene expression in plants using synthetic promoters and CRISPR-based transcription factors. Plant Methods 18, 42. https://doi.org/10.1186/s13007-022-00867-1

Keating, K.W., Young, E.M., 2019. Synthetic biology for bio-derived structural materials. Curr. Opin. Chem. Eng. 24, 107–114. https://doi.org/10.1016/j.coche.2019.03.002

Keller, N.P., 2019. Fungal secondary metabolism: regulation, function and drug discovery. Nat. Rev. Microbiol. 17, 167–180. https://doi.org/10.1038/s41579-018-0121-1

Kelly, J.M., Hynes, M.J., 1985. Transformation of Aspergillus niger by the amdS gene of Aspergillus nidulans. EMBO J. 4, 475–479. https://doi.org/10.1002/j.1460-2075.1985.tb03653.x

Khakhar, A., Starker, C.G., Chamness, J.C., Lee, N., Stokke, S., Wang, C., Swanson, R., Rizvi, F., Imaizumi, T., Voytas, D.F., 2020. Building customizable auto-luminescent luciferase-based reporters in plants. eLife 9, e52786. https://doi.org/10.7554/eLife.52786

Khang, C.H., Park, S.-Y., Rho, H.-S., Lee, Y.-H., Kang, S., 2006. Filamentous Fungi (Magnaporthe grisea and Fusarium oxysporum), in: Wang, K. (Ed.), Agrobacterium Protocols Volume 2. Humana Press, Totowa, NJ, pp. 403–420. https://doi.org/10.1385/1-59745-131-2:403

Kizhner, T., Azulay, Y., Hainrichson, M., Tekoah, Y., Arvatz, G., Shulman, A., Ruderfer, I., Aviezer, D., Shaaltiel, Y., 2015. Characterization of a chemically modified plant cell culture expressed human α-Galactosidase-A enzyme for treatment of Fabry disease. Mol. Genet. Metab. 114, 259–267. https://doi.org/10.1016/j.ymgme.2014.08.002

Kluge, J., Terfehr, D., Kück, U., 2018. Inducible promoters and functional genomic approaches for the genetic engineering of filamentous fungi. Appl. Microbiol. Biotechnol. 102, 6357–6372. https://doi.org/10.1007/s00253-018-9115-1

Köhler, H.-R., Triebskorn, R., 2013. Wildlife Ecotoxicology of Pesticides: Can We Track Effects to the Population Level and Beyond? Science 341, 759–765. https://doi.org/10.1126/science.1237591

Konermann, S., Brigham, M.D., Trevino, A.E., Joung, J., Abudayyeh, O.O., Barcena, C., Hsu, P.D., Habib, N., Gootenberg, J.S., Nishimasu, H., Nureki, O., Zhang, F., 2015. Genome-scale transcriptional activation by an engineered CRISPR-Cas9 complex. Nature 517, 583–588. https://doi.org/10.1038/nature14136

Konrad, O., Micah, S., Vu, B., Keith, W., Effendi, L., 2017. Semi-biosynthetic Production Of Fatty Alcohols And Fatty Aldehydes. WO/2017/214133.

Kotlobay, A.A., Sarkisyan, K.S., Mokrushina, Y.A., Marcet-Houben, M., Serebrovskaya, E.O., Markina, N.M., Gonzalez Somermeyer, L., Gorokhovatsky, A.Y., Vvedensky, A., Purtov, K.V., Petushkov, V.N., Rodionova, N.S., Chepurnyh, T.V., Fakhranurova, L.I., Guglya, E.B., Ziganshin, R., Tsarkova, A.S., Kaskova, Z.M., Shender, V., Abakumov, M., Abakumova, T.O., Povolotskaya, I.S., Eroshkin, F.M., Zaraisky, A.G., Mishin, A.S., Dolgov, S.V., Mitiouchkina, T.Y., Kopantzev, E.P., Waldenmaier, H.E., Oliveira, A.G.,

Oba, Y., Barsova, E., Bogdanova, E.A., Gabaldón, T., Stevani, C.V., Lukyanov, S., Smirnov, I.V., Gitelson, J.I., Kondrashov, F.A., Yampolsky, I.V., 2018. Genetically encodable bioluminescent system from fungi. Proc. Natl. Acad. Sci. 115, 12728–12732. https://doi.org/10.1073/pnas.1803615115

Krokos, F.D., Ameline, A., Bau, J., Sans, A., Konstantopoulou, M., Rot, B.F., Guerrero, A., Eizaguirre, M., Malosse, C., Etchepare, O., Albajes, R., Mazomenos, B.E., 2002. Comparative studies of female sex pheromone components and male response of the corn stalk borer *Sesamia nonagrioides* in three different populations. J. Chem. Ecol. 28, 1463–1472. https://doi.org/10.1023/A:1016256804745

Kumar, V., Pandita, S., Singh Sidhu, G.P., Sharma, A., Khanna, K., Kaur, P., Bali, A.S., Setia, R., 2021. Copper bioavailability, uptake, toxicity and tolerance in plants: A comprehensive review. Chemosphere 262, 127810. https://doi.org/10.1016/j.chemosphere.2020.127810

Kurup, V.M., Thomas, J., 2020. Edible Vaccines: Promises and Challenges. Mol. Biotechnol. 62, 79–90. https://doi.org/10.1007/s12033-019-00222-1

Lein, W., Usadel, B., Stitt, M., Reindl, A., Ehrhardt, T., Sonnewald, U., Börnke, F., 2008. Large-scale phenotyping of transgenic tobacco plants (Nicotiana tabacum) to identify essential leaf functions. Plant Biotechnol. J. 6, 246–263. https://doi.org/10.1111/j.1467-7652.2007.00313.x

Li, D., Tang, Y., Lin, J., Cai, W., 2017. Methods for genetic transformation of filamentous fungi. Microb. Cell Factories 16, 168. https://doi.org/10.1186/s12934-017-0785-7

Li, Z., Zhang, D., Xiong, X., Yan, B., Xie, W., Sheen, J., Li, J.-F., 2017. A potent Cas9-derived gene activator for plant and mammalian cells. Nat. Plants 3, 930–936. https://doi.org/10.1038/s41477-017-0046-0

Liu, G., Lin, Q., Jin, S., Gao, C., 2022. The CRISPR-Cas toolbox and gene editing technologies. Mol. Cell 82, 333–347. https://doi.org/10.1016/j.molcel.2021.12.002

Löfstedt, C., Wahlberg, N., Millar, J.G., 2016. Evolutionary Patterns of Pheromone Diversity in Lepidoptera, in: Allison, J.D., Cardé, R.T. (Eds.), Pheromone Communication in Moths. University of California Press, Berkeley, pp. 43–78.

Löfstedt, C., Xia, Y.-H., 2021. Biological production of insect pheromones in cell and plant factories, in: Blomquist, G.J., Vogt, R.G. (Eds.), Insect Pheromone Biochemistry and Molecular Biology. Academic Press, London, pp. 89–121. https://doi.org/10.1016/B978-0-12-819628-1.00003-1

Lommen, A., 2009. MetAlign: Interface-Driven, Versatile Metabolomics Tool for Hyphenated Full-Scan Mass Spectrometry Data Preprocessing. Anal. Chem. 81, 3079–3086. https://doi.org/10.1021/ac900036d

Loreto, F., Schnitzler, J.-P., 2010. Abiotic stresses and induced BVOCs. Trends Plant Sci. 15, 154–166. https://doi.org/10.1016/j.tplants.2009.12.006

Lowder, L.G., Zhou, J., Zhang, Yingxiao, Malzahn, A., Zhong, Z., Hsieh, T.-F., Voytas, D.F., Zhang, Yong, Qi, Y., 2018. Robust Transcriptional Activation in Plants Using Multiplexed

CRISPR-Act2.0 and mTALE-Act Systems. Mol. Plant 11, 245–256. https://doi.org/10.1016/j.molp.2017.11.010

Lu, C., Kang, J., 2008. Generation of transgenic plants of a potential oilseed crop Camelina sativa by Agrobacterium-mediated transformation. Plant Cell Rep. 27, 273–278. https://doi.org/10.1007/s00299-007-0454-0

Lucks, J.B., Qi, L., Whitaker, W.R., Arkin, A.P., 2008. Toward scalable parts families for predictable design of biological circuits. Curr. Opin. Microbiol. 11, 567–573. https://doi.org/10.1016/j.mib.2008.10.002

Ma, J., Ptashne, M., 1987. The carboxy-terminal 30 amino acids of GAL4 are recognized by GAL80. Cell 50, 137–142. https://doi.org/10.1016/0092-8674(87)90670-2

Madeira, L.M., Szeto, T.H., Ma, J.K.-C., Drake, P.M.W., 2016. Rhizosecretion improves the production of Cyanovirin-N in *Nicotiana tabacum* through simplified downstream processing. Biotechnol. J. 11, 910–919. https://doi.org/10.1002/biot.201500371

Mali, P., Esvelt, K.M., Church, G.M., 2013. Cas9 as a versatile tool for engineering biology. Nat. Methods 10, 957–963. https://doi.org/10.1038/nmeth.2649

Marcet-Houben, M., Ballester, A.-R., De La Fuente, B., Harries, E., Marcos, J.F., González-Candelas, L., Gabaldón, T., 2012. Genome sequence of the necrotrophic fungus Penicillium digitatum, the main postharvest pathogen of citrus. BMC Genomics 13, 646. https://doi.org/10.1186/1471-2164-13-646

Martins-Santana, L., Nora, L.C., Sanches-Medeiros, A., Lovate, G.L., Cassiano, M.H.A., Silva-Rocha, R., 2018. Systems and Synthetic Biology Approaches to Engineer Fungi for Fine Chemical Production. Front. Bioeng. Biotechnol. 6, 117. https://doi.org/10.3389/fbioe.2018.00117

Marx, F., Haas, H., Reindl, M., Stöffler, G., Lottspeich, F., Redl, B., 1995. Cloning, structural organization and regulation of expression of the Penicillium chrysogenum paf gene encoding an abundantly secreted protein with antifungal activity. Gene 167, 167–171. https://doi.org/10.1016/0378-1119(95)00701-6

Mateos-Fernández, R., Moreno-Giménez, E., Gianoglio, S., Quijano-Rubio, A., Gavaldá-García, J., Estellés, L., Rubert, A., Rambla, J.L., Vazquez-Vilar, M., Huet, E., Fernández-del-Carmen, A., Espinosa-Ruiz, A., Juteršek, M., Vacas, S., Navarro, I., Navarro-Llopis, V., Primo, J., Orzáez, D., 2021. Production of Volatile Moth Sex Pheromones in Transgenic *Nicotiana benthamiana* Plants. BioDesign Res. 2021, 2021/9891082. https://doi.org/10.34133/2021/9891082

Mateos-Fernández, R., Petek, M., Gerasymenko, I., Juteršek, M., Baebler, Š., Kallam, K., Moreno Giménez, E., Gondolf, J., Nordmann, A., Gruden, K., Orzaez, D., Patron, N.J., 2022. Insect pest management in the age of synthetic biology. Plant Biotechnol. J. 20, 25–36. https://doi.org/10.1111/pbi.13685

Mateos-Fernández, R., Vacas, S., Navarro-Fuertes, I., Navarro-Llopis, V., Orzáez, D., Gianoglio, S., 2023. Assessment of tobacco and *N. benthamiana* as biofactories of irregular

monoterpenes for sustainable crop protection. https://doi.org/10.1101/2023.08.02.551635

Matthews, N.E., Cizauskas, C.A., Layton, D.S., Stamford, L., Shapira, P., 2019. Collaborating constructively for sustainable biotechnology. Sci. Rep. 9, 19033. https://doi.org/10.1038/s41598-019-54331-7

McGovern, P.E., Zhang, J., Tang, J., Zhang, Z., Hall, G.R., Moreau, R.A., Nuñez, A., Butrym, E.D., Richards, M.P., Wang, Chen-shan, Cheng, G., Zhao, Z., Wang, Changsui, 2004. Fermented beverages of pre- and proto-historic China. Proc. Natl. Acad. Sci. 101, 17593–17598. https://doi.org/10.1073/pnas.0407921102

Mett, V., Farrance, C.E., Green, B.J., Yusibov, V., 2008. Plants as biofactories. Biologicals 36, 354–358. https://doi.org/10.1016/j.biologicals.2008.09.001

Mett, V.L., Lochhead, L.P., Reynolds, P.H., 1993. Copper-controllable gene expression system for whole plants. Proc. Natl. Acad. Sci. 90, 4567–4571. https://doi.org/10.1073/pnas.90.10.4567

Meyer, A.J., Segall-Shapiro, T.H., Glassey, E., Zhang, J., Voigt, C.A., 2019. Escherichia coli "Marionette" strains with 12 highly optimized small-molecule sensors. Nat. Chem. Biol. 15, 196–204. https://doi.org/10.1038/s41589-018-0168-3

Meyer, V., Andersen, M.R., Brakhage, A.A., Braus, G.H., Caddick, M.X., Cairns, T.C., De Vries, R.P., Haarmann, T., Hansen, K., Hertz-Fowler, C., Krappmann, S., Mortensen, U.H., Peñalva, M.A., Ram, A.F.J., Head, R.M., 2016. Current challenges of research on filamentous fungi in relation to human welfare and a sustainable bio-economy: a white paper. Fungal Biol. Biotechnol. 3, 6, s40694-016-0024–8. https://doi.org/10.1186/s40694-016-0024-8

Meyer, V., Basenko, E.Y., Benz, J.P., Braus, G.H., Caddick, M.X., Csukai, M., De Vries, R.P., Endy, D., Frisvad, J.C., Gunde-Cimerman, N., Haarmann, T., Hadar, Y., Hansen, K., Johnson, R.I., Keller, N.P., Kraševec, N., Mortensen, U.H., Perez, R., Ram, A.F.J., Record, E., Ross, P., Shapaval, V., Steiniger, C., Van Den Brink, H., Van Munster, J., Yarden, O., Wösten, H.A.B., 2020. Growing a circular economy with fungal biotechnology: a white paper. Fungal Biol. Biotechnol. 7, 5. https://doi.org/10.1186/s40694-020-00095-z

Mikkelsen, M.D., Olsen, C.E., Halkier, B.A., 2010. Production of the Cancer-Preventive Glucoraphanin in Tobacco. Mol. Plant 3, 751–759. https://doi.org/10.1093/mp/ssq020

Mitiouchkina, T., Mishin, A.S., Somermeyer, L.G., Markina, N.M., Chepurnyh, T.V., Guglya, E.B., Karataeva, T.A., Palkina, K.A., Shakhova, E.S., Fakhranurova, L.I., Chekova, S.V., Tsarkova, A.S., Golubev, Y.V., Negrebetsky, V.V., Dolgushin, S.A., Shalaev, P.V., Shlykov, D., Melnik, O.A., Shipunova, V.O., Deyev, S.M., Bubyrev, A.I., Pushin, A.S., Choob, V.V., Dolgov, S.V., Kondrashov, F.A., Yampolsky, I.V., Sarkisyan, K.S., 2020. Plants with genetically encoded autoluminescence. Nat. Biotechnol. 38, 944–946. https://doi.org/10.1038/s41587-020-0500-9

Mofikoya, A.O., Bui, T.N.T., Kivimäenpää, M., Holopainen, J.K., Himanen, S.J., Blande, J.D., 2019. Foliar behaviour of biogenic semi-volatiles: potential applications in sustainable pest

management. Arthropod-Plant Interact. 13, 193–212. https://doi.org/10.1007/s11829-019-09676-1

Molina-Hidalgo, F.J., Vazquez-Vilar, M., D'Andrea, L., Demurtas, O.C., Fraser, P., Giuliano, G., Bock, R., Orzáez, D., Goossens, A., 2020. Engineering Metabolism in Nicotiana Species: A Promising Future. Trends Biotechnol. https://doi.org/10.1016/j.tibtech.2020.11.012

Morbitzer, R., Römer, P., Boch, J., Lahaye, T., 2010. Regulation of selected genome loci using de novo-engineered transcription activator-like effector (TALE)-type transcription factors. Proc. Natl. Acad. Sci. 107, 21617–21622. https://doi.org/10.1073/pnas.1013133107

Moreno-Giménez, E., Gandía, M., Sáez, Z., Manzanares, P., Yenush, L., Orzáez, D., Marcos, J.F., Garrigues, S., 2023. FungalBraid 2.0: expanding the synthetic biology toolbox for the biotechnological exploitation of filamentous fungi. Front. Bioeng. Biotechnol. 11, 1222812. https://doi.org/10.3389/fbioe.2023.1222812

Moreno-Giménez, E., Selma, S., Calvache, C., Orzáez, D., 2022. GB_SynP: A Modular dCas9-Regulated Synthetic Promoter Collection for Fine-Tuned Recombinant Gene Expression in Plants. ACS Synth. Biol. 11, 3037–3048. https://doi.org/10.1021/acssynbio.2c00238

Mori, K., 2010. Chemical Synthesis of Hormones, Pheromones and Other Bioregulators. John Wiley & Sons Ltd., Hoboken.

Mori, K., 2007. The synthesis of insect pheromones, in: ApSimon, J. (Ed.), Total Synthesis of Natural Products. John Wiley & Sons Inc., Hoboken, pp. 1979–1989.

Mózsik, L., Hoekzema, M., De Kok, N.A.W., Bovenberg, R.A.L., Nygård, Y., Driessen, A.J.M., 2020. CRISPR-Based Transcriptional Activation Tool for Silent Genes in Filamentous Fungi (preprint). Microbiology. https://doi.org/10.1101/2020.10.13.338012

Mózsik, L., Iacovelli, R., Bovenberg, R.A.L., Driessen, A.J.M., 2022. Transcriptional Activation of Biosynthetic Gene Clusters in Filamentous Fungi. Front. Bioeng. Biotechnol. 10, 901037. https://doi.org/10.3389/fbioe.2022.901037

Mózsik, L., Pohl, C., Meyer, V., Bovenberg, R.A.L., Nygård, Y., Driessen, A.J.M., 2021. Modular Synthetic Biology Toolkit for Filamentous Fungi. ACS Synth. Biol. 10, 2850–2861. https://doi.org/10.1021/acssynbio.1c00260

Müller, K., Siegel, D., Rodriguez Jahnke, F., Gerrer, K., Wend, S., Decker, E.L., Reski, R., Weber, W., Zurbriggen, M.D., 2014. A red light-controlled synthetic gene expression switch for plant systems. Mol BioSyst 10, 1679–1688. https://doi.org/10.1039/C3MB70579J

Napier, J.A., Betancor, M.B., 2023. Engineering plant-based feedstocks for sustainable aquaculture. Curr. Opin. Plant Biol. 71, 102323. https://doi.org/10.1016/j.pbi.2022.102323

Narayanan, Z., Glick, B.R., 2023. Biotechnologically Engineered Plants. Biology 12, 601. https://doi.org/10.3390/biology12040601

Nešněrová, P., Šebek, P., Macek, T., Svatoš, A., 2004. First semi-synthetic preparation of sex pheromones. Green Chem 6, 305–307. https://doi.org/10.1039/B406814A

Nieukerken, E.J.V., Kaila, L., Kitching, I.J., Kristensen, N.P., Lees, D.C., Minet, J., Zwick, A., 2011. Order Lepidoptera, in: Zhang, Z.-Q. (Ed.), Animal Biodiversity: An Outline of Higher-Level Classification and Survey of Taxonomic Richness. Zootaxa, pp. 212–221.

Ning, P., Yang, G., Hu, L., Sun, J., Shi, L., Zhou, Y., Wang, Z., Yang, J., 2021. Recent advances in the valorization of plant biomass. Biotechnol. Biofuels 14, 102. https://doi.org/10.1186/s13068-021-01949-3

Nishida, R., 2014. Chemical ecology of insect–plant interactions: ecological significance of plant secondary metabolites. Biosci. Biotechnol. Biochem. 78, 1–13. https://doi.org/10.1080/09168451.2014.877836

Nissim, L., Perli, S.D., Fridkin, A., Perez-Pinera, P., Lu, T.K., 2014. Multiplexed and Programmable Regulation of Gene Networks with an Integrated RNA and CRISPR/Cas Toolkit in Human Cells. Mol. Cell 54, 698–710. https://doi.org/10.1016/j.molcel.2014.04.022

Ochoa-Fernandez, R., Abel, N.B., Wieland, F.-G., Schlegel, J., Koch, L.-A., Miller, J.B., Engesser, R., Giuriani, G., Brandl, S.M., Timmer, J., Weber, W., Ott, T., Simon, R., Zurbriggen, M.D., 2020. Optogenetic control of gene expression in plants in the presence of ambient white light. Nat. Methods 17, 717–725. https://doi.org/10.1038/s41592-020-0868-y

Ohno, A., Maruyama, J., Nemoto, T., Arioka, M., Kitamoto, K., 2011. A carrier fusion significantly induces unfolded protein response in heterologous protein production by Aspergillus oryzae. Appl. Microbiol. Biotechnol. 92, 1197–1206. https://doi.org/10.1007/s00253-011-3487-9

Oliveira, J.M., Van Der Veen, D., De Graaff, L.H., Qin, L., 2008. Efficient cloning system for construction of gene silencing vectors in Aspergillus niger. Appl. Microbiol. Biotechnol. 80, 917–924. https://doi.org/10.1007/s00253-008-1640-x

Orejas, M., MacCabe, A.P., Perez Gonzalez, J.A., Kumar, S., Ramon, D., 1999. Carbon catabolite repression of the Aspergillus nidulans xlnA gene. Mol. Microbiol. 31, 177–184. https://doi.org/10.1046/j.1365-2958.1999.01157.x

Ortiz, R., Geleta, M., Gustafsson, C., Lager, I., Hofvander, P., Löfstedt, C., Cahoon, E.B., Minina, E., Bozhkov, P., Stymne, S., 2020. Oil crops for the future. Curr. Opin. Plant Biol. 56, 181–189. https://doi.org/10.1016/j.pbi.2019.12.003

Ozeki, K., Kanda, A., Hamachi, M., Nunokawa, Y., 1996. Construction of a Promoter Probe Vector Autonomously Maintained in *Aspergillus* and Characterization of Promoter Regions Derived from *A. niger* and *A. oryzae* Genomes. Biosci. Biotechnol. Biochem. 60, 383–389. https://doi.org/10.1271/bbb.60.383

Paddon, C.J., Keasling, J.D., 2014. Semi-synthetic artemisinin: a model for the use of synthetic biology in pharmaceutical development. Nat. Rev. Microbiol. 12, 355–367. https://doi.org/10.1038/nrmicro3240

Palou, L., 2014. Penicillium digitatum, Penicillium italicum (Green Mold, Blue Mold), in: Postharvest Decay. Elsevier, pp. 45–102. https://doi.org/10.1016/B978-0-12-411552-1.00002-8

Pan, C., Wu, X., Markel, K., Malzahn, A.A., Kundagrami, N., Sretenovic, S., Zhang, Y., Cheng, Y., Shih, P.M., Qi, Y., 2021. CRISPR–Act3.0 for highly efficient multiplexed gene activation in plants. Nat. Plants 7, 942–953. https://doi.org/10.1038/s41477-021-00953-7

Papikian, A., Liu, W., Gallego-Bartolomé, J., Jacobsen, S.E., 2019. Site-specific manipulation of Arabidopsis loci using CRISPR-Cas9 SunTag systems. Nat. Commun. 10, 729. https://doi.org/10.1038/s41467-019-08736-7

Patel, Y.D., Brown, A.J., Zhu, J., Rosignoli, G., Gibson, S.J., Hatton, D., James, D.C., 2021. Control of Multigene Expression Stoichiometry in Mammalian Cells Using Synthetic Promoters. ACS Synth. Biol. 10, 1155–1165. https://doi.org/10.1021/acssynbio.0c00643

Patron, N.J., 2020. Beyond natural: synthetic expansions of botanical form and function. New Phytol. 227, 295–310. https://doi.org/10.1111/nph.16562

Patron, N.J., Orzaez, D., Marillonnet, S., Warzecha, H., Matthewman, C., Youles, M., Raitskin, O., Leveau, A., Farré, G., Rogers, C., Smith, A., Hibberd, J., Webb, A.A.R., Locke, J., Schornack, S., Ajioka, J., Baulcombe, D.C., Zipfel, C., Kamoun, S., Jones, J.D.G., Kuhn, H., Robatzek, S., Van Esse, H.P., Sanders, D., Oldroyd, G., Martin, C., Field, R., O'Connor, S., Fox, S., Wulff, B., Miller, B., Breakspear, A., Radhakrishnan, G., Delaux, P., Loqué, D., Granell, A., Tissier, A., Shih, P., Brutnell, T.P., Quick, W.P., Rischer, H., Fraser, P.D., Aharoni, A., Raines, C., South, P.F., Ané, J., Hamberger, B.R., Langdale, J., Stougaard, J., Bouwmeester, H., Udvardi, M., Murray, J.A.H., Ntoukakis, V., Schäfer, P., Denby, K., Edwards, K.J., Osbourn, A., Haseloff, J., 2015. Standards for plant synthetic biology: a common syntax for exchange of DNA parts. New Phytol. 208, 13–19. https://doi.org/10.1111/nph.13532

Perathoner, S., Centi, G., 2014. CO_2 Recycling: A Key Strategy to Introduce Green Energy in the Chemical Production Chain. ChemSusChem 7, 1274–1282. https://doi.org/10.1002/cssc.201300926

Pérez-González, A., Caro, E., 2019. Benefits of using genomic insulators flanking transgenes to increase expression and avoid positional effects. Sci. Rep. 9, 8474. https://doi.org/10.1038/s41598-019-44836-6

Petkevicius, K., Löfstedt, C., Borodina, I., 2020. Insect sex pheromone production in yeasts and plants. Curr. Opin. Biotechnol. 65, 259–267. https://doi.org/10.1016/j.copbio.2020.07.011

Phan, H.T., Pham, V.T., Ho, T.T., Pham, N.B., Chu, H.H., Vu, T.H., Abdelwhab, E.M., Scheibner, D., Mettenleiter, T.C., Hanh, T.X., Meister, A., Gresch, U., Conrad, U., 2020. Immunization with Plant-Derived Multimeric H5 Hemagglutinins Protect Chicken against Highly Pathogenic Avian Influenza Virus H5N1. Vaccines 8, 593. https://doi.org/10.3390/vaccines8040593

Pollak, B., Cerda, A., Delmans, M., Álamos, S., Moyano, T., West, A., Gutiérrez, R.A., Patron, N.J., Federici, F., Haseloff, J., 2019. Loop assembly: a simple and open system for recursive fabrication of DNA circuits. New Phytol. 222, 628–640. https://doi.org/10.1111/nph.15625

Polli, F., Meijrink, B., Bovenberg, R.A.L., Driessen, A.J.M., 2016. New promoters for strain engineering of Penicillium chrysogenum. Fungal Genet. Biol. 89, 62–71. https://doi.org/10.1016/j.fgb.2015.12.003

Polstein, L.R., Perez-Pinera, P., Kocak, D.D., Vockley, C.M., Bledsoe, P., Song, L., Safi, A., Crawford, G.E., Reddy, T.E., Gersbach, C.A., 2015. Genome-wide specificity of DNA binding, gene regulation, and chromatin remodeling by TALE- and CRISPR/Cas9-based transcriptional activators. Genome Res. 25, 1158–1169. https://doi.org/10.1101/gr.179044.114

Reed, J., Stephenson, M.J., Miettinen, K., Brouwer, B., Leveau, A., Brett, P., Goss, R.J.M., Goossens, A., O'Connell, M.A., Osbourn, A., 2017. A translational synthetic biology platform for rapid access to gram-scale quantities of novel drug-like molecules. Metab. Eng. 42, 185–193. https://doi.org/10.1016/j.ymben.2017.06.012

Reynolds, K.B., Taylor, M.C., Cullerne, D.P., Blanchard, C.L., Wood, C.C., Singh, S.P., Petrie, J.R., 2017. A reconfigured Kennedy pathway which promotes efficient accumulation of medium-chain fatty acids in leaf oils. Plant Biotechnol. J. 15, 1397–1408. https://doi.org/10.1111/pbi.12724

Rivaldi, J.D., Carvalho, A.K.F., Da Conceição, L.R.V., De Castro, H.F., 2017. Assessing the potential of fatty acids produced by filamentous fungi as feedstock for biodiesel production. Prep. Biochem. Biotechnol. 47, 970–976. https://doi.org/10.1080/10826068.2017.1365246

Robey, M.T., Caesar, L.K., Drott, M.T., Keller, N.P., Kelleher, N.L., 2021. An interpreted atlas of biosynthetic gene clusters from 1,000 fungal genomes. Proc. Natl. Acad. Sci. 118, e2020230118. https://doi.org/10.1073/pnas.2020230118

Rodionova, M.V., Poudyal, R.S., Tiwari, I., Voloshin, R.A., Zharmukhamedov, S.K., Nam, H.G., Zayadan, B.K., Bruce, B.D., Hou, H.J.M., Allakhverdiev, S.I., 2017. Biofuel production: Challenges and opportunities. Int. J. Hydrog. Energy 42, 8450–8461. https://doi.org/10.1016/j.ijhydene.2016.11.125

Romero-Suarez, D., Keasling, J.D., Jensen, M.K., 2022. Supplying plant natural products by yeast cell factories. Curr. Opin. Green Sustain. Chem. 33, 100567. https://doi.org/10.1016/j.cogsc.2021.100567

Ropero-Pérez, C., Bolós, B., Giner-Llorca, M., Locascio, A., Garrigues, S., Gandía, M., Manzanares, P., Marcos, J.F., 2023. Transcriptomic Profile of Penicillium digitatum Reveals Novel Aspects of the Mode of Action of the Antifungal Protein AfpB. Microbiol. Spectr. 11, e04846-22. https://doi.org/10.1128/spectrum.04846-22

Roux, I., Woodcraft, C., Hu, J., Wolters, R., Gilchrist, C.L.M., Chooi, Y.-H., 2020. CRISPR-Mediated Activation of Biosynthetic Gene Clusters for Bioactive Molecule Discovery in

Filamentous Fungi. ACS Synth. Biol. 9, 1843–1854. https://doi.org/10.1021/acssynbio.0c00197

Saijo, T., Nagasawa, A., 2014. Development of a tightly regulated and highly responsive copper-inducible gene expression system and its application to control of flowering time. Plant Cell Rep. 33, 47–59. https://doi.org/10.1007/s00299-013-1511-5

Sarmidi, M.R., Enshasy, H.A.E., 2012. Biotechnology for Wellness Industry: Concepts and Biofactories.

Sarrion-Perdigones, A., Falconi, E.E., Zandalinas, S.I., Juárez, P., Fernández-del-Carmen, A., Granell, A., Orzaez, D., 2011. GoldenBraid: An Iterative Cloning System for Standardized Assembly of Reusable Genetic Modules. PLoS ONE 6, e21622. https://doi.org/10.1371/journal.pone.0021622

Sarrion-Perdigones, A., Vazquez-Vilar, M., Palaci, J., Castelijns, B., Forment, J., Ziarsolo, P., Blanca, J., Granell, A., Orzaez, D., 2013. GoldenBraid 2.0: A Comprehensive DNA Assembly Framework for Plant Synthetic Biology. PLANT Physiol. 162, 1618–1631. https://doi.org/10.1104/pp.113.217661

Schillberg, S., Finnern, R., 2021. Plant molecular farming for the production of valuable proteins – Critical evaluation of achievements and future challenges. J. Plant Physiol. 258–259, 153359. https://doi.org/10.1016/j.jplph.2020.153359

Schmidt, J.A., McGrath, J.M., Hanson, M.R., Long, S.P., Ahner, B.A., 2019. Field-grown tobacco plants maintain robust growth while accumulating large quantities of a bacterial cellulase in chloroplasts. Nat. Plants 5, 715–721. https://doi.org/10.1038/s41477-019-0467-z

Schnee, C., Köllner, T.G., Held, M., Turlings, T.C.J., Gershenzon, J., Degenhardt, J., 2006. The products of a single maize sesquiterpene synthase form a volatile defense signal that attracts natural enemies of maize herbivores. Proc. Natl. Acad. Sci. 103, 1129–1134. https://doi.org/10.1073/pnas.0508027103

Schneeberger, R.G., Zhang, K., Tatarinova, T., Troukhan, M., Kwok, S.F., Drais, J., Klinger, K., Orejudos, F., Macy, K., Bhakta, A., Burns, J., Subramanian, G., Donson, J., Flavell, R., Feldmann, K.A., 2005. Agrobacterium T-DNA integration in Arabidopsis is correlated with DNA sequence compositions that occur frequently in gene promoter regions. Funct. Integr. Genomics 5, 240–253. https://doi.org/10.1007/s10142-005-0138-1

Schüller, A., Wolansky, L., Berger, H., Studt, L., Gacek-Matthews, A., Sulyok, M., Strauss, J., 2020. A novel fungal gene regulation system based on inducible VPR-dCas9 and nucleosome map-guided sgRNA positioning. Appl. Microbiol. Biotechnol. 104, 9801–9822. https://doi.org/10.1007/s00253-020-10900-9

Schultz, B.J., Kim, S.Y., Lau, W., Sattely, E.S., 2019. Total Biosynthesis for Milligram-Scale Production of Etoposide Intermediates in a Plant Chassis. J. Am. Chem. Soc. 141, 19231–19235. https://doi.org/10.1021/jacs.9b10717

Selma, S., Bernabé-Orts, J.M., Vazquez-Vilar, M., Diego-Martin, B., Ajenjo, M., Garcia-Carpintero, V., Granell, A., Orzaez, D., 2019. Strong gene activation in plants with

genome-wide specificity using a new orthogonal CRISPR /Cas9-based programmable transcriptional activator. Plant Biotechnol. J. 17, 1703–1705. https://doi.org/10.1111/pbi.13138

Selma, S., Gianoglio, S., Uranga, M., Vázquez-Vilar, M., Espinosa-Ruiz, A., Drapal, M., Fraser, P.D., Daròs, J., Orzáez, D., 2022a. *Potato virus X* -delivered CRISPR activation programs lead to strong endogenous gene induction and transient metabolic reprogramming in *Nicotiana benthamiana*. Plant J. 111, 1550–1564. https://doi.org/10.1111/tpj.15906

Selma, S., Sanmartín, N., Espinosa-Ruiz, A., Gianoglio, S., Lopez-Gresa, M.P., Vázquez-Vilar, M., Flors, V., Granell, A., Orzaez, D., 2022b. Custom-made design of metabolite composition in *N. benthamiana* leaves using CRISPR activators. Plant Biotechnol. J. 20, 1578–1590. https://doi.org/10.1111/pbi.13834

Shelepova, O.V., Baranova, E.N., Tkacheva, E.V., Evdokimenkova, Y.B., Ivanovskii, A.A., Konovalova, L.N., Gulevich, A.A., 2022. Aromatic Plants Metabolic Engineering: A Review. Agronomy 12, 3131. https://doi.org/10.3390/agronomy12123131

Shen, J.-Y., Zhao, Q., He, Q.-L., 2023. Application of CRISPR in Filamentous Fungi and Macrofungi: From Component Function to Development Potentiality. ACS Synth. Biol. acssynbio.3c00099. https://doi.org/10.1021/acssynbio.3c00099

Sigl, C., Handler, M., Sprenger, G., Kürnsteiner, H., Zadra, I., 2010. A novel homologous dominant selection marker for genetic transformation of Penicillium chrysogenum: Overexpression of squalene epoxidase-encoding ergA. J. Biotechnol. 150, 307–311. https://doi.org/10.1016/j.jbiotec.2010.09.941

Smith, A., Brown, K., Ogilvie, S., Rushton, K., Bates, J., 2021. Waste management options and climate change. AEA Technology.

Sonderegger, C., Galgóczy, L., Garrigues, S., Fizil, Á., Borics, A., Manzanares, P., Hegedüs, N., Huber, A., Marcos, J.F., Batta, G., Marx, F., 2016. A Penicillium chrysogenum-based expression system for the production of small, cysteine-rich antifungal proteins for structural and functional analyses. Microb. Cell Factories 15, 192. https://doi.org/10.1186/s12934-016-0586-4

Song, L., Ouedraogo, J.-P., Kolbusz, M., Nguyen, T.T.M., Tsang, A., 2018. Efficient genome editing using tRNA promoter-driven CRISPR/Cas9 gRNA in Aspergillus niger. PLOS ONE 13, e0202868. https://doi.org/10.1371/journal.pone.0202868

Spina, F., Tummino, M.L., Poli, A., Prigione, V., Ilieva, V., Cocconcelli, P., Puglisi, E., Bracco, P., Zanetti, M., Varese, G.C., 2021. Low density polyethylene degradation by filamentous fungi. Environ. Pollut. 274, 116548. https://doi.org/10.1016/j.envpol.2021.116548

Stam, M., Mol, J.N., Kooter, J.M., 1997. Review Article: The Silence of Genes in Transgenic Plants. Ann. Bot. 79, 3–12. https://doi.org/10.1006/anbo.1996.0295

Stelinski, L.L., Gut, L.J., Miller, J.R., 2013. An Attempt to Increase Efficacy of Moth Mating Disruption by Co-Releasing Pheromones With Kairomones and to Understand Possible Underlying Mechanisms of This Technique. Environ. Entomol. 42, 158–166. https://doi.org/10.1603/EN12257

Stephenson, M.J., Reed, J., Patron, N.J., Lomonossoff, G.P., Osbourn, A., 2020. Engineering Tobacco for Plant Natural Product Production, in: Comprehensive Natural Products III. Elsevier, pp. 244–262. https://doi.org/10.1016/B978-0-12-409547-2.14724-9

Storms, R., Zheng, Y., Li, H., Sillaots, S., Martinez-Perez, A., Tsang, A., 2005. Plasmid vectors for protein production, gene expression and molecular manipulations in Aspergillus niger. Plasmid 53, 191–204. https://doi.org/10.1016/j.plasmid.2004.10.001

Stothard, P., 2000. The Sequence Manipulation Suite: JavaScript Programs for Analyzing and Formatting Protein and DNA Sequences. BioTechniques 28, 1102–1104. https://doi.org/10.2144/00286ir01

Strong, P.J., Self, R., Allikian, K., Szewczyk, E., Speight, R., O'Hara, I., Harrison, M.D., 2022. Filamentous fungi for future functional food and feed. Curr. Opin. Biotechnol. 76, 102729. https://doi.org/10.1016/j.copbio.2022.102729

Süntar, I., Çetinkaya, S., Haydaroğlu, Ü.S., Habtemariam, S., 2021. Bioproduction process of natural products and biopharmaceuticals: Biotechnological aspects. Biotechnol. Adv. 50, 107768. https://doi.org/10.1016/j.biotechadv.2021.107768

Tada, S., Gomi, K., Kitamoto, K., Takahashi, K., Tamura, G., Hara, S., 1991. Construction of a fusion gene comprising the Taka-amylase A promoter and the Escherichia coli β-glucuronidase gene and analysis of its expression in Aspergillus oryzae. Mol. Gen. Genet. MGG 229, 301–306. https://doi.org/10.1007/BF00272170

Takken, F.L.W., Van Wijk, R., Michielse, C.B., Houterman, P.M., Ram, A.F.J., Cornelissen, B.J.C., 2004. A one-step method to convert vectors into binary vectors suited for Agrobacterium-mediated transformation. Curr. Genet. 45, 242–248. https://doi.org/10.1007/s00294-003-0481-5

Troiano, D., Orsat, V., Dumont, M.J., 2020. Status of filamentous fungi in integrated biorefineries. Renew. Sustain. Energy Rev. 117, 109472. https://doi.org/10.1016/j.rser.2019.109472

Tsuchiya, K., Tada, S., Gomi, K., Kitamoto, K., Kumagai, C., Jigami, Y., Tamura, G., 1992a. High level expression of the synthetic human lysozyme gene in Aspergillus oryzae. Appl. Microbiol. Biotechnol. 38. https://doi.org/10.1007/BF00169428

Tsuchiya, K., Tada, S., Gomi, K., Kitamoto, K., Kumagai, C., Tamura, G., 1992b. Deletion Analysis of the Taka-amylase A Gene Promoter Using a Homologous Transformation System in *Aspergillus oryzae*. Biosci. Biotechnol. Biochem. 56, 1849–1853. https://doi.org/10.1271/bbb.56.1849

Urnov, F.D., Rebar, E.J., Holmes, M.C., Zhang, H.S., Gregory, P.D., 2010. Genome editing with engineered zinc finger nucleases. Nat. Rev. Genet. 11, 636–646. https://doi.org/10.1038/nrg2842

van Herpen, T.W.J.M., Cankar, K., Nogueira, M., Bosch, D., Bouwmeester, H.J., Beekwilder, J., 2010. Nicotiana benthamiana as a Production Platform for Artemisinin Precursors. PLoS ONE 5, e14222. https://doi.org/10.1371/journal.pone.0014222

Vaucheret, H., Béclin, C., Elmayan, T., Feuerbach, F., Godon, C., Morel, J.-B., Mourrain, P., Palauqui, J.-C., Vernhettes, S., 1998. Transgene-induced gene silencing in plants: Transgene-induced gene silencing. Plant J. 16, 651–659. https://doi.org/10.1046/j.1365-313x.1998.00337.x

Vazquez-Vilar, M., Bernabé-Orts, J.M., Fernandez-del-Carmen, A., Ziarsolo, P., Blanca, J., Granell, A., Orzaez, D., 2016. A modular toolbox for gRNA–Cas9 genome engineering in plants based on the GoldenBraid standard. Plant Methods 12, 10. https://doi.org/10.1186/s13007-016-0101-2

Vazquez-Vilar, M., Gandía, M., García-Carpintero, V., Marqués, E., Sarrion-Perdigones, A., Yenush, L., Polaina, J., Manzanares, P., Marcos, J.F., Orzaez, D., 2020. Multigene Engineering by GoldenBraid Cloning: From Plants to Filamentous Fungi and Beyond. Curr. Protoc. Mol. Biol. 130. https://doi.org/10.1002/cpmb.116

Vazquez-Vilar, M., Quijano-Rubio, A., Fernandez-del-Carmen, A., Sarrion-Perdigones, A., Ochoa-Fernandez, R., Ziarsolo, P., Blanca, J., Granell, A., Orzaez, D., 2017. GB3.0: a platform for plant bio-design that connects functional DNA elements with associated biological data. Nucleic Acids Res. gkw1326. https://doi.org/10.1093/nar/gkw1326

Villarreal, G.U., Campos, E.V.R., De Oliveira, J.L., Fraceto, L.F., 2023. Development and commercialization of pheromone-based biopesticides, in: Development and Commercialization of Biopesticides. Elsevier, pp. 37–56. https://doi.org/10.1016/B978-0-323-95290-3.00008-X

Virdi, V., Depicker, A., 2013. Role of plant expression systems in antibody production for passive immunization. Int. J. Dev. Biol. 57, 587–593. https://doi.org/10.1387/ijdb.130266ad

Vitorino, L.C., Bessa, L.A., 2017. Technological Microbiology: Development and Applications. Front. Microbiol. 8, 827. https://doi.org/10.3389/fmicb.2017.00827

Wang, H.-L., Ding, B.-J., Dai, J.-Q., Nazarenus, T.J., Borges, R., Mafra-Neto, A., Cahoon, E.B., Hofvander, P., Stymne, S., Löfstedt, C., 2022. Insect pest management with sex pheromone precursors from engineered oilseed plants. Nat. Sustain. 5, 981–990. https://doi.org/10.1038/s41893-022-00949-x

Wang, P.-H., Kumar, S., Zeng, J., McEwan, R., Wright, T.R., Gupta, M., 2020. Transcription Terminator-Mediated Enhancement in Transgene Expression in Maize: Preponderance of the AUGAAU Motif Overlapping With Poly(A) Signals. Front. Plant Sci. 11, 570778. https://doi.org/10.3389/fpls.2020.570778

Wang, Y., Demirer, G.S., 2023. Synthetic biology for plant genetic engineering and molecular farming. Trends Biotechnol. S0167779923000884. https://doi.org/10.1016/j.tibtech.2023.03.007

Warner, T.G., 1999. Enhancing therapeutic glycoprotein production in Chinese hamster ovary cells by metabolic engineering endogenous gene control with antisense DNA and gene targeting. Glycobiology 9, 841–850. https://doi.org/10.1093/glycob/9.9.841

Weber, E., Engler, C., Gruetzner, R., Werner, S., Marillonnet, S., 2011. A Modular Cloning System for Standardized Assembly of Multigene Constructs. PLoS ONE 6, e16765. https://doi.org/10.1371/journal.pone.0016765

Wei, J., Wang, L., Zhu, J., Zhang, S., Nandi, O.I., Kang, L., 2007. Plants Attract Parasitic Wasps to Defend Themselves against Insect Pests by Releasing Hexenol. PLoS ONE 2, e852. https://doi.org/10.1371/journal.pone.0000852

Wiebe, M.G., Karandikar, A., Robson, G.D., Trinci, A.P.J., Candia, J.-L.F., Trappe, S., Wallis, G., Rinas, U., Derkx, P.M.F., Madrid, S.M., Sisniega, H., Faus, I., Montijn, R., Van Den Hondel, C.A.M.J.J., Punt, P.J., 2001. Production of tissue plasminogen activator (t-PA) inAspergillus niger. Biotechnol. Bioeng. 76, 164–174. https://doi.org/10.1002/bit.1156

Witzgall, P., Kirsch, P., Cork, A., 2010. Sex Pheromones and Their Impact on Pest Management. J Chem Ecol 36, 80–100. https://doi.org/10.1007/s10886-009-9737-y

Wu, T., Kerbler, S.M., Fernie, A.R., Zhang, Y., 2021. Plant cell cultures as heterologous bio-factories for secondary metabolite production. Plant Commun. 2, 100235. https://doi.org/10.1016/j.xplc.2021.100235

Wu, Y., Li, L., 2016. Sample normalization methods in quantitative metabolomics. J. Chromatogr. A 1430, 80–95. https://doi.org/10.1016/j.chroma.2015.12.007

Xia, X.-X., Qian, Z.-G., Ki, C.S., Park, Y.H., Kaplan, D.L., Lee, S.Y., 2010. Native-sized recombinant spider silk protein produced in metabolically engineered *Escherichia coli* results in a strong fiber. Proc. Natl. Acad. Sci. 107, 14059–14063. https://doi.org/10.1073/pnas.1003366107

Xia, Y.-H., Ding, B.-J., Dong, S.-L., Wang, H.-L., Hofvander, P., Löfstedt, C., 2022. Release of moth pheromone compounds from Nicotiana benthamiana upon transient expression of heterologous biosynthetic genes. BMC Biol. 20, 80. https://doi.org/10.1186/s12915-022-01281-8

Xia, Y.-H., Ding, B.-J., Wang, H.-L., Hofvander, P., Jarl-Sunesson, C., Löfstedt, C., 2020. Production of moth sex pheromone precursors in *Nicotiana* spp.: a worthwhile new approach to pest control. J. Pest Sci. 93, 1333–1346. https://doi.org/10.1007/s10340-020-01250-6

Xia, Y.-H., Wang, H.-L., Ding, B.-J., Svensson, G.P., Jarl-Sunesson, C., Cahoon, E.B., Hofvander, P., Löfstedt, C., 2021. Green Chemistry Production of Codlemone, the Sex Pheromone of the Codling Moth (Cydia pomonella), by Metabolic Engineering of the Oilseed Crop Camelina (Camelina sativa). J. Chem. Ecol. 47, 950–967. https://doi.org/10.1007/s10886-021-01316-4

Xiong, X., Liang, J., Li, Z., Gong, B., Li, J., 2021. Multiplex and optimization of dCas9-TV-mediated gene activation in plants. J. Integr. Plant Biol. 63, 634–645. https://doi.org/10.1111/jipb.13023

Yap, A., Glarcher, I., Misslinger, M., Haas, H., 2022. Characterization and engineering of the xylose-inducible xylP promoter for use in mold fungal species. Metab. Eng. Commun. 15, e00214. https://doi.org/10.1016/j.mec.2022.e00214

Zakrzewski, J., Grodner, J., Bobbitt, J.M., Karpińska, M., 2007. Oxidation of unsaturated primary alcohols and ω-haloalkanols with 4-acetylamino-2, 2, 6, 6-tetramethylpiperidine-1-oxoammonium tetrafluoroborate. Synthesis 16, 2491–2494. https://doi.org/10.1055/s-2007-983809

Zameitat, E., Freymark, G., Dietz, C.D., Löffler, M., Bölker, M., 2007. Functional Expression of Human Dihydroorotate Dehydrogenase (DHODH) in *pyr4* Mutants of *Ustilago maydis* Allows Target Validation of DHODH Inhibitors In Vivo. Appl. Environ. Microbiol. 73, 3371–3379. https://doi.org/10.1128/AEM.02569-06

Zarbin, P.H.G., Lorini, L.M., Ambrogi, B.G., Vidal, D.M., Lima, E.R., 2007. Sex Pheromone of *Lonomia obliqua*: Daily Rhythm of Production, Identification, and Synthesis. J. Chem. Ecol. 33, 555–565. https://doi.org/10.1007/s10886-006-9246-1

Zavada, A., Buckley, C.L., Martinez, D., Rospars, J.-P., Nowotny, T., 2011. Competition-Based Model of Pheromone Component Ratio Detection in the Moth. PLoS ONE 6, e16308. https://doi.org/10.1371/journal.pone.0016308

Zhang, Y., Malzahn, A.A., Sretenovic, S., Qi, Y., 2019. The emerging and uncultivated potential of CRISPR technology in plant science. Nat. Plants 5, 778–794. https://doi.org/10.1038/s41477-019-0461-5

Zhang, Y.-H.P., Sun, J., Ma, Y., 2017. Biomanufacturing: history and perspective. J. Ind. Microbiol. Biotechnol. 44, 773–784. https://doi.org/10.1007/s10295-016-1863-2

Zheng, N., Xia, R., Yang, C., Yin, B., Li, Y., Duan, C., Liang, L., Guo, H., Xie, Q., 2009. Boosted expression of the SARS-CoV nucleocapsid protein in tobacco and its immunogenicity in mice. Vaccine 27, 5001–5007. https://doi.org/10.1016/j.vaccine.2009.05.073

Zhou, J.-J., 2010. Odorant-Binding Proteins in Insects, in: Litwack, G. (Ed.), Vitamins & Hormones. Elsevier, pp. 241–272. https://doi.org/10.1016/S0083-6729(10)83010-9

Zou, Y., Millar, J.G., 2015. Chemistry of the pheromones of mealybug and scale insects. Nat. Prod. Rep. 32, 1067–1113. https://doi.org/10.1039/C4NP00143E